

A N N U A L   R E P O R T

1 9 6 8

U. S. WATER CONSERVATION LABORATORY  
Southwest Branch  
Soil and Water Conservation Research Division  
Agricultural Research Service  
United States Department of Agriculture  
Phoenix, Arizona

---

FOR OFFICIAL USE ONLY

This report contains unpublished and confidential information concerning work in progress. The contents of this report may not be published or reproduced in any form without the prior consent of the research workers involved.

## TABLE OF CONTENTS

	<u>Title</u>	<u>Page</u>
Introduction	Changes in Personnel	1
SWC W4-gG-1	Methods for water quality improvement and its storage underground.	
WCL 66-1	Experimental and analytical studies of the flow and oxygen regimes in soil intermittently inundated with low quality water.	44-1
WCL 67-4	Waste-water renovation by spreading treated sewage for ground-water recharge.	51-1
WCL 68-3	Column studies of the chemical, physical, and biological processes of waste-water renovation by percolation through the soil.	54-1
SWC W7-gG-2	Evaluation and control of seepage from water storage and conveyance structures.	
WCL 64-3	Clay dispersants for reduction of seepage losses from reservoirs.	37-1
WCL 64-4	Waterborne sealants to reduce seepage losses from unlined channels and reservoirs.	38-1
WCL 68-2	Fabricated in place, reinforced reservoir linings.	53-1
SWC W7-gG-3	Suppression of evaporation from water surfaces.	
WCL 67-3	Use of floating solid and granular materials to reduce evaporation from water surfaces.	50-1
SWC W7-gG-4	Principles, facilities, and systems for water harvest.	
WCL 60-7	Soil treatment to reduce infiltration and increase precipitation runoff.	7-1
WCL 65-2	Materials and methods for water harvesting and water storage in the State of Hawaii.	42-1

	<u>Title</u>	<u>Page</u>
SWC W7-gG-5	Soil water movement in relation to the conservation of water supplies.	
WCL 61-4	Measurement and calculation of unsaturated conductivity and soil water diffusivity.	13-1
WCL 64-6	Dispersion and flocculation of soil and clay materials as related to the sodium and calcium status of the ambient solution.	40-1
WCL 67-2	Physical and chemical characteristics of hydrophobic soils.	49-1
SWC W9-gG-6	Factors governing evapotranspiration of water from cropped fields.	
WCL 58-2	Consumptive use of water by crops in Arizona.	23-1
WCL 62-10	Plant response to changes in evaporative demand and soil water potential, as shown by measurements of leaf resistance, transpiration, leaf temperature, and leaf water content.	29-1
WCL 68-4	Water stresses in plants.	55-1
WCL 68-5	Assessing the energy environment of plants.	56-1
WCL 68-6	Simulation of plant communities for determining water use efficiency.	57-1
SWC W10-gG-7	Irrigation systems for efficient water use.	
WCL 60-2	Dynamic similarity in elbow flow meters.	2-1
WCL 65-3	Integrating velocity profile meters.	43-1
WCL 66-2	Irrigation outlet structures to distribute water onto erosive soils.	45-1
WCL 67-1	Flow measurement in open channels with critical depth flumes.	48-1

Title

Page

Appendix I	List of Publications.	AI-1
Appendix II	Summation of Important Findings.	AII-1

## CHANGES IN PERSONNEL

The Laboratory staff has been strengthened during 1968 by the addition of eight new members. They are as follows:

- D. A. Bucks, Agricultural Engineer
- P. B. Ealim, YOC
- G. Ekechukwu, Laboratory Technician
- E. D. Escarcega, Hydraulic Engineering Aid (Return from military furlough)
- P. Kuechelmann, Laboratory Technician
- J. C. Lance, Research Soil Scientist
- M. E. Olson, Clerk-Stenographer
- L. Shedd, YOC

During 1968 there were nine departures. They are as follows:

- D. A. Bucks, Agricultural Engineer (Military furlough)
- P. B. Ealim, YOC
- D. S. Fry, Clerk-Stenographer
- J. L. Krebs, Laboratory Technician
- R. S. Miller, Administrative Assistant
- C. D. Pullins, Physical Science Aid
- R. C. Saylor, Laboratory Technician
- L. Shedd, YOC
- C. H. Tanner, Secretary

## LABORATORY STAFF

### Professional:

- Dr. H. Bower, Research Hydraulic Engineer
- Mr. D. A. Bucks, Agricultural Engineer
- Mr. K. R. Cooley, Research Meteorologist
- Dr. W. L. Ehrler, Research Plant Physiologist
- Mr. L. J. Erie, Research Agricultural Engineer
- Dr. D. H. Fink, Research Soil Scientist
- Mr. G. W. Frasier, Research Hydraulic Engineer
- Dr. S. B. Idso, Research Soil Scientist
- Dr. R. D. Jackson, Research Physicist
- Dr. J. C. Lance, Research Soil Scientist
- Mr. L. E. Myers, Research Hydraulic Engineer and Director
- Dr. F. S. Nakayama, Research Chemist
- Mr. R. J. Reginato, Research Soil Scientist
- Dr. J. A. Replogle, Research Hydraulic Engineer
- Mr. R. C. Rice, Agricultural Engineer
- Dr. F. D. Whisler, Research Soil Scientist

Technicians:

G. Ekechukwu, Laboratory Technician  
E. D. Escarcega, Hydraulic Engineering Aid  
D. A. Forstie, Physical Science Aid  
O. F. French, Agricultural Research Technician  
J. L. Gale, Physical Science Technician  
L. P. Girdley, Engineering Draftsman  
J. R. Griggs, Physical Science Technician  
J. L. Krebs, Laboratory Technician  
P. Kuechelmann, Laboratory Technician  
J. M. R. Martinez, Engineering Aid  
J. B. Miller, Physical Science Technician  
S. T. Mitchell, Physical Science Technician  
K. G. Mullins, Physical Science Technician  
J. M. Pritchard, Physical Science Technician  
C. D. Pullins, Physical Science Aid  
B. A. Rasnick, Physical Science Technician  
R. C. Saylor, Laboratory Technician

Administrative, Clerical, and Maintenance:

O. J. Abeyta, Laborer  
I. G. Barnett, Janitor  
E. D. Bell, General Machinist  
E. E. De La Rosa, Janitor  
P. B. Ealim, YOC  
B. E. Fisher, Library Technician  
D. S. Fry, Clerk-Stenographer  
C. G. Hiesel, General Machinist  
R. C. Klapper, Refrigeration and Air Conditioning Mechanic  
R. S. Miller, Administrative Assistant  
A. H. Morse, Secretary-Dictating Machine Transcriber  
M. E. Olson, Clerk-Stenographer  
L. J. Orneside, Clerk-Stenographer  
M. A. Seiler, Clerk-Stenographer  
L. Shedd, YOC  
C. H. Tanner, Secretary  
M. F. Witcher, Clerk-Stenographer

TITLE DYNAMIC SIMILARITY IN ELBOW FLOW METERS.

CRIS WORK UNIT: SWC W10 gG-7

CODE NO.: Ariz.-WCL 60-2

INTRODUCTION:

See Annual Report for 1967.

A welded, steel elbow was calibrated for use with a portable irrigation pump. It was 4 inches in diameter, a size not previously tested in these studies.

The paper replying to discussers of the original paper "Evaluation of Pipe Elbows as Flow Meters (Sept., 1966) was published in the Journal of the Irrigation and Drainage Division, ASCE, Vol. 94, No. IR3, Sept. 1968.

Evaluation of a low-cost, turbine-type, household water meter as a shunt-meter, integrating, device for totalizing flow through large elbow meters was continued. The tests were made on the 10-inch diameter elbow, numbered 32 in previous reports. The turbine-type meter was a half-inch Tempe "magnetic-drive" water meter number 408199.

PROCEDURE:

The turbine-type water meter was connected in a shunt configuration across the elbow so that water from the tap on the outside of the elbow bend flowed through the water meter and into the inside tap on the elbow bend. A manometer connected across the elbow near each tap could be read to determine discharge through the main line and elbow when a valve in the water meter, or shunt line, was closed. When the valve was open, the manometer indicated the pressure drop across the water meter and the water meter accumulated total flow through the shunt. This flow was related to the total flow in the main line through the following developed relationships:

In terms of the differential head,  $H$ , between the outside and inside of a pipe elbow, the discharge,  $Q$ , can be expressed by a relation of the form

$$Q = M H^E \quad (1)$$

where M is a constant, depending on the diameter and radius of bend of the elbow, and E is an exponent, usually 0.5 for 3-inch diameter elbows, but increasing to about 0.52 for 12-inch diameter elbows.

In the shunt loop formed by connecting an ordinary water meter between pressure taps placed on the outside and inside of the elbow bend, the flow, q, is related to H by the pipe friction equation

$$H = f \frac{L}{D} \frac{v^2}{2g} \quad (2)$$

where f is the shunt pipe friction factor, L is the shunt pipe length, D is the shunt pipe diameter, v is the velocity in the shunt pipe, and g the acceleration due to gravity.

Since  $q = av$ , where a is the shunt pipe cross-sectional area, Equation (2) can be rewritten as

$$H = f \frac{L}{D} \frac{q^2}{a^2 2g} \quad (3)$$

Combining Equations (1) and (3)

$$Q = M \left[ f \frac{L}{D} \frac{q^2}{a^2 2g} \right]^E \quad (4)$$

or

$$Q = C q^{(2E)} \quad (5)$$

where C is a new constant combining M with the other dimensions and constants.

It may be noted that if E is 0.5, the relationship is linear between Q and q, and the accumulated total flow recorded on the household type shunt meter is directly related to the total flow through the main line independent of H. In reality, because of

bearing friction in the shunt meter, zero reading on the shunt meter would be expected to occur before flow actually reached zero in the main line. If this is correct, the actual form of the equation relating the flow in the main line to the flow in the shunt meter is

$$Q = K + C q^{(2E)} \quad (6)$$

where K represents the intercept on the zero axis of a plot of Q versus q.

The welded steel elbow meter mentioned earlier was 4 inches in diameter and had a radius of curvature for the flow centerline of 6 inches. The theoretical calibration curve was computed with the previously derived equation (see Annual Report, 1966). Because the approach piping was only about 4-feet long, which is less than the recommended 20 pipe diameters, and because this type elbow had not been previously tested, the pump system was laboratory calibrated with the meter in place on the pump system.

#### RESULTS AND DISCUSSION:

The "wethead" meter (see Annual Report 1966, 1967) was not further tested since it failed to turn freely after remaining idle for several months. The dryhead turbine-type meter that transmits its turbine rotation to the meter-dial mechanism through magnetic linkage has been tested. At first the results were erratic and the calibration could not be repeated. Calibration results shown in Figure 1 were obtained. The difficulty was ultimately traced to incomplete purging of air from the shunt meter housing. The air was finally removed by high pressure flushing through the meter. Air could be detected in the meter by pressurizing the shunt meter line when the valves installed between the meter and the pressure taps were closed. When one of the valves was opened rapidly, the flow indicator would spin if there was major air expansion forcing

flow past the rotor. Purging was continued until the rotation of the turbine shaft (or flow indicator) was less than about a quarter turn.

With the air removed, the calibration was stable and nearly linear, curving only slightly more than would be predicted by fitting an equation of the form of Equation (6) to the data. This was done by letting  $y = q^{(2E)}$  in Equation (6) and then fitting a least squares equation to the transformed data. The plotted line can hardly be distinguished from the straight line that would result if  $E = 0.5$ , except on a plot to a larger scale than that of Figure 1.

The linear calibration assuming  $E = 0.5$  is indicated in Figure 1. The data points at low flow rates tend to curve slightly to the left, probably due to the tendency for the turbine meter to under-indicate slightly at its lower operating limit. The meter has not been individually calibrated as yet, but the general class of meter behaves in this way.

Since air trapped in the meter can be a problem, it is desirable that some method be devised to easily or automatically remove the air and keep it out of the meter. Air bleeds on the side of the meter may be one solution. Another would be to use a meter style that fits into a vertical line which reduces the chance of trapping air.

Another source of calibration shift can be eliminated by removing the strainer in the meter. Relatively clean water should be used with these meters anyway, and sand type particles readily pass the meter rotor with little difficulty. If a filter is needed, it should be in the main line, or if in the shunt line, at least should be large enough to have negligible change in head loss with plugging.

Computation of discharge. Equation (6) is linear if  $E = 0.5$ . This linear equation is the basis for inferring total flow through the main line from observation of total flow through the household meter in the shunt line. The total flow,  $Q_T$ , could be expressed by summing the individual flow rates, each multiplied by the respective

time, that the particular flow rate prevailed. Expressed in terms of the symbols in Equation (6), with subscripts to denote flow rate and time periods 1, 2, n, etc., this becomes

$$Q_{\text{total}} = Q_1 T_1 + Q_2 T_2 + \dots + Q_n T_n \quad (7)$$

or

$$Q_{\text{total}} = (K + Cq_1) T_1 + (K + Cq_2) T_2 + \dots + (K + Cq_n) T_n \quad (8)$$

or

$$Q_{\text{total}} = Cq_{\text{total}} + KT_{\text{total}} \quad (9)$$

$$\begin{aligned} \text{where } q_{\text{total}} &= \sum q_n T_n \\ T_{\text{total}} &= \sum T_n \end{aligned}$$

Equation (9) shows that K must be zero if  $Q_{\text{total}}$  is to be inferred with only knowledge of  $q_{\text{total}}$ . If K is not zero then a quantity that is dependent on the total time of meter operation must be added.

Two obvious approaches are available to handle the problem. The first is to monitor the meter whenever it operates so that  $T_{\text{total}}$  is known. This is not convenient if the meter is to indicate total delivered flows to a field or water user for a season, since each application time would have to be recorded.

The second method would consist of assuming that deliveries would be near the maximum flow rate consistent with the pipe diameter and seldom if ever lower than, say, 2/3 of this maximum rate. The calibration curve is then fit through this upper range of data points and forced through zero, thus eliminating K.

Typical errors introduced by the second method can be evaluated for the 10-inch elbow used in this study (Figure 2). For this elbow,  $K = 102.3$  and  $C = 2406$ , with both Q and q expressed in gallons and T in minutes. Thus

$$Q_{\text{total}} = 2406 q_{\text{total}} + 102.3 T_{\text{total}} \quad (10)$$

For the case where the calibration curve is forced through zero, the equation for the 10-inch elbow is

$$Q_{\text{total}} = 2576 q_{\text{total}} \quad (11)$$

Consider a typical application in a 24-hour period at an average rate of 1500 gpm or a total application of 2,160,000 gallons (6.63 acre-feet). For ease of computation, assume that the water was applied for 8 hours (440-min.) at 2000 gpm, 8 hours at 1000 gpm, and 8 hours at 1500 gpm, averaging 1500 gpm.

From Equation (10),  $q_{\text{total}}$  can be calculated to be 836.5 gallons using either the total for each 8-hour period or the average for 24 hours.

Using the approximation of Equation (11), and inserting this same value for  $q_{\text{total}}$ ,  $Q_{\text{total}} = 2,155,000$  gallons, or a systematic error of less than 0.24%. Even if the entire amount had been applied at the lower flow rate of 1000 gpm requiring 36 hours (2160 min.), the shunt meter would have recorded 805.9 gallons (Equation (10)), which applied to Equation (11) would yield 2,076,000 gallons, or a systematic error of -3.9%. Likewise, at the highest flow rate, which would require 18 hours (1080 min.), the shunt meter would record 851.8 gallons, which applied to Equation (11) would yield 2,194,000 gallons, or a systematic error of +1.6%. It thus appears that use of the simplified form of Equation (11) is justified.

The calibration for the welded-steel, 4-inch elbow meter produces a discharge-differential head relation that was about 5 percent lower than calculated from the theoretical equations. This can be expected since the piping arrangement was inadequate.

The calibration equation was

$$Q = .169 H^{.497} \quad (12)$$

as compared to the theoretical equation which is

$$Q = 0.175 H^5 \quad (13)$$

where Q is in cubic feet per second and H is in inches of water.

#### SUMMARY AND CONCLUSIONS:

Studies toward incorporating low-cost integrating devices with elbow meters to convert them from rate devices to total quantity meters are continuing. Turbine-type household water meters have been used as a shunt meter across the pressure taps of the elbow meters. The expected linear relationship between the main line flow and the shunt flow was obtained with both "wethead" type meters and "dryhead", magnetic-linked meters. The wethead meters failed to restart after lying idle several weeks, probably due to deposits on the readout gears. The magnetic-linked type has no rotating liquid seals and no water in contact with the gears. Restarting after several months was no problem.

Since the relationship between the shunt meter and the main flow is affected by shunt-line friction losses, the relationship should be field checked several times per season. This is readily done with a manometer reading between the elbow pressure taps when the shunt meter line is closed. For the flow rate calculated from the manometer reading, the shunt meter is allowed to operate for a timed interval and the shunt flow rate determined. This is repeated for three or more flow rates and the curve plotted, main flow vs shunt meter flow.

The calibration plot will usually not intersect the origin, leaving a time dependent term in the total discharge equation. The

problem of keeping time records on the length of time the meter has operated can be avoided by forcing the calibration through the origin and through calibration points in the upper two-thirds of the flow range for the meter. Systematic errors resulting from this procedure would depend on the individual installation, but for a particular 10-inch diameter elbow and shunt meter system studied, typical systematic errors were less than 3.9%. It thus appears that this simplification is justified where time records are not easily kept.

PERSONNEL: J. A. Replogle.

CURRENT TERMINATION DATE: December 1970.

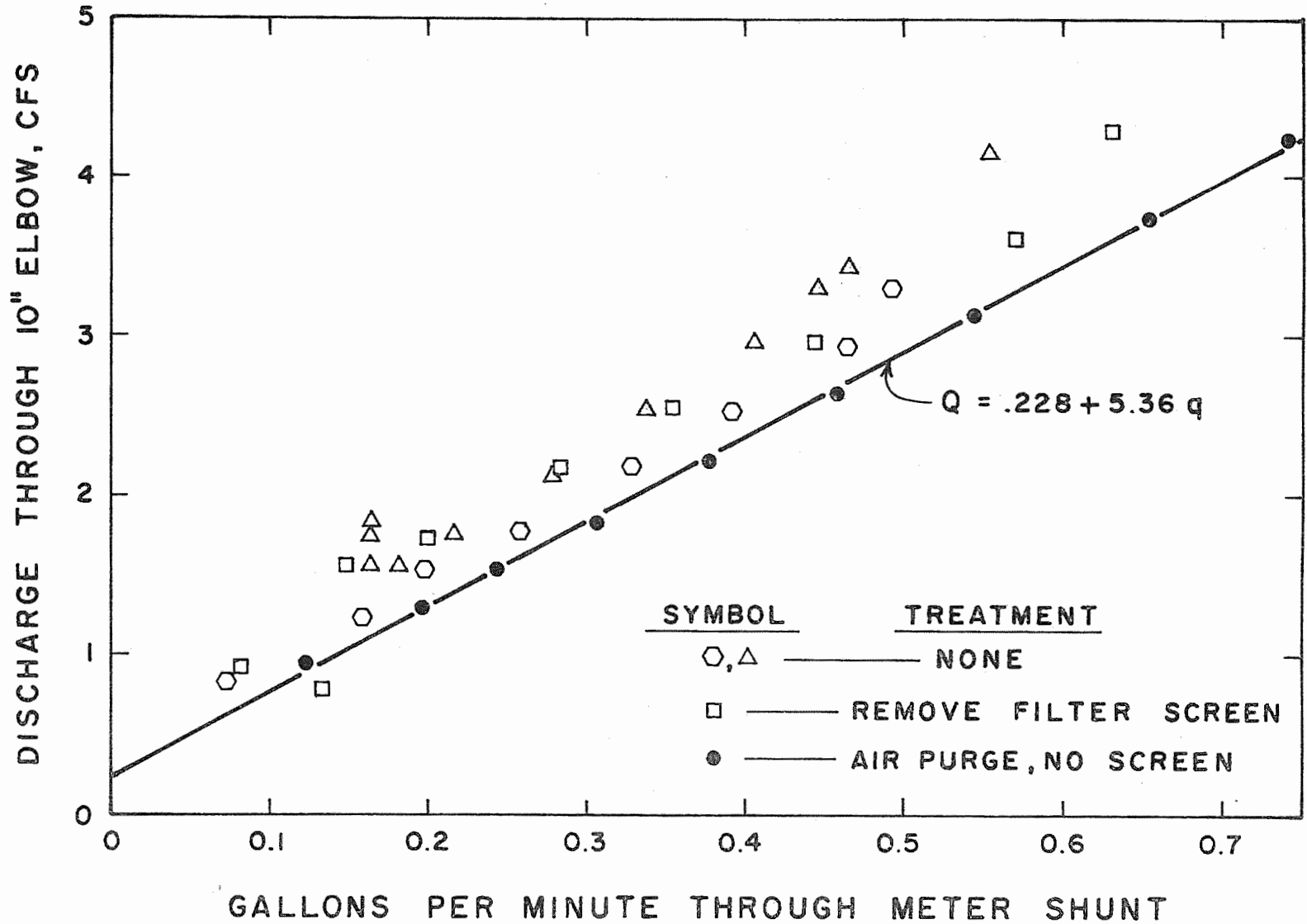


Figure 1. Calibration curves for 1-inch elbow meter with shunt meter attachment.

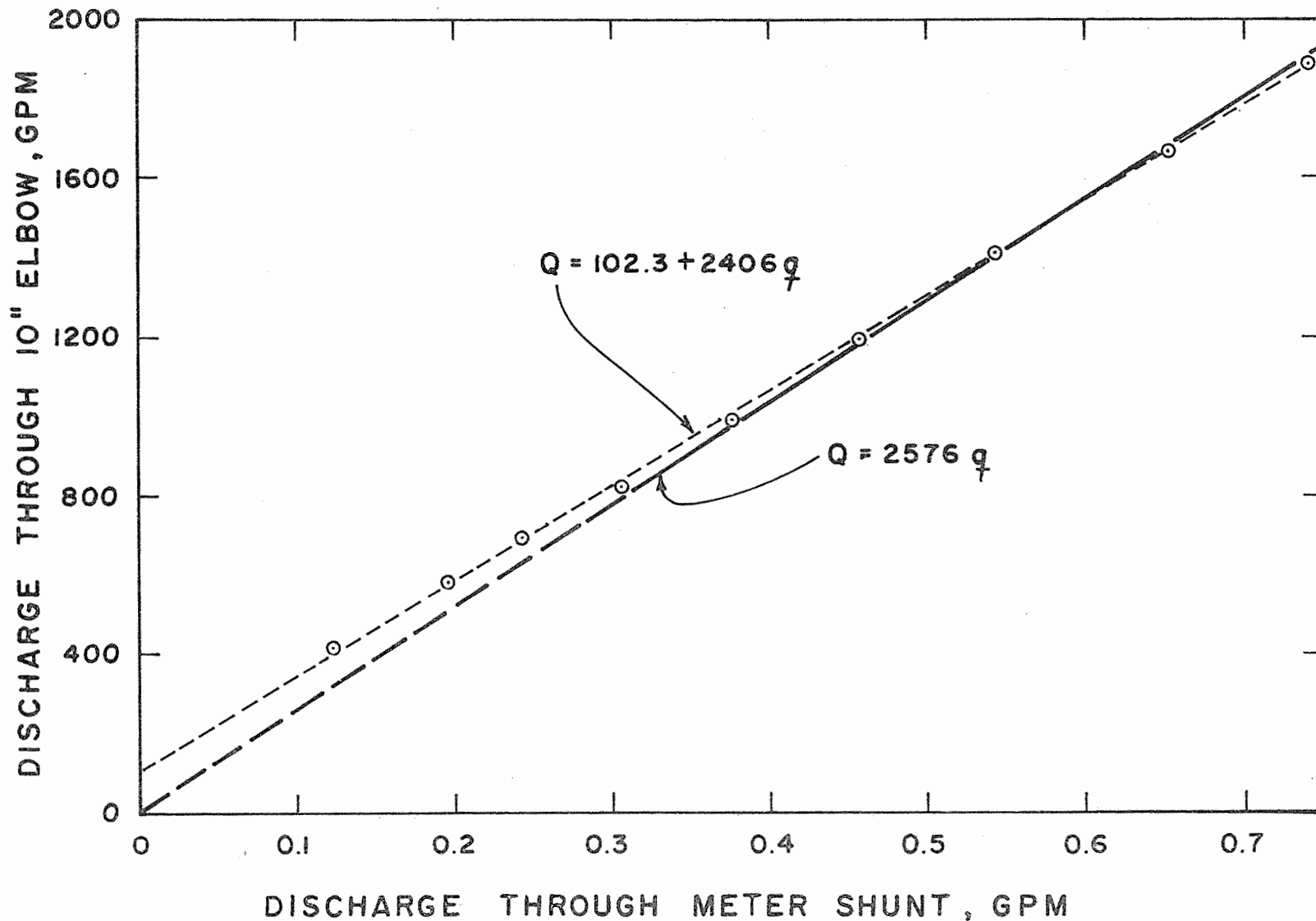


Figure 2. Calibration curve, forced zero. Annual Report of the U.S. Water Conservation Laboratory

TITLE: SOIL TREATMENT TO REDUCE INFILTRATION AND INCREASE  
PRECIPITATION RUNOFF

CRIS WORK UNIT: SWC W7 gG-4 CODE NO.: Ariz.-WCL 60-7

INTRODUCTION:

With the exception of the Seneca catchment, all previously reported operational water harvesting installations were turned over to the respective cooperators. This was accomplished in June 1968 with the final treatment of the Metate and Blue Mountain catchments. These catchments will be inspected at periodic intervals to observe the weathering performance of the treatments, but further maintenance will be done by the cooperators. A new catchment near Safford, Arizona, was treated in cooperation with the Bureau of Land Management. Measurement of rainfall and runoff was continued at the Monument Tank test site in the pretreatment phase of the study to evaluate water harvesting techniques on larger areas.

Observations and measurements were continued at the Granite Reef testing site in the evaluation of different surface treatments for increasing precipitation runoff. Laboratory studies were concerned with continued evaluation of the effectiveness of low-cost soil stabilizers and water-repellent treatments.

PART I. OPERATIONAL FIELD CATCHMENTS

With the exception of the Seneca and Guthrie Peak catchments, all operational field catchments were turned over to the respective cooperating agency. These catchments will continue to be observed under fully operational use. The Flagstaff cinders catchment and the two dual-purpose butyl catchments were not visited the past year nor was any report received on their performance.

Nelson Road Catchment. This catchment, with a two-phase asphalt pavement applied during the summer of 1964, was considered in good condition when inspected in May 1968. There were some soft spots in the pavement caused by water penetrating through cracks in the

asphalt. There were a few small holes where weeds had been removed. Repair could easily be made in an hour with 10 gallons of asphalt emulsion. The asphalt-fiberglass lining in the reservoir was in excellent condition. Asphalt-clay emulsion on the fiberglass appeared to be weathering exceptionally well.

Blue Mountain Catchment. This catchment, with a two-phase asphalt pavement applied in August 1967, was given a final protective spray coating of aluminized asphalt on 27 May 1968. The coating was applied, using a 3-gallon garden sprayer, at a rate of 0.017 liter of solution  $m^{-2}$  (0.075 gal  $yd^{-2}$ ). The aluminum coating appeared to give complete coverage and should protect the pavement for several years if weed growth is kept under control. Removal of weeds before applying the aluminized asphalt left about ten 2-inch diameter holes in the pavement. The catchment was considered in good condition.

Metate Catchment. The Metate catchment was re-treated 18 June 1968. A light tack coat of SS2H asphalt emulsion was sprayed on the old polyethylene cover. Then 5-ft wide, 3/4-oz  $ft^{-2}$  fiberglass was unrolled on the tack coat. Four-inch laps were made between the strips. Asphalt emulsion was sprayed on the surface at a rate which would completely fill the voids in the fiberglass plus penetrate through it to the catchment surface. A total of 0.75 gal  $yd^{-2}$  was applied. The previously installed asphalt-fiberglass lining in the reservoir is in excellent condition.

San Vicente Catchment. This catchment and reservoir, covered and lined with 20-mil chlorinated polyethylene sheeting in June 1965, was not inspected during the year. Reports from the Papago Indian Reservation are that the unit is in good condition, and they are using the water collected.

Mescal Catchment. This catchment, covered with chlorinated polyethylene sheeting in September 1965, was considered in good

condition when inspected in October 1968. The catchment had not been maintained during the previous 12 months. Two large weeds had grown through the cover and coyotes had dug two holes about 12 inches in diameter through the sheeting. There were indications that the sheeting was starting to deteriorate where stretched over small pebbles or sticks. In spite of these flaws, this catchment is still supplying adequate water for an area which previously was undergrazed because of insufficient water supplies.

Seneca Catchment. Original plans had called for treatment of this catchment in September 1967 after the grass had depleted soil moisture from the summer rain and prior to the winter precipitation. It had been hoped that creating a water-repellent soil surface over a relatively dry subsoil would greatly retard growth of grass on the catchment. Damage to the reservoir lining by a bathing bear, and the subsequent loss of water in the reservoir, prevented treatment until the Spring of 1968. As a result, the subsoil at the time of treatment contained sufficient water for luxurious grass growth after treatment.

Dry grass was burned off the catchment on 26 February 1968. On 17 April 1968 the plot was sprayed with a 3% solution of R-20 in water at a rate of 2.4 liters  $m^{-2}$ . Analysis of rainfall and runoff data shows that measured pretreatment runoff averaged 2.1% of the 500 mm precipitation during the period 12 July 1967 to 3 April 1968. Posttreatment measured runoff averaged 3.3% of the 148 mm precipitation during the period 5 July to 26 December 1968. This is not a satisfactory increase in runoff.

Failure of the treatment was probably the result of several factors. Growing vegetation undoubtedly disrupted the soil surface. The nozzles used to spray the plot produced a fine mist, and a strong wind blowing during the spray application blew part of the solution away. Application of the R-20 solution may have been inadequate. Possible reasons for treatment failure will be

investigated and will be eliminated before the catchment is treated again in 1969.

Guthrie Peak Catchment. This is a new catchment installed 14 May 1968 in cooperation with the Bureau of Land Management on top of a mountain near Safford, Arizona. There was a 1000 m<sup>2</sup> catchment of butyl sheeting and a large metal tank already on the site which is located so that water in excess of local needs can easily be piped to other locations. It was decided that an expansion of the catchment area would be desirable. Because the road to the site is very rough and steep, and soil conditions at the site restrict the amount of plot preparation, low-cost, sprayable, water repellent plus stabilizer treatment offered many advantages. A total area of 580 m<sup>2</sup> was sprayed with about 2 liters m<sup>-2</sup> of a mixture containing 10% DCA-70 and 3% R-20 by weight. The mixture was sprayed with a small centrifugal pump and a 4-nozzle spray bar with full-cone nozzles. A moderate growth of grass and small brush covered part of the sprayed area and was not removed prior to spraying. The catchment will be inspected at periodic intervals to observe the performance of the treatment.

#### PART II. MONUMENT TANK TESTING SITE

A description of the test site is presented in the 1967 Annual Report. A 2-ft contour topographic map of the area was made by aerial survey in the summer of 1968. Pretreatment rainfall and runoff measurements were continued during the year.

#### PROCEDURE:

On 18 March 1968 the two runoff collection ditches on areas 2 and 3 were sprayed with 1 kg asphalt m<sup>-2</sup> MC-250 cutback asphalt. On 22 April 1968 the two ditches were sprayed with 1.3 kg m<sup>-2</sup> RS-2 asphalt emulsion.

On 7 October 1968 three additional raingages were installed on area 4. This gives a total of 14 gages for the 30-hectare study

area. All raingages are read once a month. Lightweight transformer oil is placed in the raingages to prevent evaporative losses between readings. During the summer months it was observed that there was a considerable loss of water by evaporation from the stilling wells on the flumes. When runoff occurred it was necessary for the stilling wells to refill before the float was correctly recording the stage. This problem has been solved by using transformer oil in the stilling well to stop the evaporation.

#### RESULTS:

The waterstage recorder charts have not been analyzed at this time so the quantity of runoff from the four areas is not known. There has been sufficient runoff from the areas to maintain some water in the earth reservoir below the watersheds the entire year with the exception of approximately 30 days in June and July. We are told this had never previously occurred. The larger quantity of water reaching the reservoir is probably the result of two factors. One - the natural channel within the fenced study area was cleaned and straightened which reduced the retention time in an area of high intake rate. Two - the asphalt-lined ditches on areas 2 and 3 intercept the water before it reaches the channel. These two areas drain over 4 hectares with no channel losses occurring.

The asphalt-lined ditches are holding up exceptionally well. There are a few plants growing on the upper edge of the ditch on area 2. These will be removed and the ditch patched the early part of 1969.

The raingage network showed that there was no major variation in rainfall over the area. The variation is approximately 10% on a monthly basis. Comparison of the raingage catch by months indicates that the variation is random. A total of 439.7 mm was recorded for the year. The vector pluviometer shows that for the

year the percentage of the total collected by the four openings was: North - 20, East - 24, South - 14, West - 42.

For a remote site, damage caused by vandals has been essentially absent. One exception was a storage raingage which was taken from the stand and severely bent by rocks being thrown at it.

### PART III. GRANITE REEF TESTING SITE

In July 1968 the 5300-liter steel collection tanks at the lower edge of the L-plots, R-plots, and A-plots were replaced with 7500-liter covered concrete storage tanks. These new tanks eliminate a number of operational problems and simplify the analysis of the data. It was found that the bottoms of the tanks had cracked after installation, permitting water to leak out. The bottoms of the tanks were sealed with an asphaltic crack sealer in November 1968. Runoff measurements during the period of July to November were inaccurate because of the leaky tanks and have been omitted from this report. Concurrent with the tank installation, new water meters were installed on all the plots. These new meters have less internal friction and are less susceptible to stoppage by fine sand than the older nutating disk meters.

A 10 x 30 foot metal storage building was installed at the site. Rainfall runoff from the roof of the building is being measured to evaluate the relative effectiveness of roof-type catchments.

The water storage pond for the L-plots was reshaped to 13 x 40 x 2 meters deep and lined with 30-mil nylon reinforced butyl. The reservoir will be used in future evaporation studies and can also be a water supply for the underground pipe system that makes water available to all study plots. A second water storage tank was installed in the spring of 1968. This tank consists of the sides only of a standard metal grain bin 3 meters high by 5.5 meters in diameter. The tank is buried 1.5 meters in the ground

with the sides supported on soil cement. A liner for the tank was constructed from 20-mil blue vinyl. Seams in the lining have failed and the manufacturer has been unable to repair them satisfactorily. This liner will be removed and a more durable liner installed. The tank will be connected to the underground water supply as an alternate source of water.

A total of 219.9 mm of rainfall was measured in 19 separate storms. Following are the results of the runoff measurements for the different storms as compared to the standard 20.32-cm storage raingage.

Esso Plots. The runoff from the four-plot test unit constructed in cooperation with Esso Research Corporation of Linden, New Jersey, in December 1964 with a one-phase treatment of Venezuelan asphalt, has decreased as expected, but the runoff is still a significant portion of the rainfall. For the year, Plot E-1, treated with 1.95 kg asphalt  $m^{-2}$ , averaged 69% runoff; Plot E-2, treated with 1.85 kg asphalt  $m^{-2}$ , averaged 57% runoff; and Plot E-4, treated with 2.2 kg asphalt  $m^{-2}$ , averaged 69% runoff. This is only 3 to 5% lower than was measured the previous year.

Paved Plots. Treatments applied to the paved plots are listed in Table 1 and the runoff results presented in Table 2.

In May 1968 a sheeting of 30-mil chlorinated polyethylene was installed on Plot L-1. The sheeting was laid in strips 4 ft wide and the laps solvent welded. The underlying asphalt basecoat was in excellent condition at the time of installation. Heating of the polyethylene by the sun softened the asphalt, and the sheeting is now partially bonded to the soil. To date there has been no evidence of asphalt migration through the sheeting. Since installation, the treatment has averaged 101% runoff.

Runoff from Plot L-4, 15-mil butyl sheeting averaged 94% for the year. The decrease in efficiency of the plot is apparently

caused by increased wrinkling and the development of some small holes.

Runoff from the two-phase asphalt treatment, Plots L-5 and L-6 was 99.7% and 102.9%, respectively, for the year. The increased efficiency of L-6 compared to 1967 is a result of repairing the lower edge of the plot to reduce retention. The effect of plot aspect did not appear to be a factor in 1968. The vector pluviometer data shows the rainfall was essentially uniform with respect to direction. The percent of the total collected by each orifice for the storms used in the runoff analysis was: North - 23.8, East - 28.4, South - 20.1, and West - 27.7. In January 1968 a polyethylene netting with 5 mm cord spacing was installed around Plot L-5 in an attempt to increase the collection efficiency of the plot. Preliminary analysis of the data indicates that the netting did not affect the quantity collected.

The runoff from Plot L-7, 1-mil bonded aluminum foil, averaged 94% runoff for the year. Water retention by surface wrinkles appears to be a significant factor with this treatment.

Plot A-1, covered with asphalt-fiberglass, was given a vinyl-aluminum top spray in January 1968 to reduce water discoloration. The coating has performed very well, and the runoff water is colorless. Runoff from the plot for the year averaged 100%.

The standard roofing covering on Plot A-1 is performing satisfactorily. During the year, it was necessary to add approximately 100 lb of rock to the surface to cover spots where the rag felt base was showing through. Runoff measured from the plot averaged 96%. Runoff during the summer months was not measured because of construction at the site. Runoff for the summer months would be less than that measured for the winter months because of evaporative losses from the water retained in the gravel.

Bare Soil Plots. The bare soil plots include all treatments where soil is not completely covered or paved. A description of

these treatments at the Granite Reef site is presented in Table 3 with runoff data listed in Table 4.

Ridge-and-furrow Plot R-2, with 10% side slope, averaged 26% runoff in 1968. Plot R-1, with 20% side slope averaged 23% runoff. For the years 1965 through 1968 Plots R<sub>1</sub> and R<sub>2</sub> averaged 35% and 34% runoff, respectively. It must be concluded that there was no significant difference in runoff between 10% and 20% slopes on these plots.

Ridge-and-furrow Plot R-4, treated with sodium carbonate in May 1966, averaged 34% runoff for 1968. This is 7% more runoff of total rainfall than was obtained from a similar Plot R-2 that had not been treated with salt. Using runoff from R-2 as a base, runoff from R-4 was 148% in 1966, 138% in 1967, and 125% in 1968. Although effectiveness is declining, the salt treatment is still causing some increase in runoff.

Watershed W-3, hand-cleared of brush in 1963, gave 27% runoff in 1968, compared to an average of 19% runoff from Watersheds W-1 and W-2 which are still covered with scattered brush. For the years 1964 through 1968, W-3 has averaged 30% runoff while W-1 and W-2 averaged 21%. W-1 and W-2 have no channel losses. Runoff from natural areas, including channel losses, is estimated at 5%, or 66 mm since 1963. W-3 has produced 389 mm. Cost of brush clearing was \$40 per acre. This means that water collected to date from W-3 has cost 9.5 cents per 1,000 gallons. It should be noted that W-3 produces almost no runoff from December to July. This means that increased storage requirements could offset the apparently low cost of the water collected.

Plot L-3, treated with a water repellent in August 1965, yielded 64% runoff in 1968, which is essentially identical to percent runoff in 1967. Contrary to a statement in the 1967 annual report, there is no evidence that the treatment is deteriorating. Rainfall amounts and intensities vary from year to year. Annual

runoff percentages do not consider this variation and can be misleading. The effectiveness of the water repellent on L-3 is better determined by comparison with Plot L-2, which is nearly identical except that it has not been treated with water repellent. Using runoff from L-2 as a base, runoff from L-3 was 232% in 1965, 223% in 1966, 218% in 1967, and 227% in 1968. These figures do not indicate any significant deterioration in the water repellent. Contrary to the brush-cleared watershed W-3, the water repellent plot L-3 does produce significant quantities of runoff during the January to July period. Total on-site cost of preparing and treating L-3 would be about 5 cents per yd<sup>2</sup>. Assuming 5% runoff from natural areas, L-3 has produced over 600 mm more water since August 1965 than would an untreated area. The cost of the water collected to date would be 31 cents per 1,000 gallons. Rainfall for these four years averaged 10.0 inches. At least twice as much runoff would be obtained in a 20-inch precipitation zone. These figures indicate that the water repellent treatment can produce water in a 20-inch precipitation area for less than 20 cents per 1,000 gallons.

#### PART IV. SOIL STABILIZATION

Only a small amount of exploratory work was done utilizing procedures described on pages 7-1 and 7-2 in the 1967 Annual Report and on page 7-1 in the 1964 Annual Report. Soil from a Monument Tank site was used in addition to Granite Reef soil. A brief comparison of the soils is as follows:

Soil	Chemical analysis meq/100 g			Physical analysis		
	Na	CaMg	CEC	% clay	% silt	% sand
Granite Reef	0.02	28	10	7	37	58
Monument Tank 1	0.15	14	15	16	29	55

Both soils are classified as sandy loams but they react quite differently to treatment.

Granite Reef and Monument Tank 1 soils were both made water repellent with 3% solutions of sodium methyl silanolate (SMS) alone. SMS was then mixed with emulsions containing 10% solids of polyvinyl acetate emulsion (PAE) and vinyl acrylic terpolymer (VAT) and with 2% solutions of polyvinyl alcohol (PVA) and applied to both soils. Granite Reef soil was made water repellent when these mixtures contained 3% SMS. Monument Tank 1 soil was not made water repellent until the SMS concentration was increased to 12.5% for PAE and PVA and to 25% for VAT. The reason for this is not yet known.

Granite Reef soil did not crack when treated with water repellent SMS and stabilizers PAE, VAT, and PVA, separately or in combination. Granite Reef soil was not treated with mixtures containing more than 5% SMS. Monument Tank 1 soil did not crack when treated with stabilizers without SMS, or when treated with SMS solutions up to 3% concentration. SMS solutions exceeding 3% caused Monument Tank 1 soil to crack. Adding the plastic soil stabilizers did not alleviate the cracking. Soil cracking is caused by dispersion of the soil resulting from the production of sodium hydroxide when SMS reacts with calcium in the soil.

#### SUMMARY AND CONCLUSIONS:

All previously reported operational water harvesting installations except Seneca were turned over to the respective cooperators. These catchments will be observed at periodic intervals, but further maintenance will be done by the cooperators. The two-phase asphalt pavement on the Nelson Road catchment is in good condition after 4 years with a minimum of maintenance. The Blue Mountain catchment was given a final protective spray coating of aluminized asphalt which should protect the pavement for several years if weed growth is kept under control. The Metate catchment was covered with

asphalt-fiberglass. The 20-mil chlorinated polyethylene on the Mescal and San Vicente catchments is in good condition, although there were indications that it is starting to deteriorate where stretched over small pebbles or sticks. Asphalt-fiberglass linings in the Metate and Nelson Road reservoirs, after 6 years of severe exposure, including trampling by deer and cattle, were in excellent condition.

Seneca catchment was treated in the spring of 1968 with R-20 water repellent. The grass had previously been burned off, but there was considerable moisture in the subsurface soil and heavy regrowth of grass occurred after treatment. Analysis of the rainfall and runoff data shows that measured pretreatment runoff averaged 2.1% of 500 mm precipitation for a 9-month period. Post-treatment measured runoff averaged 3.3% of 148 mm precipitation for a 7-month period. This is not a satisfactory increase in runoff. Failure of the treatment was caused by the growing vegetation and/or inadequate application of the water repellent. Reasons for the treatment failure will be investigated before the catchment is treated again in 1969.

Guthrie Peak catchment was installed 14 May 1968 in cooperation with the Bureau of Land Management. This catchment was sprayed with a low-cost, water repellent plus soil stabilizer. It will be inspected at periodic intervals to observe the performance of the treatment.

Pretreatment rainfall and runoff measurements were continued at the Monument Tank site during the year. Waterstage recorder charts have not yet been analyzed. Monthly rainfall as measured by the raingage network has approximately a 10% variation among locations which appears to be random throughout the year.

Laboratory studies with sprayable plastic soil stabilizers in combination with SMS water repellent were continued on Granite Reef

and Monument Tank soils. Both soils are classified as sandy loams, but they react quite differently to treatment. Treatment rates which were effective on the Granite Reef soil were insufficient for the Monument Tank soil. There appeared to be some masking of SMS by the soil stabilizer on Monument Tank soil that did not occur on Granite Reef soil. Increasing the amount of SMS applied caused the soil to crack because sodium hydroxide is produced when the SMS reacts with calcium in the soil.

At the Granite Reef testing site new water meters were installed on all metered plots, and the open steel collection tanks were replaced with 7500-liter covered concrete storage tanks. The evaporation study pond was reshaped to 44 × 130 ft and lined with butyl sheeting. A 10-ft deep by 18-ft diameter water storage tank was built from the sides only of a standard metal grain bin with a plastic liner. A 10 × 30 ft steel storage building was erected and rainfall runoff from the roof is being metered.

Runoff from the three plots treated with a one-phase treatment of Venezuelan asphalt in 1964 was 57 to 69%, only slightly lower than was measured the previous year. The two plots with the two-phase asphalt treatment continue to produce essentially 100% runoff 5 years after installation.

A new 20-mil modified chlorinated polyethylene sheeting was installed on an asphaltic basecoat. To date there has been no evidence of asphalt migration through the sheeting, and the catchment has averaged 101% runoff. The 15-mil butyl sheeting catchment averaged 94% for the year. Wrinkles in the butyl are causing some retention. The 1-mil bonded aluminum foil plot averaged 94%. Water retention by wrinkles is also a factor on this plot. Runoff from the asphalt-fiberglass plot averaged 100% for the year, and discoloration of runoff water has been eliminated by application of a vinyl-aluminum top spray. Measured runoff from the standard roofing catchment averaged 96%. Runoff for the summer months was

not measured because of construction at the site. Runoff for the summer months would be less than that measured for the winter months because of evaporation losses from the water retained in the gravel.

Runoff measurements from the ridge-and-furrow plots indicate there is no significant difference between 10 and 20% slopes. Runoff from a ridge-and-furrow plot treated with sodium carbonate in May 1966 was 125% of runoff from a similar untreated plot. Although effectiveness is declining, the salt treatment is still causing some increase in runoff. Runoff measurements for cleared and un-cleared watersheds show brush clearing alone has produced water at a cost of 9.5 cents per 1000 gallons. Because of essentially no runoff between December and July, the low cost of water could be offset by increased storage requirements.

Contrary to previous statements, the water repellent treatment on the 180 m<sup>2</sup> bare soil plot L-3 has not degraded. Using runoff from a similar untreated plot as a base, runoff from L-3 was 232% in 1965, 223% in 1966, 218% in 1967, and 227% in 1968. On-site costs for the treatment on L-3 are 5 cents yd<sup>-2</sup>. A similar plot in a 20-inch precipitation zone could produce water for less than 20 cents per 1,000 gallons.

PERSONNEL: L. E. Myers and G. W. Frasier

CURRENT TERMINATION DATE: December 1970

Table 1. Waterproof treatments on large plots at Granite Reef testing site.

Plot	Treatment Date	Treatment
L-1	8 Aug 1967	<u>Basecoat.</u> MC-250 at 1.5 kg asphalt m <sup>-2</sup>
	22 Aug 1967	<u>Topcoat.</u> RSK asphalt emulsion at 0.7 kg asphalt m <sup>-2</sup>
	20 May 1968	<u>Top Sheeting.</u> 30-mil chlorinated black polyethylene
L-4	30 Nov 1961	<u>Butyl Rubber Sheeting.</u> 15 mil
L-5	18 Sept 1962	<u>Basecoat.</u> S-1 at 1.04 kg asphalt m <sup>-2</sup>
	16 Mar 1966	<u>Topcoat.</u> RSK asphalt emulsion at 0.6 kg asphalt m <sup>-2</sup>
L-6	19 Apr 1963	<u>Basecoat.</u> RC-special at 1.5 kg asphalt m <sup>-2</sup>
	8 May 1963	<u>Topcoat South Half.</u> SS-2 special asphalt emulsion at 0.65 kg asphalt m <sup>-2</sup> with 3% butyl latex
	9 Jul 1963	<u>Topcoat North Half.</u> S-1 at 0.5 kg asphalt m <sup>-2</sup> with 3% butyl latex
	17 Feb 1966	<u>Top Spray.</u> Aluminum coating TS-A-1 at 0.16 kg material m <sup>-2</sup>
L-7	3 Aug 1967	<u>Basecoat.</u> MC-250 at 1.5 kg asphalt m <sup>-2</sup>
	22 Aug 1967	<u>Top Sheeting.</u> 1 mil aluminum foil bonded with RSK asphalt emulsion at 0.7 kg asphalt m <sup>-2</sup>
A-1	3 Aug 1967	<u>Basecoat.</u> MC-250 at 1.5 kg asphalt m <sup>-2</sup>
	22 Aug 1967	<u>Top Sheeting.</u> 3/4 oz chopped fiberglass matting bonded with RSK asphalt emulsion at 1.4 kg asphalt m <sup>-2</sup>
	Jan 1968	<u>Top Spray.</u> Vinyl aluminum coating at 0.1 gal yd <sup>-2</sup>

Table 1. Waterproof treatments on large plots at Granite Reef testing site - Continued.

Plot	Treatment Date	Treatment
A-2	3 Aug 1967	<u>Basecoat.</u> MC-250 at 1.5 kg asphalt m <sup>-2</sup>
	12 Sept 1967	<u>Top Sheeting.</u> Standard rag felt-rock roofing treatment

Table 2. Runoff results from rainfall on waterproof treatments at Granite Reef testing site.

Date	Total rainfall	L-1		L-4		L-5		L-6		L-7		A-1		A-2	
		runoff		runoff		runoff		runoff		runoff		runoff		runoff	
1968	mm	mm	%	mm	%	mm	%	mm	%	mm	%	mm	%	mm	%
26-27 Jan	5.1			5.2	102.0	5.9	115.7	5.2	102.1	5.6	109.8	6.0	117.8	5.1	100.0
28 Jan	0.7			0.8	114.3	0.7	100.0	0.6	85.7	0.6	85.7	0.8	114.3	0.7	100.0
9-10 Feb	9.6			9.4	97.9	10.7	111.8	10.0	104.2	9.7	101.0	10.2	106.3	9.7	101.0
12 Feb	19.3			18.4	95.3	20.8	107.8	20.2	104.7	18.8	97.4	19.6	101.7	18.9	97.9
13 Feb	11.0			10.1	91.8	11.3	103.1	11.3	102.7	10.3	93.6	10.8	98.2	10.6	96.4
14 Feb	2.1			1.6	76.2	1.8	85.9	1.8	85.7	1.7	81.0	1.8	85.7	0.9	42.9
8-10 Mar	34.2	35.0	102.3	31.4	91.9	30.7	89.8	35.7	104.4	33.4	97.6	34.9	102.0	33.6	98.2
13-14 Nov	27.2	27.3	100.5	26.3	96.7	27.2	100.0 <sup>a</sup>	27.8	102.2	25.0	91.9	27.2	100.0 <sup>a</sup>	27.2	100.0
15 Nov	8.2	7.9	96.2	5.9	72.4	8.2	100.0 <sup>a</sup>	7.6	92.8	6.9	84.1	7.3	89.0	6.5	79.3
20 Dec	5.3	5.5	104.3	4.3	81.0	5.3	100.0 <sup>a</sup>	4.5	84.9	3.8	71.7	4.8	90.7	3.5	66.0
26 Dec	18.1	18.2	100.7	18.1	100.0 <sup>a</sup>	17.8	98.3	18.8	103.9	16.4	90.8	17.5	96.7	17.0	93.9
26 Dec	9.9	10.1	102.0	9.9	100.0 <sup>a</sup>	9.9	100.0 <sup>a</sup>	11.6	117.2	9.5	96.0	9.8	99.0	10.2	103.0
Total <sup>b</sup>	150.7	104.0 <sup>c</sup>	101.1	141.4	93.8	150.3	99.7	155.1	102.9	141.7	94.0	150.7	100.0	143.9	95.9

<sup>a</sup> Meter failure, runoff estimated at 100%.

<sup>b</sup> Runoff and rainfall from period 3 July through 4 October omitted. Measurements inaccurate because of construction and leaks in storage tanks.

<sup>c</sup> Rainfall for period of treatment was 102.9 mm.

Table 3. Smooth soil treatments on large plots at Granite Reef testing site.

Plot	Treatment Date	Treatment
L-2	30 Nov 1961	Smoothed soil, 14.14 m × 14.14 m plot
L-3	4 Aug 1965	Smoothed soil, 14.14 m × 14.14 m plot treated with R-9 at 0.057 kg m <sup>2</sup>
A-3	1 Aug 1967	Smoothed soil, 6 m × 30 m plot
E-3	10 Dec 1964	Smoothed soil, 7.6 m × 15.2 m plot
W-1	1 Dec 1963	Uncleared watershed
W-2	1 Dec 1963	Uncleared watershed
W-3	1 Dec 1963	Cleared watershed
R-1	1 Mar 1965	Ridge and furrow - 20% side slope
R-2	1 Mar 1965	Ridge and furrow - 10% side slope
R-3	1 Mar 1965	Ridge and furrow - 20% side slope
R-4	13 May 1966	Ridge and furrow - 10% side slope treated with 44.9 g m <sup>-2</sup> sodium carbonate

Table 4. Runoff results from rainfall on bare soil plots at Granite Reef testing site.

Date	Total rainfall	L-2		L-3		A-3	
		runoff		runoff		runoff	
1968	mm	mm	%	mm	%	mm	%
26-27 Jan	5.1	0	0	0	0	0	0
28 Jan	0.7	0	0	0.7	100.0	0	0
9-10 Feb	9.6	0	0	2.7	28.1	0	0
12 Feb	19.3	13.5	70.1	17.4	90.3	12.7	65.8
13 Feb	11.0	2.3	21.0	6.5	58.1	2.6	23.6
14 Feb	2.1	0.4	19.2	1.0	47.6	0.4	19.0
8-10 Mar	34.2	3.9	11.4	25.7	75.1	11.3	33.2
3-5 Jul	19.0	(a)		(a)		(a)	
26 Jul	8.3						
2 Aug	8.7						
5 Aug	19.8						
6 Aug	1.5						
11 Aug	1.1						
3-4 Oct	10.8						
13-14 Nov	27.2	13.6	50.0 <sup>b</sup>	19.2	70.6	13.1	48.1
15 Nov	8.2	0.9	11.0	3.7	45.1	1.3	15.9
20 Dec	5.3	0	0	1.4	26.4	0.6	11.3
26 Dec	18.1	2.2	11.9	10.8	59.7	4.5	24.9
26 Dec	9.9	5.9	59.6	7.9	79.8	6.1	61.6
Total <sup>d</sup>	219.9	42.7 <sup>d</sup>	28.3	97.0 <sup>d</sup>	64.4	52.6 <sup>d</sup>	34.9

<sup>a</sup> Runoff and rainfall from period 3 July through 4 October omitted. Measurements inaccurate because of construction and leaks in concrete storage tanks.

<sup>b</sup> Meter error, runoff estimated at 50% from similar storms 1967.

<sup>c</sup> Storage lining damage, runoff estimated from plot W-2.

<sup>d</sup> Total rainfall for plots with omitted data was 150.7 mm.

Table 4. Runoff results from rainfall on bare soil plots at Granite Reef testing site - Continued.

Date	Total rainfall	E-3		W-1		W-2		W-3	
		runoff		runoff		runoff		runoff	
1968	mm	mm	%	mm	%	mm	%	mm	%
26-27 Jan	5.1	0	0	0	0	0	0	0	0
28 Jan	0.7	0	0	0	0	0	0	0	0
9-10 Feb	9.6	0	0	0	0	0	0	0	0
12 Feb	19.3	12.5	64.8	14.3	73.9	11.8	61.1	14.6	75.6
13 Feb	11.0	2.6	23.6	2.4	21.8	1.8	16.4	2.4	21.8
14 Feb	2.1	0.3	14.3	0.1	4.8	0	0	0.1	4.8
8-10 Mar	34.2	8.6	25.1	7.6	22.2	8.3	24.2	8.0	23.4
3-5 Jul	19.0	7.7	40.7	5.7	30.0	3.2	16.6	4.0	21.1
26 Jul	8.3	1.2	14.6	0.3	3.6	0	0	0.5	6.0
2 Aug	8.7	5.5	62.8	3.8	43.7	2.9	33.3	4.3	49.4
5 Aug	19.8	6.7	33.8	1.7	8.6	0.9	4.5	8.5	42.9
6 Aug	1.5	0	0	0	0	0	0	0	0
11 Aug	1.1	0	0	0	0	0	0	0	0
3-4 Oct	10.8	1.7	15.7	0.5	4.6	0.4	3.7	1.4	13.0
13-14 Nov	27.2	9.9	36.4	6.5	23.9	5.0	18.4	9.0	33.1
15 Nov	8.2	1.2	14.6	0	0	0	0	0	0
20 Dec	5.3	0.9	17.0	0	0	0	0	0	0
26 Dec	18.1	2.3	12.7	0	0	0	0	2.2	12.2
26 Dec	9.9	4.7	47.5	2.7	27.3 <sup>c</sup>	2.7	27.3	4.7	47.5
Total <sup>d</sup>	219.9	65.8	29.9	45.6	20.7	37.0	16.8	59.7	27.1

<sup>a</sup> Runoff and rainfall from period 3 July through 4 October omitted. Measurements inaccurate because of construction and leaks in concrete storage tanks.

<sup>b</sup> Meter error, runoff estimated at 50% from similar storms 1967.

<sup>c</sup> Storage lining damage, runoff estimated from plot W-2.

<sup>d</sup> Total rainfall for plots with omitted data was 150.7.

Table 4. Runoff results from rainfall on bare soil plots at Granite Reef testing site - Continued.

Date	Total rainfall	R-1		R-2		R-3		R-4	
		runoff		runoff		runoff		runoff	
1968	mm	mm	%	mm	%	mm	%	mm	%
26-27 Jan	5.1	0	0	0	0	0	0	0	0
28 Jan	0.7	0	0	0	0	0	0	0	0
9-10 Feb	9.6	0	0	0	0	0	0	0	0
12 Feb	19.3	11.6	60.1	12.6	65.3	13.1	68.0	10.1	52.3
13 Feb	11.0	2.0	18.2	2.2	20.0	2.1	19.3	7.9	71.8
14 Feb	2.1	0.4	19.3	0.5	23.8	0.4	18.9	0.5	23.8
8-10 Mar	34.2	4.3	12.6	6.4	18.7	4.5	13.3	9.3	27.3
3-5 Jul	19.0	(a)		(a)		(a)		(a)	
26 Jul	8.3								
2 Aug	8.7								
5 Aug	19.8								
6 Aug	1.5								
11 Aug	1.1								
3-4 Oct	10.8								
13-14 Nov	27.2	8.1	29.9	9.8	36.0	8.4	30.9	13.6	50.0 <sup>b</sup>
15 Nov	8.2	0.6	7.5	0.8	9.8	0.5	6.1	1.0	12.2
20 Dec	5.3	0	0	0.5	9.4	0.1	2.3	0.4	7.5
26 Dec	18.1	2.5	14.0	2.8	15.5	1.8	9.9	2.8	15.5
26 Dec	9.9	5.0	50.5	5.5	55.7	4.9	49.5	5.7	57.6
Total <sup>d</sup>	219.9	34.5 <sup>d</sup>	22.9	41.1 <sup>d</sup>	27.3	35.8 <sup>d</sup>	23.7	51.3 <sup>d</sup>	34.0

<sup>a</sup> Runoff and rainfall from period 3 July through 4 October omitted. Measurements inaccurate because of construction and leaks in concrete storage tanks.

<sup>b</sup> Meter error, runoff estimated at 50% from similar storms 1967.

<sup>c</sup> Storage lining damage, runoff estimated from plot W-2.

<sup>d</sup> Total rainfall for plots with omitted data was 150.7.

TITLE: MEASUREMENT AND CALCULATION OF UNSATURATED CONDUCTIVITY  
AND SOIL WATER DIFFUSIVITY

CRIS WORK UNIT: SWC W7 gG-5 CODE NO.: Ariz.-WCL 61-4

INTRODUCTION:

The objectives and need for study for this project were given in the 1961 Annual Report of the U. S. Water Conservation Laboratory. Annual Reports for 1962, 1963, and 1965 reported work concerning conductivity and soil water diffusivity measurements at several porosities and temperatures. The 1966 report concerned deviations from Darcy's law for flow of water through fine pores. The 1967 report contains data on the flow of several polar and nonpolar liquids through two ceramic plates. The purpose was to elucidate the effect of structuring of polar molecules and electrokinetic effects on flow through very fine pores. This report contains more extensive data on electrokinetic flow retardation for the same ceramic plates and for a porous glass having pores of 20 Angstrom nominal radii.

Water permeates through finely porous materials at a lower rate than is predicted by Poiseuille's law. This flow retardation has been attributed to the effect of an electric double layer that exists at a solid-solution interface. If there is relative movement between the two phases caused by pressure applied to the fluid, a streaming potential is generated that creates back electroosmotic movement to occur. The net fluid transfer is therefore less than that which would occur in the absence of the double layer. This effect has been known for well over a century and has been extensively studied (2, 3, 4).

Electrokinetic theory has been developed largely for single capillaries whose radii were so large that the effect of the double layer was not felt at the center of the capillary (2, 3). Recently Burgreen and Nakache (1) solved the electrokinetic equation for flow through a slit of any width. Rice and Whitehead (6) solved the electrokinetic equation for flow through cylindrical capillaries, valid only for low values of surface ionic potential. Street (7) showed that

the pore size distribution of a porous material could be taken into account in electrokinetic calculations.

Electrokinetic flow theory is based upon the observation that a potential  $\psi_0$  (relative to the fluid far from the solid surface) exists at the interface of a nonconducting surface and a dilute solution, whose magnitude depends upon the character of the surface and the solution. The presence of  $\psi_0$  disturbs the equilibrium ionic distribution resulting in a nonzero net electric charge at various points in the solution. This resulting ionic distribution is called the Boltzmann distribution. The net charge per unit volume  $\rho$  is given by

$$\rho = -2nez \sinh(\alpha\psi/\psi_0) , \quad (1)$$

Where  $n$  is Avogadro's number,  $e$  is the electronic charge,  $z$  is the valence and  $\alpha$  is a composite of constants. The charge density and potential are related by

$$d^2\psi/dx^2 = -4\pi\rho/D \quad (2)$$

where  $x$  is distance and  $D$  the dielectric constant. Equation (2) is combined with the hydrodynamic equations to obtain the relations which describe electroosmotic flow retardation. Davies and Rideal's (2) equation (3.23) leads to

$$\bar{u}_r = \frac{-pR^2}{8\eta L} \left( 1 - \frac{D^2 \psi_0^2}{2\pi^2 \eta R^2 (\lambda + 2\lambda_s/R)} \right) \quad (3)$$

where  $\bar{u}_r$  is the average resultant velocity in a pore,  $p$  the hydrostatic pressure,  $R$  the pore radius,  $\eta$  the viscosity,  $L$  the length of the pore,  $\lambda$  the electrical conductivity.

Equation (3) is restricted to cases where the radius of the capillary is large compared to the double layer thickness. Rice and Whitehead (6) removed this restriction and obtained

$$\bar{u}_r = \frac{-pR^2}{8\eta L} \left[ 1 - \frac{8\beta \left[ 1 - \frac{2I_1(\omega R)}{\omega R I_0(\omega R)} \right]^2}{(\omega R)^2 \left[ 1 - \beta \left\{ 1 - \frac{2I_1(\omega R)}{\omega R I_0(\omega R)} - \frac{I_1^2(\omega R)}{I_0^2(\omega R)} \right\} \right]} \right] \quad (4)$$

Where  $\beta$  and  $\omega$  are composites of constants and  $I_0$  and  $I_1$  are Bessel functions of the second kind and zero and first order respectively. This equation is subject to the restriction that  $\psi_0 < 25$  mv, because it was assumed that  $\sinh(\alpha\psi/\psi_0) = \alpha\psi/\psi_0$  in equation (1). Burgreen and Nakache (1) had previously solved the equation exactly for flow through a rectangular slit of width  $2h$ . Their result is

$$\bar{u}_r = - \frac{ph^2}{3\eta L} \left[ 1 - \frac{3\beta(1-G)^2}{(\omega h)^2(1 + I_t/I_c)} \right] \quad (5)$$

where  $G$  is an integral that must be solved numerically. Equation (5) is not restricted by the relative magnitudes of the double layer and the slit. It is, however, a continuum model and may not be valid in capillaries less than, say, 50 Angstroms.

Equations (3), (4), and (5) assume that the dielectric constant  $D$  and the viscosity  $\eta$  are constant. Furthermore, they are derived for a single capillary. In porous materials a range of pore sizes exist. The electroosmotic effect will be different for each pore size. Following the suggestion of Street (7) we can write equations (3), (4), and (5) in terms of a reduced radius and sum the electroosmotic effect over the various pore sizes. Forming the ratio

of the reduced flow velocity  $\bar{u}_r$  to the velocity if no electroosmotic effects are present we find  $\bar{u}_r/\bar{u} = R_r^2/R^2$ , where  $R_r$  is the apparent reduced radius of the pore. The resulting equations, for Davies and Rideal (DR), Rice and Whitehead (RW) and Burgreen and Nakache (BN) are for DR,

$$R_r^2 = R^2 - \frac{D_o^2 \psi_o^2}{2\pi^2 \eta (\lambda + 2\lambda_s/R)} = R^2 - 8\beta \frac{\lambda}{\omega^2 (\lambda + 2\lambda_s/R)} \quad (6)$$

for RW,

$$R_r^2 = R^2 - \frac{8\beta \left[ 1 - \frac{2I_1(\omega R)}{\omega R I_o(\omega R)} \right]^2}{\omega^2 \left[ 1 - \beta \left\{ 1 - \frac{2I_1(\omega R)}{\omega R I_o(\omega R)} - \frac{I_1^2(\omega R)}{I_o^2(\omega R)} \right\} \right]} \quad (7)$$

for BN,

$$R_r^2 = R^2 - \frac{6\beta}{\omega^2} \frac{(1 - G)^2}{1 + I_t/I_c} \quad (8)$$

where in equation (8) the electrokinetic radius  $R$  is taken as  $2h$ .

The value of  $R_r^2$  for each of the equations is now substituted into Millington and Quirk's (5) permeability calculation equation:

$$k = \frac{\theta^{4/3}}{8m^2} \left[ R_{r1}^2 + 3R_{r2}^2 + 5R_{r3}^2 + \dots + (2m-1) R_{rm}^2 \right] \quad (9)$$

to obtain

$$k_r = k - \frac{\theta^{4/3}}{8m^2} \left[ A_1 + 3A_2 + 5A_3 + \dots + (2m-1) A_m \right] \quad (10)$$

Where  $k_r$  is the reduced permeability,  $\theta$  is the porosity,  $m$  the number of pore intervals taken and, for the DR equation

$$A = \frac{8\beta}{\omega^2} \frac{\lambda}{\lambda + 2\lambda_s/R} \quad (11)$$

for RW equation,

$$A = \frac{8\beta \left[ 1 - \frac{2I_1(\omega R)}{\omega R I_0(\omega R)} \right]^2}{\omega^2 \left[ 1 - \beta \left\{ 1 - \frac{2I_1(\omega R)}{\omega R I_0(\omega R)} - \frac{I_1^2(\omega R)}{I_0^2(\omega R)} \right\} \right]} \quad (12)$$

and for BN equation, and

$$A = \frac{6\beta}{\omega^2} \frac{(1 - G)^2}{\left( 1 + I_t/I_c \right)} \quad (13)$$

Values of  $k_r$  for various solution concentrations are obtained by evaluation of equations (9) and (10) on a computer.

#### MATERIALS AND METHODS:

Two ceramic plates of nominal pore radius of  $1.5 \times 10^{-5}$  and  $5 \times 10^{-6}$  cm, and a porous glass of nominal pore radius of  $2 \times 10^{-7}$  cm were used in the experiments. The ceramic plates were epoxied into

acrylic plastic cells and the glass plate into a brass cell. The cells were connected to a constant head water source. Flow was measured gravimetrically for the ceramic plates and by an oil bubble in a calibrated capillary tube for the glass plate. Steady state values of the permeability were obtained.

#### RESULTS AND DISCUSSION:

Figure 1 shows the results of permeability measurements: A is for the porous glass (pore radius about  $2 \times 10^{-7}$  cm) whose permeability is on the order of  $6 \times 10^{-16}$  cm<sup>2</sup>; B is for the ceramic of  $5 \times 10^{-6}$  cm nominal pore size whose permeability is about  $7.8 \times 10^{-14}$  cm<sup>2</sup>; C is for the ceramic having  $1.5 \times 10^{-5}$  cm pores whose permeability is about  $2.2 \times 10^{-12}$  cm<sup>2</sup>. For the ceramic plates, B and C, the permeability increases with concentration, reaching a maximum at about 0.5 N KCl concentration. The glass permeability reaches a maximum near 0.1 N and drops off as the concentration is increased. At present only five data points are available for the glass, therefore this reduction in permeability with increasing concentration may be due to experimental error. The experiment is still in progress. Because of the few experimental points, data from the glass plate will not be used in the subsequent calculations.

In order to calculate permeability for the three plates it was necessary to obtain pore size distribution data. Figure 2 depicts the pore size distribution of the three plates; A is the glass plate, B and C are the ceramic plates. Data for curves B and C were obtained at this laboratory with a 15,000 psi mercury intrusion porosimeter. Data for curve A was furnished by a commercial company using a 60,000 psi mercury intrusion porosimeter. The pore size distributions were divided into ten intervals and the permeabilities calculated using equations (9) and (10). The ratio of the reduced permeability  $k_r$  to the permeability,  $k$ , (when no electroosmotic flow reduction took place) was formed. The experimental value of  $k$  was taken as the value of 0.5 N KCl concentration.

Figure 3 shows experimental values of  $k_r/k$  and calculated values using the three different equations for calculations  $k_r$ . All theoretical equations overestimated the permeability ratio at higher concentrations and underestimated the ratio at lower concentrations. This may be due to the value of  $\psi_0$  used in the calculations. Figure 4 shows the values of  $\psi_0$  used, as taken from Davies and Rideal (2, page 118). Equations were fit to the data in Figure 4 for use in the calculations.

The theoretical equations all assume a constant viscosity and a constant dielectric constant. Possibly these factors vary with distance from the pore wall. It may be possible to take these factors as variables in the equations. If so, this should lead to information on the structuring of water near pore walls. This point will be pursued during 1969.

Figure 3 shows that the three equations, DR, RW and BN yield similar results for the permeabilities of the two ceramics. For the ceramic with the larger pores (C) at low concentrations the DR equation deviates considerably from the more exact RW and BN equations. At higher concentrations the three equations yield identical results. Initial calculations concerning the effect of viscosity and dielectric changes will be made using the DR equation because of its simplicity. Use of the DR equation for concentrations greater than  $10^{-3}$  should lead to little error. This may not be the case for the glass plate.

#### SUMMARY AND CONCLUSIONS:

Permeabilities at various KCl concentrations were measured for a glass plate and two ceramic plates. The nominal pore radii were  $2 \times 10^{-7}$  cm for the glass and  $5 \times 10^{-6}$  and  $1.5 \times 10^{-5}$  for the ceramics. For the ceramics the permeability increased about 10% in going from a  $10^{-4}$  N KCl solution to 0.5 N KCl. The few data for the glass plate indicated a reduction in permeability with an increase in concentration from 0.1 to 0.5 N.

Theoretical calculations using three different equations did not accurately match the experimental data. The deviation is possibly due to increased viscosity near the pore walls and a change in the dielectric constant. Further calculations should clarify this point and lead to conclusions concerning the viscosity and structure of water near pore walls.

REFERENCES:

1. Burgreen, D., and Nakache, F. R. Electrokinetic flow in ultrafine capillary slits. Jour. Phys. Chem. 68:1084-1091. 1964.
2. Davies, J. T., and Rideal, E. K. Interfacial Phenomena. Academic Press, New York. 1961.
3. Elton, G. A. H. Electroviscosity I. The flow of liquids between surfaces in close proximity. Proc. Roy. Soc. London A194:259-274. 1948.
4. Henniker, J. C. The depth of the surface zone of a liquid. Rev. of Mod. Phys. 21:322-341. 1949.
5. Millington, R. J., and Quirk, J. P. Permeability of porous medici. Nature 183:387-388. 1959.
6. Rice, C. L., and Whitehead, R. Electrokinetic flow in a narrow cylindrical capillary. Jour. Phys. Chem. 69:4017-4024. 1965.
7. Street, N. Electrokinetic effects in fluid flow. Soil Sci. 105:65-66. 1968.

PERSONNEL: R. D. Jackson and F. S. Nakayama

CURRENT TERMINATION DATE: December 1970.

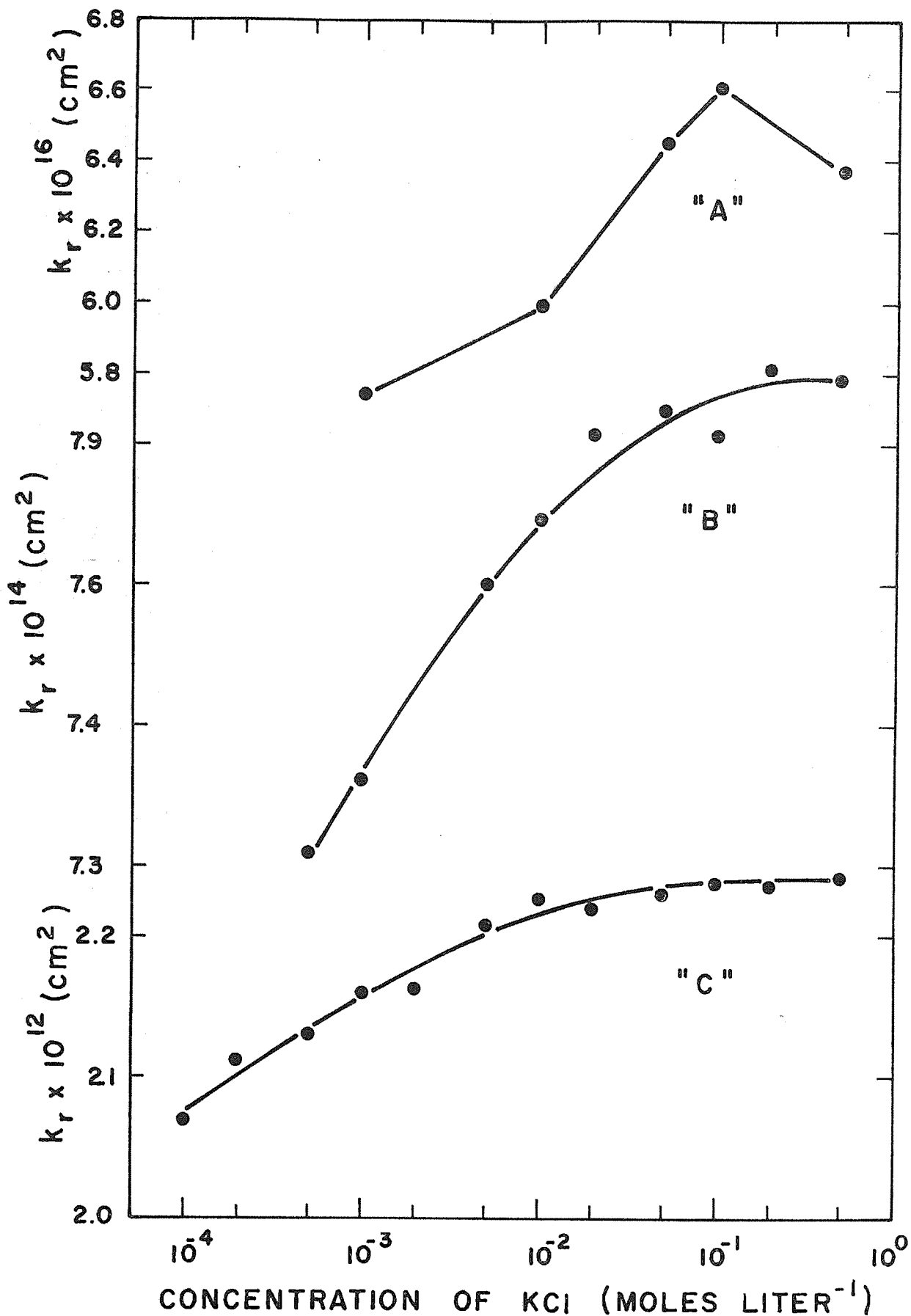


Figure 1. Permeabilities of A the glass plate, B and C the ceramic plates. Annual Report of the U.S. Water Conservation Laboratory 13-9

# FRACTION OF TOTAL PORE VOLUME

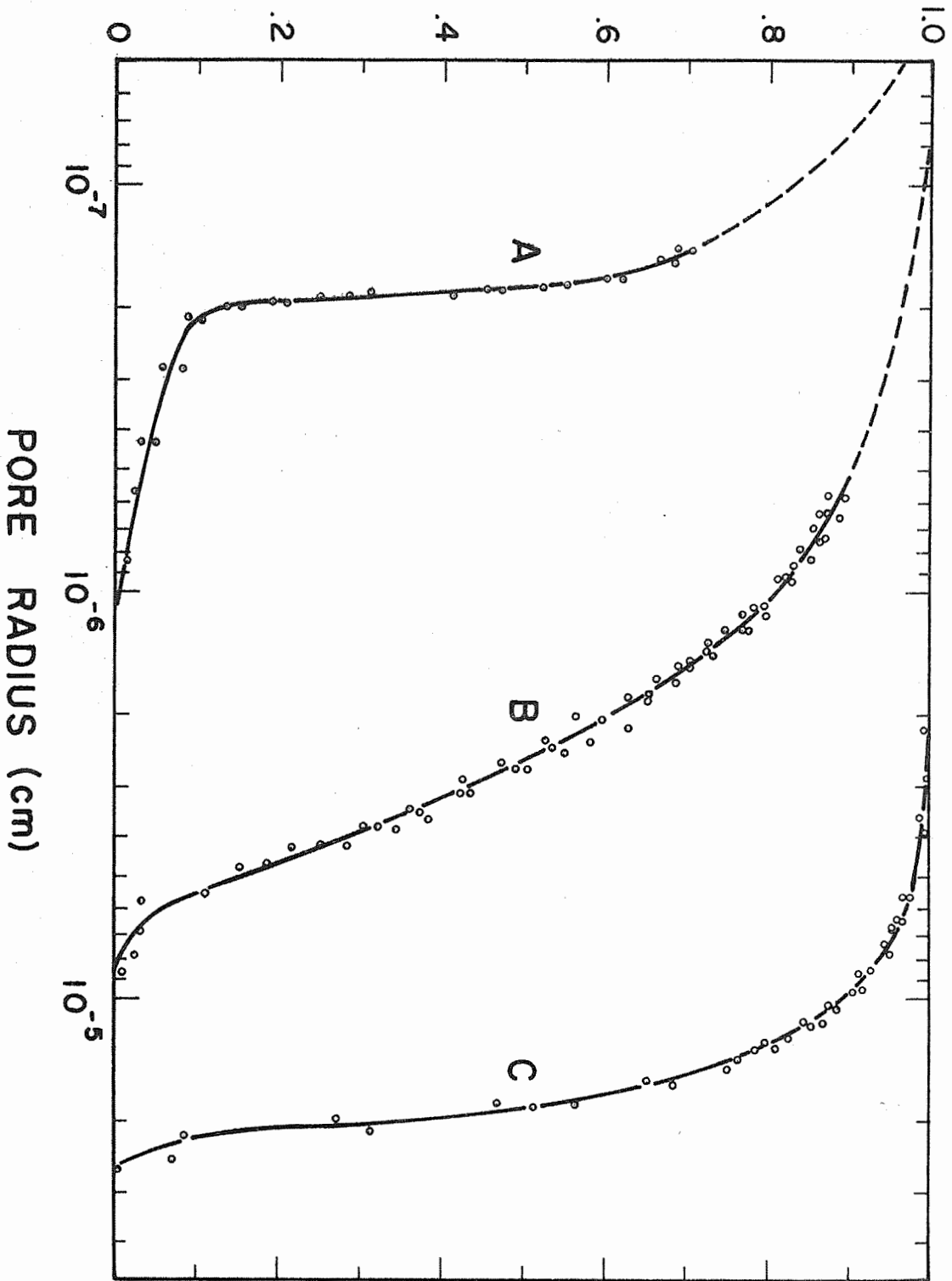


Figure 2. Pore size distributions for A, the glass plate, B and C for the ceramic plates.

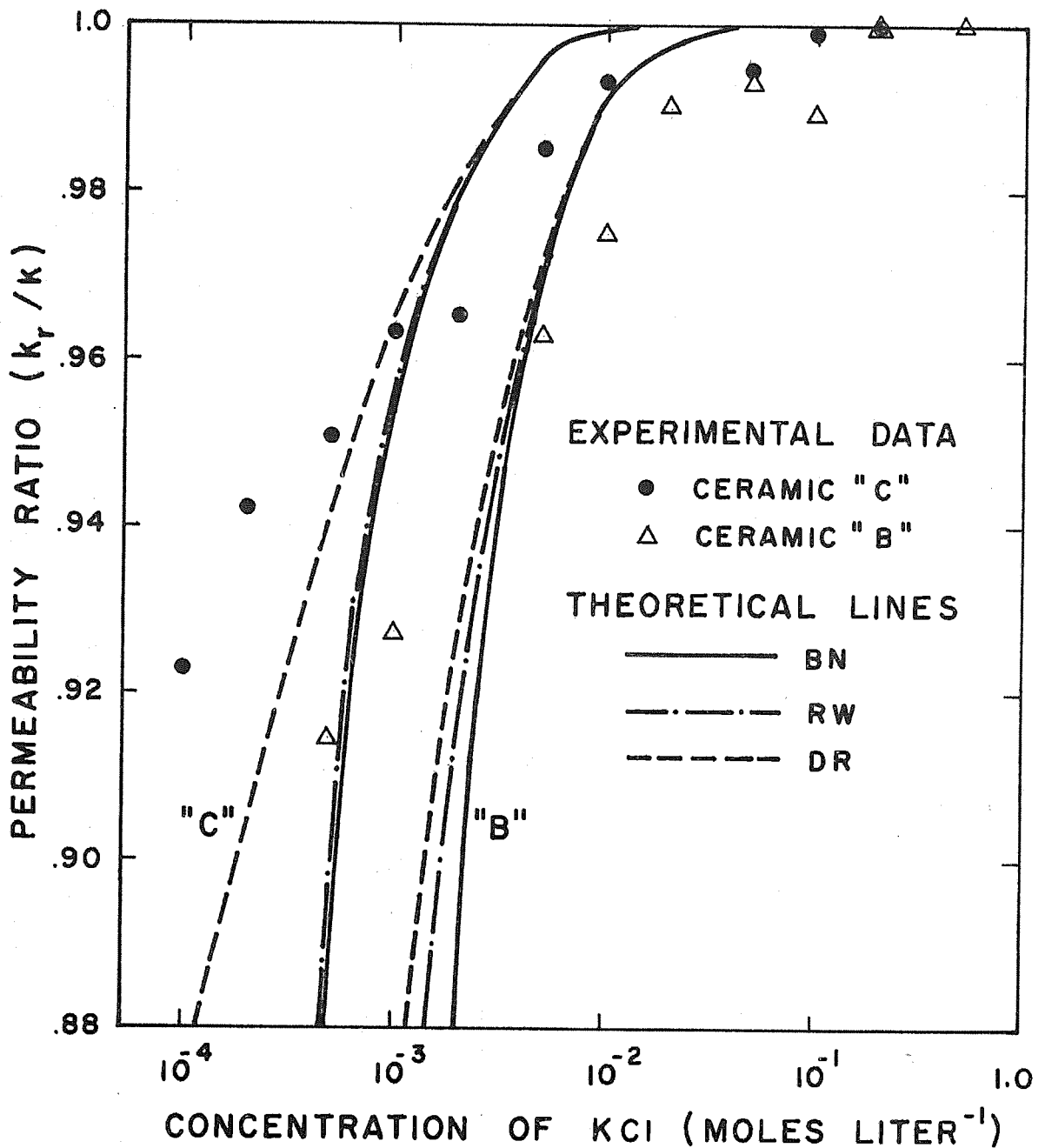


Figure 3. Permeability ratio for ceramics B and C. The solid line was calculated using Burgreen and Nakache's (1) equation, the dash-dot line from Rice and Whitehead's (6) equation, and the dashed line from Davies and Rideal (2).

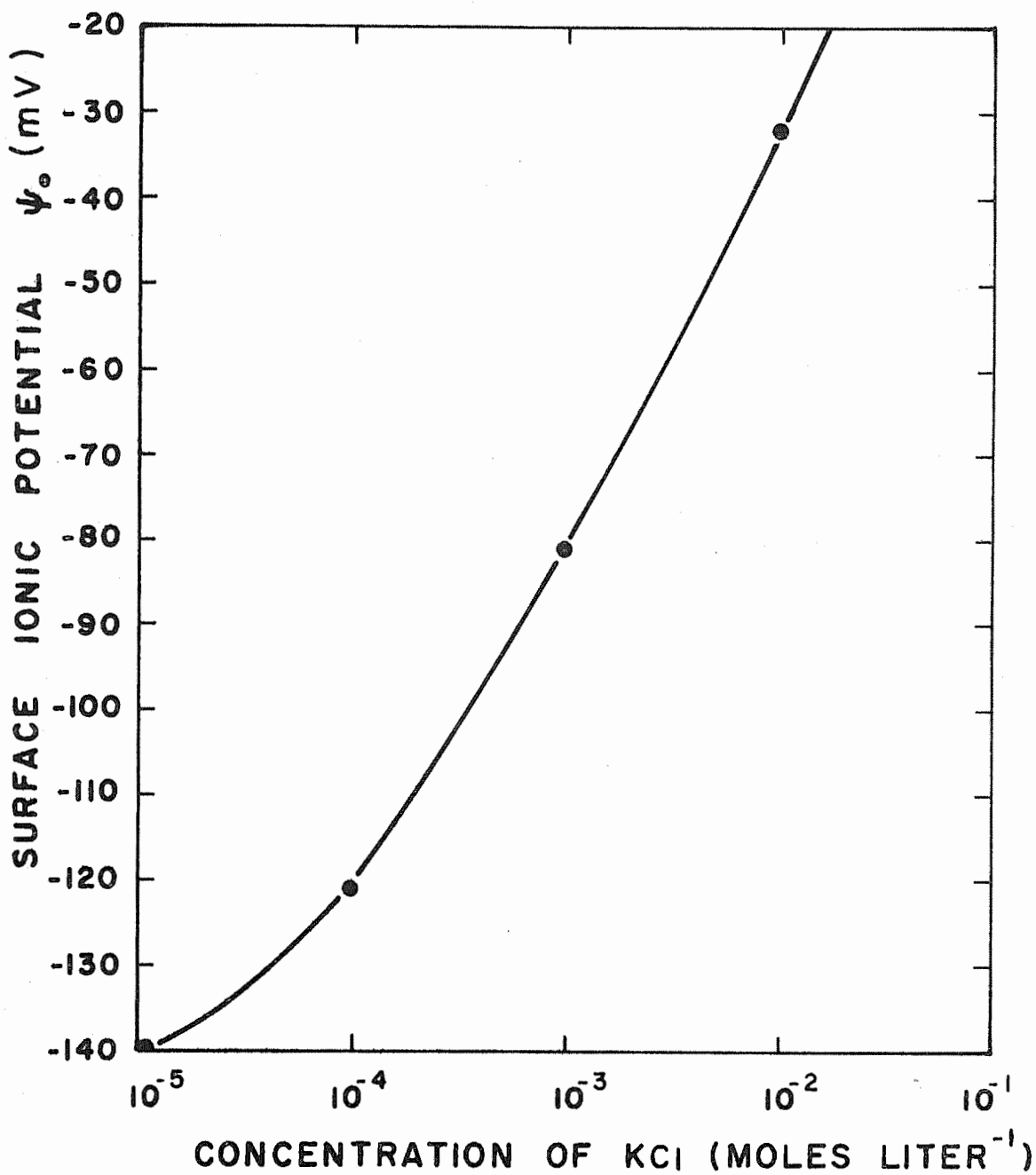


Figure 4. Surface ionic potential at several KCl concentrations, data from Davies and Rideal (2).

TITLE: CONSUMPTIVE USE OF WATER BY CROPS IN ARIZONA  
CRIS WORK UNIT: SWC W9 gG-6 CODE NO.: Ariz.-WCL 58-2

INTRODUCTION:

For need of study, see Annual Reports for 1957, 1958, and 1966. This year's report is a continuation of the study reported under Part I of the 1967 Annual Report on Ariz. WCL-23.

OBJECTIVES:

1. To correlate certain meteorological measurements with water management on cotton.
2. To check two irrigation schedules on three present-day cotton varieties.
3. To obtain data on accumulative production of blossoms, bolls, and yield on three varieties of cotton, as affected by two irrigation regimes and an early irrigation cut-off date.

PROCEDURE:

The experiment is located on Field C-1 at the University of Arizona Cotton Research Center, Phoenix, Arizona. The field was planted to cotton in 1966 and 1967, and to alfalfa during the previous two years.

Cotton stalks from the 1967 crop were plowed under, fertilizer was applied, and Arivat barley was planted. This was used as a green manure crop to iron out residual effects, as an aid in pink bollworm control, and to improve intake rates.

Urea was applied to the field on 28 February 1968, at the rate of 300 pounds per acre, and the barley was plowed under. The field was furrowed out into 40-inch furrows and the pre-plant irrigation was given on 11 March.

On 27 March, a buffer area of twelve rows of Deltapine-16 were planted, beginning on the west side of the field. After the buffer zone was planted, DpL-16, Hopicala and Pima S-4 were planted in 4-row plots in a random block design, replicated 5 times. Within each replication, there were two moisture treatments; 65% (medium)

and 50% (wet) moisture used from the top 3 ft. In addition, two more blocks of three varieties were planted for a leaf temperature study.

Timing of irrigations was based mainly on results of gravimetric soil moisture determinations and aided by visual plant leaf symptoms.

Two 30-ft lengths of row, beginning 80 ft from the north end of the field in each 4-row plot on replications 2, 3 and 4, were used for tagging of blossoms. Four 12-ft lengths of row, each comprising 16 plants, were selected and designated as quadrants 1, 2, 3, and 4. Blossoms in quadrant 2 were tagged daily throughout the flowering period.

On 15 August 1968, a border dike was built through the middle of the tagging area, across the entire study area. This was to facilitate an early season cutoff of irrigation water to the lower portion of the field. At about the same time, tagging was begun in quadrants 1 and 3, and continued in quadrant 2.

Machine-picked yield measurements were made on 80 ft of the two inside rows of the 4-row plots, on both sides of the border dike which divided the field in half, creating the areas referred to as 'upper' and 'lower'. Additional yield and boll count measurements were made on quadrants 3 and 4 tagging areas by hand picking.

Atmographs, net radiometers, anemometers and a hygrothermograph were installed in the East portion of the field on 13 June 1968.

Soil moisture depletion measurements were made in two replications of each moisture treatment for three varieties.

#### RESULTS AND DISCUSSION:

A good stand was attained, temperatures were normal through April and May and excellent vegetative growth occurred. Blossoming began around the 15th of June.

All irrigations met pre-determined levels except the July irrigation on the medium treatment. At this time, soil moisture conditions were somewhat dryer than the desired 65% level.

Insect populations were low in the early season with no noticeable damage. However, around the first of August, leaf perforators became very prevalent. The insecticide program did not control populations and because of extensive damage to the vegetative growth, all cotton was defoliated on 14 September 1968. Damage by the leaf perforators curtailed blossoming in August and September, thus affecting total yield and especially late-season set. In addition, the early defoliation made void the results of comparison between the early irrigation cutoff and normal irrigation practice.

#### SUMMARY AND CONCLUSIONS:

All final yields were affected by the leaf perforator, and it could be expected that the medium irrigation regime was damaged more than the wet treatment. Normally, the medium treatment has a heavy late-season set which did not occur this year, not only because of the leaf perforator, but because of the decision to mechanically defoliate early. It is felt that the plants were not seriously affected by the perforators until after August 18.

In Tables 2 and 4, yield data show that only minor yield differences existed between comparable irrigation treatments, though medium treatments were given two less irrigations (Table 1). The number of bolls developed from blossoms opened by August 18 (Table 3) show that only DpL-16 had more bolls on the wet treatment. On the basis of previous years' data, the medium treatment bolls could be expected to increase more than the wet, if a late season set had been possible. In Figure 4, the DpL-16 shows the beginning of a late set, but defoliation prevented maturity. Comparisons between the upper and lower field yields (late irrigation value phase of the study) are questionable because of defoliation; however, production was decreased by not irrigating in early September. Under more normal producing conditions, a greater difference could be expected.

The consumptive use figures are lower than they would have been if a full crop of leaves had been maintained. The difference in consumptive use between varieties was negligible (Table 2, and Figures 1, 2 and 3).

The efficiency of bolls from blossoms was approximately the same for the wet and medium treatments (Table 3). The weight per boll on the wet treatments showed a slight trend toward being heavier than for the dryer treatment on DpL-16 and Pima S-4 (Table 4).

Quadrant 2 was tagged during the entire blossoming season, but quadrant 3 bolls were counted but not tagged. Data shows that the total number of mature bolls was reduced in quadrant 2, but the weight per boll was increased (Table 4). Comparisons between quadrants 3 and 4 showed that the number of bolls and weight per boll were reduced by not giving the early September irrigation to quadrant 4. Figures 4 through 9 show the blossom and boll counts per day, with high efficiency early in the blossoming period and low efficiency for a 2-week period immediately after July 15, regardless of the soil moisture status. All treatments and varieties show a desirable cut-out date (before August 20), indicating that late-season sets could have been expected with desirable growing conditions.

PERSONNEL: Leonard J. Erie and Orrin F. French.

CURRENT TERMINATION DATE: December 1970.

Table 1. Irrigation Schedule for Cotton, 1968.

IRRIGATION DATES

	5/28	6/14	6/20	6/27	7/11	7/25	8/5	8/12	8/26 <sup>a</sup>
Wet	X	X		X	X	X		X	X
Medium	X		X		X		X		X

<sup>a</sup> 8/26 irrigation applied only to upper half of field.

Table 2. Yield and Consumptive Use of Water by Cotton, 1968.<sup>a</sup>

Varieties	Irrigations no.	Seed <sup>b</sup> lb/plot	Lint <sup>b</sup> %	Lint <sup>b</sup>		Consumptive Use in.
				lb/plot	bales/A	
<u>Hopi</u>						
Wet (upper)	7	48.0	39.5	19.0	3.10	38.8
Wet (lower)	6	45.1	39.0	17.6	2.88	
Medium (upper)	5	46.1	39.2	17.7	2.95	34.8
Medium (lower)	4	40.3	38.7	15.6	2.55	
<u>DpL-16</u>						
Wet (upper)	7	55.6	38.9	21.6	3.54	37.2
Wet (lower)	6	52.2	38.6	20.1	3.29	
Medium (upper)	5	53.0	39.3	20.8	3.41	32.0
Medium (lower)	4	46.3	38.5	17.8	2.91	
<u>Pima S-4</u>						
Wet (upper)	7	38.7	36.2	14.0	2.29	36.0
Wet (lower)	6	32.9	35.4	11.6	1.90	
Medium (upper)	5	38.3	35.2	13.5	2.20	31.0
Medium (lower)	4	32.4	35.8	11.6	1.90	

<sup>a</sup> All yields and consumptive use affected by early insect damage and mechanical defoliation.

<sup>b</sup> Mean, five replications.

TABLE 3. Number of Blossoms and Bolls in Quadrant Two, 1968.  
(3 replications. 16 plants/12 lineal ft per plot)

TOTAL GROWING SEASON						
	WET (7 irrigations)			MEDIUM (5 irrigations)		
	Hopicala	DpL-16	Pima S-4	Hopicala	DpL-16	Pima S-4
Blossoms	2478	2646	3125	2601	2476	2971
Bolls	796	1091	1587	842	1008	1585
Efficiency (%)	32.1	40.9	50.8	32.4	40.7	53.3
TO AUGUST 18th <sup>a</sup>						
Blossoms	2274	2534	2880	2361	2375	2734
Bolls	725	1073	1545	772	995	1546
Efficiency (%)	31.9	41.9	53.6	32.7	41.9	56.5

<sup>a</sup> Probably minimum damage by perforators, up to this date.

Table 4. Bolls and Yield by Quadrants, 1968 Season.

VARIETY	WET (7 irrigations)				MEDIUM (5 irrigations)			
	Bolls no.	Weight gm	Lint bales/A	Wt/boll gm	Bolls no.	Weight gm	Lint bales/A	Wt/boll gm
Hopicala								
q2	796	4662.0	2.85	5.86	842	4721.6	2.98	5.61
q3	852	4884.3	2.98	5.73	867	4676.5	2.95	5.39
q4 <sup>a</sup>	779	4410.1	2.68	5.65	807	4264.5	2.59	5.28
DpL-16								
q2	1091	5058.9	3.16	4.64	1008	4689.9	2.94	4.65
q3	1251	5773.7	3.61	4.59	1128	5260.2	3.30	4.66
q4 <sup>a</sup>	1122	5076.2	3.15	4.52	1092	4975.8	3.01	4.56
Pima								
q2	1587	4402.6	2.49	2.77	1585	4298.4	2.41	2.71
q3	1662	4538.5	2.56	2.73	1539	4177.2	2.34	2.71
q4 <sup>a</sup>	1536	4268.6	2.37	2.78	1482	3935.3	2.20	2.66

<sup>a</sup> q4 received 1 less irrigation in each regime.

23-8

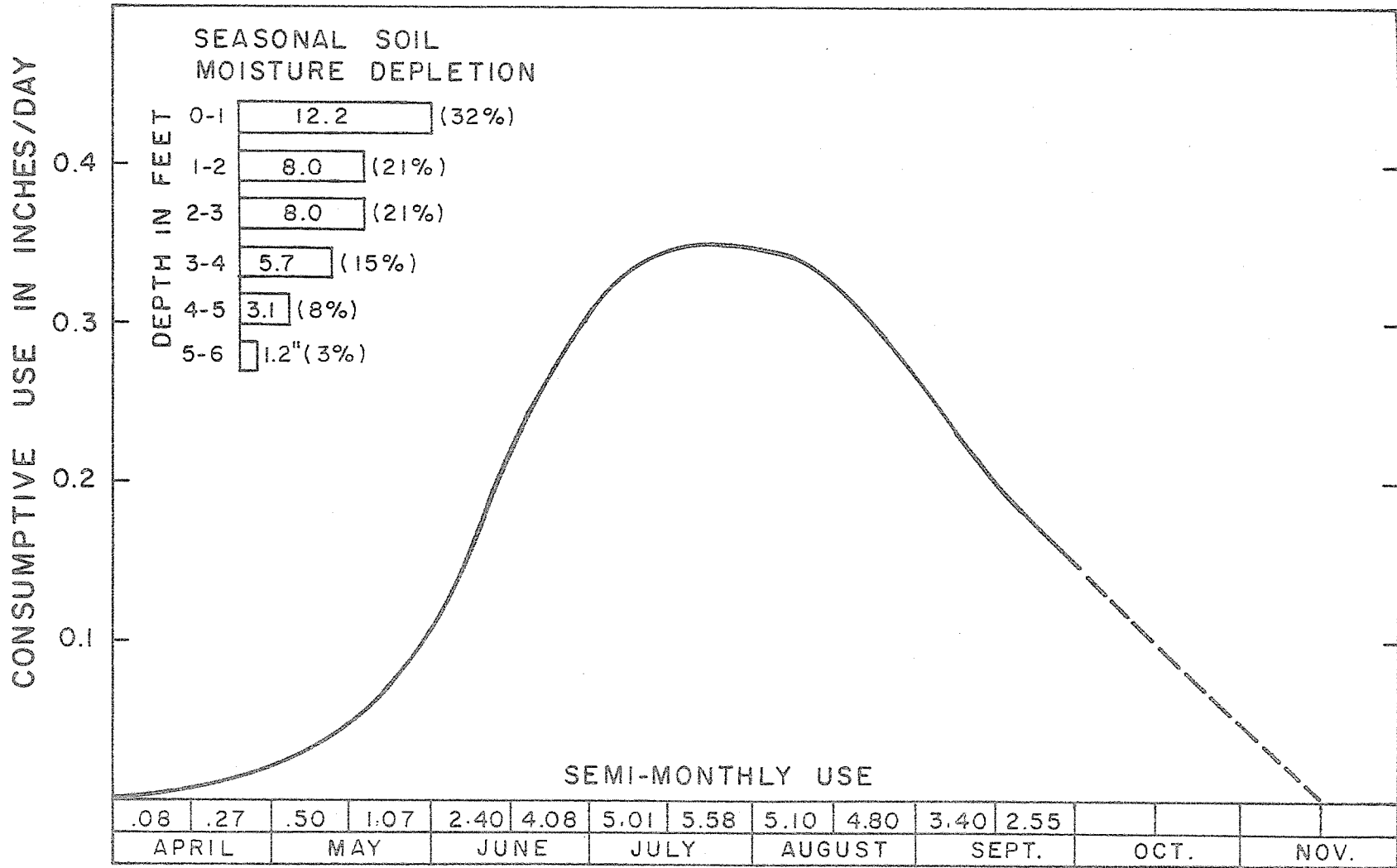


Figure 1. Consumptive use for cotton (Hopicala -- medium treatment). Phoenix, Arizona. 1968.

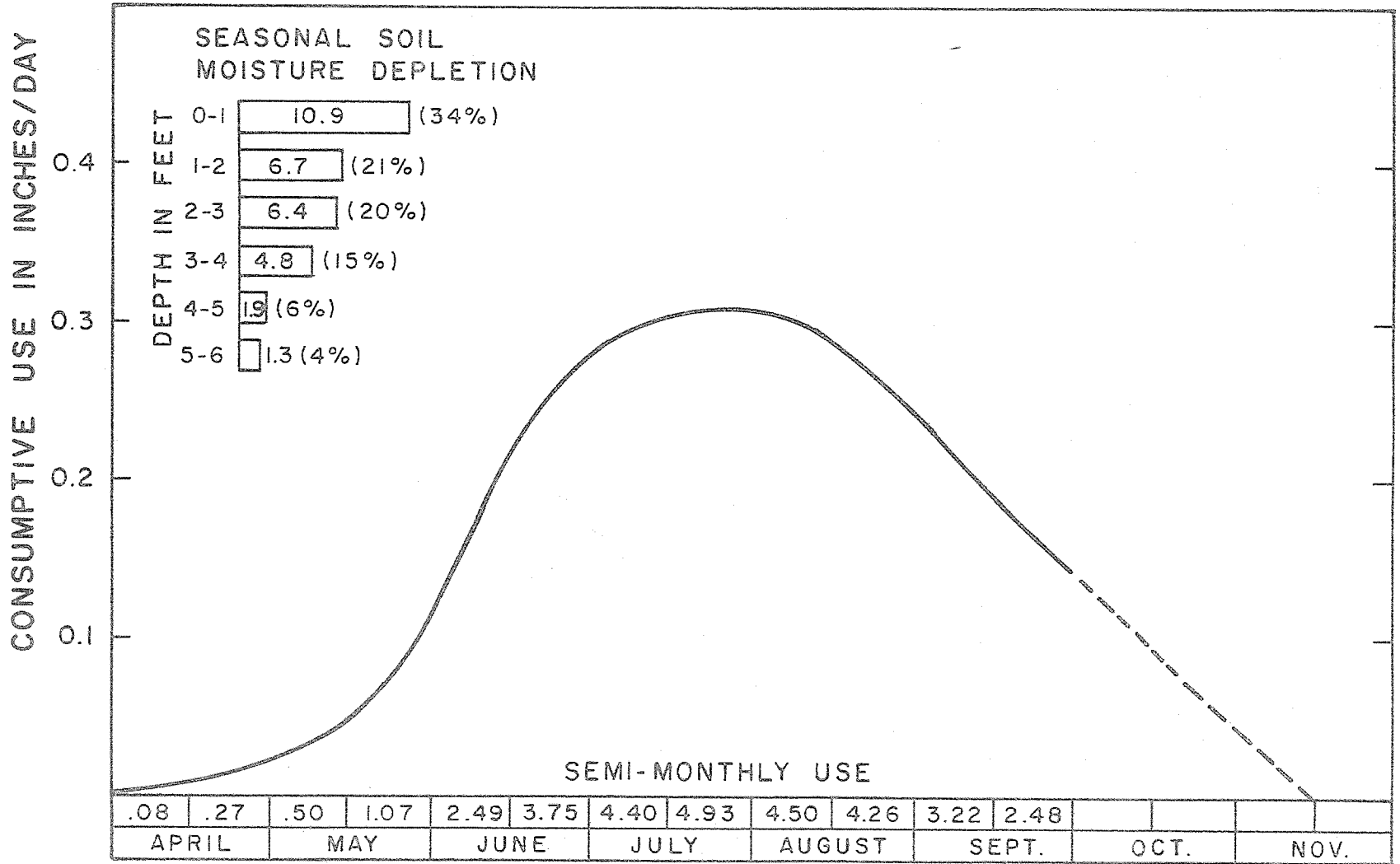


Figure 2. Consumptive use for cotton (DpI-16 -- medium treatment). Phoenix, Arizona. 1968.

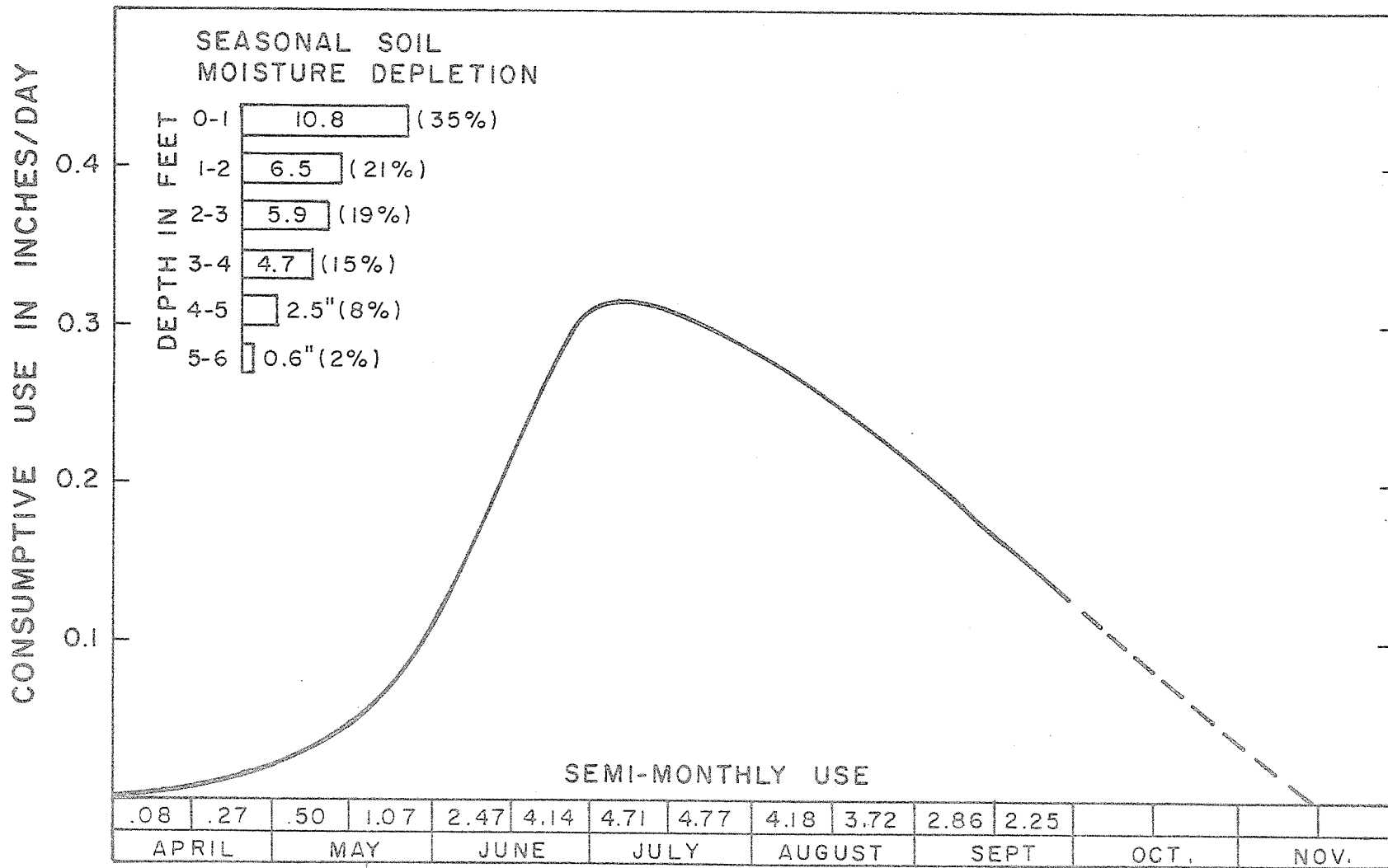
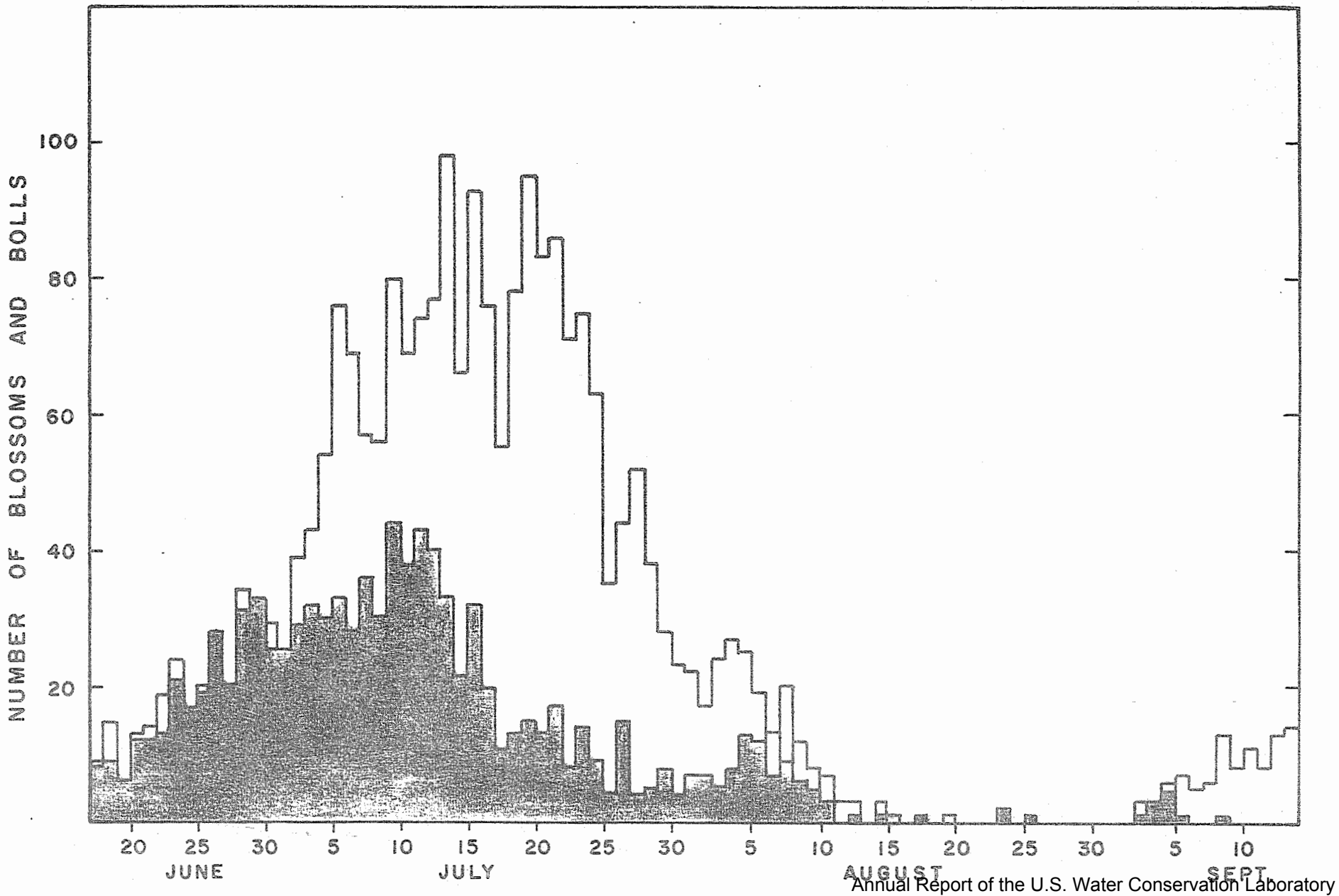
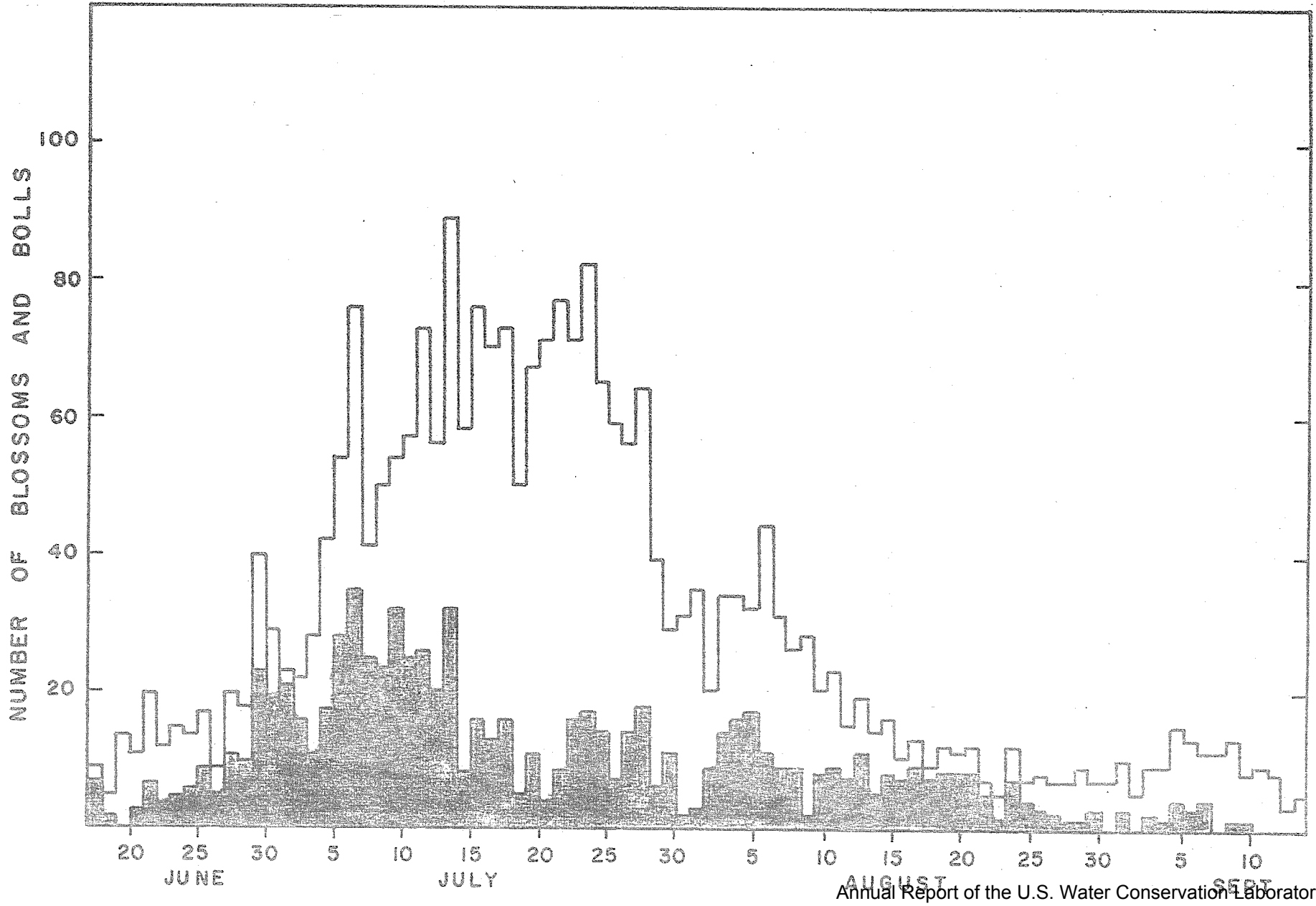


Figure 3. Consumptive use for cotton (Pima S-4 -- medium treatment). Phoenix, Arizona, 1968.



Annual Report of the U.S. Water Conservation Laboratory

Figure 4. Blossom and boll count - cotton (DpL-16 -- medium treatment). 1968.



Annual Report of the U.S. Water Conservation Laboratory

Figure 5. Blossom and boll count - cotton (Hopicala -- medium treatment), 1968.

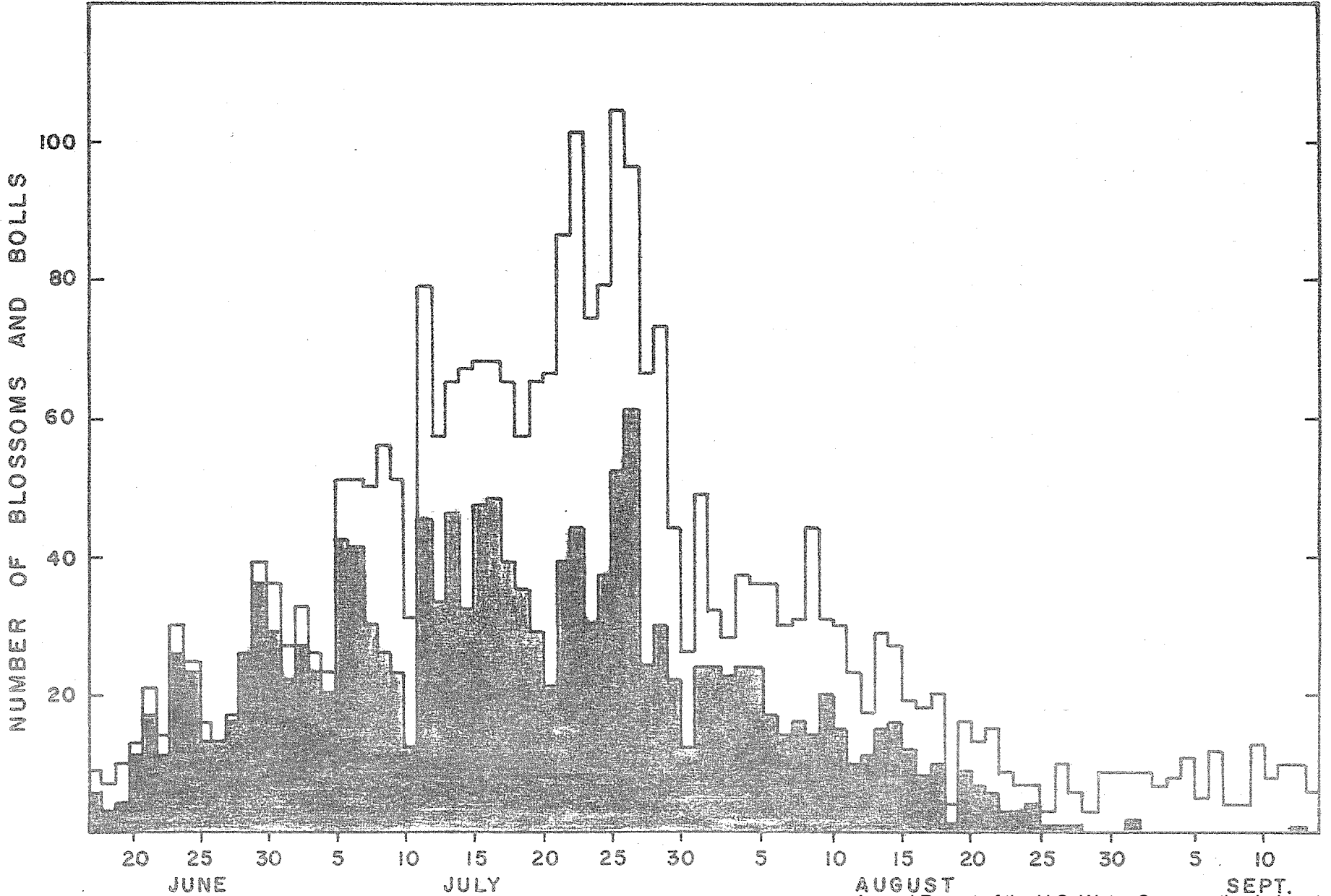


Figure 6. Blossom and boll count - cotton (Pima S-4 -- medium treatment), 1968. Annual Report of the U.S. Water Conservation Laboratory

23-15

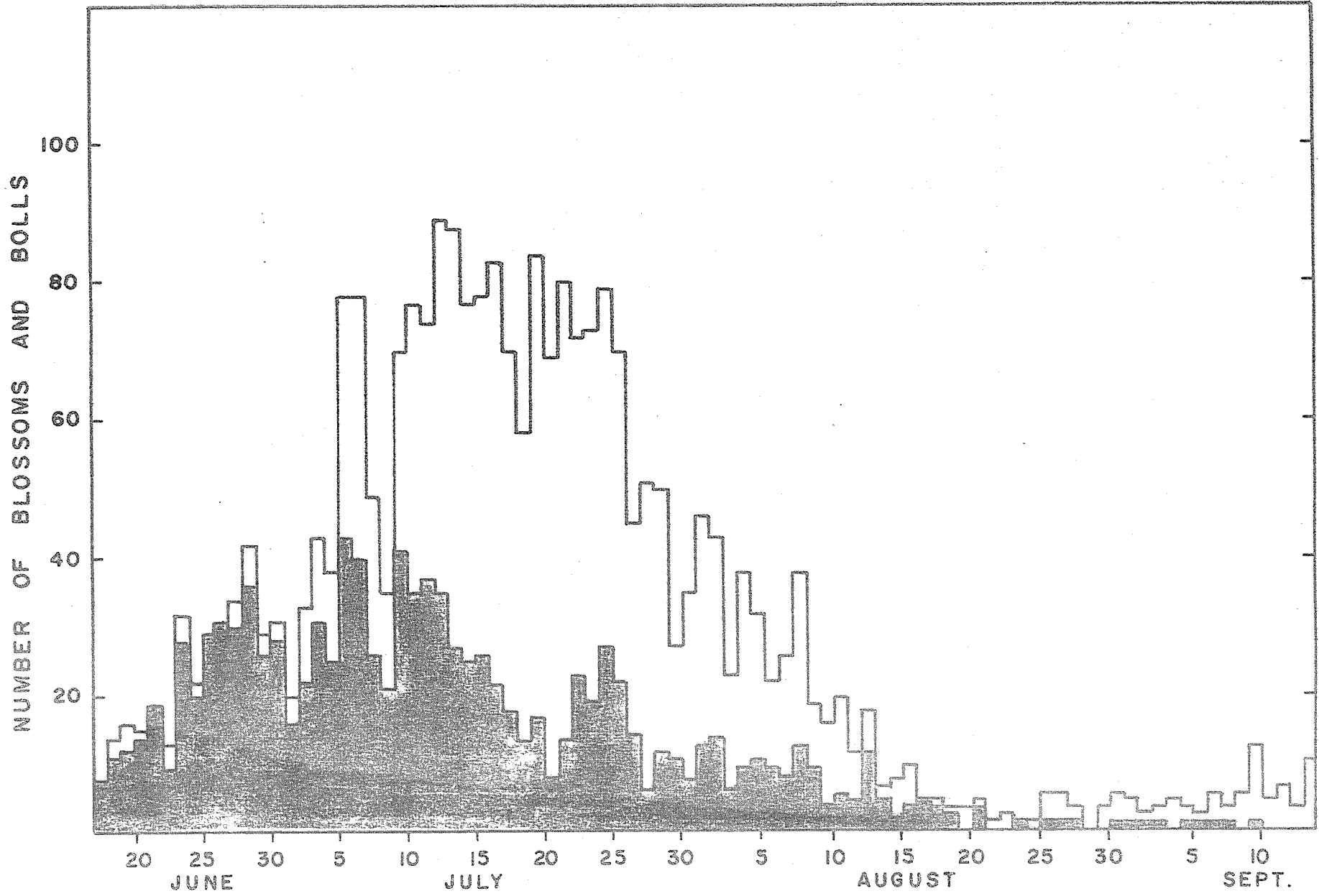


Figure 7. Blossom and boll count - cotton (DpL-16 -- wet treatment), 1968. Annual Report of the U.S. Water Conservation Laboratory

23-16

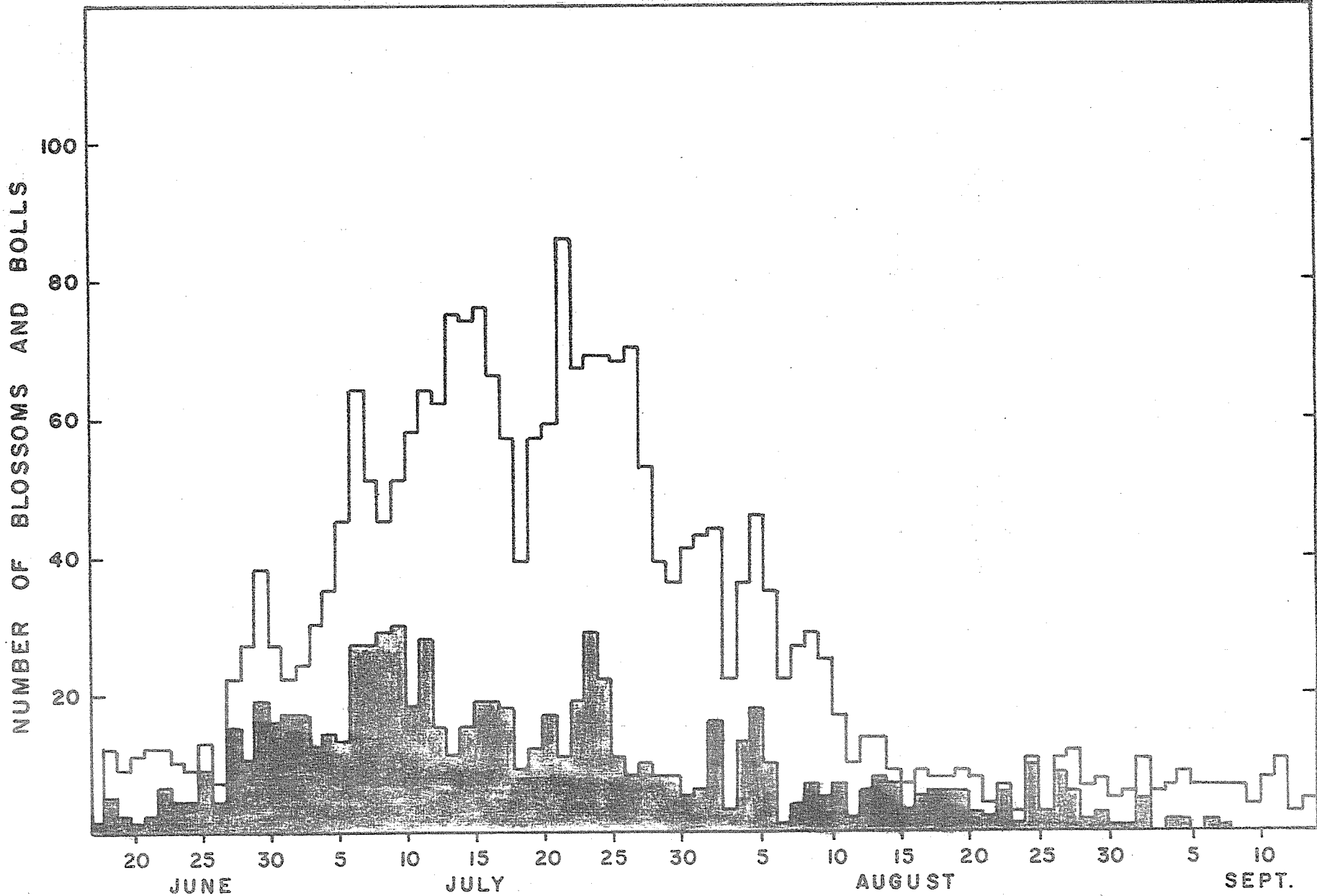


Figure 8. Blossom and boll count - cotton (Hopicala -- wet treatment) Annual Report 1968 U.S. Water Conservation Laboratory

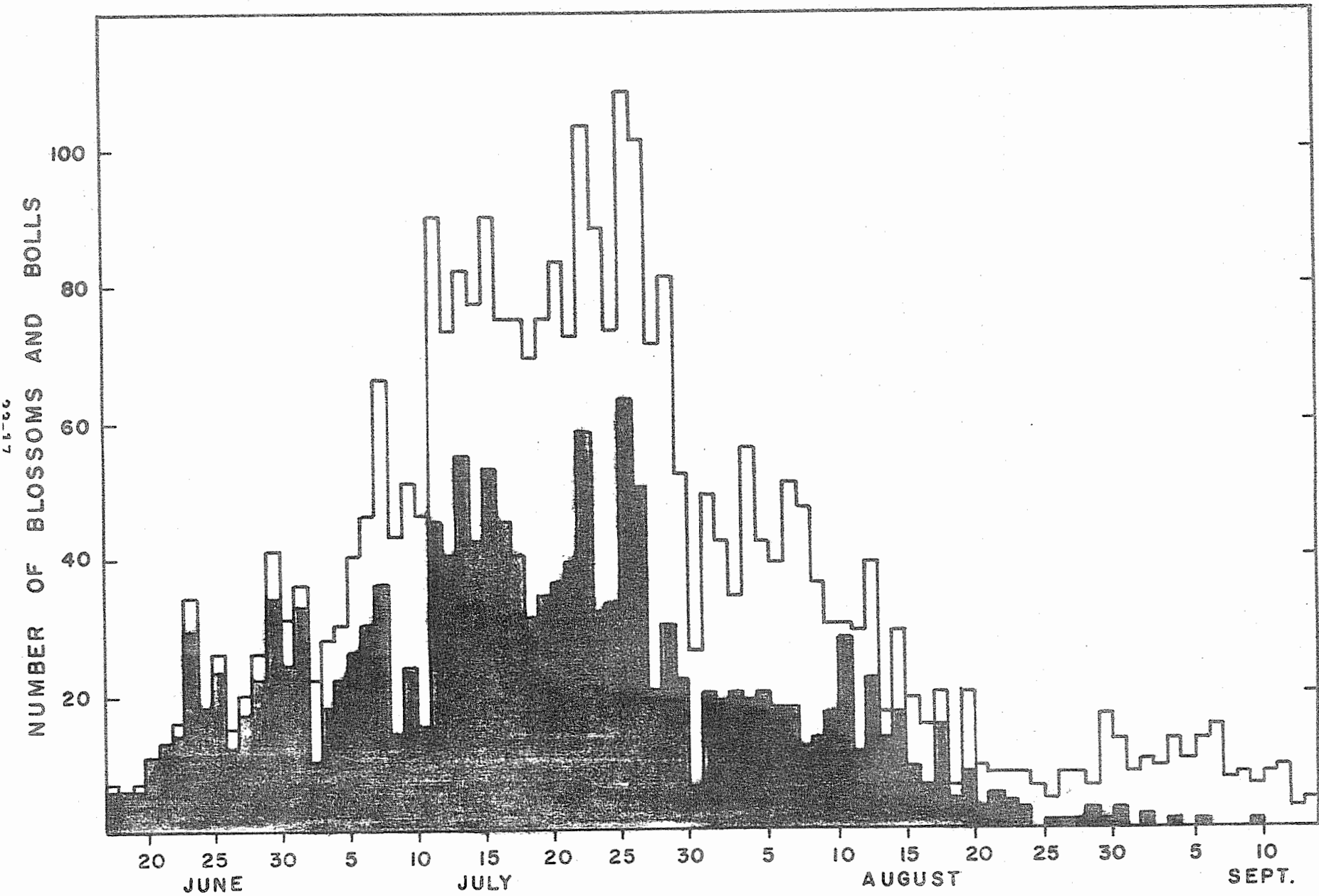


Figure 9. Blossom and boll count - cotton (Pima S-4 -- wet treatment), 1968. Annual Report of the U.S. Water Conservation Laboratory

TITLE: PLANT RESPONSE TO CHANGES IN EVAPORATIVE DEMAND AND SOIL WATER POTENTIAL, AS SHOWN BY MEASUREMENTS OF LEAF RESISTANCE, TRANSPIRATION, LEAF TEMPERATURE AND LEAF WATER CONTENT.

CRIS WORK UNIT: SWC W9 gG-6 CODE NO.: Ariz.-WCL 62-10  
PART I. A FIELD STUDY OF COTTON GROWTH AS AFFECTED BY IRRIGATION FREQUENCY.

#### INTRODUCTION:

At this Laboratory previous field experiments have shown that stomatal closure eventually occurs in response to soil water depletion. However, a sufficient plant reaction to bring about a 50% reduction in transpiration does not occur until far into a drying cycle - about thirty days for alfalfa and sorghum, for example. Although stomatal closure can be detected at this time by measurements of leaf resistance ( $R_L$ ) or a rise in leaf temperature ( $T_L$ ), it is likely that growth reduction already has occurred. Therefore, an irrigation guided by criteria of changes in  $R_L$  or  $T_A$  may be too late to maintain a rapid growth rate. In view of this delayed plant indicator response, attention was focussed on direct measurements of plant growth, to determine if there were differences in the growth rate of cotton plants subjected to three irrigation frequencies. The hypothesis was that various aspects of plant growth might be more sensitive indicators of the need for irrigation than changes in  $R_L$  or  $T_A$ .

#### PROCEDURE:

Growth was measured in three ways: (1) by periodically determining the leaf area index (LAI), defined as the leaf area corresponding to a given area of ground, and primarily a function of the growth in fresh weight of the leaves, (2) by documenting the increase in total dry weight of the plant per unit ground area, which is an indirect measure of net photosynthesis, and (3) by measuring the rate of height increase of the crop, a function of cell turgor

pressure that is quite sensitive to soil water depletion.

The study was carried out in conjunction with the field experiment of L. J. Erie, reported as WCL 58-2 of this report. A 9-acre field (C-1 of the University of Arizona Cotton Research Center), consisting of 184 north-south rows with 40-inch spacing, was divided into blocks for irrigation at different frequencies. The medium treatment, the one recommended for maximum lint production, was irrigated when the available soil water in the upper three feet of the soil was 65% depleted, as measured by gravimetric soil sampling. The wet treatment was irrigated when only 30% of the available water was depleted. There were five 4-row replications of both these treatments for each of three cultivars of cotton: Deltapine-16 and Hopicala, both a type of short-staple cotton (Gossypium hirsutum), and Pima S-4, a long staple cotton (G. barbadense). Later in the season another block (12 rows) was designated the dry treatment, in which the irrigation normally scheduled was delayed until  $T_L$  rose several degrees above air temperature and the plants showed a visible wilt. Data on the time of irrigation, the degree of soil water depletion in response to different irrigation frequencies, amount of flowering and boll set, as well as lint yield, can be found in L. J. Erie's report, referred to above.

The LAI was measured by cutting off at ground level the four plants that occurred in 1 m of row length (in a stand of about 17,000 plants per acre). Since the rows were virtually 1 m apart, the results were valid for  $1 \text{ m}^2$  of ground area. After being cut off, the plants immediately were placed in large polyethylene bags, taken to the laboratory in less than five minutes, and quickly stripped of all leaf blades; care was taken to minimize transpiration during leaf removal. After the leaf fresh weight was obtained, three 0.02 subsamples of the total were removed for leaf area determination by photocopying the five to 10 leaves of a subsample and planimentering the leaf images. The principle underlying this

subsampling procedure is that leaf area is linearly related to fresh weight, a relation that was verified directly from field data for Deltapine-16 on 23 July. It was assumed that the linear relation held for the whole sampling period, and also was valid for Hopicala and Pima S-4.

The LAI was determined on four dates encompassing the active growing period only for Deltapine-16 (medium treatment); the most comprehensive information was obtained on the last date, 06 August, at which time data were obtained for all three cultivars and the three treatments. At this time the canopy was complete and there was no significant leaf loss due to senescence or insect damage. After the LAI measurements were finished, all Deltapine-16 plant material harvested from the square meter of ground was dried in a forced draft oven at 70 C at each of the four times mentioned previously and on two additional dates, the last of which was on 20 August. Only four harvest dates were used for Hopicala and Pima S-4.

Height measurements of the crop were taken five times during the season, beginning on 16 July and ending on 03 September. The readings were obtained by a visual sighting along the top of the canopy from the observer's position near the northern edge of the field to the measuring stake 10 m away, located in a fixed position and graduated in 10-cm increments. There was a measuring stake for each of the three treatments and for each cultivar, making a total of nine reference sites. Sighting along the top of the canopy from three different positions gave a reasonable measurement of the average height of the crop as a whole, a value that is believed to be equivalent to numerous height measurements of randomly selected plants.

Accompanying the height measurements was an estimate of the average distance between rows, to assess the rate of lateral spread of the plants with time - an indirect evaluation of axillary growth

rate.

#### RESULTS:

Table 1 shows the LAI at a time when the crop had achieved full cover, but before any significant leaf senescence had occurred. The data are the mean of two replications for each cultivar, each replication in turn consisting of duplicate or triplicate subsamples. The subsamples agreed to within 15%, but the replicates only to within 50%. In view of such variation between replicates, no significance can be attached to small differences shown in the table. Therefore, the approximately 20% greater LAI for the "medium" than for the "wet" or "dry" treatments may not be significant. However, the considerably smaller LAI of Pima S-4 than of the two short staple cultivars seems to be a real difference, and also is consistent with the height data for this same date, 06 August. It appears that different irrigation scheduling does not significantly change the final LAI from a characteristic value for either long or short staple cotton. For the plant population cited, this characteristic value tends to be about 3 for short staple (Deltapine-16 and Hopicala) and only slightly above 2 for Pima S-4.

The dry weight data in Table 2 represent the total above-ground production of plant material in grams per square meter of ground area, given as the mean of two replications. Multiplying this figure by 10 gives the production in kg/hectare. The total dry weight should be highly correlated with the photosynthetic capacity of the crop. The dry weight yield does not necessarily correlate with the lint yield, however. The six harvests for Deltapine-16 "medium" show the typical sigmoid growth curve, which peaked on 13 August. The "wet" treatment produced similar yields to the "medium." Of interest is the spurt in growth shown by the "dry" treatment late in the season, undoubtedly caused by the irrigation that alleviated the considerable drought stress. The yield of

Pima S-4 also showed this effect of stress, where the "dry" treatment caused the least early growth, but ended up with the greatest dry weight by 20 August. For Hopicala there was no clear effect of treatment on dry weight production throughout the period.

In Table 3 it can be seen that for Deltapine-16 "dry" treatment the height growth consistently was less than that in the "wet" and "medium" treatments; these latter two treatments probably were not significantly different from each other. This pattern held until 03 September, at which time the height was essentially the same for all three treatments.

In Hopicala, in contrast, the heights were greater as the treatment had more moisture, for every harvest except the last. At the last harvest, on 03 September, the "medium" treatment was the shortest.

In Pima S-4 there was a trend for the "dry" treatment to cause the least height growth, but again at the last harvest the "dry" treatment height ended up essentially equal to that of the other treatments.

Summary and Conclusions. Although a lack of soil water brought about considerable height reductions in the "dry" treatment as compared to the "wet" and "medium" treatments, in both Deltapine-16 and Hopicala, a delayed spurt of growth by plants in the "dry" treatment canceled the early difference. Although not so pronounced, the same behavior was evidenced in regard to dry weight accumulation. It is concluded that a soil-induced internal water deficit in the cotton plant does not seriously interfere with the final dry weight and plant height, since compensatory growth makes up for the initial growth depression, once the drought is broken by an irrigation. This kind of response has been documented in the literature on a short term basis, and is attributed to an accumulation of reserves during water stress that can bring about faster-than-normal growth when the stress is removed. It is obvious, however, that the

length of the growth period after the stress is removed would have a bearing on the final yield. In certain instances a stress is bound to be detrimental to final production, since a delay in maturity can prolong the season until low temperature effects or a killing frost intervene.

PART II. THE WATER USE EFFICIENCY OF AGAVE AND OPUNTIA PLANTS  
IN THE DESERT.

INTRODUCTION:

Part III of this report cites the experimentally determined high water use efficiency of the agave (Century plant, Agave americana), as evidenced by a transpiration ratio (TR) only half as high as that of corn grown at the same time in the greenhouse. The high efficiency of agave is attributed to its behavior as a succulent, a chief feature of which is daytime stomatal closure accompanied by nocturnal opening and dark fixation of carbon dioxide. Opuntia (Opuntia Ficus-Indica, the spineless prickly pear) also is a succulent. Both species are native to an arid region of Mexico. Since the succulent nature of both these species presumably permits them to limit daytime water loss effectively, and since they are well adapted to arid conditions, agave and opuntia are likely candidates for a field test designed to find the highest possible water use efficiency in an extremely arid environment.

Accordingly, it was decided to compare the drought tolerance and measure the water use efficiency of both agave and opuntia at the Granite Reef experimental site, thirty miles northwest of this Laboratory, an area probably more arid than that of the native habitat of the two species. The objective was to measure the water use efficiency under two levels of soil water content: (a) a low level, as governed by the natural rainfall and perhaps a minimal amount of supplementary irrigation, and (b) a higher level provided by a somewhat greater amount of irrigation, sufficient to promote a rapid growth rate.

PROCEDURE:

Plots. At a level site halfway between rain gauges No.'s 18 and 19 at Granite Reef, a 12.2-m square of ground was enclosed by a redwood border. At the corners of the main plot four subplots also were bordered by redwood berms 10 cm above the ground surface, each

square subplot having an area of 1/500-hectare. Pathways allowed adequate plot separation and thus facilitated different levels of soil water content to be maintained in separate plots without mutual interference. In the center of each plot an access tube was installed to a depth of 160 cm for measurements of soil water with a neutron meter. A Young pan for measuring free water evaporation was buried in the soil in the prescribed manner at the center of the main plot.

Plants. Each agave plot has four rows of plants, the rows being spaced 1 m apart. The planting dates were 9 and 10 October 1968. Plots I and IV were planted to agave offshoots, with six plants per row, spaced equidistantly. All the offshoots came originally from the same parent plant. Those which had been maintained in the greenhouse nursery had viable roots and were placed in the third and fourth row. However, those taken from the parent plant and stored in the greenhouse without soil had no functional roots, and were segregated by being placed in the first and second rows of the two subplots. The agave transplants were less than six months old, and had from six to 12 leaves, none longer than 40 cm. The fresh weight of the offshoots ranged from 208 to 4,110 g, averaging 1,100 g. The plants were grouped into matched pairs not differing in weight by more than 20%. Then each member of the pair was put in the corresponding location in plots I and IV.

The opuntia stem segments came from one parent plant. Of the total of 12 plants per plot, 10 were rootless cuttings. The other two had been rooted earlier in the year. The plants were placed in four rows 1 m apart, and at a spacing of 1 m between plants. The rooted cuttings were the only ones having more than one stem segment, and were placed in row 4 in plots II and III. In every instance, a plant at a given location had a matched plant at the analogous location in the replicate plot.

Since part of the desired information for the transpiration ratio is the gain in dry matter, it was necessary to estimate the initial dry weight percentage of the transplants. This was done by obtaining fresh and dry weight data from three agave and two opuntia plants from the same group as used for transplanting.

Irrigation Scheduling. Since one objective was to manipulate the water use efficiency by establishing two different levels of soil water content, two irrigation schedules will be followed. When the plants become established, probably by the spring of 1969, one of the paired plots for each species will be irrigated more frequently than the other. The criteria for irrigation scheduling will be plant appearance, a difference in growth rate, if discernible, and changes in soil water tension (SWT) as inferred from changes in soil water content. In addition, tensiometers have been installed 10 cm below the soil surface in plots I and II.

The objective is to maintain a relatively low SWT in the active root zone for the "wet" treatment and a considerably higher SWT for the "dry" treatment. The range of difference in SWT between the two treatments will have to be determined by experience, but will depend strongly on the objective of keeping supplementary irrigations to a bare minimum in the dry treatment, consistent with at least a slow growth rate. In this regard, a goal to strive for in the dry treatment might be a total application of water, including rainfall of not more than 600 mm per year, provided that such a low amount could maintain at least a slow growth rate, rather than merely sustain life. If attainable, such an amount of evapotranspiration by a perennial would be as low as the values obtained for small grains growing under the low evaporative demand of early spring and for only a fraction of the year. There is reason to believe that low total water use by a succulent nevertheless could be accompanied by a rather large dry matter accumulation.

It is planned to take neutron meter readings once a week at 20-cm increments, starting at 20 cm and ending at 160 cm below the soil surface. Irrigations will be the minimum number necessary to replenish the active root zone, so as to avoid completely, or at least to minimize, deep percolation. Equipment will be obtained to permit accurate metering of water, such that as small a quantity as 10 mm can be applied rapidly and evenly to the 20 m<sup>2</sup> area of each plot.

**RESULTS:**

The data will consist of accurate measurements of all the irrigation water applied after transplanting, a record of the rainfall, as the average of the two rain gauges 20 m to the north and south of the main plot, and the total gain in dry weight over a long period, as given by an initial and a final weighing of the plant material from each plot. The length of the period will depend on the rate of plant growth. More than one harvest may be possible by thinning out plants that become too crowded.

PART III. THE TRANSPIRATION RATIO OF AGAVE AND CORN PLANTS AS  
AFFECTED BY LOW SOIL WATER POTENTIAL.

INTRODUCTION:

The transpiration ratio (TR), defined as the number of units of water transpired per unit gain in dry weight, ranges up to 1,000 or more for some plants. The lower the TR, the more efficient the water use. As water becomes more expensive, the TR will assume greater importance. In a previous greenhouse experiment the TR for corn was low, 140, but for agave (the Century Plant) only 70 over a 10-week period. This means that the agave, a succulent, was twice as efficient in its water use as corn. The lower TR of agave was associated with daytime stomatal closure and nocturnal opening, a pattern of behavior diametrically opposite to that for corn. Such daytime closure effectively reduces transpiration, but also stops the access of carbon dioxide ( $\text{CO}_2$ ) for photosynthesis. However, a gain in  $\text{CO}_2$  during nocturnal opening would help compensate for the daytime closure. Presumably the agave behaves like other succulents known to rely primarily on dark fixation of  $\text{CO}_2$ , a capability common in the Crassulaceae, a family containing many succulent species.

In the previous experiment all the plants were irrigated at a low soil water tension (SWT), 50 cb. However, in their natural habitat agaves frequently must undergo a considerable rise in SWT during extended droughts, and yet they thrive. Also, some recent work in Australia has shown a lower TR in agave subjected to a leaf water deficit than in plants with freely available water. Such an adaptation to drought makes it likely that the already low TR could be lowered even further by growing the plants in a substrate deficient in available water. Therefore, an experiment dealing with the effect of low soil water potential on the TR of agave and corn might help elucidate the relative importance of partial stomatal closure on photosynthesis and transpiration, in addition to demonstrating a method to obtain an extremely low TR. Corn represents

the normal, non-succulent plant, whose response to soil drought might be just the opposite from that of agave, in that the TR might be higher under drought.

In view of the foregoing considerations, an experiment was designed to contrast the behavior of corn (Zea mays, cv. Mexican June) and agave (Agave americana) to a low soil water potential.

#### PROCEDURE:

On 27 February 1968 six uniform agave offshoots from a plant growing out-of-doors at the Laboratory were transplanted to a standard soil mixture in 1-gallon crocks. Three pots had irrometers installed at the 6-inch depth. The soil was watered with nutrient solution in a prescribed manner (described in the Annual Report, 1967) that involved soil saturation followed by vacuum filtration to remove the excess solution. This process left the soil at a volumetric water content of 0.39, the pot capacity, at which the soil water tension (SWT) was quite low, 2 cb. Reirrigation occurred when SWT reached 20 cb, a point at which 64% of the available water had been depleted. Previous experiments in a controlled environment had shown no decrease from the potential rate of transpiration in bean and lemon until the SWT exceeded 20 cb, even under a high radiant load and evaporative demand quite similar to greenhouse conditions. Three other agave plants were partitioned into roots, leaves, and stems, and oven dried, to serve as a guide for estimating the initial dry weight of the six plants. The objective was to measure the increase in dry weight over a long period in comparison to the total transpiration, to obtain data for the transpiration ratio.

After the agave plants were well established, Mexican June corn was germinated. On 19 December the corn seedlings were transplanted, one to each of six pots, in soil irrigated in the same way as for the agaves. The three pots destined to be in the "wet" treatment had irrometers installed at the 6-inch depth. All pots had a

polyethylene cover over the soil surface to minimize soil water evaporation. During the long establishment period the agaves each added six new leaves and increased their daily transpiration from 5 to 45 g.

The corn plants now are transpiring 75 g per day. Within a few days the "dry" treatment will be started for both species. For both corn and agave the "wet" treatment will continue to be irrigated when the SWT reaches 20 cb. Corn plants subjected to the "dry" treatment will be irrigated when the SWT reaches 100 cb, this value to be determined by weight loss and knowledge of the soil water characteristic curve. Estimates of the soil water potential will be made by knowledge of both the SWT and the osmotic potential, the latter obtained from periodic measurements of the saturation extract, followed by appropriate adjustment for soil water depletion.

For agave the SWT will be permitted to attain 15 bars, since an irrigation would cause the SWT to fall to a low value and remain there for as long as three weeks, which time is a significant fraction of the contemplated 10-week duration of the "dry" treatment.

#### RESULTS:

The data will be summarized in the next annual report. In determining the transpiration ratio as affected by soil water potential, the experiment will help to answer the question of whether partial stomatal closure due to a leaf water deficit affects photosynthesis more than transpiration, and therefore takes on both theoretical and practical importance.

PERSONNEL: W. L. Ehrler

TERMINATION DATE: December 1970

Table 1. Maximum leaf area index for cotton in the field  
 (on 06 August 1968) in response to irrigation frequency.

Crop	<u>Treatment</u>			Mean
	Wet	Med.	Dry	
Deltapine-16	2.8	3.2	2.9	3.0
Hopicala	3.4	3.3	3.2	3.3
Pima S-4	2.0	3.0	1.8	2.3
Mean	2.7	3.2	2.6	

Table 2. The dry weight accumulation in cotton, in response to irrigation frequency.

<u>Dry Weight Yield in Grams Per Square Meter of Ground Area</u>						
<u>Treat-</u> <u>ment</u>	<u>16 July</u>	<u>23 July</u>	<u>30 July</u>	<u>06 Aug</u>	<u>13 Aug</u>	<u>20 Aug</u>
<u>Deltapine-16</u>						
Wet	-	-	706	760	951	670
Med.	412	482	544	781	1086	955
Dry	-	-	574	741	790	1568
<u>Hopicala</u>						
Wet	-	-	-	736	1044	1036
Med.	-	-	-	738	1046	784
Dry	-	-	-	714	838	976
<u>Pima S-4</u>						
Wet	-	-	-	521	690	774
Med.	-	-	-	684	704	662
Dry	-	-	-	432	646	960

Table 3. The rate of height increase in cotton in the field in response to irrigation frequency.

<u>Height in cm</u>						
Treat- ment	16 July	23 July	30 July	06 Aug	03 Sept	
<u>Deltapine-16</u>						
Wet	110	120	117	110	95	
Med.	107	118	112	100	100	
Dry	85	90	95	80	100	
<u>Hopicala</u>						
Wet	133	148	145	145	140	
Med.	128	138	135	137	120	
Dry	113	120	120	120	150	
<u>Pima S-4</u>						
Wet	87	100	105	110	120	
Med.	90	112	107	105	105	
Dry	80	87	82	80	110	

TITLE: CLAY DISPERSANTS FOR THE REDUCTION OF SEEPAGE LOSSES  
FROM RESERVOIRS.

CRIS WORK UNIT: SWC W7 gG2 CODE NO.: Ariz.-WCL 64-3

INTRODUCTION:

Water loss observations and soil and water analyses were made during 1968 on three ponds treated with sodium carbonate to reduce seepage. Two other tanks were treated to reduce seepage.

Dick Mason. This pond had a pretreatment seepage rate of 120 mm/day. In August 1962 the pond was treated with tetrasodium pyrophosphate at the rate of 7000 lb/acre. The treatment failed after about 20 months and the pond was retreated in July 1965 with sodium carbonate at the rate of 5500 lb/acre. Both treatments were aimed at establishing an exchangeable sodium percentage (ESP) of 15 in the top 10 cm of soil.

House Mountain Pond No. 1. The pretreatment seepage rate on this pond is unknown, but was estimated to be between 50 and 100 mm/day. In July 1963, the pond was treated with sodium carbonate at the rate of 8000 lb/acre (a design ESP of 15 in the top 10 cm of soil). A low seepage rate after treatment (3 to 4 mm/day) persisted for nearly 3 years, but then started to increase (7 mm/day). In November 1966 200 lbs of sodium carbonate and 300 lbs of sodium chloride were broadcast in the pond water for a "booster shot" to try and restore a low seepage rate.

Swan Lake. In May 1967 this pond was treated with sodium carbonate at the rate of 2400 lbs/acre (a design ESP of 15). The pretreatment seepage rate varied from 475 mm/day at a water depth of 700 mm to 180 mm/day at the 400-mm water depth. Seepage was reduced to 52 mm/day which was still too high. In November 1967, additional sodium carbonate was broadcast on the soil in a band around the bank of the pond between the 520- and 730-cm level above the pond bottom. Water loss measurements were made during June and July 1968.

Tombstone. Two stock tanks in Tombstone, Arizona were treated in May 1968 with sodium carbonate to reduce seepage.

PROCEDURE:

See 1967 Annual Report for water loss measurement techniques on Dick Mason, House Mountain, and Swan Lake. The two tanks in Tombstone, No. 7 and No. 23, which have areas of 1.25 and 0.70 acres, were treated with 3,200 and 2,000 lbs of sodium carbonate, respectively. The salt was uniformly applied with a commercial 6-ft fertilizer spreader and mixed into the soil with an offset disk. Both implements were pulled behind a jeep.

RESULTS AND DISCUSSION:

Dick Mason Pond. At an average depth of 725 mm the seepage rate was measured at 3 mm/day during the latter part of June 1968. This same low rate persisted in October with the water depth at 250 mm. Soil water extracts taken in October are shown in Table 1. Even though sodium has been leached from the profile, the seepage loss is still low. These results verify those reported in 1967: low seepage rates can persist even at low SAR values (2 to 5). The sodium carbonate treatment on Dick Mason has now lasted  $3\frac{1}{2}$  years, whereas the tetrasodium pyrophosphate treatment lasted for about  $1\frac{1}{2}$  years.

House Mountain No. 1. Seepage losses during the latter part of June 1968 averaged 5 mm/day at an average water depth of 635 mm. Because of extremely low rainfall (117 mm) from April through October 1968, the pond went dry. Analysis of soil samples taken in October showed an ESP of 2.5 at all depths down to 60 cm. This means that the average amount of exchangeable sodium has decreased 4 to 10% since July 1967 but is still 2% greater than the original pretreatment values. Observations during 1969 should show if another booster shot will be necessary.

Swan Lake. Retreatment of the pond banks in November 1967 was successful. The total water loss (seepage + evaporation) was 14 mm/day as measured during June and July 1968 at an average water depth of

650 mm. This is a 94% reduction in the pretreatment seepage rate.

Tombstone. There is insufficient data to analyze the effectiveness of the salt treatment, but preliminary observations indicate that there is a good chance for success.

**SUMMARY:**

The use of sodium carbonate as a dispersing agent to reduce seepage on five ponds was evaluated. Although sodium is slowly being leached from the soil, Dick Mason pond still has a seepage rate of only 3 mm/day 3½ years after treatment with sodium carbonate. The original treatment of this pond with tetrasodium pyrophosphate maintained a low seepage rate for only 1½ years.

House Mountain No. 1 has a seepage rate of 5 mm/day even though the exchangeable sodium in the upper 60 cm of soil decreased 4 to 10 percent during the past year to 2.5 percent. The 500 lbs of sodium carbonate and sodium chloride added to the pond water in November 1966 has been effective in maintaining low seepage rates for 2 yrs.

Swan Lake water loss has been reduced to 14 mm/day at an average water depth of 650 mm. This is a 94% reduction in the pretreatment rate of 292 mm/day at the same depth.

Two stock tanks in Tombstone, Arizona were treated with sodium carbonate. The salt was dispensed through a fertilizer spreader and mixed into the soil with a disk, both implements pulled behind a jeep. There is insufficient data to analyze the effectiveness of the treatment.

**PERSONNEL:** Robert J. Reginato and Lloyd E. Myers.

**CURRENT TERMINATION DATE:** December 1970.

Table 1. Sodium adsorption ratio (SAR) of soil water extracts from Dick Mason pond.

DEPTH (cm)	SAR		
	DATE SAMPLED		
	11/66	10/67	10/68
5	12.0	7.7	4.8
10	11.1	6.7	1.9
22	6.2	*	*
Pond water	0.5	1.7	0.9

\* not enough extract for analysis

TITLE: WATERBORNE SEALANTS TO REDUCE SEEPAGE LOSSES FROM  
UNLINED CHANNELS AND RESERVOIRS

CRIS WORK UNIT: SWC W7 gG-2 CODE NO.: Ariz.-WCL 64-4

INTRODUCTION:

Water loss measurements were made on two ponds near Salome, Arizona, that had been treated with different waterborne sealants. See 1966 and 1967 Annual Reports for treatment details.

PROCEDURE AND RESULTS:

Pond No. 1 had a pretreatment water loss rate of  $3.00 \text{ ft day}^{-1}$  at its operating level (4.7 ft deep). It was treated with sealant 10A (a rapid setting type asphalt emulsion) in October 1966 at the rate of  $0.8 \text{ gal yd}^{-2}$ . Water loss measurements were made in May 1968 with an F-1 water stage recorder. The test was started when the water level was 0.15 ft below the spillway, and the water level decline was measured for 7 days. The water loss, seepage plus evaporation, was  $0.04 \text{ ft day}^{-1}$ , indicating a 99% reduction in the original loss rate.

Located adjacent to No. 1, pond No. 2 had an initial water loss of  $2.53 \text{ ft day}^{-1}$  at its operating level (5.5 ft deep). It was treated in May 1967 with sealant 13 MR (a slow setting type asphalt emulsion) at the rate of  $1 \text{ gal yd}^{-2}$ . The measurements taken in May 1968 started with the water level at spillway height and proceeded for 7 days. Total loss was  $0.04 \text{ ft day}^{-1}$  for a 97% reduction in the pretreatment loss rate.

Seepage reduction in ponds 1 and 2 is excellent 19 and 12 months after treatment, respectively. The sealant used on pond 2 is being manufactured commercially. Our findings from these and previous tests were used by the U. S. Soil Conservation Service to prepare a national engineering standard and specifications guide for seepage reduction with waterborne asphalt sealants.

SUMMARY:

Seepage reduction by waterborne asphalt sealants was evaluated in two ponds near Salome, Arizona. Nineteen months after treatment with  $0.8 \text{ gal yd}^{-2}$ , the original loss rate of  $3.00 \text{ ft day}^{-1}$  in pond 1 was reduced to  $0.04 \text{ ft day}^{-1}$ . Twelve months after treatment with  $1.0 \text{ gal yd}^{-2}$ , the original loss rate of  $2.53 \text{ ft day}^{-1}$  in pond 2 was also reduced to  $0.04 \text{ ft day}^{-1}$ . This posttreatment loss, which includes evaporation, represents seepage reduction in ponds 1 and 2 of 99% and 97%, respectively.

As a direct result of this research project, which included previously reported laboratory and field work, a waterborne asphalt sealant is being manufactured commercially and the U. S. Soil Conservation Service has prepared a national engineering standards and specifications guide for reducing seepage with waterborne asphalt sealants.

PERSONNEL: Robert J. Reginato and Lloyd E. Myers.

CURRENT TERMINATION DATE: December 1970.

TITLE:                   DISPERSION AND FLOCCULATION OF SOIL AND CLAY  
                          MATERIALS AS RELATED TO THE Na AND Ca STATUS  
                          OF THE AMBIENT SOLUTION.

CRIS WORK UNIT:  SWC W7 gG5                   CODE NO.:  Ariz.-WCL 64-6

PART I.  MAGNESIUM ION-PAIRS AND COMPLEXES

INTRODUCTION:

The measurement of the complexes and ion-pairs for the alkaline-earth species was extended to Mg in a manner similar to those developed for Ca reported in the 1967 Annual Report, which also included the theoretical development.

PROCEDURE:

In the case of  $MgCO_3$ , solution concentrations giving ionic strengths ranging from 0.04 to 0.15 were used. pH and Mg activity were measured after equilibrating with various partial pressures of  $CO_2$ . For  $MgCl_2$ , a 99.98%  $CO_2$  composition was used with only H activity measurements made on the equilibrium solution.

Calculation procedures follow that for the  $CaCO_3-CO_2$  system presented in 1967.

RESULTS AND DISCUSSION:

A typical set of results for a  $5.59 \times 10^{-2}$  M  $MgCO_3$  solution equilibrated with various  $CO_2$  partial pressures is listed in Table 1. The pH and  $Mg^{+2}$  activities are measured quantities, whereas  $[HCO_3^-]$  and  $[CO_3^{-2}]$  were calculated from pH,  $K_{1A}$ , and  $K_{2A}$ , and  $[MgHCO_3^+]$  and  $[MgCO_3^0]$  were estimated from the experimentally determined dissociation constants. The

$$([Mg_T]/[Mg^{+2}]-1)/[HCO_3^-] \gamma_{Mg^{+2}} \text{ versus } \gamma_{MgHCO_3^+}/(H^+)$$

relations obtained by computer calculation and which were used to calculate  $K_1$  and  $K_2$  are plotted in Figure 1 for the same set of experimental data. The linear correlation coefficient

was 0.99, which agrees well with the value of 1 predicted by theory.

The K results obtained for other concentrations of  $\text{MgCO}_3$  are presented in Figure 2. If the theory developed and the Debye-Hückel corrections were completely adequate to describe the  $\text{MgCO}_3\text{-CO}_2$  system, the pK values should be independent of the ionic strength. The results, however, show a dependency of the K's to ionic strength as described by the relation  $\text{pK}_1 = 1.31 - 3.28 \mu$ ,  $\text{p}(1/\text{K}_2) = 8.64 - 6.14 \mu$ , and  $\text{pK}_3 = 3.02 + 3.10 \mu$ . The standard free energies of formation for  $\text{MgHCO}_3^+$  and  $\text{MgCO}_3^0$  are -251.1 and -239.3 kcal per mole, respectively.

The  $\text{pK}_1$  values obtained from the  $\text{MgCl}_2\text{-CO}_2$  system are presented in Table 2.  $\text{pK}_1$  at  $\mu = 0$  is 1.27 and compares favorably with the  $\text{pK}_1 = 1.31$  obtained independently through the  $\text{MgCO}_3\text{-CO}_2$  system, using both H and Mg ion activity measurements.

## PART II. BARIUM AND STRONTIUM COMPLEXES

### PROCEDURE:

The  $\text{BaCl}_2$  and  $\text{SrCl}_2$  solutions were treated in a similar manner as the preceding  $\text{MgCl}_2\text{-CO}_2$  system.

### RESULTS AND DISCUSSION:

The measurement and computation for the dissociation constant of  $\text{BaHCO}_3^+$  and  $\text{SrHCO}_3^+$  are presented in Tables 3 and 4, respectively. The presence of  $\text{SrHCO}_3^+$  and  $\text{BaHCO}_3^+$  is apparent. The dissociation constants and free energy of formation for  $\text{BaHCO}_3^+$  are  $3.0 \times 10^{-2}$  and -276.39 kcal/mole, respectively, and for  $\text{SrHCO}_3^+$  are  $5.26 \times 10^{-2}$  and -275.25 kcal/mole.

The lower  $\text{K}_{\text{BaHCO}_3^+}$  compared to that for  $\text{MgHCO}_3^+$ ,  $\text{CaHCO}_3^+$ , and  $\text{SrHCO}_3^+$  indicates that the  $\text{Ba}^{+2}\text{-HCO}_3^-$  interaction is stronger than the  $\text{Mg}^{+2}$ ,  $\text{Ca}^{+2}$ , or  $\text{Sr}^{+2}$ . Unlike the hydroxide complexes of  $\text{K}_{\text{MgOH}^+} = 2.63 \times 10^{-3}$ ,  $\text{K}_{\text{CaOH}^+} = 4 \times 10^{-2}$ ,  $\text{K}_{\text{SrOH}^+} = 1.49 \times 10^{-1}$ , and  $\text{K}_{\text{BaOH}^+} = 2.27 \times 10^{-1}$ , the  $\text{HCO}_3^+$  complexes do not follow a definite

electronegativity pattern. The dissociation constant of the  $\text{MgHCO}_3^+$  complex is smaller than the  $\text{MgOH}^+$ , whereas that for the  $\text{SrHCO}_3^+$  and  $\text{BaHCO}_3^+$  complexes are larger than their respective  $\text{MOH}^+$  complexes.

### PART III. HYDROLYSIS OF $\text{Na}_2\text{CO}_3$

#### INTRODUCTION:

The use of sodium carbonate for pond sealing required a simple and reliable method for predicting the pH when  $\text{Na}_2\text{CO}_3$  hydrolyzes in water. At the rate of  $\text{Na}_2\text{CO}_3$  addition, the equations developed in handbooks were found to be inadequate because of the simplifying assumptions used to treat the mathematical problem. Several methods were tested to correct this shortcoming.

#### THEORY:

The analysis of  $\text{Na}_2\text{CO}_3$  hydrolysis requires a combination of the following relationships for C moles of material, depending on the method of solution used:

##### A. Mass balance

$$C = [\text{H}_2\text{CO}_3] + [\text{HCO}_3^-] + [\text{CO}_3^{-2}] \quad (1a)$$

$$[\text{Na}^+] = 2C \quad (1b)$$

##### B. Charge balance

$$[\text{Na}^+] + [\text{H}^+] = [\text{HCO}_3^-] + 2[\text{CO}_3^{-2}] + [\text{OH}^-] \quad (2)$$

##### C. Proton balance

$$[\text{H}^+] + 2[\text{H}_2\text{CO}_3] + [\text{HCO}_3^-] = [\text{OH}^-] \quad (3)$$

D. Equilibrium constants

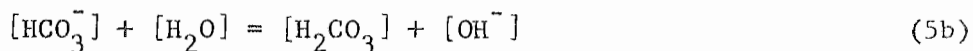
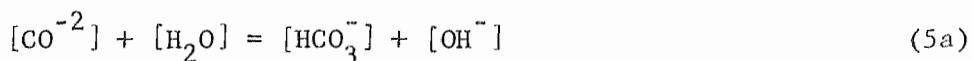
$$K_{1A} = \frac{[H^+][HCO_3^-]}{[H_2CO_3]} = 4.4 \times 10^{-7} \quad (4a)$$

$$K_{2A} = \frac{[H^+][CO_3^{2-}]}{[HCO_3^-]} = 5.6 \times 10^{-11} \quad (4b)$$

$$K_w = [H^+][OH^-] = 1 \times 10^{-14} \quad (4c)$$

$$K_h = \frac{K_w}{K_{2A}} = 1.78 \times 10^{-4} \quad (4d)$$

E. Hydrolysis reaction



In all cases to follow, it has been assumed that (a) total carbonate is constant, (b) K values remain constant, (c) concentrations and activities are the same, and (d) complex such as  $NaCO_3^-$  is absent.

PROCEDURE:

Method 1. In this method, which is the simplest and most frequently used example in elementary textbooks, it is assumed that the reaction described by equation (5a) is dominant and (5b) is negligible, and also that  $[HCO_3^-] = [OH^-]$ .

The equilibrium describing (5a) is

$$K_h = \frac{K_w}{K_{2A}} = \frac{[\text{OH}^-][\text{HCO}_3^-]}{[\text{CO}_3^{-2}]} = \frac{[\text{OH}^-]^2}{[\text{CO}_3^{-2}]} \quad (6)$$

Substituting the relationship for  $[\text{OH}^-]$  from (4c) into (6), and assuming negligible hydrolysis, i.e. implying that  $[\text{CO}_3^{-2}] = C$ , a new relationship is obtained such that

$$[\text{H}^+] = (K_{2A} K_w / C)^{1/2} \quad (7)$$

for which the pH can be readily estimated as

$$\text{pH} = \frac{1}{2} \text{p}K_{2A} + \frac{1}{2} \text{p}K_w + \frac{1}{2} \log C \quad (7a)$$

Method 2. If hydrolysis occurs to any significant extent, the original concentration of carbonate cannot be used as it stands. The concentration of  $\text{CO}_3^{-2}$  will be less than  $C$  and in this case  $[\text{CO}_3^{-2}][C - \text{HCO}_3^-]$  or since we are assuming  $[\text{HCO}_3^-] = [\text{OH}^-]$ ,  $[\text{CO}_3^{-2}] = C - [\text{OH}^-]$ . Substituting this improved  $C - [\text{OH}^-]$  instead of  $[\text{CO}_3^{-2}]$  and also  $[\text{OH}^-]$  relation from (4c) into (6), the new estimate for  $[\text{H}^+]$  is obtained as

$$[\text{H}^+] = \frac{K_h K_w + \sqrt{(K_h K_w)^2 + 4CK_h K_w^2}}{2CK_h} \quad (8)$$

This relation appears more formidable than (7), but nevertheless solvable in a straightforward manner.

Method 3. The graphical technique for resolving equilibrium data provides another method for estimating  $[H^+]$ . Complete details are presented by Butler (2). With this technique, an essential consideration is that we assume that  $[HCO_3^-] = [OH^-]$ . It thus follows from the proton balance equation (3), that  $H^+$  and  $H_2CO_3$  concentrations must be negligible in relation to  $[HCO_3^-]$  and  $[OH^-]$ . Consequently, the pH of the  $Na_2CO_3$  solution is estimated at the intersection of the  $[OH^-]$  and  $[HCO_3^-]$  curves in the graphical analysis.

Method 4. The three preceding methods are reliable for calculating the pH of the more concentrated  $Na_2CO_3$  solution. However, with less concentrated solutions, the hydrolysis will increase, the pH will decrease, and the hydrolysis reaction represented by equation (5b) cannot then be ignored. Furthermore, the estimate of the component concentrations ( $HCO_3^-$ ,  $CO_3^{2-}$ ,  $H_2CO_3$ ) is less reliable because of the simplifying assumptions made in order to calculate  $[H^+]$ .

To overcome these shortcomings, and to check on the accuracy of the preceding methods, the digital computer technique for chemical equilibrium calculations proposed by Bard and King (1) was adapted for  $Na_2CO_3$  hydrolysis with the necessary transposition from their FORTRAN language to one compatible to the General Electric 235 digital computer.

In brief, equations (1a) and (2) are rewritten as

$$Y(1) = [H_2CO_3] + [HCO_3^-] + [CO_3^{2-}] - C \quad (9)$$

$$Y(2) = [HCO_3^-] + 2[CO_3^{2-}] + [OH^-] - [Na^+] - [H^+] \quad (10)$$

The method involves initial guesses of  $[H^+]$  and the least concentrated species to get the computational process started. In this case, at the high pH's a guess of the  $H_2CO_3$  concentration instead of  $[HCO_3^-]$  and  $[CO_3^{2-}]$  is appropriate, whereas at the low pH's a guess of the  $CO_3^{2-}$  in place of  $[HCO_3^-]$  and  $[H_2CO_3]$  is made.

By using the mass and charge balance equations together with the dissociation constants ( $K_{1A}$ ,  $K_{2A}$ ,  $K_w$ ), the computer is programmed to minimize the difference between Y(1) and Y(2) by an appropriate and systematic change in  $[H_2CO_3]$  or  $[CO_3^{2-}]$  and  $[H^+]$  by an iteration procedure. Details for the technique involving a hypothetical acid dissociation are adequately discussed by Bard and King (1).

An alternate to Method 4 which also does not require any assumption regarding the degree of hydrolysis or the relation between  $[HCO_3^-]$  and  $[OH^-]$  can be derived.

Method 5. Solving for  $[H_2CO_3]$ ,  $[CO_3^{2-}]$ , and  $[OH^-]$  in terms of  $[H^+]$ ,  $[HCO_3^-]$  and the equilibrium constants, and substituting these into the mass and charge balanced equations (1a) and (2), a pair of simultaneous equations is obtained as follows:

$$C = [H^+][HCO_3^-]/K_{1A} + [HCO_3^-] + K_{2A}[HCO_3^-]/[H^+] \quad (11a)$$

$$2C + H^+ = K_w/[H^+] + [HCO_3^-] + 2K_{2A}[HCO_3^-]/[H^+] \quad (11b)$$

The algebraic solution of (11a) and (11b) in terms of  $[H^+]$  is a quartric equation of the form

$$\begin{aligned}
& [\text{H}^+]^4 + (2C + K_{1A})[\text{H}^+]^3 + (CK_{1A} + K_{1A}K_{2A} - K_w)[\text{H}^+]^2 \\
& - K_{1A}K_w[\text{H}^+] - K_{1A}K_{2A}K_w = 0 \quad (12)
\end{aligned}$$

The concentrations of  $\text{H}^+$  at different  $\text{Na}_2\text{CO}_3$  concentrations were also calculated using equation (12) on the digital computer. With the  $\text{H}^+$  value thus obtained  $[\text{HCO}_3^-]$  was consequently estimated from equation (11a), and the other components were computed from the definition of the equilibrium constants.

#### RESULTS AND DISCUSSION:

The pH's of  $\text{Na}_2\text{CO}_3$  solutions at different concentrations obtained by the five methods are compared in Table 5. The pH values derived by Methods 2, 3, 4, and 5 are comparable at all  $\text{Na}_2\text{CO}_3$  concentrations. The results for Methods 4 and 5 are the same. Values estimated by Method 1 are in good agreement with those estimated by the other methods at the higher  $\text{Na}_2\text{CO}_3$  concentrations, but not at the lower concentrations. The reason for the poor agreement between Method 1 and the others is illustrated in Tables 5 and 6, where the concentrations of the different components and the degree of hydrolysis of  $\text{Na}_2\text{CO}_3$  at various solution concentrations are compared for Methods 2 and 4. The greater hydrolysis of  $\text{Na}_2\text{CO}_3$  at lower concentrations will affect Method 1 because its derivation requires the assumption that hydrolysis is negligible and not corrected for. On the other hand, Methods 2 and 3 agree well with 4 and 5 because the assumption that  $[\text{OH}^-] = [\text{HCO}_3^-]$  holds throughout most of the  $\text{Na}_2\text{CO}_3$  concentration ranges as shown by the  $[\text{OH}^-]$  and  $[\text{HCO}_3^-]$  values calculated from Method 4 in Table 6. Methods 2, 4, and 5 are more convenient than the graphical technique (Method 3), since they provide a direct method for estimating concentrations of carbonate components. Thus,

in essence, Methods 2 and 3 provide suitable means for predicting hydrolysis of salts, but the digital computer analysis of hydrolysis used in conjunction with these methods provides us with a better insight into the hydrolysis process and into the reliability of the assumptions made for simplifying some of the computational procedures. Furthermore, it is apparent that the numerical methods 4 and 5 give concentration relations of the different components that are more reliable than the others since assumptions relative to the degree of hydrolysis, equality of  $\text{OH}^-$  and  $\text{HCO}_3^-$ , and single estimates of  $[\text{CO}_3^{-2}]$  or  $[\text{H}_2\text{CO}_3]$  are not made.

#### PART IV. PREDICTING THE pH OF A $\text{Na}_2\text{CO}_3$ - $\text{CO}_2$ SYSTEM

In the preceding section the hydrolysis of  $\text{Na}_2\text{CO}_3$  was described in systems where  $\text{CO}_2$  in the atmosphere was absent. Where  $\text{CO}_2$  is present, the prediction equation must be modified to account for this additional factor.

#### THEORY:

The charge balance for the dissociation of  $\text{Na}_2\text{CO}_3$  is

$$[\text{Na}^+] + [\text{H}^+] = [\text{HCO}_3^-] + 2[\text{CO}_3^{-2}] + [\text{OH}^-] \quad (13)$$

Substituting the equivalent values for  $[\text{HCO}_3^-]$ ,  $[\text{CO}_3^{-2}]$ , and  $[\text{OH}^-]$  in terms of  $[\text{H}^+]$  and the dissociation constants and activity coefficients, we have a cubic equation of the form

$$[\text{H}^+]^3 + [\text{Na}^+][\text{H}^+]^2 - \left( \frac{K_w}{\gamma_{\text{H}^+} \gamma_{\text{OH}^-}} + \frac{K_1 k P_{\text{CO}_2}}{\gamma_{\text{H}^+} \gamma_{\text{HCO}_3^-}} \right) [\text{H}^+] - \frac{2K_{1A} K_{2A} k P_{\text{CO}_2}}{\gamma_{\text{H}^+}^2 + \gamma_{\text{CO}_3^{-2}}} = 0, \quad (14)$$

where  $k$  is Henry's law constant,  $P_{\text{CO}_2}$  the partial pressure of  $\text{CO}_2$ , and  $\gamma$  the activity coefficient.

## PROCEDURE:

Equation (14) was solved for  $[H^+]$  and pH on a digital computer at different  $Na_2CO_3$  concentrations at a partial pressure of 0.93 atmospheres. pH's were also measured with a glass-calomel electrode system of the different  $Na_2CO_3$  solutions at  $P_{CO_2} = .93$ .

## RESULTS AND DISCUSSION:

The comparison of the theoretical and experimental data is presented in Table 7, which indicates that the equation (14) developed is suitable for making predictions of the pH of  $Na_2CO_3$  solutions at a prescribed  $CO_2$  partial pressure.

## PART V. THEORETICAL ASPECTS OF THE CALCIUM SULFATE-BICARBONATE-CARBONATE INTERRELATION IN SOIL SOLUTION

An understanding of the solution chemistry of the  $Ca^{+2}-SO_4^{-2}-HCO_3^- - CO_3^{-2}$  system should prove invaluable for use in both sealing and reclamation projects for artificially controlling the physical and chemical properties of soils. Much interest and knowledge have resulted already concerning solubility of Ca carbonate and phosphate in the presence of  $CaSO_4$ , but the behavior of ionic and ion-pair interactions of the various species in solution has not been fully explored. That complexes and ion-pairs such as  $CaHCO_3^+$  and  $CaCO_3^0$ , and  $CaSO_4^0$  can exist in solution under certain conditions which resemble that of the soil solution has been demonstrated experimentally and data for the formation and dissociation constants of the species are presently available (Annual Reports 1966 and 1967). In this section the possible interactions among the calcium, sulfate, bicarbonate, carbonate ions will be presented and the importance of the relation Ca to these different anions will be related to that of the ion-pair and complex formation and distribution.

$\text{CaSO}_4^{\circ}-\text{CO}_3^{-2}$  and  $\text{CaSO}_4^{\circ}-\text{HCO}_3^{-}$  relations. The two equations which relate the reactions among Ca sulfate ion-pair ( $\text{CaSO}_4^{\circ}$ ), Ca carbonate ion-pair ( $\text{CaCO}_3^{\circ}$ ), Ca bicarbonate complex ( $\text{CaHCO}_3^{+}$ ), sulfate, bicarbonate, and carbonate with their respective equilibrium constants in the solution phase are



$$K_1 = (\text{CaCO}_3^{\circ})(\text{SO}_4^{-2}) / (\text{CaSO}_4^{\circ})(\text{CO}_3^{-2}) \quad (15a)$$



$$K_2 = (\text{CaHCO}_3^{+})(\text{SO}_4^{-2}) / (\text{CaSO}_4^{\circ})(\text{HCO}_3^{-}) \quad (16a)$$

The equilibrium constants for these reactions were obtained by estimating first the free energy change of the reactions,  $\Delta F_r$ , namely

$$\Delta F_r^I = (\Delta F_{\text{CaCO}_3^{\circ}} + \Delta F_{\text{SO}_4^{-2}}) - (\Delta F_{\text{CaSO}_4^{\circ}} + \Delta F_{\text{CO}_3^{-2}}) \quad (15b)$$

$$\Delta F_r^{II} = (\Delta F_{\text{CaHCO}_3^{+}} + \Delta F_{\text{SO}_4^{-2}}) - (\Delta F_{\text{CaSO}_4^{\circ}} + \Delta F_{\text{HCO}_3^{-}}) \quad (16b)$$

and then using the general relation  $K = \exp(-\Delta F_r / RT)$  where R is the gas constant and T the Kelvin temperature. The  $\Delta F$  of formation for the various species used in this report are listed in Table 8.

$\Delta F_r$  for reactions 1 and 2 were -3.01 and +1.40 kcal/mole, respectively, with  $K_1 = 4.66 \times 10^2$  and  $K_2 = 4.89 \times 10^{-2}$  at 25 C. It is evident from the  $\Delta F_r$ 's that the interaction between

$\text{CaSO}_4^0$  with  $\text{CO}_3^{-2}$  is toward the formation of the  $\text{CaCO}_3^0$  ion-pair, whereas that between  $\text{CaHCO}_3^+$  and  $\text{SO}_4^{-2}$  is that of  $\text{CaSO}_4^0$  ion-pair.

The distributions of  $\text{CaSO}_4^0\text{-CaCO}_3^0$ , and  $\text{CaSO}_4^0\text{-CaHCO}_3^+$  combinations as functions of  $\text{SO}_4^{-2}\text{-CO}_3^{-2}$  and  $\text{SO}_4^{-2}\text{-HCO}_3^-$  activities are presented in Figures 1 and 2, respectively, following the method discussed by Hem (3) and Sillén (8). In both figures the solid diagonal line represents the condition under which the activity  $\text{CaCO}_3^0 = \text{CaSO}_4^0$  or  $\text{CaHCO}_3^+ = \text{CaSO}_4^0$ . Under these conditions then from Equation (15a)  $(\text{CO}_3^{-2}) = (\text{SO}_4^{-2})/K_1$ , and from Equation (16a)  $(\text{SO}_4^{-2}) = (\text{HCO}_3^-)K_2$ . Other ratios of  $\text{CaCO}_3^0$  to  $\text{CaSO}_4^0$  and  $\text{CaSO}_4^0$  to  $\text{CaHCO}_3^+$  were selected (1:100, 1:10, 1:5, 1:2, 2:1, 5:1, 10:1, 100:1), giving straight lines paralleling both sides of the 1:1 ratio presented in the figures. For every ratio the intersection of these lines with the activities of  $\text{SO}_4^{-2}$  and  $\text{CO}_3^{-2}$ , or  $\text{SO}_4^{-2}$  and  $\text{HCO}_3^-$ , which would give a certain percentage of complexing (90, 80, 70, 60, 50, 40, 30, 20, 10, 5), was determined. Referring to the 1:1 ratio of  $\text{CaCO}_3^0$  to  $\text{CaSO}_4^0$ , at 90% complexing there will be 45%  $\text{CaCO}_3^0$ , 45%  $\text{CaSO}_4^0$ , and 10%  $\text{Ca}^{+2}$ . The  $\text{SO}_4^{-2}$  activity under these conditions will then be  $(\text{SO}_4^{-2}) = \text{percent complex} \times K_{\text{CaSO}_4^0} / (\text{percent Ca}^{+2} \times (\text{ratio} + 1)) = 90 \times 5.32 \times 10^{-3} / (10 \times 2) = 2.39 \times 10^{-2}$ . The dissociation constants K are presented in Table 9. The calculation and resultant graphs were made in terms of activities and thus concentrations must be converted to activities before the graphs can be used.

The contour lines in both figures represent the percent of the total Ca as the  $\text{CaSO}_4^0 + \text{CaCO}_3^0$  or  $\text{CaSO}_4^0 + \text{CaHCO}_3^+$  forms in solution for the different anion combinations. The region below the 1:1 activity ratio line represents conditions where the  $\text{CaSO}_4^0$  (Figure 3 and 4) form will predominate, whereas that above the line represents conditions where the  $\text{CaCO}_3^0$  or  $\text{CaHCO}_3^+$  will predominate, respectively. To achieve equivalent  $\text{CaSO}_4^0$  and  $\text{CaCO}_3^0$  activities, the activity of  $\text{SO}_4^{-2}$  must be approximately 450 times greater than the  $\text{CO}_3^{-2}$  activity. In the case of a saturated  $\text{CaCO}_3 - \text{CaSO}_4$

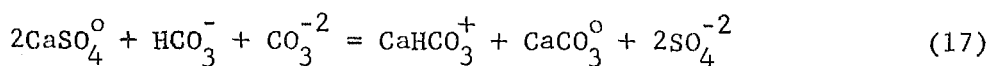
solution (disregarding enhanced solubility effects and  $\text{HCO}_3^-$  for the moment) where  $(\text{CO}_3^{-2})$  is in the order of  $1 \times 10^{-5}$ , and  $(\text{SO}_4^{-2})$  of  $5 \times 10^{-3}$ , it is evident that the equilibrium condition will be located in a region where  $\text{CaCO}_3^0$  will predominate over the  $\text{CaSO}_4^0$  form and, furthermore, that a large portion ( $> 90\%$ ) of the total Ca in solution is nonionic. The discussion presented would be applicable primarily to the alkali soils ( $\text{pH} > 8.5$ ) where the  $(\text{CO}_3^{-2})$  becomes very much larger than the  $(\text{HCO}_3^-)$ .

The addition of Ca to an alkali soil system high in  $\text{CO}_3^{-2}$  and Na results in the removal of  $\text{CO}_3^{-2}$  by precipitation of  $\text{CaCO}_3$  and consequent lowering of pH and replacement of Na with Ca. This is illustrated in Figure 3, describing the equilibrium distribution of  $\text{H}_2\text{CO}_3$ ,  $\text{HCO}_3^-$ , and  $\text{CO}_3^{-2}$  as a function of pH. Thus, there are several restrictive conditions that arise in the use of gypsum for supplying  $\text{Ca}^{+2}$  ions compared to other Ca sources. The two which have been generally understood and accounted for in the past are (1) limited solubility of  $\text{CaSO}_4$  and (2) limited solubility of  $\text{CaCO}_3$  which is also a function of solution pH, decreasing with increasing pH; the third, as indicated by the calculations presented in (3), is the much lower  $\text{Ca}^{+2}$  ion activity in solution than formerly assumed because of the association of the ionic calcium into both the sulfate and particularly the carbonate anions with consequent reduction in the Ca activity involved in such processes as ion exchange for the replacement of Na ions from the soil complex. Furthermore, it appears that the reaction rate of the complex and ion-pair forms is much lower than the ionic form (5).

Under more "normal" soil conditions, the  $\text{HCO}_3^-$  is the chief functioning carbonate species. In such cases, Figure 2 can be used to demonstrate the distribution of the  $\text{CaHCO}_3^+$

and  $\text{CaSO}_4^0$  forms. First, at equal  $\text{CaSO}_4^0$  and  $\text{CaHCO}_3^+$  activities, the  $\text{HCO}_3^-$  activity is approximately 10 times greater than the  $\text{SO}_4^{2-}$  activity. Assuming a typical  $\text{HCO}_3^-$  and  $\text{SO}_4^{2-}$  activity of  $1 \times 10^{-3}$  and  $1 \times 10^{-2}$  in soil solution, about 26% of the total solution calcium is in the complex and ion-pair forms with one-half of this as the  $\text{CaSO}_4^0$  species and the other half as the  $\text{CaHCO}_3^+$ . The significance and interpretation of less ( $\text{Ca}^{+2}$ ) in solution than assumed from total Ca analysis (correcting for ionic strength, non-ideality effects) will depend upon the accuracy to which one ascribes his results.

$\text{CaCO}_3^0$ - $\text{CaHCO}_3^+$  relation. The two preceding equilibria involved the  $\text{HCO}_3^-$  and  $\text{CO}_3^{2-}$  forms taken as separate entities in their relation to  $\text{CaSO}_4^0$ , but in reality the soil solution contains both  $\text{HCO}_3^-$  and  $\text{CO}_3^{2-}$  anions in equilibrium with each other and other ions as a function of solution pH and partial pressure of soil  $\text{CO}_2$ . The reason for separating the two reactions will become evident from the discussion to follow. In the case then where  $\text{HCO}_3^-$ ,  $\text{CO}_3^{2-}$ , and  $\text{CaSO}_4^0$  equilibria are treated simultaneously, we have



$$K_3 = (\text{CaHCO}_3^+) (\text{CaCO}_3^0) (\text{SO}_4^{2-})^2 / (\text{CaSO}_4^0)^2 (\text{HCO}_3^-) (\text{CO}_3^{2-}) \quad (17a)$$

for which  $\Delta F_r = -1.29$  kcal/mole and  $K_3 = 8.83$ .

The reaction is difficult to interpret in a practical manner similar to that exemplified by Figures 3 and 4 because of the ion activity product factor  $(\text{HCO}_3^-)(\text{CO}_3^{-2})$  in equation (17a). Thus, it is easily observed that we cannot differentiate between  $(1 \times 10^{-2} \text{HCO}_3^-) \times (1 \times 10^{-4} \text{CO}_3^{-2})$  and  $(1 \times 10^{-4} \text{HCO}_3^-) \times (1 \times 10^{-2} \text{CO}_3^{-2})$ .

To evaluate this condition, therefore, requires an understanding of the interrelation between  $\text{CaCO}_3^0$ ,  $\text{CaHCO}_3^+$ ,  $\text{CO}_3^{-2}$ ,  $\text{HCO}_3^-$ , and also pH. The pH,  $\text{HCO}_3^-$ , and  $\text{CO}_3^{-2}$  relation are presented graphically in Figure 5. In going from acid to basic conditions, the  $\text{CO}_3^{-2}$  becomes the significant form over the  $\text{HCO}_3^-$ . The interaction between  $\text{CaHCO}_3^+$  and  $\text{CO}_3^{-2}$  can be written as



$$K_4 = (\text{CaCO}_3^0)(\text{HCO}_3^-) / (\text{CaHCO}_3^+)(\text{CO}_3^{-2}) \quad (18a)$$

where  $\Delta F_r = -4.41$  kcal/mole and  $K_4 = 1.71 \times 10^3$ .

The distribution relation  $\text{CaCO}_3^0$  and  $\text{CaHCO}_3^+$  as a function of  $\text{HCO}_3^-$  and  $\text{CO}_3^{-2}$  activities is presented in Figure 6 and was obtained in a similar manner as that for the  $\text{CaSO}_4^0$ - $\text{CaCO}_3^0$  and  $\text{CaSO}_4$ - $\text{CaHCO}_3^+$  cases. Following the diagonal equi-activity ration line, it is evident that there must be approximately  $10^3$  times more  $\text{HCO}_3^-$  than  $\text{CO}_3^{-2}$  activity to have  $(\text{CaHCO}_3^+)$  equal to  $(\text{CaCO}_3^0)$ . As noted earlier,  $\text{CO}_3^{-2}$  becomes dominant over  $\text{HCO}_3^-$  as the pH increases. In Figure 7 is shown the relation of  $\text{CaHCO}_3^+$  and  $\text{CaCO}_3^0$  as function of pH. Equi-activity occurs at pH 7.10. Furthermore, it is clearly observable that some  $\text{CaCO}_3^0$  form can exist in the acidic pH range, even though the fraction of  $\text{CO}_3^{-2}$  compared to  $\text{HCO}_3^-$  may be small.

Confining the attention to the saturated  $\text{CaCO}_3$  solution in equilibrium with atmospheric  $\text{CO}_2$  partial pressure of 350 ppm where the  $(\text{HCO}_3^-)$  and  $(\text{CO}_3^{2-})$  are in the order of magnitude  $1 \times 10^{-3}$  and  $1 \times 10^{-5}$ , respectively, the use of the graphs (Figure 6) indicates that from 20 to 25% of the total solution Ca is in the ion-pair and complex forms. Since the pH of the saturated  $\text{CaCO}_3$  solution is 8.4, graphical interpolation shows that approximately 95% of the ion-pair + complex species is in the  $\text{CaCO}_3^0$  form.

From the preceding discussions it can be seen that the  $\text{CaSO}_4^0$  - carbonate equilibrium is pH dependent whereby at the low pH's the  $\text{CaSO}_4^0\text{-HCO}_3^-$  reaction will be predominant and at the high pH's that for  $\text{CaSO}_4^0\text{-CO}_3^{2-}$  will be dominant. For an illustrative example let us compare a solution with a pH of 6,  $\text{HCO}_3^- = 1 \times 10^{-3}$  and  $\text{SO}_4^{2-} = 1 \times 10^{-3}$  and one with pH of 7 at the same  $\text{HCO}_3^-$  and  $\text{SO}_4^{2-}$  activities. In both cases  $\text{CO}_3^{2-}$  will not be detectable by ordinary chemical methods. However, by using the second dissociation constant of carbonic acid in conjunction with the pH and  $\text{HCO}_3^-$ ,  $\text{CO}_3^{2-}$  activities are  $5.6 \times 10^{-8}$  and  $5.6 \times 10^{-7}$  for pH 6 and 7, respectively. At pH 6 the  $\text{CaSO}_4^0$  species will predominate and the complexed Ca will be approximately 19% of the total Ca in solution. For pH 7, however,  $\text{CaCO}_3^0 \cong \text{CaHCO}_3^+$  and furthermore, approximately 20% of the total Ca is tied up with the  $\text{CaSO}_4^0$  species predominating over the  $\text{CaCO}_3^0$  species. The next incremental increase in pH to 8 will result in an equilibrium condition where the  $\text{CaCO}_3^0$  species will be dominant and also where a greater fraction of the total dissolved Ca becomes complexed.

The preceding discussion may be a reasonable explanation as to why we do not obtain a rapid and dramatic improvement in soil properties when soils high in free alkali carbonates are treated with Ca salt amendments; namely, that a large part of the Ca which eventually gets into solution is not in the  $\text{Ca}^{+2}$  form and consequently unavailable for Na replacement.

Considerably more experimental work must be done in this area to improve upon one presented understanding of ion-pair and complex formation in soil solutions. Of particular use are the ion selective electrodes, but these have their limitations because of their sensitivity of high  $\text{H}^+$  and  $\text{Na}^+$  activities and the presence of divalent ions, even at low activities, and the requirement of a good knowledge of the ionic strength of the solution. Accurate knowledge of both inorganic and organic complex association constants of the major soil solution constituents, together with the treatment developed here, should provide a reliable means of separating out the "active" fraction of the different solution components.

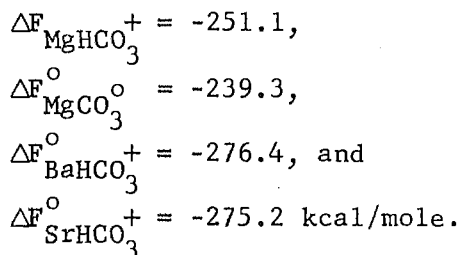
#### SUMMARY AND CONCLUSIONS:

The dissociation constants of the bicarbonate complexes of Mg, Ba, and Sr were

$$\begin{aligned} K_{\text{MgHCO}_3^+} &= 5.37 \times 10^{-2}, \\ K_{\text{BaHCO}_3^+} &= 3.00 \times 10^{-2}, \text{ and} \\ K_{\text{SrHCO}_3^+} &= 5.26 \times 10^{-2} \end{aligned}$$

as determined in the  $\text{MCl}_2\text{-CO}_2$  system. These values did not follow the electronegativity or ionic radii pattern of the  $\text{MOH}^+$  alkaline earth series. K for the  $\text{MgCO}_3^0$  species in the  $\text{MgCO}_3\text{-CO}_2$

system is  $9.55 \times 10^{-4}$ . The standard free energies of formation of these compounds are:



The interrelation of the sulfate, bicarbonate, and carbonate anions with Ca were investigated theoretically based on thermodynamic principles, using the equilibrium constants obtained from laboratory measurements. Graphical solutions are possible in which predictions concerning the relative proportions of  $\text{CaSO}_4^0$ ,  $\text{CaHCO}_3^+$ ,  $\text{CaCO}_3^0$ , and  $\text{Ca}^{+2}$  forms of dissolved calcium in the  $\text{SO}_4\text{-CO}_3$ ,  $\text{SO}_4\text{-HCO}_3$ , and  $\text{HCO}_3\text{-CO}_3$  can be made.

Several equations were developed which are suitable for predicting the pH of sodium carbonate solutions as a consequence of the hydrolysis of the salt. These equations work equally well at low and high concentrations, whereas, the equations usually used were applicable only at the high salt concentrations. In addition, the partial pressure of  $\text{CO}_2$  was accounted for where necessary.

#### REFERENCES:

1. Bard, A. J., and King, D. M. General digital computer program for chemical equilibrium calculations. Jour. Chem. Ed. 42:127-131. 1965.
2. Butler, J. N. Ionic equilibrium - A mathematical approach. p. 221. Addison-Wesley, Reading, Mass. 1964.
3. Hem, J. D. Manganese complexes with bicarbonate and sulfate in natural water. Jour. Chem. Engin. Data 8:99-101. 1963.

4. Latimer, W. M. The oxidation states of the elements and their potentials in aqueous solutions. pp. 72, 128. Prentice-Hall, New York. 1952.
5. Morgan, J. J. Chemical equilibria and kinetic properties of manganese in natural waters. In Faust, S. D. and Hunter, J. V. (eds.) Principles and application of water chemistry. pp. 561-624. John Wiley and Sons, New York. 1967.
6. Nakayama, F. S. Calcium activity, complex and ion-pair in saturated  $\text{CaCO}_3$  solution. Soil Sci. 106:429-434. 1968.
7. Nakayama, F. S., and Rasnick, B. A. Calcium electrode method for measuring dissociation and solubility of calcium sulfate dihydrates. Analyt. Chem. 39:1022-1023. 1967.
8. Sillén, L. G. Graphic presentation of equilibrium data. In Kolthoff, I. M., and others (ed.) Treatise on analytical chemistry. Part I, Vol. 1. pp. 277-317. Interscience Encyclopedia, Inc., New York. 1964.
9. Wagman, D. D., and others. Selected values of chemical thermodynamic properties. N.B.S. Tech. Notes. pp. 270-273. 1968.

PERSONNEL: F. S. Nakayama and B. A. Rasnick

CURRENT TERMINATION DATE: December 1970

Table 1. Typical results used for estimating  $K_1$  and  $K_2$ ,<sup>a/</sup> and the concentration of the various Mg species in  $5.59 \times 10^{-2}$  M  $MgCO_3$ .

$P_{CO_2}$	pH	$(Mg^{+2})$	$[Mg^{+2}]$	$[MgHCO_3^+]$	$[MgCO_3^0]$	$[HCO_3^-]$	$[CO_3^{-2}]$
Atm.		$\times 10^2$	$\times 10^2, \underline{M}$				
.9353	6.714	1.74	4.21	1.30	.081	9.78	.0054
.1841	7.393	1.65	3.94	1.27	.38	9.15	.0238
.09529	7.655	1.61	3.80	1.15	.63	8.63	.0405
.04861	7.907	1.58	3.64	.96	.94	7.82	.0647
.01857	8.254	1.52	3.47	.66	1.46	6.59	.118
.008906	8.457	1.47	3.27	.51	1.81	4.99	.139
.005042	8.614	1.35	2.97	.43	2.24	4.01	.155

<sup>a/</sup>  $K_1 = (Mg^{+2})(HCO_3^-) / (MgHCO_3^+)$ ;  $K_2 = (MgHCO_3^+) / (MgCO_3^0)(H^+)$

40-20

Table 2.  $pK_1$  values obtained from the  $MgCl_2-CO_2$  system.

$MgCl_2, M$	pH	$\mu$	$pK_1$
0.006	3.907	0.018	1.29
0.0075	3.903	0.022	1.27
0.01	3.899	0.030	1.26
0.0233	3.877	0.070	1.23
0.035	3.860	0.115	1.25
0.050	3.845	0.150	1.22
0.060	3.834	0.180	1.23
0.070	3.824	0.210	1.25

Table 3.  $K_{\text{BaHCO}_3^+}$  values in the  $\text{BaCl}_2\text{-CO}_2$  system.

Conc. <u>M</u>	pH	$\mu$	$K_{\text{BaHCO}_3^+}$ $\times 10^{23}$
.005	3.903	.010	2.80
.010	3.888	.020	3.03
.020	3.872	.040	3.74
.030	3.839	.060	2.85
.040	3.829	.080	3.07
.060	3.799	.120	2.89
.080	3.786	.160	3.07
.120	3.764	.240	3.24
.160	3.735	.320	3.03
.200	3.716	.400	2.98

Table 4.  $K_{\text{SrHCO}_3^+}$  values in the  $\text{SrCl}_2\text{-CO}_2$  system.

Conc. <u>M</u>	pH	$\mu$	$K_{\text{SrHCO}_3^+}$ $\times 10^{23}$
.02	3.884	.040	5.10
.03	3.877	.060	5.75
.04	3.861	.080	5.25
.06	3.856	.120	6.22
.08	3.832	.160	5.34
.12	3.767	.240	3.38
.16	3.782	.320	4.69
.20	3.764	.400	4.49

Table 5. pH values of various  $\text{Na}_2\text{CO}_3$  solution concentrations obtained by different methods.

Conc. $\text{Na}_2\text{CO}_3, \underline{\text{M}}$	<u>M E T H O D</u>				
	1 pH	2 pH	3 pH	4 pH	5 pH
1	12.13	12.13	12.15	12.12	12.12
$1 \times 10^{-1}$	11.63	11.62	11.65	11.62	11.62
$1 \times 10^{-2}$	11.13	11.10	11.15	11.10	11.10
$1 \times 10^{-3}$	10.63	10.54	10.55	10.53	10.53
$1 \times 10^{-4}$	10.13	9.85	9.90	9.85	9.85
$1 \times 10^{-5}$	9.63	8.98	9.00	8.98	8.98
$1 \times 10^{-6}$	9.13	8.00	8.00	8.01	8.01
$1 \times 10^{-7}$	8.63	7.00	7.00	7.23	7.23

Table 6. Carbonates and hydroxyl concentrations, and degree hydrolysis of  $\text{Na}_2\text{CO}_3$  estimated by methods 2 and 4.

Conc. $\text{Na}_2\text{CO}_3$ , M	$[\text{CO}_3^{2-}]$		$[\text{HCO}_3^-]$		$[\text{H}_2\text{CO}_3]$		$[\text{OH}^-]$		Hydrolysis, %	
	2	4	2	4	2	4	2	4	2	4
1	9.87E-1	9.87E-1	1.34E-2	1.33E-2	2.27E-8	2.27E-8	1.34E-2	1.33E-2	1.3	1.3
1E-1	9.58E-2	9.59E-2	4.17E-3	4.14E-3	"	"	4.17E-3	4.14E-3	4.2	4.1
1E-2	8.74E-3	8.75E-3	1.26E-3	1.25E-3	"	"	1.26E-3	1.25E-3	12.6	12.5
1E-3	6.55E-4	6.57E-4	3.45E-4	3.43E-4	"	"	3.45E-4	3.43E-4	34.5	34.3
1E-4	2.83E-5	2.86E-5	7.17E-5	7.14E-5	"	"	7.17E-5	7.14E-5	71.7	71.4
1E-5	4.97E-7	5.05E-7	9.50E-6	9.47E-6	"	2.26E-8	9.50E-6	9.52E-6	95.0	95.0
1E-6	5.44E-9	5.54E-9	9.94E-7	9.73E-7	"	2.16E-8	9.94E-7	1.03E-6	99.4	99.4
1E-7	5.49E-11	8.41E-11	9.99E-8	8.82E-8	"	1.18E-8	9.99E-8	1.70E-7	99.9	99.9

40-25

Table 7. pH of  $\text{Na}_2\text{CO}_3$  solutions in equilibrium with  $\text{CO}_2$

Conc. $\text{Na}_2\text{CO}_3, \text{M}$	Exptl.	pH Theoretical
1	7.96	8.17
$1 \times 10^{-1}$	6.96	7.03
$1 \times 10^{-2}$	6.06	6.09
$1 \times 10^{-3}$	5.11	5.13
$1 \times 10^{-4}$	4.27	4.25
$1 \times 10^{-5}$	3.98	3.96
$1 \times 10^{-6}$	3.95	3.93
$1 \times 10^{-7}$	3.95	3.93

Table 8. Free energies of formation used in calculating equilibrium constants.

Species	$\Delta F$ , kcal/mole	Source
$\text{SO}_4^{-2}$	-177.97	Wagman (9)
$\text{HCO}_3^-$	-140.31	Latimer (4)
$\text{CO}_3^{-2}$	-126.22	Latimer (4)
$\text{CaSO}_4^0$	-313.25	Nakayama and Rasnick (7)
$\text{CaHCO}_3^+$	-274.29	Nakayama (6)
$\text{CaCO}_3^0$	-264.61	Nakayama (6)

Table 9. Dissociation and association constants  
of Ca sulfate and carbonates at 25 C.

Reaction	K
$\text{CaSO}_4^0 = \text{Ca}^{+2} + \text{SO}_4^{-2}$	$5.32 \times 10^{-3}$ (7)
$\text{CaHCO}_3^+ = \text{Ca}^{+2} + \text{HCO}_3^-$	$5.64 \times 10^{-2}$ (6)
$\text{CaCO}_3^0 + \text{H}^+ = \text{CaHCO}_3^+$	$1.24 \times 10^{-7}$ (6)
$\text{CaCO}_3^0 = \text{Ca}^{+2} + \text{CO}_3^{-2}$	$3.29 \times 10^{-5}$ (6)

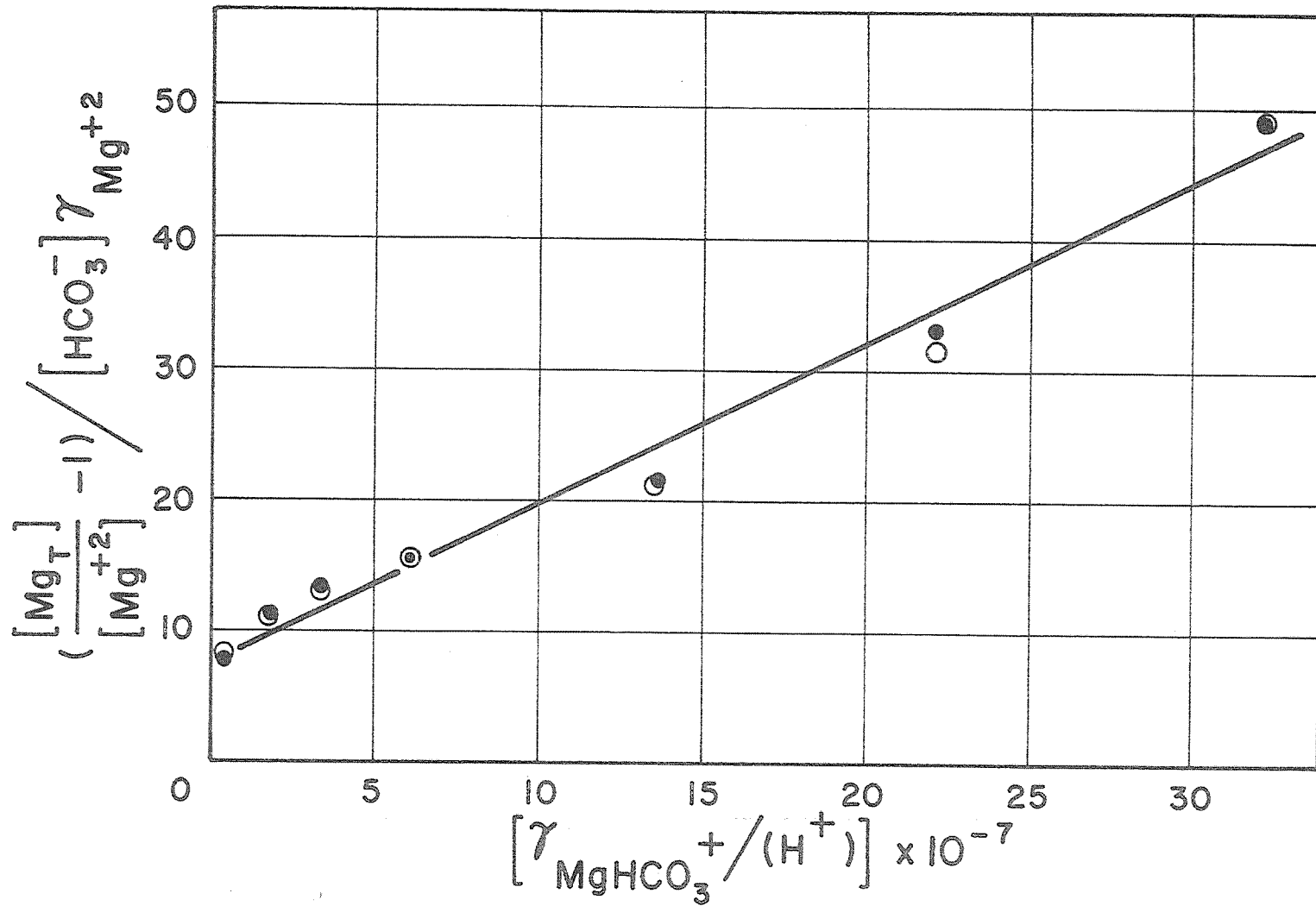


Figure 1. Plot of data from final iterative computation used for estimating  $K_1$  and  $K_2$ .

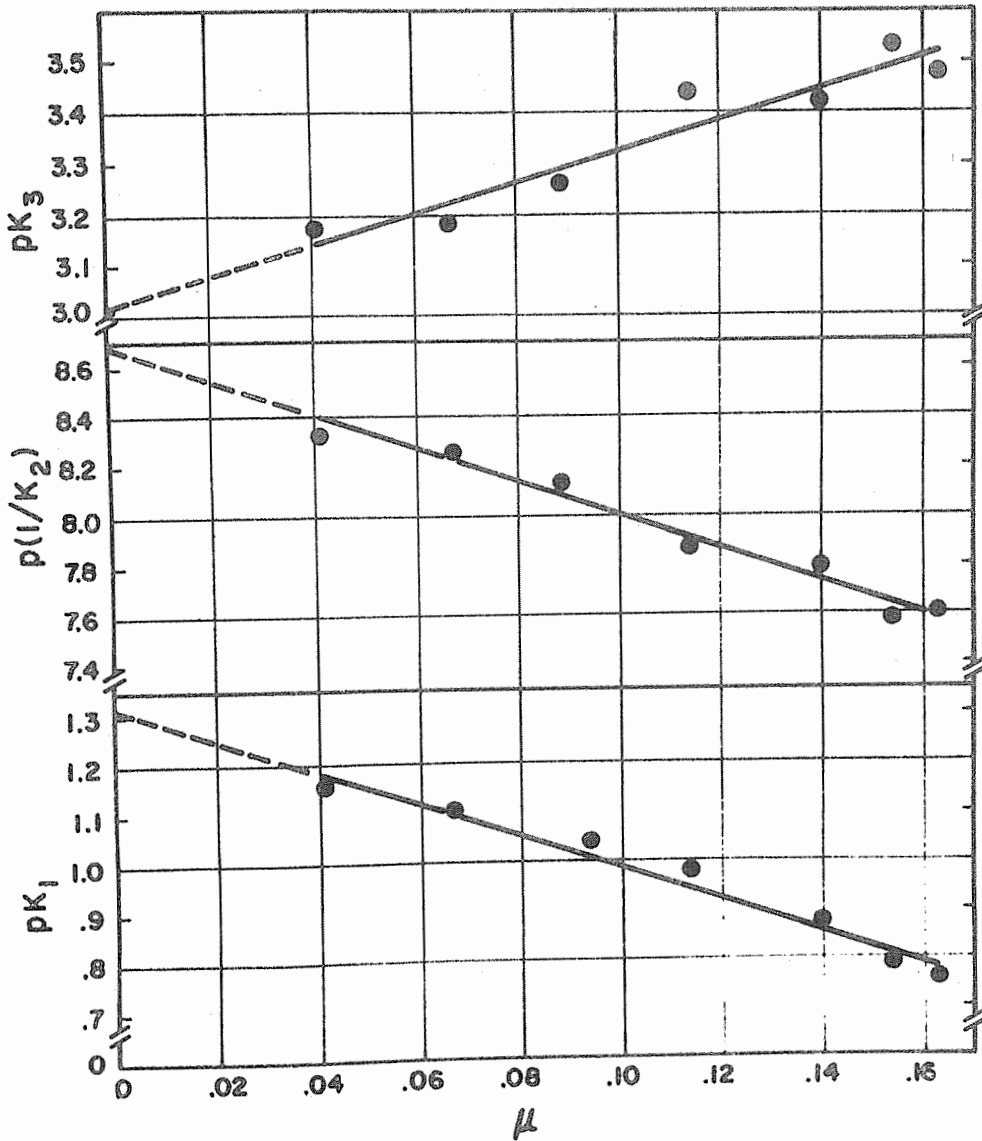


Figure 2. Relation of  $pK$ ,  $p(1/K_2)$  and  $pK_3$  to ionic strength.

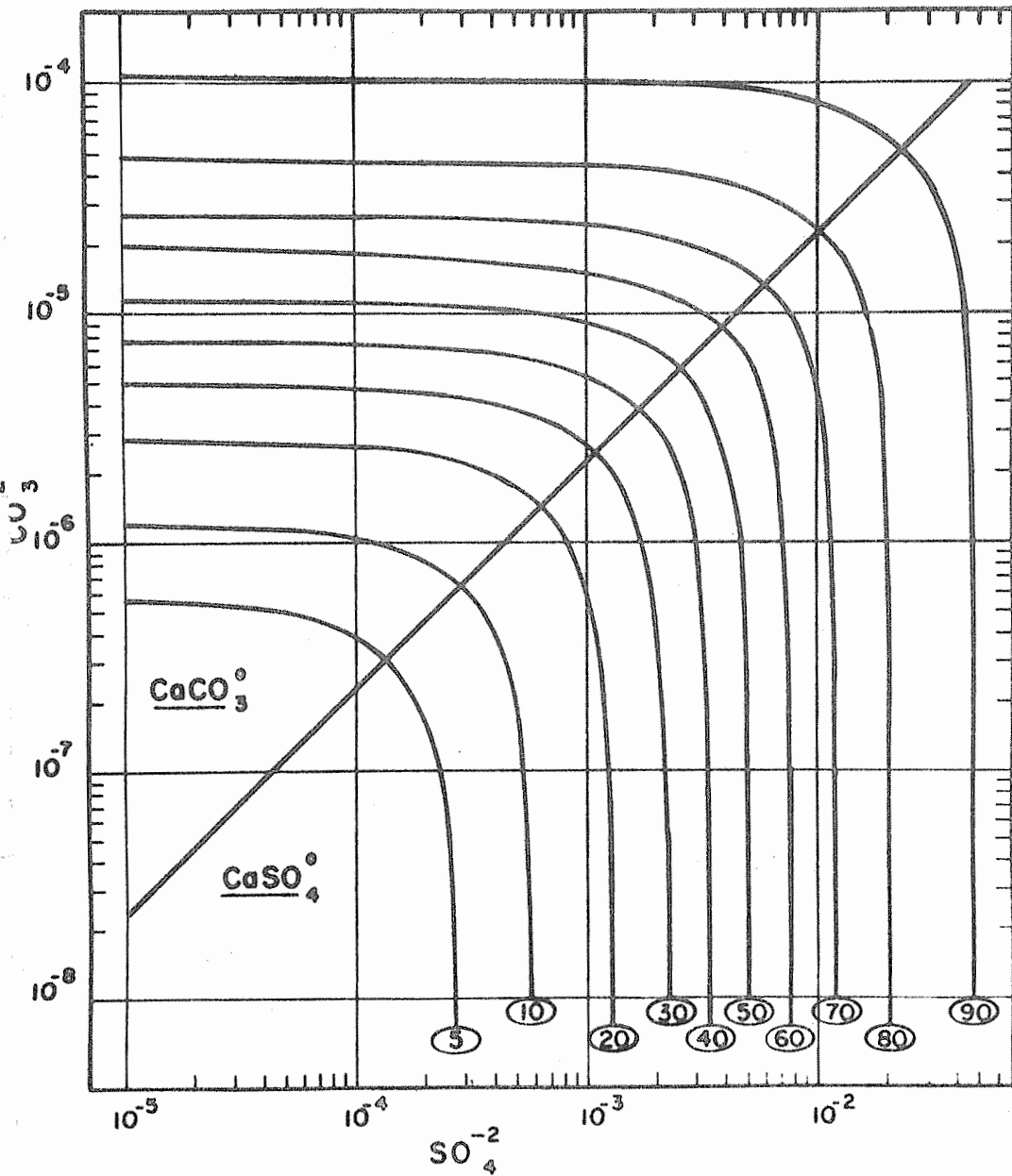


Figure 3. Distribution of  $CaSO_4^0$  and  $CaCO_3^0$  as function of  $SO_4^{-2}$  and  $CO_3^{-2}$  activities.

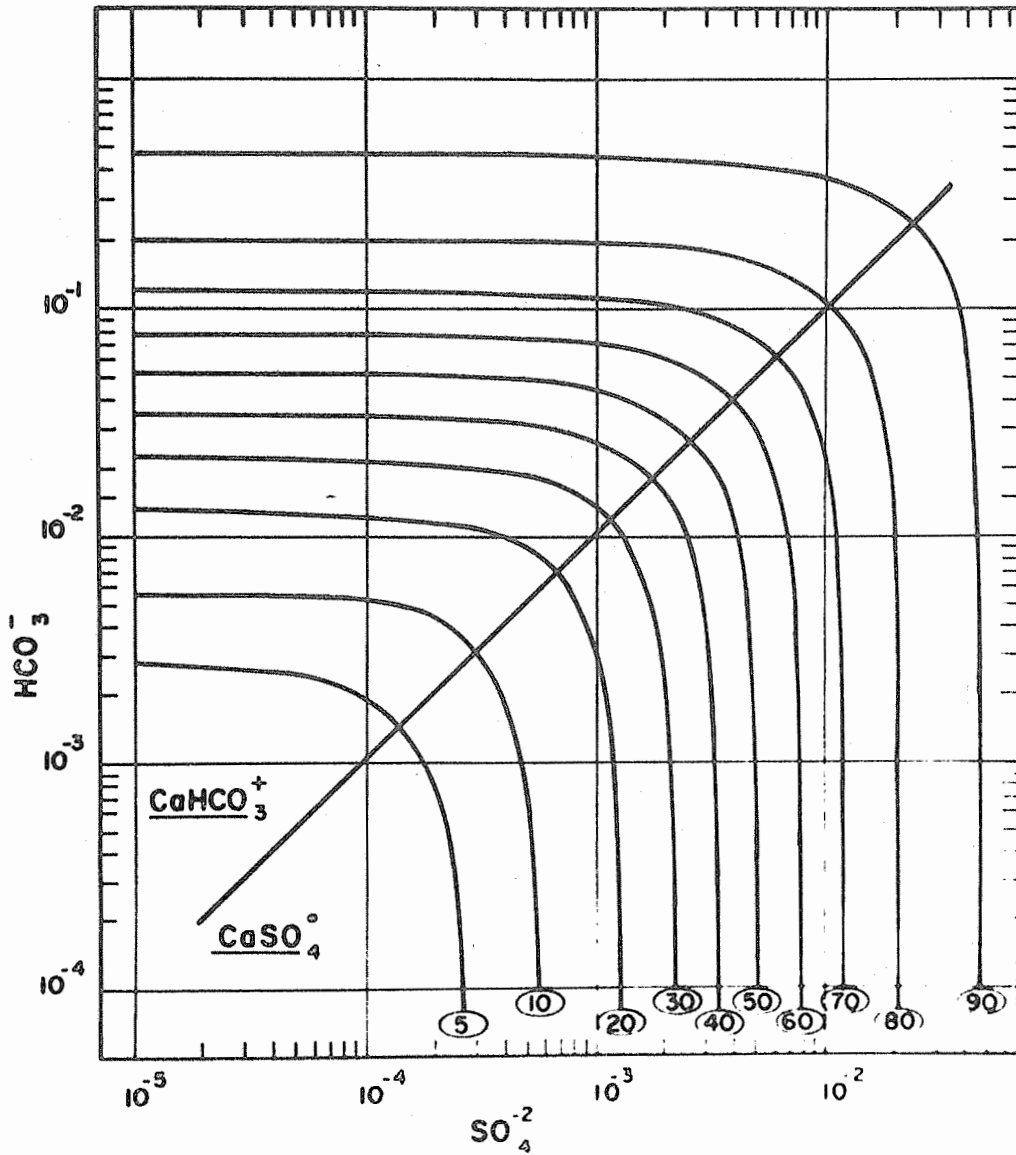


Figure 4. Distribution of  $CaSO_4^0$  and  $CaHCO_3^+$  as function of  $SO_4^{-2}$  and  $HCO_3^-$  activities.

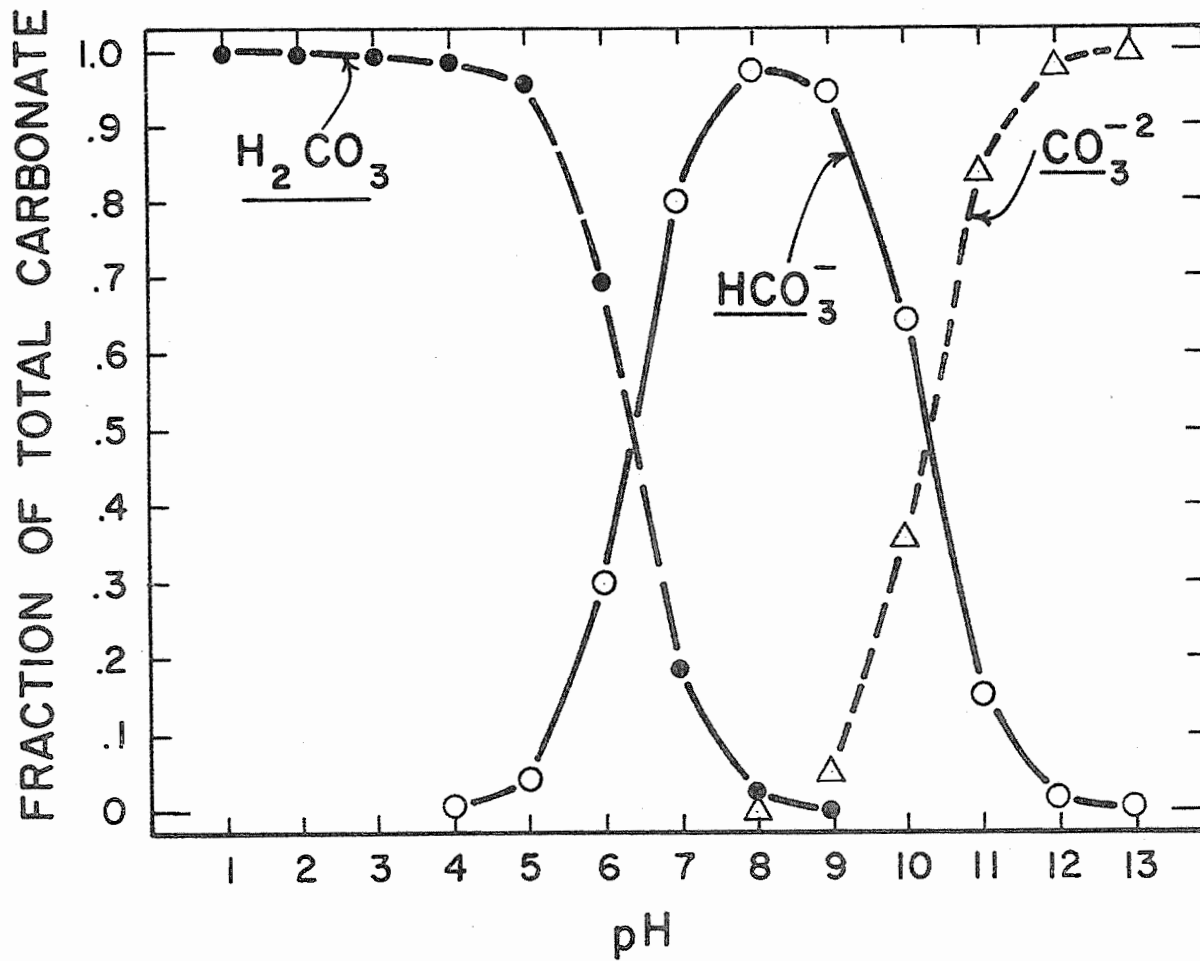


Figure 5. Distribution of  $\text{H}_2\text{CO}_3$  ( $\text{H}_2\text{CO}_3 + \text{CO}_2$ ),  $\text{HCO}_3^-$ , and  $\text{CO}_3^{2-}$  as function of pH.

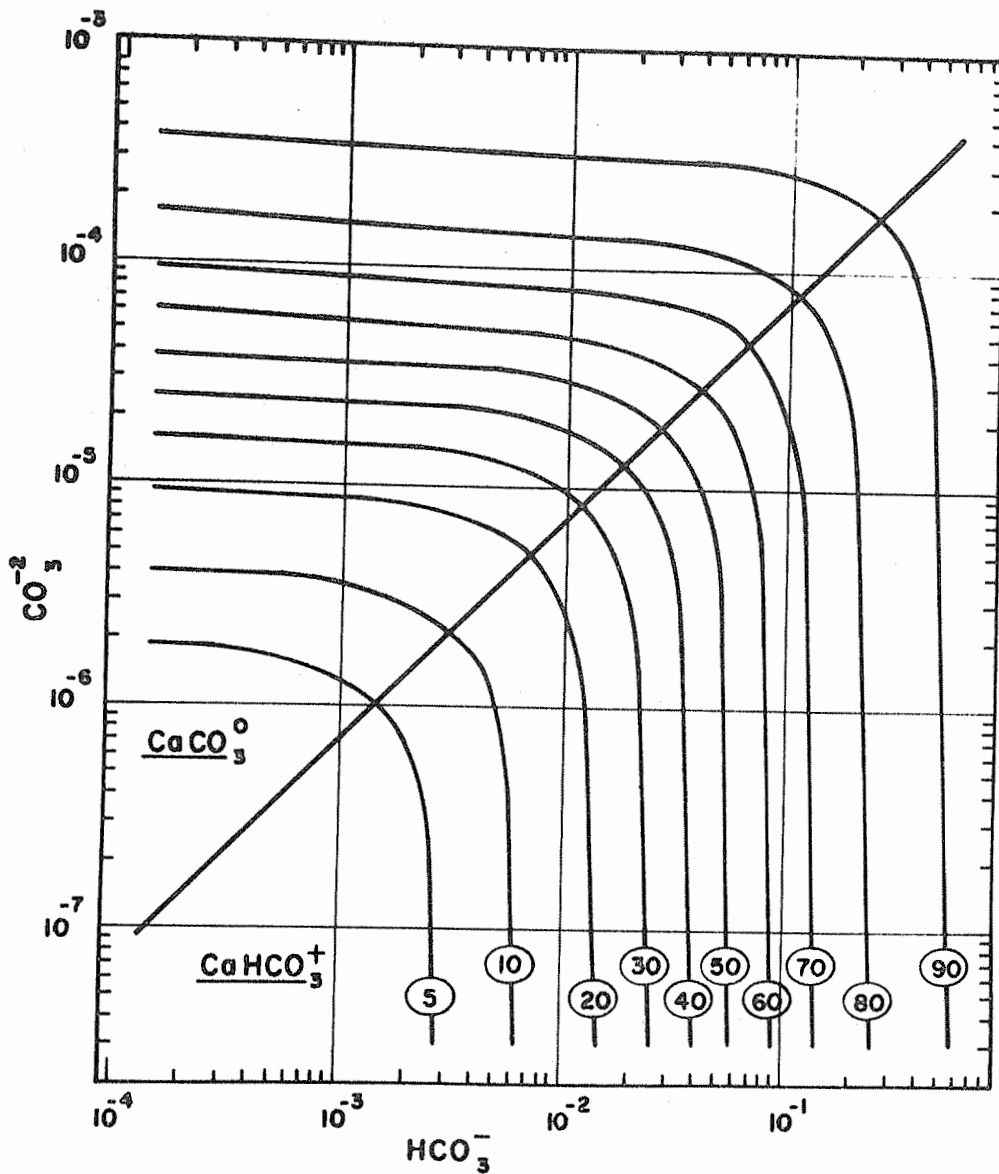


Figure 6. Distribution of  $\text{CaCO}_3^0$  and  $\text{CaHCO}_3^+$  as function of  $\text{CO}_3^{2-}$  and  $\text{HCO}_3^-$  activities.

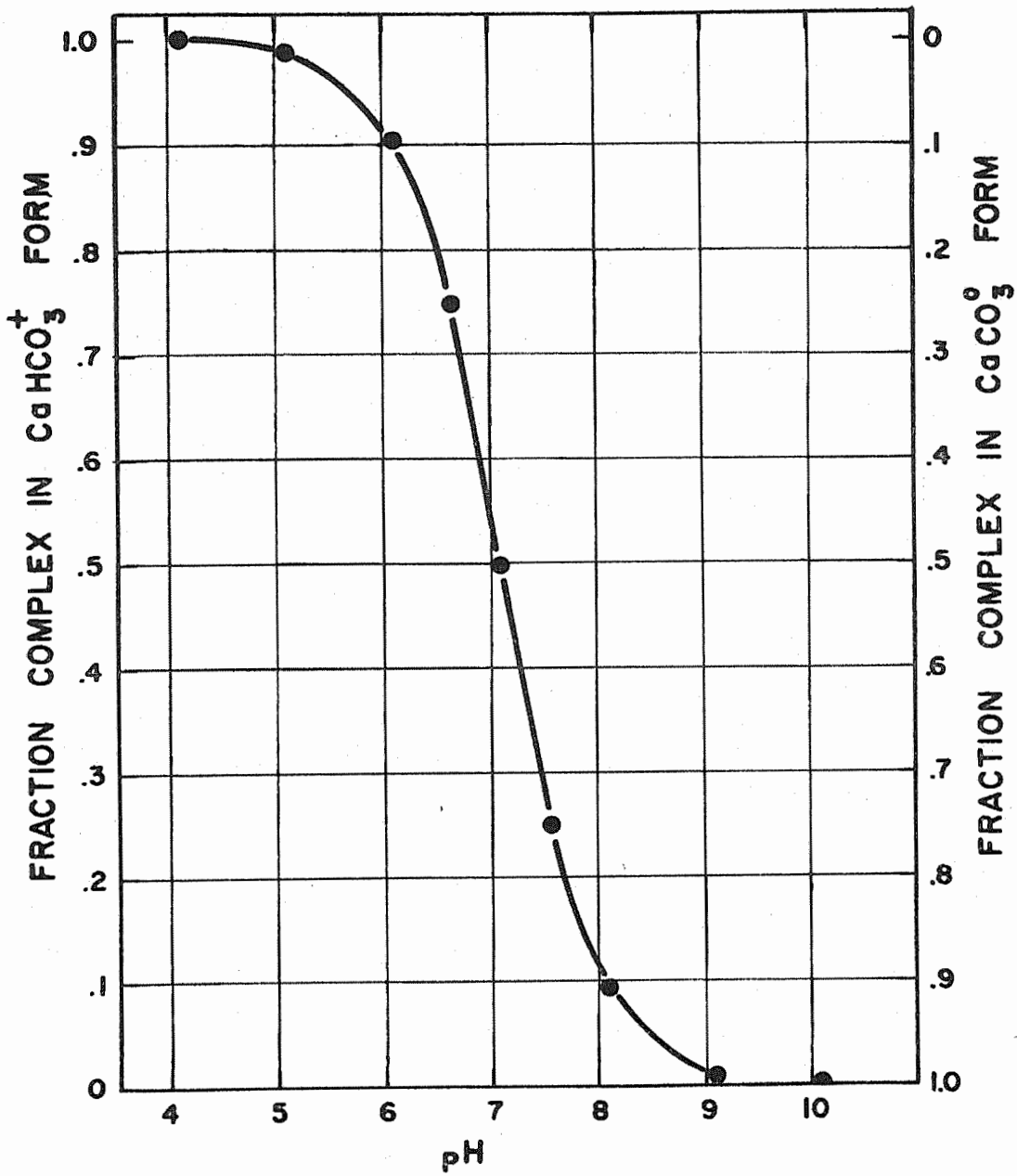


Figure 7. Distribution of  $\text{CaCO}_3^0$  and  $\text{CaHCO}_3^+$  as function of pH.

TITLE: MATERIALS AND METHODS FOR WATER HARVESTING AND  
WATER STORAGE IN THE STATE OF HAWAII

CRIS WORK UNIT: SWC W7 gG-4 CODE NO.: Ariz.-WCL 65-2

INTRODUCTION:

A description of the installation is given in previous annual reports. Data collected at the two sites by cooperators is forwarded monthly to the U. S. Water Conservation Laboratory for analysis. Both sites were visited by Laboratory personnel in February 1968 and in September 1968.

PROCEDURE:

There was no procedure change. See Annual Report for 1966.

RESULTS AND DISCUSSION:

Kukaiiau Catchment. The storage reservoir was completely full when inspected in February and September. The modified polyethylene sheeting on the catchment was in excellent condition in February 1968. The September inspection revealed that several of the seams were starting to fail. The reservoir lining material was still in excellent condition, although the problem of ground water seepage from the area around the pond collecting under the lining and causing the sheeting to balloon upwards, still exists. This does not appear to be causing any damage to the lining. For the period 1 January 1968 through 31 December 1968, a total of 2839.2 mm of rainfall was recorded. For the second year, over 7 million liters of water was collected from the combined catchment and reservoir.

Maui Catchments: For a description of the plots see previous annual reports. The Hypalon sheeting on Plot No. 1 has shown no indication of deterioration or damage. The material was found to be stretched taut when inspected because of shrinkage of the material.

Plot No. 2, covered with butyl, was in excellent condition when inspected in February 1968. The butyl was bonded quite well to the underlying soil. When the plot was inspected in September 1968,

there were a number of wrinkles in the sheeting which retained a portion of the rainfall. The retained water would then evaporate from the catchment between rainfall events. Also, a considerable quantity of soil had blown or washed onto the surface of the plot. This soil deposition was unexpected because the surrounding area is grassed.

The asphalt on Plot No. 3 was considered very good when inspected in February 1968. The base was quite firm and there were no signs of cracking or asphalt deterioration. There were approximately one dozen plants growing on the upper edge and berms of the plot. When inspected in September 1968, the plot had some spongy spots. Grass encroachment is a continuous problem.

Runoff data from the Maui plots were improved by the installation of new clocks on the recorders in February 1968. Analysis of the data is not completed, but some typical runoff data by weeks are presented in Table 1. For the period of 14 May 1968 through the week of 27 June 1968, a total of 130.8 mm of rainfall was measured. Percent rainfall runoff was: butyl - 98, asphalt - 97, and grass - zero. Soil washed or blown onto the butyl plot settles out in the flume as flow decreases and gradually plugs the tubing to the recorder stilling well. This caused the loss of some data. The personnel maintaining the recorders have been asked to keep tubing free.

For the year a total of 2100 mm of rainfall was recorded at the site. The 360 m<sup>2</sup> (428 yd<sup>2</sup>) plots of Hypalon, butyl and asphalt each collected over 750,000 liters (200,000 gal.). Even though the total rainfall at the site is quite high, inspection of the rain gage charts shows that most of the rain falls in small showers of less than 3 mm each. One exception the past year was on 11 March 1968 when over 140 mm of rain occurred in an 8 hour period.

#### SUMMARY AND CONCLUSIONS:

The experimental water harvesting structures installed in Hawaii in June 1966 were in excellent condition when inspected in September

1968. The Kukaiau catchment and storage combination on the Island of Hawaii has provided more than 7 million liters of water for livestock use. Minor seam failure was noted on the modified polyethylene sheeting in September 1968. The reservoir lining material has shown no signs of deterioration. Ground water seepage from outside the reservoir sometimes causes one area of the lining to balloon upward, but this has not damaged the lining.

The quality of runoff data from the four-plot test unit on the Island of Maui was improved by the installation of new waterstage recorder clocks in February 1968. Analysis of all runoff data is not complete at this time. Analysis of data for a period of 7 weeks starting 14 May shows that for a total measured rainfall of 130 mm, percent rainfall runoff from the plots was: butyl - 98, asphalt - 97, and grass - zero. Wrinkles in the butyl sheeting retain some water and reduce runoff efficiency. The asphalt plot is performing very well, but inspection in September 1968 indicated that the pavement may be starting to fail. Grass encroachment is also a problem. Even though the total rainfall at the Maui site is relatively high, over 2,000 mm annually, inspection of the rain gage charts shows that most of the rain falls in small showers of less than 3 mm each. This shows the desirability of a catchment treatment that causes nearly 100 percent runoff of small, low-intensity rain showers.

PERSONNEL: L. E. Myers and G. W. Frasier.

CURRENT TERMINATION DATE: December 1970.

Table 1. Rainfall runoff from 15 × 24 meter plots at the Maui test site.

Date	Total Rainfall	Butyl Plot Runoff		Asphalt Plot Runoff	
	(mm)	(mm)	(%)	(mm)	(%)
1968					
14 May	6.35	6.20	97.6	5.31	83.6
23 May	11.68	12.76	109.2	12.21	104.5
31 May	0.76	1.66	218.4	1.29	169.7
6 Jun	41.91	43.71	104.3	39.92	95.3
14 Jun	48.77	41.57	85.2	49.42	101.3
21 Jun	18.80	18.90	100.5	16.49	87.71
27 Jun	2.54	3.11	122.4	2.28	89.8
Total	130.81	127.91	97.8	126.92	97.0

TITLE: INTEGRATING VELOCITY PROFILE METERS.

CRIS WORK UNIT: SWC W10 gG-7

CODE NO.: Ariz.-WCL 65-3

INTRODUCTION:

See Annual Report for 1967.

The project has been inactive during the past year awaiting completion of a glass-sided tilting channel being constructed at the Laboratory.

PROCEDURE:

Further tests of the type previously made (see Annual Report, 1967) on shaped blades are planned, using the basic facilities now available with completion of the laboratory channel.

RESULTS AND DISCUSSION:

Channel Construction. The glass-sided channel is 123.5 cm (approx. 48 5/8 inches) wide, 60 cm (approx. 23 5/8 inches) deep, and 15.3 meters (approx. 50 feet) long. It is capable of slope variations up to 8%, and with special blocking, up to 10% or more.

Two welded steel trusses support the channel. The truss design was controlled by deflection limitations of not more than 0.012 foot at any point under the maximum anticipated design loads. The maximum depth of each truss is about 4 feet and the pair of trusses are capable of supporting a uniform load of 800 pounds per foot of channel while maintaining the above mentioned deflection limitations.

Special Features. The channel slope is adjusted by a special scissors jack built to accommodate existing vertical space limitations. The jack is capable of lifting between 8 and 20 tons, depending on the channel slope. The channel may be completely filled with water or a combination of water and sand when the flume is in the near level position. An overload spring device assists the jack in the low, or most disadvantaged position, but enough load is maintained on the jack to provide positive position control.

The entrance tank, built of 60-61-T6 aluminum, is designed to accept input flow through a distributor in the bottom of tank. The tank is approximately 8-feet tall, 5-feet long and as wide as the channel. Flow exits from the tank front at about the 5-foot level. The bottom entrance contraction to the channel from the tank has a radius of 2 feet. There are no side contractions for the flow. Side contractions were deliberately avoided in an attempt to eliminate cross-wave patterns in the channel.

The exit tank, also of aluminum, was built with two, 12-inch diameter butterfly valves in the bottom to control tail water elevations. By allowing the channel flow to enter a flooded tail water tank, the flow pattern would be somewhat less disturbed near the end of the channel than it would be if it were exiting over a weir or raised hinged floor section and thus would increase the usable length of the channel.

The sides of the channel are made of nominal 2-feet by 10-feet long, half-inch thick, plate glass panels. The floor is eight-inch thick stainless-steel sheets layed on half-inch steel plate. All water seals were made with a silicone caulking compound.

The hydraulic features include a maximum water flow rate of 10 cfs from a recirculatory pump and sump system. Flow will be metered to the channel through a 12-inch Venturi meter, a 4-inch turbine meter, or a 1.5-inch turbine meter for a total flow range from about 0.01 cfs (4.5 gpm) to 10 cfs (4500 gpm), to an accuracy of better than  $\pm 0.5\%$  of rate. The turbine meters are designed to be accurate to  $\pm 0.25\%$  of rate and operate up to about 1 cfs.

#### SUMMARY AND CONCLUSIONS:

The project has been inactive during the past year awaiting completion of glass-sided laboratory channel approximately 4-feet wide, 2-feet deep and 50-feet long. The channel has variable slope capabilities up to 10%, 10 cfs water supply, tail water control, and

measuring devices capable of accuracy to  $\pm 0.5\%$  of rate down to 0.01 cfs. The tilting channel will be used to test shaped-blade response to a variety of flows in several channel cross-sectional shapes that will be mounted in the tilting channel.

PERSONNEL: J. A. Replogle.

CURRENT TERMINATION DATE: December 1970.

TITLE:                   EXPERIMENTAL AND ANALYTICAL STUDIES OF THE FLOW  
                          AND OXYGEN REGIMES IN SOIL INTERMITTENTLY  
                          INUNDATED WITH LOW QUALITY WATER.

CRIS WORK UNIT: SWC W4 gG-1                   CODE NO.: Ariz.--WCL 66-1

INTRODUCTION:

The need for this study and the preliminary results are given in the 1966 Annual Report. The results of the numerical technique reported by Whisler and Watson (7) indicate that the numerical procedure gives a very good description of the drainage of vertical soil columns. This type of analysis is very complicated and needs the availability of a high-speed digital computer to be handled economically. Where one is interested in only total volumes and rates of drainage and infiltration, there are other simpler methods of analysis. There is a need to compare the results of these simpler methods against the more complicated numerical techniques and, where possible, against experimental results. If any of these simpler techniques are sufficiently accurate in predicting the amounts of drainage and infiltration under field conditions, then they may be used to predict the amounts of drainage and infiltration during intermittent inundation schedules. This report will be divided into two sections: (1) the first dealing with the comparison problem and (2) the second dealing with the intermittent scheduling problem.

PART I. COMPARISON OF METHODS FOR CALCULATING VERTICAL  
          DRAINAGE AND INFILTRATION INTO SOILS

THEORY:

The heading of this section is the title of a paper by Frank D. Whisler and Herman Bower, submitted to the Division for approval for publication in the Journal of Hydrology. This part of the report is a condensation of that paper. The

only methods of calculation studied were those with physical significance and physically measurable parameters. The methods of calculating the amount of drainage from a vertical soil column proposed by Youngs (8), Gardner (3), and Ligon, et al. (5) were compared theoretically to the numerical results and where possible to the experimental data. From a theoretical basis it can be shown that at the start of drainage the Gardner equation is off by a factor of 2; i.e., the prediction of the drainage rate is one-half of what it should be. No further comparisons were made using the Gardner approach.

In order to calculate the amounts of infiltration, the methods of Green and Ampt (4), as interpreted by Bouwer (1), and Philip (6) were used. These methods were compared to the numerical technique and, where possible, to experimental results.

#### RESULTS:

Figure 1 shows the amount of drainage,  $Q$ , versus time,  $t$ , as measured experimentally (solid curve), or calculated numerically (dashed curves), for a column of #17 sand. The curve labeled  $K_s$  used the water content - hydraulic conductivity - pressure head relationship for drainage from true saturation. The curve labeled  $K_r$  used the relationships for a column originally drained, rewet, and then drained again. This figure shows the good agreement between experimental and numerically predicted results. If the total amount of drainage from such a column,  $Q_{\infty}$ , is calculated by integrating the water content profile with depth at the start of drainage and subtracting the integral at equilibrium, a value of 33.65 cm is obtained. If the water content - pressure head relationship for drainage is replaced by a step function after the manner of Bouwer (2), a value of 41.90 cm is calculated

for  $Q_{\infty}$ . Figure 2 shows a comparison of the value of  $Q$  as calculated by Youngs' and Ligon's equations and that measured experimentally. It can be seen that the Youngs equation gave the best fit. An even better fit was obtained where  $Q_{\infty} = 33.65$  cm was used in the Youngs equation (although not as good as the numerical fit). In addition to better predicting the amount of drainage with time, the Youngs equation was also easier to use than the Ligon equation.

The amount of infiltration,  $I$ , versus time is shown in Figure 3 for a column of Botany sand as predicted numerically (solid curve) or by using the Green and Ampt equation (dashed curves). The dashed curves differ as to which value of the water-entry pressure,  $P_w$ , is used in the calculation, either the experimentally determined value or an estimate based on one-half of the air-entry pressure,  $P_a$ . In order to use the Philip method of predicting the amount of infiltration one needs the diffusivity - water content relationship, and thus needs the water content - pressure head relationship. For the Botany sand this latter relationship is almost discontinuous at the water-entry value,  $P_w$ ; i.e., a different value for the diffusivity is obtained depending upon the direction of approach. The two values of the diffusivity,  $D_o$ , are  $132,000 \text{ cm}^2/\text{day}$  and  $1,320 \text{ cm}^2/\text{day}$  when approaching  $P_w$  from right or left, respectively. Figure 4 shows the Philips equation predictions (dashed curves) compared to the numerical prediction (solid curve). The results using an intermediate value of  $D_o$  are also shown. It can be seen that the Green and Ampt predictions are as good as the Philip predictions and are easier to calculate. Other materials and comparisons are reported in the above-mentioned paper by Whisler and Bower.

## PART II. THE CALCULATION OF INUNDATION CYCLES

### THEORY:

From the previous study it was seen that the Youngs and Green and Ampt methods of calculating amounts of drainage and infiltration gave good agreement with experimental results and numerical analysis. On that basis one can calculate the amount of drainage from a resaturated soil column and the amount of infiltration up to the point when the column is resaturated (but still has entrapped air). The amount of additional water infiltrated after resaturation can be calculated using Darcy's law.

As the profile drains, approximately 240 mg of  $O_2$  enter the soil profile from the atmosphere per liter of drainage. This oxygen will be used to satisfy the total oxygen demand (TOD) of the sewage effluent that will enter the soil in the ensuing inundation period. For short inundation periods with complete aerobic digestion, the TOD can be calculated as the COD plus the oxygen for oxidation of ammonium to nitrate. If the inundation periods are sufficiently long for biodenitrification to occur, the TOD will be less because oxygen used for oxidation of ammonium to nitrate will subsequently be used to satisfy the COD.

When inundation is started, some of the air in the profile will escape to the atmosphere (bubbling phenomenon!). Also, perfect mixing of the oxygen in the soil profile and the downward moving effluent will probably not occur. Thus, it is necessary to introduce an efficiency term,  $E$ , which describes the fraction of the oxygen volume that entered the soil during a dryup that is used to satisfy the TOD of the effluent. Thus, each liter of air that has entered the soil can satisfy the total oxygen demand of  $240/TOD/E$  liters of effluent.

The amount of air entering during the dryup will be equal to the amount of water draining from the soil profile, which can be computed with Youngs' equation. The amount of effluent entering during inundation can be calculated with Green and Ampt's method. Thus, for a given value of  $240/TOD/E$ , length of dryup and inundation periods can be compared so that the oxygen that has entered during a dryup will be completely used by the effluent entering during the following inundation before a new dryup period is started.

The maximum volume of air that can enter during dryup is primarily determined by the depth of the water table. Thus, inundation schedules are principally controlled by the depth of the water table, the hydraulic conductivity of the soil, the TOD of the effluent, and the value of E. Quantitative information regarding E is scarce to nonexistent. Laboratory studies with soil columns intermittently inundated with sewage effluent are presently being conducted to evaluate E.

#### RESULTS:

Using data collected on the Salt River bed sand (see 1967 Annual Report) and the Youngs and Green and Ampt equations, the accumulated amount of drainage flow versus time was calculated as shown in Figure 5. In this figure it was assumed that it was 5 meters to the water table. If one assumed that the ratio of  $240/TOD/E$  was 1, the amounts of effluent in  $cc/cm^2$  per month versus the amount of effluent in  $cc/cm^2$  per cycle are shown in Figure 6 for infiltration rates of 1, 2, 4, and 8 ft/day. (The infiltration rates can be varied by varying the head.) Figure 7 shows the amounts of effluent recharged per month versus amounts of effluent per cycle in  $cc/cm^2$  for different ratios of  $240/TOD/E$ . A ratio of 0.5 indicates 0.5 ml of effluent per milliliter of air, whereas a ratio of

5 indicates 5 ml of effluent per milliliter of air. Figure 7 is calculated for a depth of 5 meters to the water table. Figure 8 shows the amount of effluent per month versus the amount per cycle for a ratio of 240/TOD/E of 5 for different depths to the water table. From these figures it can be seen that (1) the cleaner the effluent (the lower the TOD), the more can be recharged per month and per cycle, (2) the greater the distance to the water table, the more effluent can be infiltrated per cycle for a selected recharge rate, (3) the higher the infiltration rate, the more can be infiltrated per month and per cycle (all of which would be expected), and (4) short, frequent cycles yield more recharge per month than long cycles. An economic evaluation would have to be made to dictate the operating conditions in light of this latter point; also, oxygen diffusion, nitrate levels, soil clogging, and other factors have to be considered (see WCL 67-4).

#### SUMMARY:

The Youngs equation and Green and Ampt equation predict the amounts of drainage and infiltration with sufficient accuracy for many field situations. They can be used to predict the amounts of drainage and infiltration which occur during intermittent inundation with sewage effluent. By assuming sets of values for the total oxygen demand of the effluent, the efficiency of the utilization of oxygen in the soil profile, the hydraulic conductivity of the soil, and the water table depth, the long-term amount of effluent recharge can be computed for different operating schedules. Based on the oxygen use only, the short inundation periods and dryups will recharge more water than longer cycles. However, other effects such as oxygen diffusion, nitrates and soil clogging must also be taken into account.

REFERENCES:

1. Bower, Herman. Field measurement of saturated hydraulic conductivity in initially unsaturated soil. Proc., IAHS-UNESCO Symposium on Artificial Recharge and Management of Aquifers, Haifa, Isreal. pp. 243-251. 1967.
2. Bower, Herman. Rapid field measurement of air entry value and hydraulic conductivity of soil as significant parameters in flow system analysis. Water Resources Res. 2:729-738. 1966.
3. Gardner, W. R. Approximate solutions of a non-steady-state drainage problem. Soil Sci. Soc. Amer. Proc. 22:129-132. 1962.
4. Green, W. Heber, and G. A. Ampt. Studies on soil physics. I. The flow of air and water through soils. Jour. Agr. Sci. 4:1-24. 1911.
5. Ligon, James T., Howard P. Johnson, and Don Kirkham. Unsteady-state drainage of fluid from a vertical column of porous material. Jour. Geophys. Res. 67:5199-5204. 1962.
6. Philip, J. R. An infiltration equation with physical significance. Soil Sci. 77:153-157. 1954.
7. Whisler, F. D., and K. K. Watson. One-dimensional gravity drainage of uniform columns of porous materials. Jour. of Hydrol. 6:277-296. 1968.
8. Youngs, E. G. The drainage of liquids from porous materials. Jour. Geophys. Res. 65:4025-4030. 1960.

PERSONNEL: Herman Bower and Frank D. Whisler

CURRENT TERMINATION DATE: December 1970

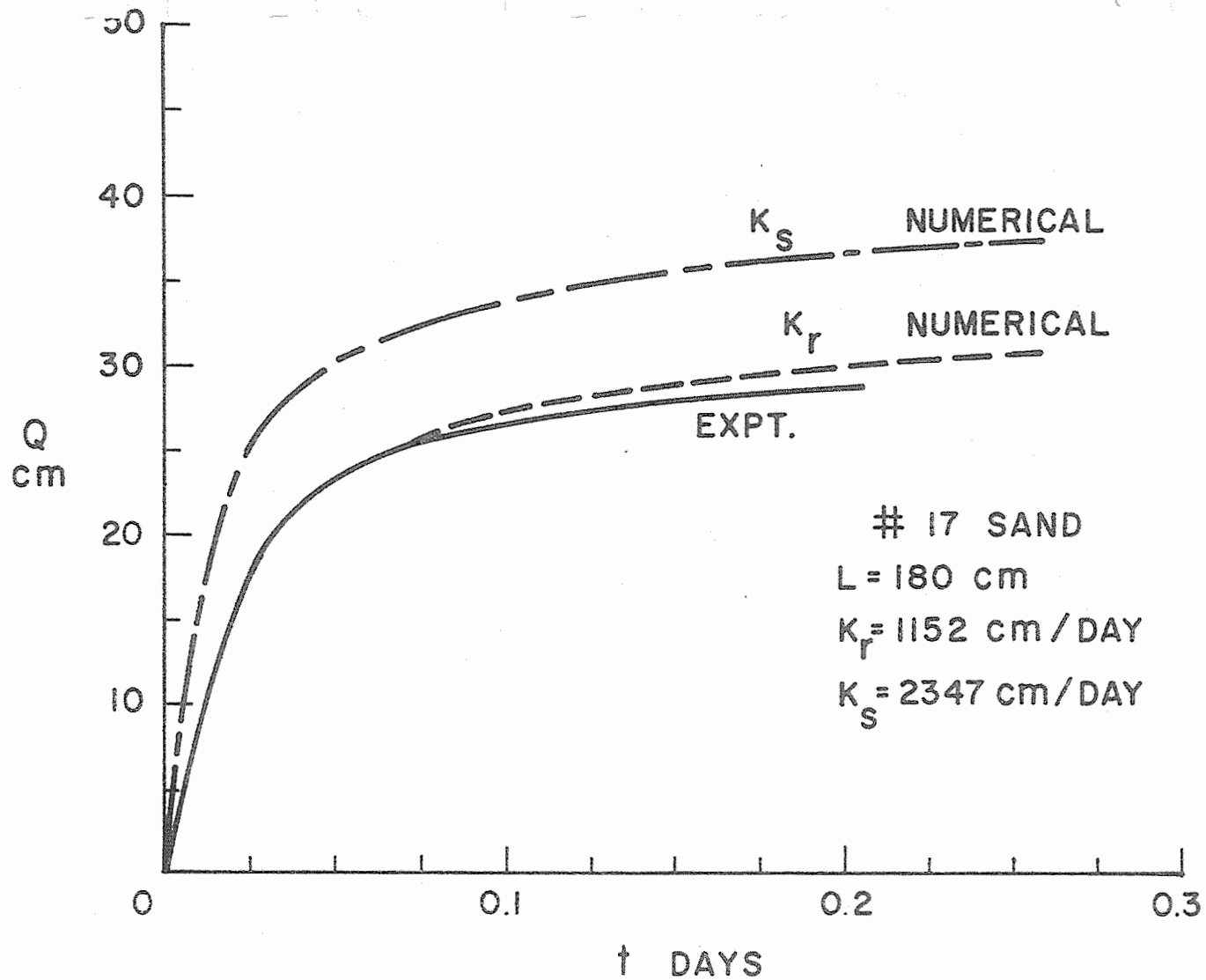


Figure 1. The amount of drainage versus time for #17 sand. The solid curve is the experimental observation. The dashed curves are numerical predictions using either saturated or resaturated curve data.

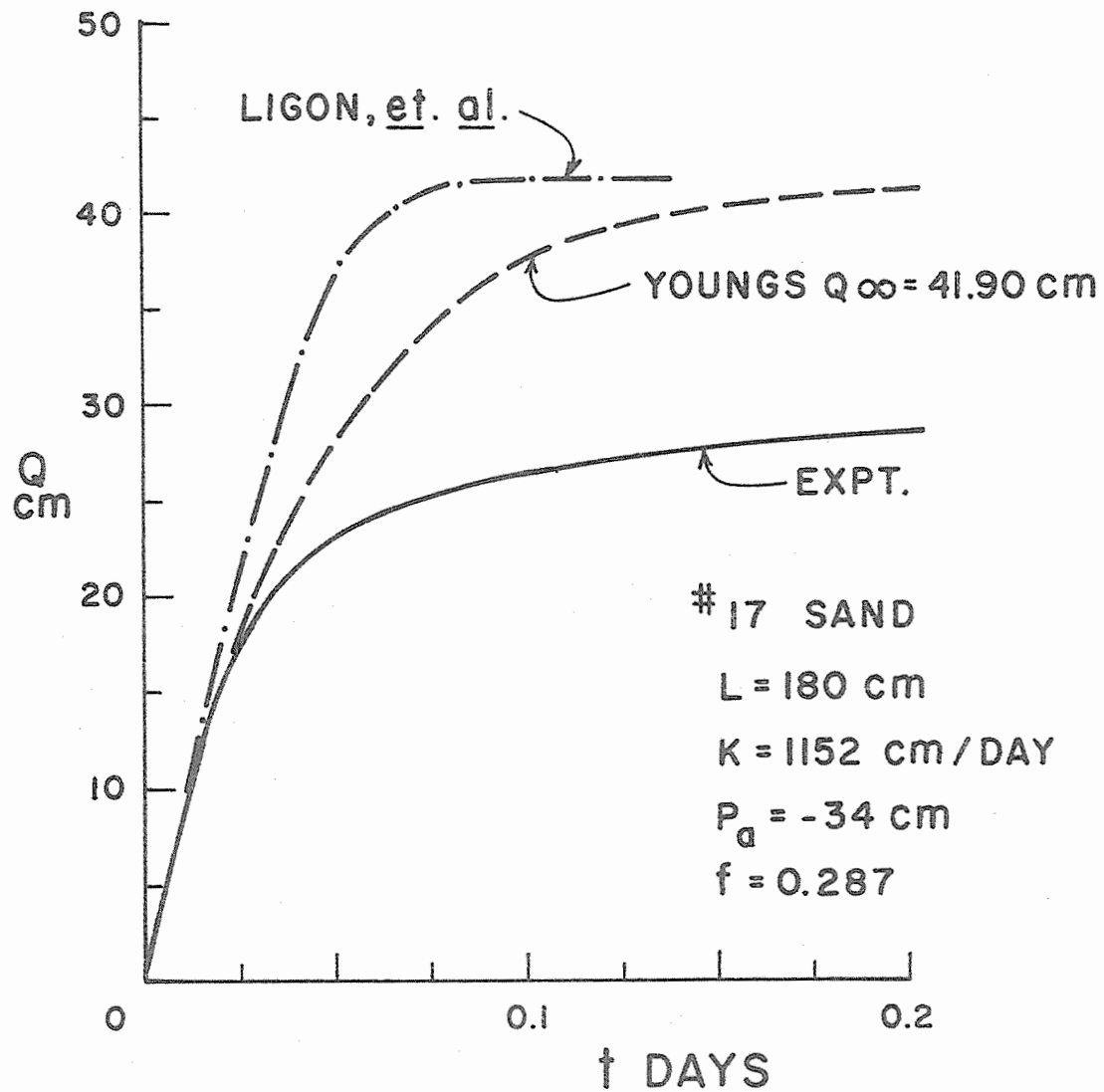


Figure 2. The amount of drainage versus time for #17 sand. The solid curve is the same as in Figure 1. The dashed curves are the Youngs and Ligon predictions, as indicated.

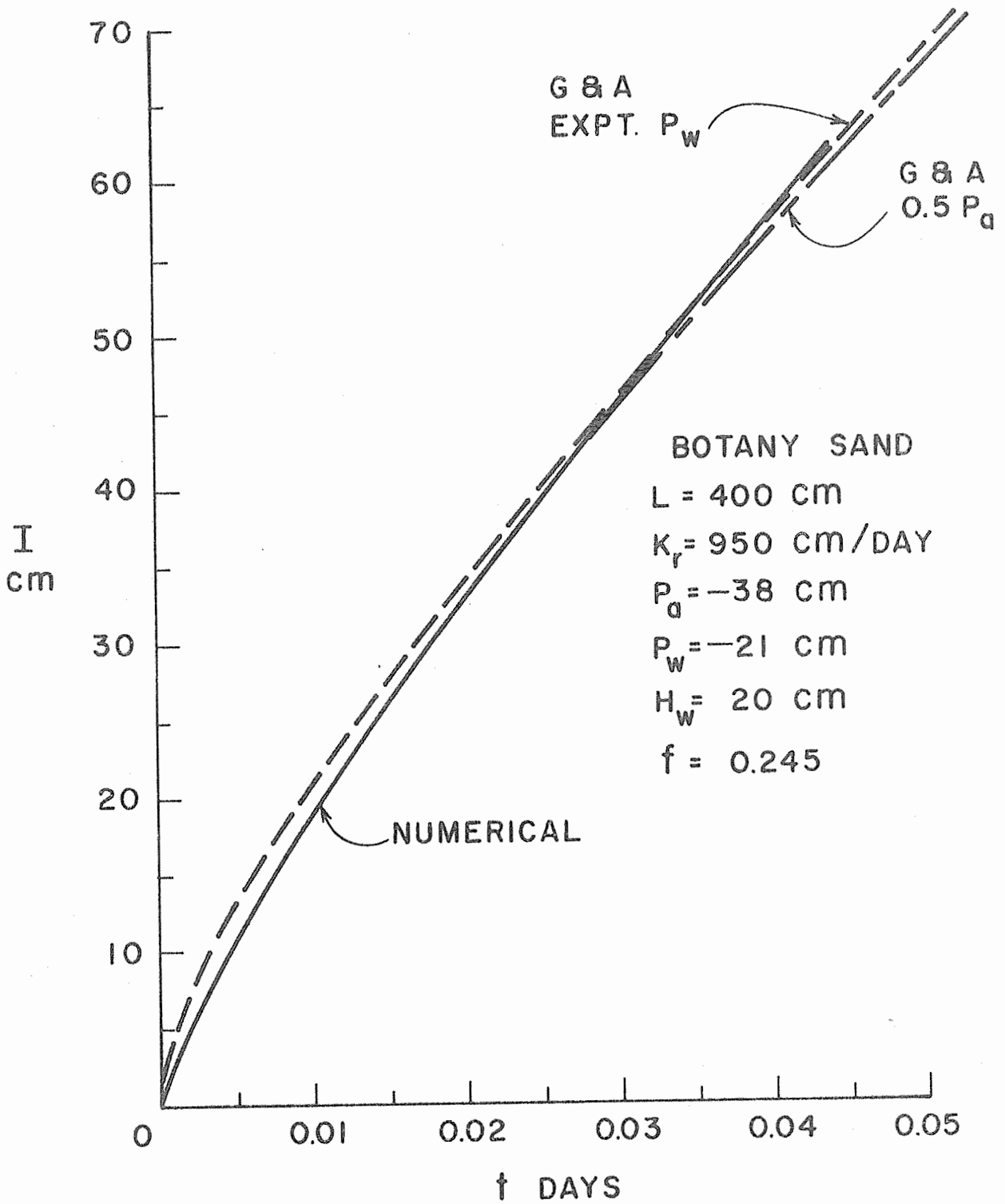


Figure 3. The amount of infiltration versus time for Botany sand. The solid curve is the numerical predictions. The dashed curves are the Green and Ampt predictions.

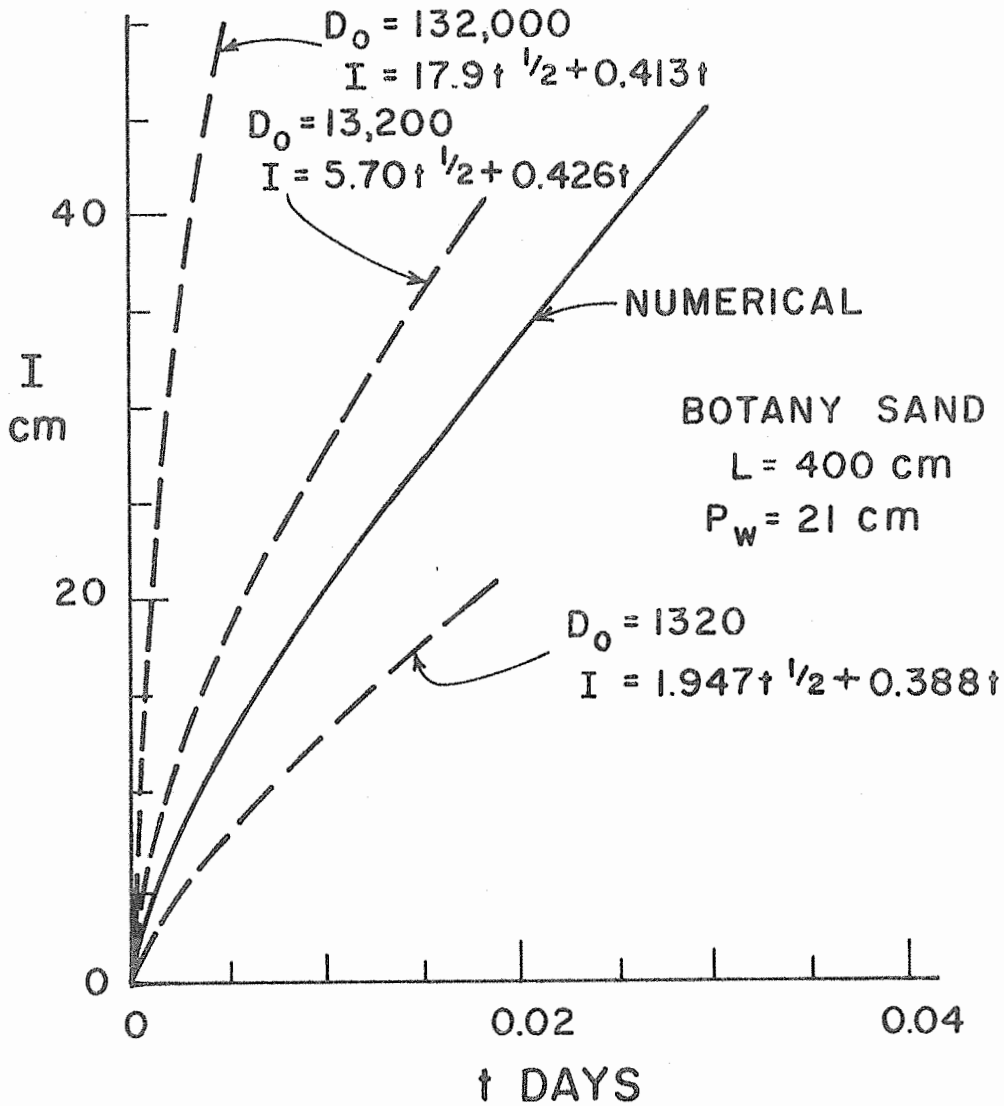


Figure 4. The amount of infiltration versus time for Botany sand. The solid curve is the same as in Figure 3, and the dashed curves are the Philip predictions.

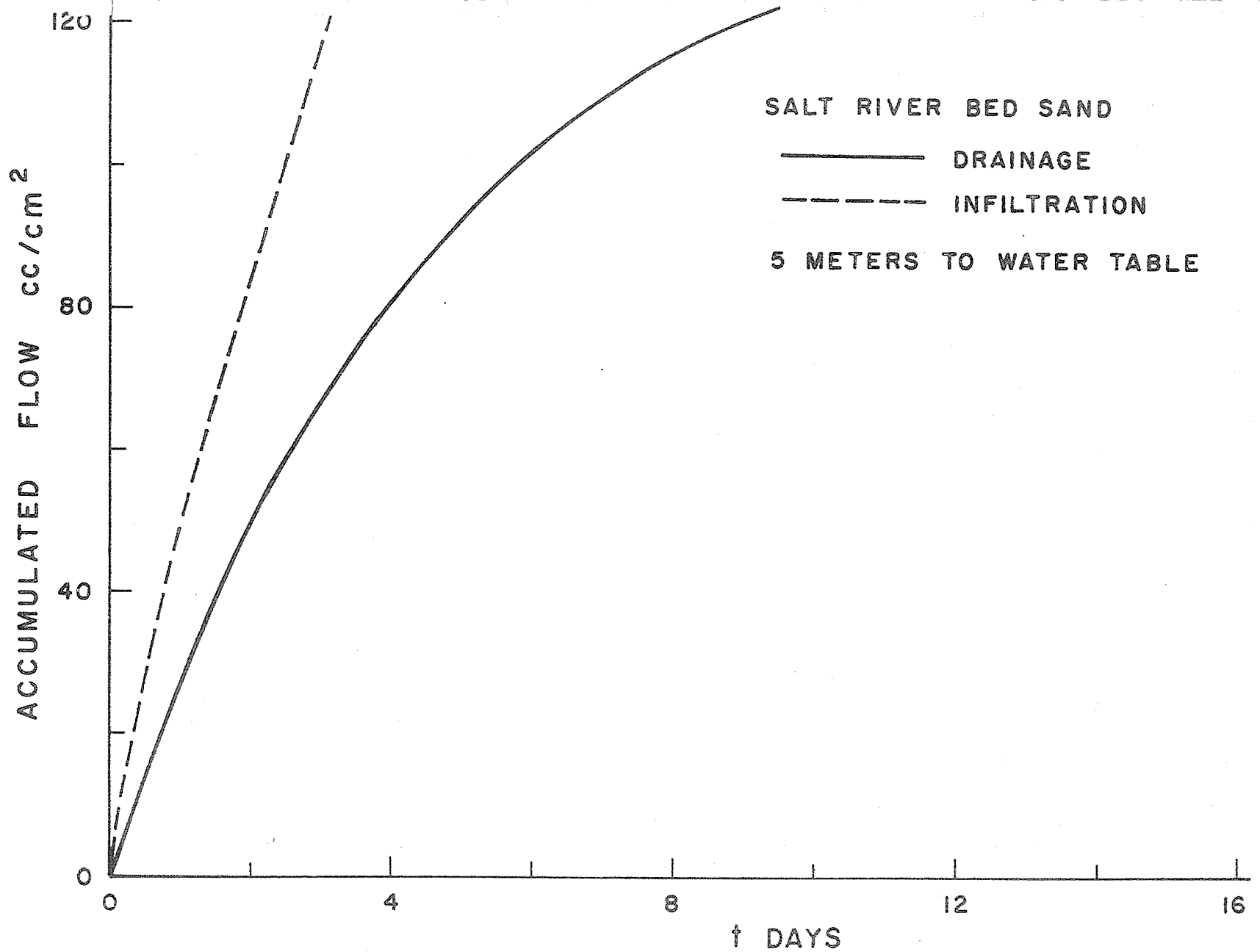


Figure 5. The accumulated amount of drainage or infiltration versus time for salt river bed sand.

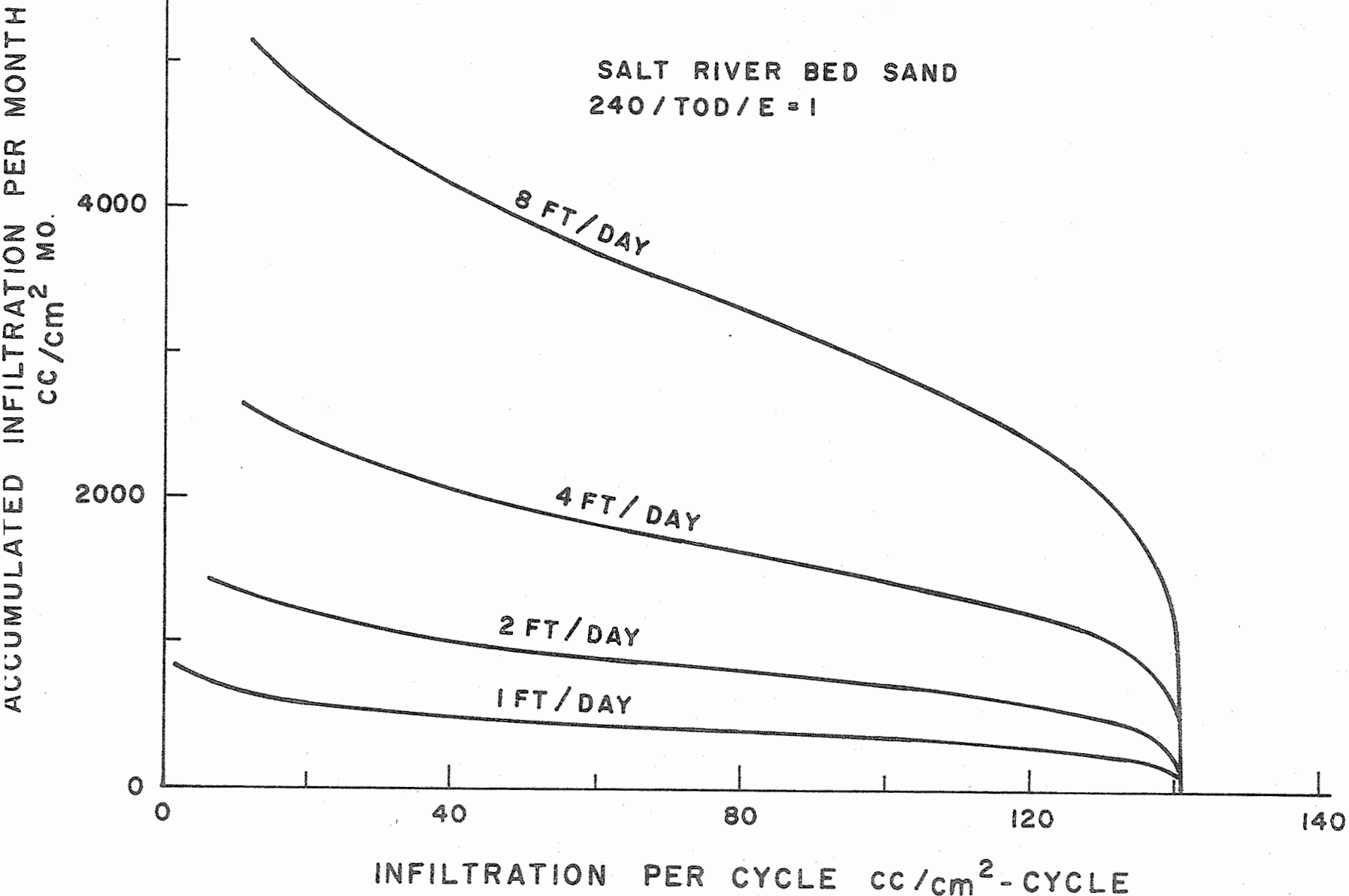


Figure 6. The accumulated amount of infiltration per month versus the amount of infiltration per cycle for the Salt River bed sand, assuming 5 meters to the water table and a ratio of  $240/10D^2/E = 1$ . The curves differ by the infiltration rate.

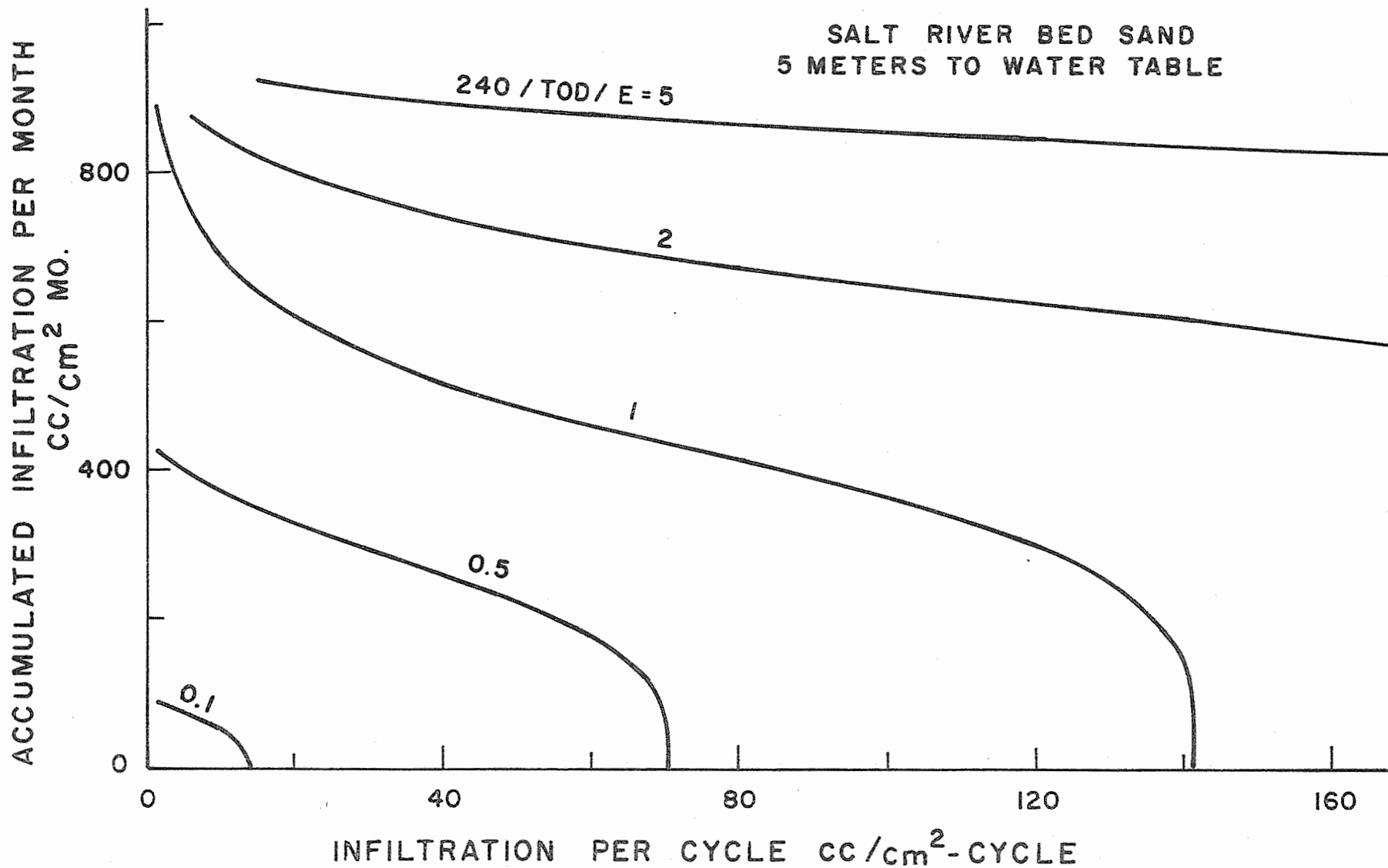


Figure 7. The accumulated amount of infiltration per month versus the amount of infiltration per cycle for the Salt River bed sand, assuming 5 meters to the water table and an Annual Report of the U.S. Water Conservation Laboratory. The curves differ by the ratio of 240/TOD/E.

SI-77

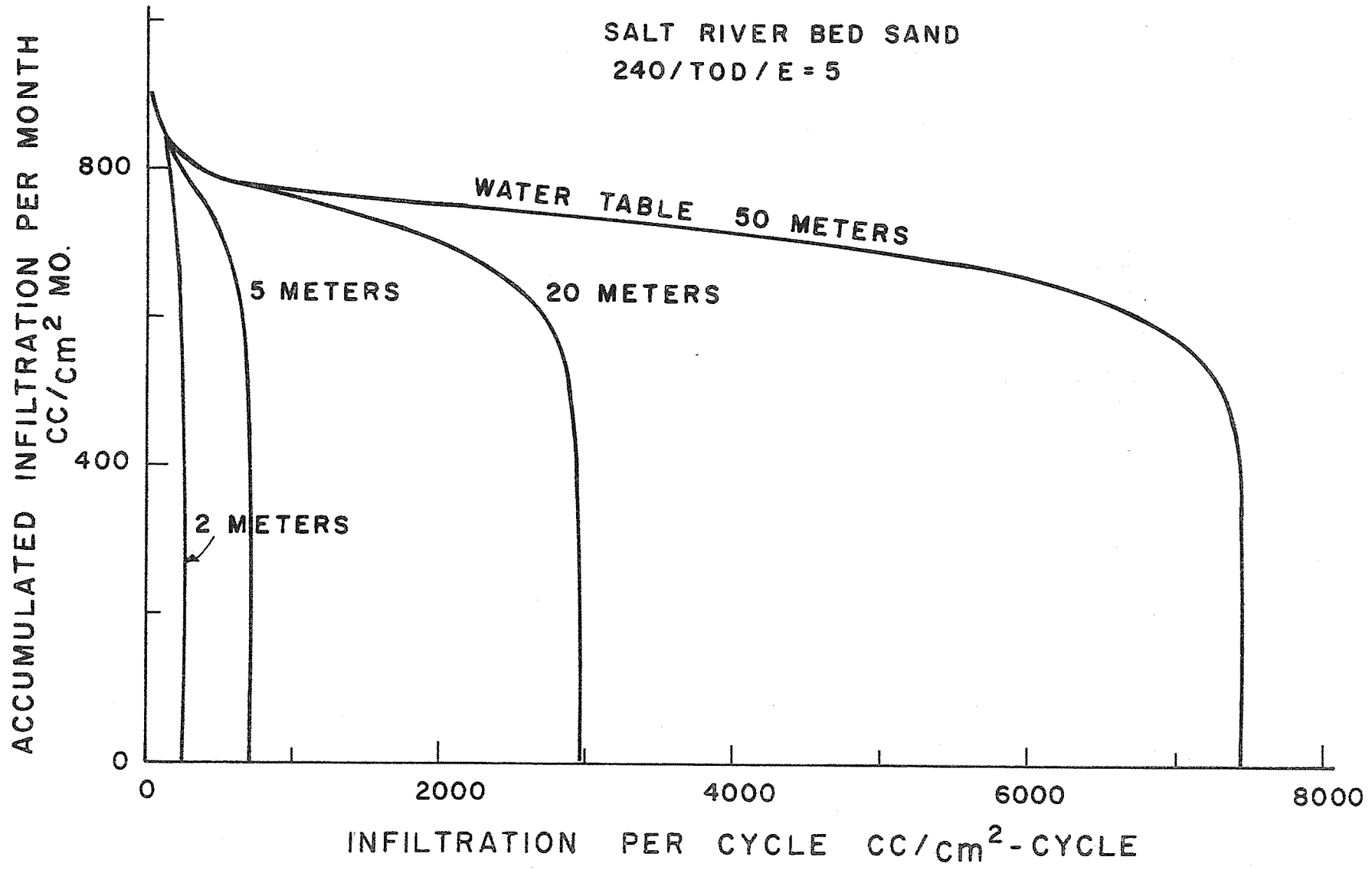


Figure 8. The accumulated amount of infiltration per month versus the amount of infiltration per cycle for the Salt River bed sand, assuming an infiltration rate of 1 ft/day and a ratio of 240/TOD/E = 5. The curves differ by the depth to the water table.

TITLE: IRRIGATION OUTLET STRUCTURE TO DISTRIBUTE WATER  
ONTO EROSIVE SOILS.

CRIS WORK UNIT: SWC W10 gG-7 CODE NO.: Ariz.-WCL 66-2

INTRODUCTION:

For need of study, see Annual Report, 1966.

OBJECTIVES:

1. To obtain design criteria for low-cost irrigation outlets that will distribute large streams of water without excessive erosion.

PROCEDURE:

The major activity on this project has been to construct outlets at farm sites where erosion problems exist, observe their operation, determine their weaknesses, then repair or reconstruct them and continue to observe. Nearly twenty structures remained after the 1967 season. These were observed throughout 1968, and twelve new outlets were constructed. One structure on the Bruce Church Ranch and two on the Currie Ranch were for 18-inch outlets carrying 8 cfs streams from main supply ditches constructed on high railroad fills. The three new structures on the Floyd Sparr Ranch were for 18-inch outlets carrying 5 cfs streams, vulnerable to machinery damage and subject to high back-up water. Two square dissipator boxes were used and one chip-out equipped with a flat front. All aprons were 30 inches and stepped down.

Four new structures were built on a proposed 6,000 acre citrus ranch now under development. These consisted of two standard concrete-type structures, one fiber glass structure covered with SS-2 anionic asphalt emulsion, and one structure with only a high-dissipator box equipped with an 18-inch apron with no back or shoulders. Two of these structures were built in cooperation with Soil Conservation Service personnel, who have designed, planned and built 16 types of structures and established various outlet elevations on this ranch, owned by Taubman and Parker.

Two new structures were built on the Spencer and Spencer Ranch, one using the fiber glass and SS-2 asphalt on a standard plan, and the other using a high dissipator box with 18-inch apron and no back or shoulders.

Additional investigations were made on the Bruce Church and Bob Woodhouse ranches relative to structures for preventing erosion by water from 3-foot-wide jack gates.

**SUMMARY AND CONCLUSIONS:**

Structure inspections this year complement last year's results, showing that a square dissipator box attached to an outlet tile, then equipped with appropriate back, shoulders and a step-down apron, will discharge a non-erosive stream of water.

The major problems connected with these structures are those of Bermuda grass, machinery breakage, and perhaps the labor problems associated with construction. The step-down apron has solved the problem of platform breakage by machinery but not the machinery shoulder breakage problems. By placing a small amount of wire or metal on the edge of the dissipator boxes where the platform attaches, Bermuda grass emergence has been prevented. The problem of cement cracking can probably be solved by using thicker concrete, reinforcing, or by doing a better job of packing the soil adjacent to the concrete. It is hoped the use of fiber glass and SS-2 asphalt will cut down labor construction requirements.

PERSONNEL: Leonard J. Erie and John A. Replogle.

CURRENT TERMINATION DATE: December, 1970.

TITLE: FLOW MEASUREMENT IN OPEN CHANNELS WITH CRITICAL  
DEPTH FLUMES.

CRIS WORK UNIT: SWC W10 gG-7

CODE NO.: Ariz.-WCL 67-1

INTRODUCTION:

Previous reports (see Annual Reports for 1966, 1967) summarized results of studies on critical-depth flumes of the trapezoidal throated type. The term "trapezoidal" is used here to include the limiting cases of triangular-throated flumes and rectangular throated flumes.

A technical paper titled "Flow measurements with critical-depth flumes" was presented before the U. S. Committee of the International Committee on Irrigation and Drainage and was subsequently submitted for the VII Congress ICID, Mexico City, April 1969. The paper included results for studies on eight sizes of flumes, all triangular throated except one, which was a trapezoidal throated flume patterned after a flume used by the U. S. Bureau of Reclamation (USBR). The report presents the theoretical aspects for predicting the calibration results for flumes and summarizes the effects of installation anomalies. These include effects of torsional twist of the flume, deflection of the sides, elevating or lowering the outlet end, sedimentation in the flume, approach conditions, removal or addition of diverging sections at the outlet, and submergence.

A second paper submitted as a discussion of the "Rectangular cut-throat flow measuring flumes" by G. V. Skogerboe and Leon Hyatt, (published December 1967 by ASCE) was published in the September 1968 issue of the American Society of Civil Engineers Proceedings, Journal of the Irrigation and Drainage Division (Vol. 94, No. IR3). The discussion cautioned against using the high-water mark in ditches and streams to determine if free-flow will exist through a flume to be installed and thus avoid submergence, as advocated by the authors. In many cases, the flow depth that should be checked is the low flow rates or perhaps some mid-range rate, depending on the shape of the flume throat and the shape of the ditch into which it is to be installed.

## PROCEDURE:

The laboratory calibrations were accomplished as previously described using a weighing system to determine discharge rate. Head in the flumes was referenced to the bottom of the outlet end of the throat section, but measured in the approach section of the flume by means of a stilling well and point gage.

Theoretical studies were extended to include prediction of calibration curves for circular-throated flumes. Computer programs were written in BASIC for both trapezoidal and circular throated flumes. The computer was also used to evaluate effects of friction through the flume and velocity distribution in both the approach section and throat section of the flume. The friction evaluation depends somewhat on the "model" chosen to represent the actual losses. A boundary-layer model appears to give the best and most consistent results so far devised. With this "model", various shapes of flumes were subjected to the computation procedure in order to study characteristic trends in friction losses with changes in flow depth.

## RESULTS AND DISCUSSION:

The computer programs developed were rather simple in that they solved the previously derived equations with a routine iteration process. There was no problem with convergence when solving for any of the trapezoidal types of flumes. Some difficulty was encountered in getting the solution for circular throated flumes to converge. Even these converged if the initial guess was good enough. Considerable effort was required to determine what caused divergence and how to prevent it for the particular equations involved. A simplified flow diagram appears in Figure 1 for the circular flumes. The flow diagram for rectangular flumes is similar except the subroutine portion is less complicated. Listings of the BASIC language programs for both are included in Appendix A and B.

Laboratory Calibrations. Several additional calibrations were made since the previous report on flumes of various designs and sizes.

1. Trapezoidal Flume. The flume that was built to the dimensions of the USBR flume (see Annual Report, 1967) has been tested. The calibration agrees with the theoretically derived equations, but differs from their results by as much as 6 or 7 percent. Because the USBR flume had downstream sections, it was suspected that these may have produced the difference, although theoretically they should not.

An additional (divergent) section was added to the constructed model. At heads of 1.3 feet, a decrease of approximately 0.003 feet could be detected in the stilling well when the end section was removed. This might be expected, based on curving streamlines and the experience with other flumes concerning flow depth and throat length. However, based on the same experience, the difference should not have been detectable at a head of 0.5 feet, but differences of as much as 0.002 feet were noted. This has yet to be entirely resolved.

2. Triangular Flume. Some flumes, intended for field plot studies, were constructed by the Southwest Irrigation Field Station at Brawley, California. Through an undetected dimensioning error, part of the flumes were constructed with 53.5 degree openings, instead of the intended 60°. Theoretical curves were provided and one of the deviates brought to the Laboratory for verification. The results agreed with the theoretical calibration.

3. Circular Throated Flumes. Two flumes, each with a circular approach section and a circular throat section connected by a truncated-oblique-cone transition section, have been built and tested. Their application to sewer flows and tile drains seems promising. As with the other flumes, the bottom points in the flume sections are in the same horizontal plane permitting complete drainage of the upstream channel when flow is discontinued.

One flume had a 12-inch diameter pipe two-feet long for the entrance section and a 10-inch diameter pipe, also two-feet long, for the throat section. The other flume used an 8-inch diameter pipe in

the throat section. Neither flume was fitted with divergent sections or downstream piping beyond the throat section.

With the first mentioned flume, standing waves were present in the approach section and the calibration was not stable, especially at low flow rates. The Froude number in this section was calculated to be about 0.67 at the lowest flow rate to about 0.58 at the highest flow rate. This would appear to be low enough to avoid any problems with standing waves. Further calculations revealed that critical depth in the flume at say 0.30 foot of head was 0.24 foot, a difference of only 0.06 foot. The abrupt entrance to the approach section from the supply tank could easily cause a disturbance in the water surface of this magnitude and maintain the condition of standing waves at relatively low Froude numbers.

It appears that knowledge of the Froude number is insufficient and that some information on the size of disturbances is necessary. If the disturbances initiate a wave whose depth is nearly the same size as the difference between the mean flow depth and critical depth, then the water surface will not be stable enough to get a good reading on the depth in the approach section.

The flume whose throat was 8 inches in diameter had much less tendency to form standing waves. At the same head of 0.3 foot referred to above for the first flume, the difference between critical depth and head was about 0.87 foot. This proved to be adequate for this particular installation. In long pipeline approaches, the problem should be decreased if the interior of the pipe has few abrupt joints in the vicinity of the flume.

4. Friction Loss Studies. Recognizing that friction losses occur between the point of depth measurement and the point of critical depth, some method of estimating the loss was sought. The reference literature (see Annual Report, 1966, Reference (2), Ackers and Harrison's report)) proposed a boundary layer development method that was used as the model for this study. The flumes were calibrated and

the results compared to theoretical, frictionless, flow calculations, that is, with no terms included to allow for friction losses, velocity distribution in the throat, or velocity distribution in the approach section. The difference obtained by this comparison was attributed to these three possible causes. Assuming the velocity distribution coefficients to be unity, the general effects of the expected friction loss as calculated with the boundary layer model is shown in Figure 2. The length of throat,  $L$ , divided by the roughness height,  $k$ , is indicated in the figure. The significance of the figure lies in the general shapes of the various characteristic curves. The curves for triangular and trapezoidal flumes indicate an almost constant deduction for friction loss regardless of flow depth.

The rectangular and circular flumes indicate increasing friction with increasing depth. Measured values for the 8-inch circular flume, calculated as stated above, are shown for comparison. Trapezoidal flume measurements, not shown, had the indicated trend but were about 50% lower than calculated. The rectangular trend line shown is for a narrow flume and can be changed to almost horizontal if the throat is wide compared to its length; this appears to be about 30:1.

Associated with the friction-trend study is the study of the effects of velocity distribution in both the approach section and the throat section of the flumes. This is a computer oriented study which has not been completed. Preliminary results would indicate only minor effects from this source. The effect of a high value for the velocity distribution coefficient in the approach section appears to cancel some of the effect noted for friction losses, whereas, the effects of a high value in the throat section adds to the effects of friction. Both effects are nearly linear with flow depth for given values of the coefficient.

5. Field Installations. Flumes have been installed in consultation with the Laboratory in several locations. A concrete, 50° opening, triangular flume was installed near Beardsly, Arizona, on

an irrigation project. Several have been installed in connection with other Laboratory field studies located on Hawaii, the San Carlos Indian Reservation, and on the Granite Reef experimental plots. The head detecting method has given trouble on almost all the sites. The piezometer tap tends to plug if there is sediment in the flow. Other means of head detection should be studied.

The city of Tempe, Arizona, has adapted the design for use in measuring sewage flows. The detecting device is a float placed directly in the flow. It clears floating debris fairly well. Some sedimentation upstream is occurring.

#### SUMMARY AND CONCLUSIONS:

Stage-discharge relations for critical depth flumes generally have been determined empirically because the application of the theoretical equations was tedious and required detailed computations. With the aid of computers, the theoretical knowledge can now be applied routinely. In general, a computation of the minor friction losses through a flume permits the application of energy concepts to predict the laboratory calibration to within  $\pm 2\%$  for a flow range that frequently exceeds 100:1, depending on the flume size. In many cases, for heads exceeding one-foot deep, the energy equations are sufficiently accurate even when the friction loss is ignored.

For the low-flow rates and the instances where maximum accuracy is desired, methods of predicting the friction loss are being investigated. Preliminary tests and laboratory calibrations have been completed on trapezoidal, triangular, and circular throated flumes. A friction loss computation model based on boundary layer development appears to give the most consistent results. The calculated values and those obtained from the calibration data have similar trends but do not necessarily agree in absolute value, the measured values being as much as half the computed values. This difference is usually not serious since large variations in the friction losses are required to cause significant changes in the calibration.

PERSONNEL: J. A. Replogle

CURRENT TERMINATION DATE: December 1970.

APPENDIX A  
Circular Flumes

CIRC            21:10    PX SYSF 9/02/68

```

100 READ D1,D3,S,I,L,R,G
101 DATA 1,.833333
102 DATA .05,.05,.75
103 DATA 6,32.16
110 LET A=0
120 LET L1=0
130 LET E=1E-6
135 LET Y0=S-I
140 LET Q=0
150 LET Y0=Y0+I
160 LET Y1=Y0
170 LET K=1
180 LET Y=Y1
185 GOSUB 700
190 LET F=Q/(A1*SQR(G*A1/T1))
200 LET F= INT(F*10↑4+.5)/10↑4
270 LET Q=INT ( Q*10↑R + .5 ) / 10↑R
280 IF K=1 THEN 310
290 LET Q4=Q
291 LET Y5=INT(Y3*10↑4+.5)/10↑4
295 LET F4=F
300 GOTO 380
310 LET Q1=Q
311 LET Y6=INT(Y3*10↑4+.5)/10↑4
320 LET Y4 = Y0 + 45*I
325 LET F1=F
330 IF Y4>L THEN 370
340 LET K=4
350 LET Y=Y4
355 LET F1=F
360 GOTO 185
370 LET Q4=Q
380 LET L1=L1+1
390 IF L1 =1 THEN 410
400 GOTO 450
410 LET A=A+1
411 PRINT "CIRCULAR FLUME:  D1=";TAB(21);D1;TAB(38);
412 PRINT "D3=";TAB(42); D3; TAB(64);"PAGE " ;A
413 PRINT
420 PRINT"    Y-F            Q        CRITICAL FROUDE *";
421 PRINT TAB(38);"Y-F            Q        CRITICAL FROUDE"
430 PRINT"    FT.            CFS        DEPTH-FT NO.AT Y*";
431 PRINT TAB(38);"FT.            CFS        DEPTH-FT NO.AT Y"
440 PRINT "=====*"
441 PRINT "=====*"

```

APPENDIX A (continued)

```

450 IF D4=0 THEN 480
460 PRINTTAB(1);Y1;TAB(8);D1;TAB(17);Y6;TAB(26);F1;TAB(34);"*";
461 PRINT TAB(36);Y4;TAB(43);D4;TAB(52);Y5;TAB(61);F4
470 GO TO 490
480 PRINTTAB(1);Y1;TAB(8);D1;TAB(17);Y6;TAB(26);F1;TAB(34);"*"
490 IF (L1/5)-INT(L1/5)=0 THEN 510
500 GO TO 520
510 PRINT
520 IF L1=45 THEN 540
530 GO TO 590
540 FOR P=1 TO 7
550 PRINT
560 NEXT P
570 LET L1=0
580 LET Y0=Y4
590 IF Y0>=L-I THEN 999
600 GO TO 140
700 LET T1=2*SQR(D1*Y-Y*Y)
710 LET X9=(2*Y/D1)-1
720 LET S9=ATN(X9/SQR(1-X9*X9))
730 LET A1=(2*Y-D1)*T1/4 + D1*D1*3.14159/8 + S9*D1*D1/4
731 LET T2=2*SQR(D3*.8*Y-.64*Y*Y)
732 LET X7=(2*Y*.8/D3)-1
733 LET S7=ATN(X7/SQR(1-X7*X7))
734 LET A2=(2*.8*Y-D3)*T2/4+D3*D3*3.14159/8 + S7*D3*D3/4
735 LET D=SQR(A2+3*G/T2)
736 LET A3=A2
737 LET T3=T2
740 LET H3=Y+D*0/(2*G*A1*A1)
750 LET Y3=H3- A3/(2*T3)
751 LET C=0
760 LET T3=2*SQR(D3*Y3-Y3*Y3)
770 LET X8=(2*Y3/D3)-1
780 LET S8=ATN(X8/SQR(1-X8*X8))
790 LET A3=(2*Y3-D3)*T3/4+D3*D3*3.14159/8 + S8*D3*D3/4
800 LET Y9= H3-A3/(2*T3)
810 LET E3=ABS(Y9-Y3)
820 LET Y3=Y9-(Y9-Y3)/2
821 LET C=C+1
822 IF C<1000 THEN 830
825 PRINT"NOT CONVERGING"
826 STOP
830 IF E3>E THEN 760
840 LET T = SQR(6*A3+3/T3)
850 LET E3=ABS(T-0)
860 LET D=T+.5*(T-0)
870 IF E3>E THEN 740
880 RETURN
899 END

```

APPENDIX B  
Trapezoidal Flumes

TRAPF1      13:42      PX SYSP 11/19/8

```

90 READ A1,A3
99 DATA 1,1.10
100 READ B1,B3,Z1,Z3,S,I,L,R,G
101 DATA .6666667,0
102 DATA .57735,.57735
103 DATA .1,.1,1.5
104 DATA 6,32.16
110 LET A=0
120 LET L1=0
130 LET E=1E-6
135 LET Y0=S-I
140 LET Q=0
150 LET Y0=Y0+I
160 LET Y1=Y0
170 LET K=1
180 LET Y=Y1
185 GOSUB 700
270 LET Q=INT ( Q*10↑R + .5 ) / 10↑R
280 IF K=1 THEN 310
290 LET Q4=Q
291 LET Y5=INT(Y3*10↑4+.5)/10↑4
300 GØ TØ 380
310 LET Q1=Q
311 LET Y6=INT(Y3*10↑4+.5)/10↑4
320 LET Y4 = Y0 + 45*I
330 IF Y4>L THEN 370
340 LET K=4
350 LET Y=Y4
360 GØ TØ 185
370 LET Q4=0
380 LET L1=L1+1
390 IF L1 =1 THEN 410
400 GØ TØ 450
410 LET A=A+1
411 PRINT"TRAPEZOIDAL FLUME:  B1=";TAB(22);B1;TAB(33);"B3=";
412 PRINT TAB(36);B3;TAB(45);"Z1=";TAB(48);Z1;TAB(60);"Z3=";
414 PRINT TAB(63);Z3
416 PRINT TAB(6);"ALPHA 1=";A1;TAB(42);"ALPHA 3=";A3
420 PRINT TAB(3);"Y-F";TAB(15);"Q";TAB(22);"CRITICAL";
422 PRINT TAB(34);"*";TAB(38);"Y-F";TAB(50);"Q";TAB(57);
424 PRINT "CRITICAL";TAB(68);A
430 PRINT TAB(3);"FT." ;TAB(14);"CFS";TAB(22);"DEPTH-FT";TAB(34);
431 PRINT "*" ;TAB(38); "FT." ;TAB(49);"CFS";TAB(57);"DEPTH-FT"
440 PRINT "=====*"

```

APPENDIX B (continued)

```

441 PRINT "=====
450 IF Q4=0 THEN 480
460 PRINT TAB(2);Y1;TAB(11);Q1;TAB(22);Y6;TAB(34);"*";TAB(37);
461 PRINT Y4;TAB(46);Q4;TAB(56);Y5
470 GØ TØ 490
480 PRINT TAB(2);Y1;TAB(11);Q1;TAB(22);Y6;TAB(34);"*"
490 IF (L1/5)-INT(L1/5)=0 THEN 510
500 GØ TØ 520
510 PRINT
520 IF L1=45 THEN 540
530 GØ TØ 590
540 FOR P=1TØ7
550 PRINT
560 NEXT P
570 LET L1=0
580 LET Y0=Y4
590 IF Y0>=L-I THEN 999
600 GØ TØ 140
700 LET C9=0
710 LET H=Y+A1*Q*Q/(2*G*Y*Y*(B1+Z1*Y)+2)
720 LET X=(4*Z3*H)-3*B3
730 LET C = (SOR(X*X+40*Z3*B3*H)+X)/10
740 LET D =((B3+C)/(3*B3+5*C))+ (3/2)
750 LET T=H+(3/2)*SOR(2*G/A3)*(2*B3+4*C)*D
760 LET E3=ABS(T-Q)
770 LET C9=C9+1
780 IF C9<1000 THEN 810
790 PRINT"NOT CONVERGING"
800 STØP
810 LET Q = T
820 IF E3>E THEN 710
821 IF Z3=0 THEN 833
830 LET Y3=C/Z3
831 GØ TØ 840
833 LET Y3=2*H/3
840 RETURN
999 END

```

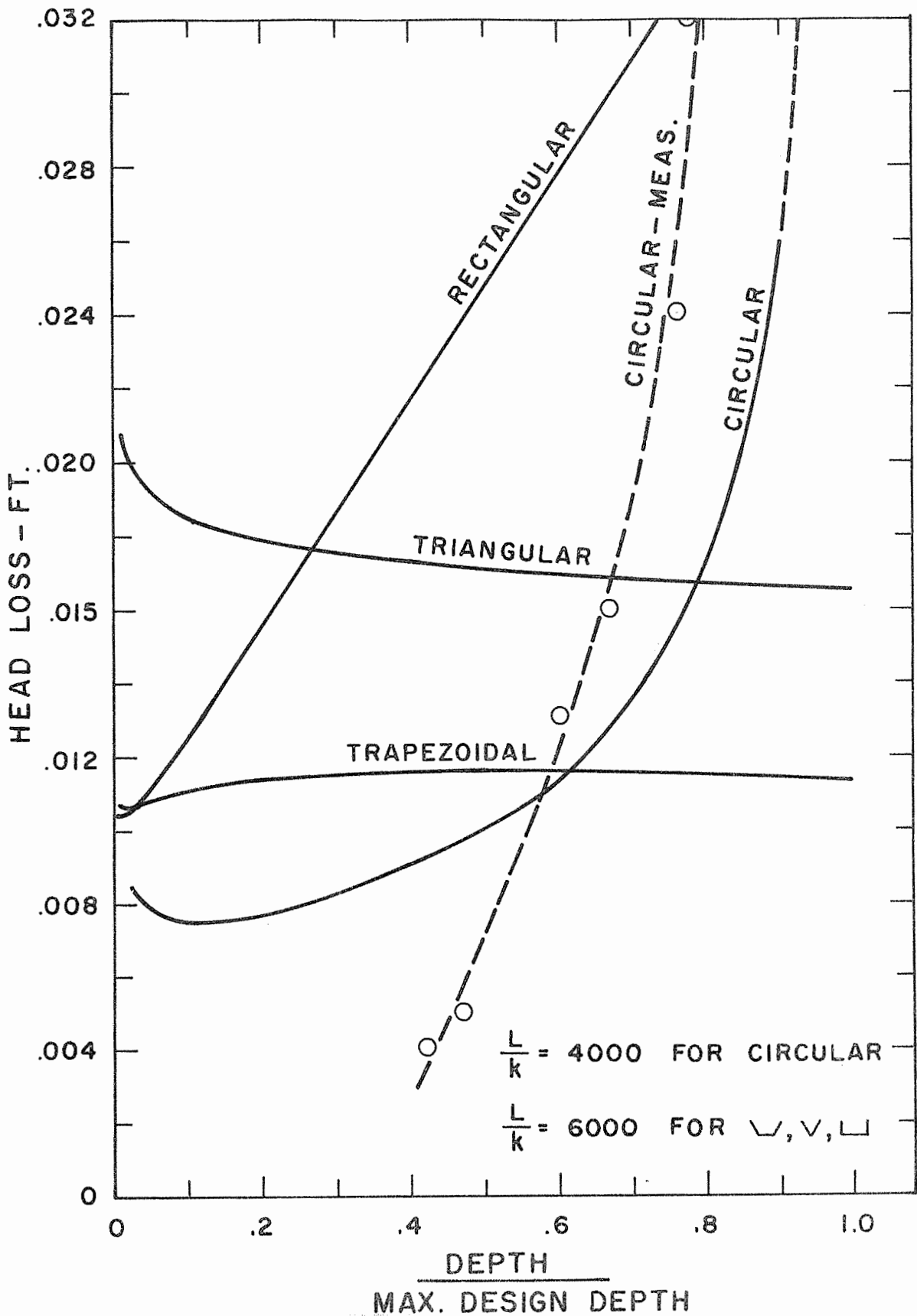


Figure 1. Simplified flow diagram for the circular flumes.

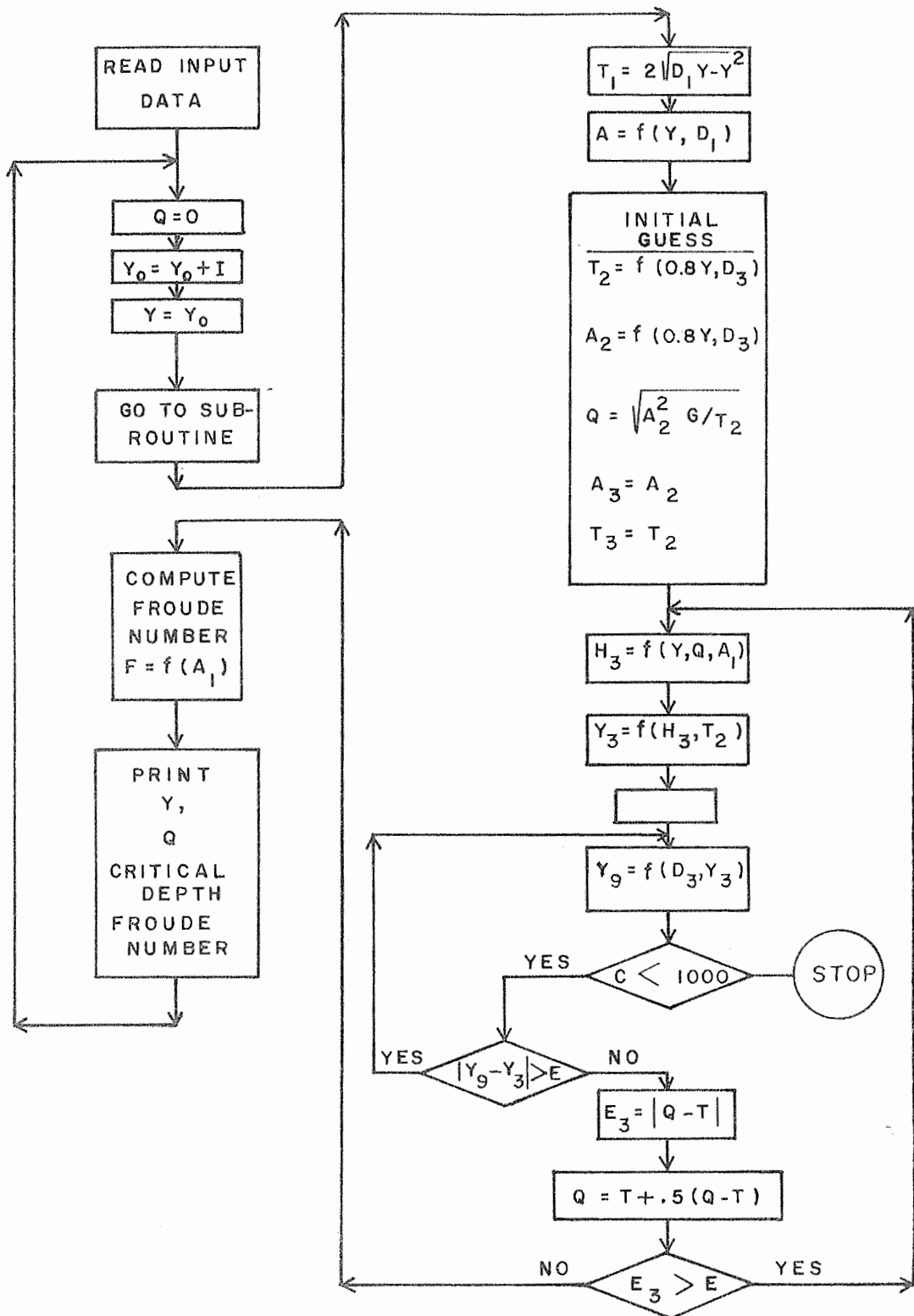


Figure 2. Expected friction loss as calculated with the boundary layer model.

TITLE: PHYSICAL AND CHEMICAL CHARACTERISTICS OF HYDROPHOBIC SOILS

CRIS WORK UNIT: SWC W7 gG-5 CODE NO.: Ariz.-WGL 67-2

PART I. WATERPROOFING OF SOILS - AN EVALUATION OF TREATMENTS AND INFLUENCING FACTORS.

INTRODUCTION:

The need for this study is covered in Annual Reports for 1966 and 1967.

OBJECTIVES:

The overall objectives of the present phase of the study were to evaluate the effectiveness of waterproofing treatments on soils both as a function of the chemical and physical properties of the waterproofing agent, and of the soil. In particular, (1) what effects, if any, do the physical and chemical properties of the soil have on the water-repellency?, (2) what organics would do a good job of making soil water-repellent?, and (3) could the performance of a specific coating material be predicted from the molecular structure of the organic molecule?

PROCEDURE:

Several soils were used. They were selected to provide a fairly large range of particle size distributions and surface areas. The pertinent physical data appear in Table 1. The organic coating materials were selected from groups of materials which were advertised as having, or thought to have, water-repellent characteristics, and whose general chemical structures were known. All coatings, except one, were added as solutions or dispersions, of varying concentrations, to loose, air-dried < 2mm soils in a manner as reported in the 1967 Annual Report. The one exception, methyltrichlorosilane, was added as a gas.

The two techniques used for evaluating the waterproofing characteristics of the treated soils were (1) the breakthrough pressure, and (2) the contact angle. The mechanical and theoretical particulars for these two methods are covered in the 1967 Annual Report.

## RESULTS AND DISCUSSION:

Variation in degree or quality of waterproofing due to accompanying variations in the physical and chemical properties of soil was studied using only one organic, water-repellent, coating (Silicone-R-20) on five soils. Figure 1 shows that soil type had no significantly measurable effects on the contact angle of water -- thus, indicating that any variations in the surface energy between untreated soils is effectively masked by the organic coating. Figure 1 also shows that the contact angle increases with increasing surface coverage -- rapidly at low coverages, then levels out at about  $150^{\circ}$ . An inflection point in the rate of this increase in contact angle occurs at approximately the same coverage per unit area of soil for all the soils tested, i.e.,  $2 \times 10^{-5}$  g R-20/m<sup>2</sup>. This inflection point undoubtedly corresponds to monolayer coverage by the organic coating.

The breakthrough pressure curves for these same treated soils have already been shown (3) and Annual Report, 1967)). Recapitulating, briefly: at low surface coverages the breakthrough pressure ( $h_w$ ) also increased markedly for rather small increment increases in surface coverage -- this undoubtedly being due to corresponding marked increases in the contact angle of the water phase in contact with the partially coated soil surfaces. As with the related contact angle measurements on these soils, a distinct inflection occurred in the rate of change of  $h_w$  (also at about  $2$  to  $3 \times 10^{-5}$  g R-20/m<sup>2</sup>), after which  $h_w$  leveled off at some maximum value. Contrary to the contact angle case, where the leveling off of  $\theta_s$  was the same for all soils, the leveling off or maximum values of  $h_w$  were different for each soil -- this, of course, being predicted from the breakthrough pressure equation which states that:

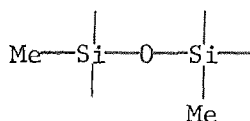
$$h_w \propto \frac{\cos \theta_w}{r}$$

That is,  $h_w$  is directly proportional to the cosine of the effective

contact angle ( $\theta_w$ ) of water (already shown to be constant for any one organic coating material), and is inversely proportional to the effective pore radius ( $r$ ). As predicted by the equation, the fine-textured soils had higher breakthrough pressures than the sandy soils.

Variation in degree or quality of waterproofing of treated soils due to the type of organic coating materials also were effectively studied using contact angle ( $\theta_s$ ) and breakthrough pressure ( $h_w$ ) measurements. Only one soil (Flushing Meadow sand) was used -- this to eliminate variation due to soil physical properties. Several types of organics were studied.

A group of commercial silicone materials were tested. Contact angle data are shown in Figure 2. The materials all produced similar contact angles at equal coverages per unit soil area, thus suggesting that all the silicones had similar surface energies. The R-20 and Dri-Sil 37 were aqueous solutions of sodium methyl silicate; SS-X-3601 and MAS were alkoxy silanes stored in methanol and toluene, respectively, but diluted and emulsified in water just prior to application. All polymerize in the presence of  $CO_2$  and  $H_2O$  to form a resinous film of the type:



which is thought to enmesh the soil particulate matter; also, they may be chemically bound to the soil through the silanol groups, or in other ways. In any case, the water-repellency characteristics derive from the exposed alkyl groups (normally methyl), which effectively cover the soil.

The methyltrichlorosilane was added to the air-dry soil as a gas at its saturated vapor pressure. The chlorosilane apparently

reacted with all the hygroscopic water present, and, again, possibly with the exposed silanol groups to form a continuous, resinous coating on the soil. In spite of the large coverage per unit area, which suggests multilayer formation, the contact angle of water on the treated soil was essentially the same as that for the other silicone materials at monolayer coverage.

The breakthrough pressure measurements for these silicone materials, also, were nearly identical; the average curve of  $h_w$  vs. coverage is shown in Figure 4.

Figure 3 shows breakthrough pressure data for several related types of organics having nitrogen present in the molecular structure. The Armac trade name denotes a group of acetic acid salts of fatty amines. Variation between the three Armac materials is in the R group. Armac 8D, which was not water repellent, had an alkyl group eight carbons long; 18D, which was repellent, had an alkyl group 18 carbons long; T was similar to 18D except the R group of T was highly mono-unsaturated. The C = C group resulted in a lower  $h_w$  at the monolayer coverage point, and, also, seems to have resulted in an inversion of the second molecular layer.

The quaternary ammonium salts, the Arquads, were less effective water-repellents than the long chain fatty amines. Weiss (8) has shown that asymmetrical quaternary alkylammonium ions are as tightly bound to mica-type clays as are primary ammonium ions. This suggests that the degree of water repellency of these materials is primarily a function of how well the nitrogen is shielded from the water phase.

Breakthrough pressure measurements were also run on an amine- and a hydroxy-substituted phenol. The lines for the two materials coincided and is shown in Figure 4. The hydrophilic end is reported to chemically bond to the soil surface, thus exposing the hydrophobic tertiary-butyl group. A fluoro-carbon material was also run (Figure 4). The rather low breakthrough for this material probably is related to the presence of several sulfur and nitrogen groups in the molecule.

There are other materials which will give water-repellent surfaces. The present study was not intended to be all inclusive in this regard. Theoretically, any material which produces a breakthrough pressure greater than zero, or a contact angle greater than  $90^{\circ}$ , should shed water when it runs off as a thin sheet. For water harvesting purposes, the treated soil surface also must resist the impact of the falling raindrops - anything beyond that is merely a margin of safety.

SUMMARY:

Soils may be effectively water proofed with monolayer coatings of certain types of low-surface-energy organics. The measured contact angle of water on soils treated with thin films of such organic waterproofing materials is not significantly affected by the chemical and physical properties of the soil, but is affected by the chemical properties of the coating material. The breakthrough pressure of such treated soils is affected both by the type of coating and by the soil texture (i.e., effective pore radius), and by the type of organic coating the soil. Optimum water-repellency for any coating material is obtained at monolayer coverage, thus suggesting that (1) application of the coatings should be applied to soil on the basis of some convenient units of the organic per unit of surface area of the soil, and (2) that coarse textured sands will be cheaper to treat than fine textured soils. Theoretically, any organic coating which produces a breakthrough pressure greater than zero, or a contact angle greater than  $90^{\circ}$ , should shed water as a thin film, but, of course, for use in water harvesting a margin of safety is required so that the water repellent soil will also resist the impact of the falling water drop. A number of the materials tested were extremely water repellent and, in this regard, show promise for use in water harvesting work.

## PART II. Na-Ca-DEMIXING IN FREE-SWELLING MONTMORILLONITE.

### INTRODUCTION:

Despite the large amount of information available on the swelling of homoionic clays, relatively few workers have treated the more practical problem of clay swelling in mixed-ion systems. The tendency of Ca-saturated clays to exist as aggregates of platelets as opposed to the nearly monodisperse behavior of Na-saturated clays, causes more than an academic interest in the extent to which the behavior of mixed Na-, Ca-clays reflects the behavior of the homoionic clays themselves. Recent suggestions that ion demixing (segregation of interlayer ions into essentially Na-saturated and Ca-saturated regions) occurs in swollen mixed-ion clays (5, 7) as well as in natural bentonites and in relatively dry clays (6), also raise the question of the extent to which models assuming nearly uniform distribution of ions over all mineral surfaces of swollen clays are applicable.

To study this problem, hypothetical models of interlayer swelling for Na-, Ca-montmorillonites in water, assuming both the randomly mixed and demixed cases, were prepared using the approach of Fink et al. (2). The approach can assess the amount of internal surface area attributable to the freely-swelling portion of the clay, and by difference assigns the rest to limited or non-swelling surfaces; thus, it was hoped this approach might serve to deduce the extent to which ion demixing occurs. Preliminary experimental data are presented and compared to the hypothetical models.

### THEORY:

The expansion of a free-swelling montmorillonite in a water system may be described by:

$$d = 9.4 + u(W_t - W_e)/S_i \quad (1)$$

where  $d$  is the  $d$ -spacing of the expanded montmorillonite in Angstroms;

$9.4\overset{\circ}{A}$  is the thickness of the individual montmorillonite sheets;  $W_t$  is the total weight of water in the system;  $W_e$  is the summation of the water associated with external surfaces and non-free-swelling internal surfaces;  $S_i$  is the internal area of the free-swelling portion of the clay; and  $u$  is a combined constant and conversion factor equal to  $2 \times 10^4 \text{ A}\cdot\text{m}^2/\text{g}$ .

In a salt-free, free-swelling system,  $W_e$  can be expected to remain nearly constant over much of the free-swelling range, therefore, equation (1) may be written as

$$d = (9.4 - uW_e/S_i) + uW_t/S_i \quad (2)$$

Thus, from plots of  $d$  versus  $W_t$ , one may obtain  $S_i$  from the slope and  $W_e$  from the intercept. It was thought that these relationships might help solve the cation mix, demix controversy - at least for the moisture ranges where the above free-swelling relationships have been shown to apply.

Conjectured plots for Na-, Ca-montmorillonite, with ESP equal to 50 and 100%, and assuming either complete random mixing or complete demixing are shown in Figure 5. The extended legend lists the equations describing each line, along with the appropriately imposed conditions and restrictions.

Briefly, in summary of Figure 5: for the demix model, where separate Na and Ca diffracting domains are formed, the slope of the swelling line of  $d$  vs  $W_t$  should increase as the ESP decreases, while the Ca-saturated packets should swell to a maximum of  $19.6A$ ; for the random cation mix model the swelling line for the high ESP's should coincide roughly with the line for a pure Na-system, but at low ESP's the platelets should collapse to  $19.6A$ .

#### Explanation of Figure 5

Curve I:  $d = 19.6A$

For: Actual plot of completely Ca-saturated montmorillonite and

conjectured plot of limited-swelling packets in Na, Ca-saturated montmorillonite systems.

$$\text{Curve II: } d = \left( 9.4 - \frac{uW_e}{S_i} \right) + \frac{uW_t}{S_i}$$

For: (1) Theoretical plot for Na-saturated montmorillonite (ESP = 100%). (2) Theoretical plot for Na-, Ca-saturated montmorillonite where cations are randomly distributed on exchange sites, and where free-swelling characteristics of a sodium system predominate.

Assumptions: (1) Complete random distribution of the two types of cations on exchange sites; (2) salt-free; (3)  $S_i = 720 \text{ m}^2/\text{g}$ ; (4)  $W_e = 0.10 \text{ g/g}$ .

$$\text{Curve III: } d = \left( 9.4 - \frac{uW_e}{S_i} \right) + \frac{uW_t}{S_i}$$

For: Theoretical plot of free-swelling for Na-, Ca-saturated montmorillonite where cations completely demix to give separate Na and Ca diffracting domains.

Assumptions: (1) Complete demixing of cations to form separate diffracting domains; (2) salt-free; (3) ESP = 50%; therefore,  $S_i = 360 \text{ m}^2/\text{g}$ ; (4)  $W_e = 0.28 \text{ g/g}$ , based on  $0.10 \text{ g/g}$  for water on external surfaces, plus  $0.18 \text{ g/g}$  for water hydrating interlayer portions of Ca-saturated packets.

$$\text{Curve IV: } d = \left[ 19.6 + \left( 9.4 - \frac{uW_e}{S_i} \right) \right] + \frac{uW_t}{S_i}$$

For: Theoretical plot of free-swelling for mixed Na-, Ca-saturated montmorillonite where cations completely demix into alternate layers to give a regular, alternating interstratification.

Assumptions: (1) Complete demixing of cations to form a regular, alternating sequence of Na-, and Ca-saturated layers and

where Ca-layers expand to  $19.6\overset{\circ}{\text{A}}$ , and where Na-layers are free-swelling; (2) salt-free; (3) ESP = 50%; therefore,  $S_1 = 360 \text{ m}^2/\text{g}$ ; (4)  $W_e = 0.28 \text{ g/g}$ .

Curve V:  $\hat{d} = 21 + 15 W_t$

For: Actual curve obtained for mixed Na-, Ca-saturated montmorillonite for both ESP: 61 and 90%.  $\hat{d}$  denotes a least squares estimate of  $d$ .

#### PROCEDURE:

The specimen montmorillonite used in this study was Wyoming bentonite. Dispersion, fractionation, and purification, including removal of carbonates and free iron oxides, were carried out according to methods proposed by Jackson (4). Excess salt was removed by repeated washes and extractions with a pressure membrane apparatus.

The  $< 2\mu$  fraction was Na-saturated by passing dilute clay suspensions through Na-Amberlite IR-120 exchange resin. A subsample of this Na-clay was selected to represent ESP = 100%. The remaining clay was Ca-saturated and finally converted to mixed Na-, Ca-montmorillonite by stirring subsamples with various quantities of Na-resin. The clay was passed through a sieve to remove the resin particles; excess water was removed by a final pass through the pressure membrane, and all the materials were freeze-dried and ground.

Two gram samples of clay were thoroughly mixed with desired amounts of water, then equilibrated for two weeks. The  $d$ -spacings of the wet samples were determined using low-angle X-ray diffraction (1). Peak locations were corrected by dividing the recorded intensity data by the combined Lorentz and polarization factors for oriented samples. Water contents of the X-rayed samples were determined gravimetrically on  $300^\circ\text{C}$  dried material. Soluble salts were determined on the samples by electrical conductivity, and exchangeable cations were extracted using  $\text{NH}_4\text{OAC}$ .

## RESULTS AND DISCUSSION:

The experimental data for these mixed ion systems are presented in Table 2. Included are the ESP, the water contents, the corrected d-spacings of the two major peaks of each diffractogram, the peak intensity ratio of the low-angle peak divided by the high angle peak, and the salt concentration of each sample.

The diffractograms at ESP 1.4 and 12.1 were dominated in all cases by a strong peak near 19.6A, the spacing of which was invariant with water content within the range tested. The peaks at 35-40A roughly coincide with the expected second order for this 19.6A peak, but were found to persist even after air-drying the sample. The peak probably arose from a small quantity of resin particles which remained in the clay following the sample preparation procedure. The locations of these peaks have been placed in parentheses in Table 2, as they appear to be experimental artifacts and should be disregarded during analysis of the data.

The intensity of the 19.6A peaks remained quite strong throughout the water range used, but intensity did gradually decrease as water content increased. This gradual decrease in intensity is undoubtedly due primarily to the absorption and random scattering of the X-rays by the water phase, rather than to a diminution of the 19.6A phase, i.e., there was no X-ray evidence for a highly expanded, freely-swelling phase. Thus, the data suggest (but do not necessarily prove) that complete ion-demixing does not occur for  $ESP \leq 12$ .

The data for  $ESP = 41$  is even more insecure. Again the two peaks at about 20 and 40A were present, but the intensities of the 20A phase were consistently lower than for the two lower ESP's. Also, these 20A peaks were quite broad (even at the lowest water contents); they became more diffuse as more water was added, and finally became unresolvable from the 40A peaks.

The low intensities of the 20A peaks could be due to a reduced number of diffracting platelets of this spacing, caused by the presence of a highly expanded phase; however, no positive evidence for

such a freely-expanding, separate diffracting phase existed. So, again, there was no direct X-ray evidence for a highly expanded, free-swelling phase, but again, such a phase cannot necessarily be precluded.

Plots of d-spacing versus total water content ( $W_t$ ) for both ESP, 60.1 and 91.2% were linear, and both conformed to the line  $\hat{d} = 21 + 15 W_t$ , as shown by line V in Figure 5 ( $\hat{d}$  denotes a least squares estimate). Thus, a freely expanding phase was definitely present. There was no evidence for cation demixing into separate, coherently diffracting domains, i.e., there were no stable 19.6A peaks. Unfortunately, one cannot infer from this that random mixing definitely occurred. This is simply because the line of d-spacing vs.  $W_t$  for ESP 60 and 91% did not even come close to conforming to the required line, i.e., line II in Figure 5. Obviously, the amount of external water in the system increased proportionately as  $W_t$  increased. Apparently, the excess salt in the system (Table 2) partially restricted the double layer, thus forcing water into the external gel structure. The discovery of this salt, almost as an afterthought near the end of the experiment, came as a surprise and a disappointment. Silver nitrate and conductivity tests on the extract from the pressure membrane had indicated that all excess salts had been removed, but apparently this was not so. An attempt is currently in progress to extend equation (1) to situations where salt is present, and an attempt is also being made to utilize the principles of double-layer theory to explain the present data.

#### SUMMARY AND CONCLUSIONS:

Swelling properties of mixed Na-, and Ca-montmorillonites were examined using X-ray diffraction in an attempt to settle the existing conflict as to whether the cations demix in such systems into mono-saturated sub-units. For ESP  $\leq 40\%$ , only the Ca-controlled 19.6A spacing was observed. Results showed that free-swelling occurred at ESP 60 and 90% and that the swelling plots of d-spacing versus total water content ( $W_t$ ) for these two ESP's were identical, both following the line:  $d = 20 + 15 W_t$ . Absence of a 19.6A X-ray peak for ESP  $> 60\%$

strongly suggests that cation demixing into separate, coherently, diffracting domains does not occur. However, since the free-swelling line did not conform to the expected theoretical line for random mixing of cations, the complete solution of the demixing problem remains obscure.

REFERENCES:

1. Fink, D. H. and Thomas, G. W. A technique for low-angle X-ray diffraction studies on expanded three-layer clays. Soil Sci. Soc. Am. Proc., 27:241-242. 1963.
2. \_\_\_\_\_, Rich, C. I. and Thomas, G. W. Determination of internal surface area, external water, and amount of montmorillonite in clay-water systems. Soil Sci. 105:71-77. 1968.
3. \_\_\_\_\_, and Myers, L. E. Synthetic hydrophobic soils for harvesting precipitation. Soil Wettability Symp. Proc., Riverside, Calif., 6-10 May 1968.
4. Jackson, M. L. "Soil Chemical Analysis-Advance Course", University of Wisconsin, Madison, Wisconsin.
5. McNeal, B. L., Norvell, W. A. and Coleman, N. T. Effect of solution composition on the swelling of extracted soil clays. Soil Sci. Soc. Am. Proc., 30:313-317. 1966.
6. McAtee, J. L. Heterogeneity in montmorillonite. Clays and Clay Minerals 5:279-288. 1958.
7. Shainberg, I. and W. D. Kemper. Electrostatic forces between clay and cations as calculated and inferred from electrical conductivity. Clays and Clay Minerals 14:117-132.
8. Weiss, A. Organic derivatives of mica-type layer-silicates. Angew. Chem., 2:134-143. 1963.

PERSONNEL: D. H. Fink.

CURRENT TERMINATION DATE: December 1970.

Table 1. Soils and physical constants

Soil	Particle size			Surface area $\text{m}^2/\text{g}$	Effective pore radii	
	Sand	Silt	Clay		Air entry ( $L_a$ ) cm water	Radii (r) cm ( $\times 10^3$ )
	%					
Play sand	96.8	0.5	2.7	16.4	-20	7.43
Salt River bed sand	87.3	10.7	2.0	23.4	-37	4.02
Flushing Meadow	90.4	5.3	4.3	21.5	-52	2.86
Control sand	39.8	60.2	6.9	32.2	-120	1.24
Pachappa	50.3	41.9	7.8	22.2	-132	1.12
Granite Reef	51.9	41.3	6.8	71.5	-112	1.33

49-13

Table 2. Experimental data for mixed ion clays.

ESP	Water Content	X-Ray Peak Locations		Peak Intensity Ratio ( $I_{low L}/I_{high L}$ )	Average Salt
		° A			Concentration
%	%				(meq/l)
91.2	127	39	21	6.4	39.4
	169	47	26	3.7	29.6
	204	52	30	3.4	24.6
	239	61	32	2.6	21.0
	286	62	33	1.1	17.5
60.1	79	33	19.7	0.23	58.9
	124	38	22	2.0	37.5
	168	49	27	5.1	27.7
	209	50	28	4.2	22.2
	263	61	34	3.3	17.7
41.0	79	19.3	37	7.6	130.4
	99	20.3	44	5.8	104.0
	120	20.2	45	4.8	85.8
	189	*	*	*	54.5
	272	*	*	*	37.9
12.1	61	19.3	(36)	14.4	33.9
	84	19.8	(38)	12.9	24.6
	126	19.5	(36)	24.8	16.4
	180	19.9	(35)	14.4	11.5
	242	19.8	(41)	12.8	8.6
1.4	63	19.7	(36)	12.4	32.1
	91	19.5	(43)	17.2	22.2
	118	19.7	(35)	16.7	17.1
	223	19.6	(37)	22.2	9.1

\* Broad, poorly defined peak systems.

47-67

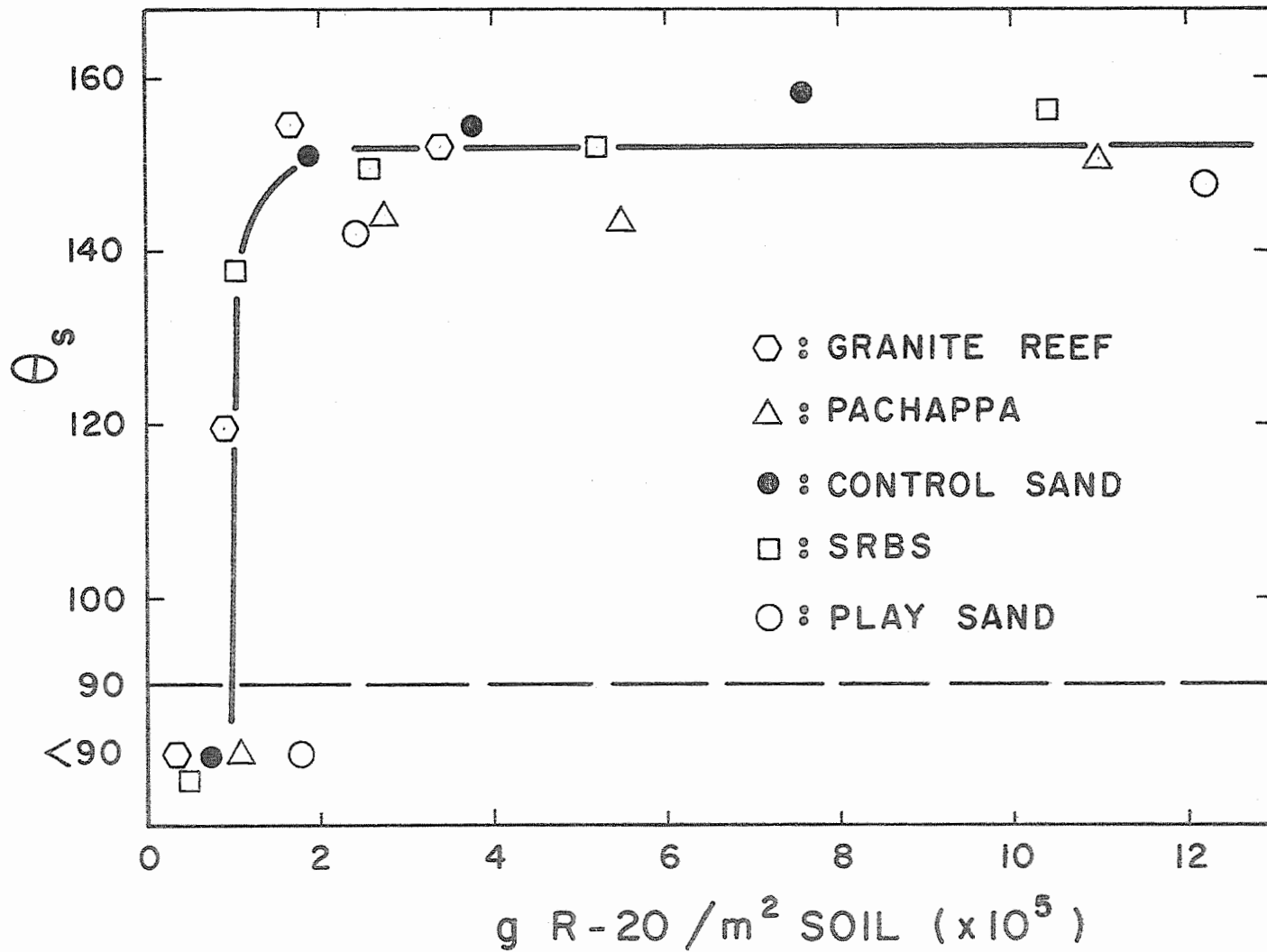


Figure 1. Contact angle of water on soil surfaces treated with R-20.

91-67

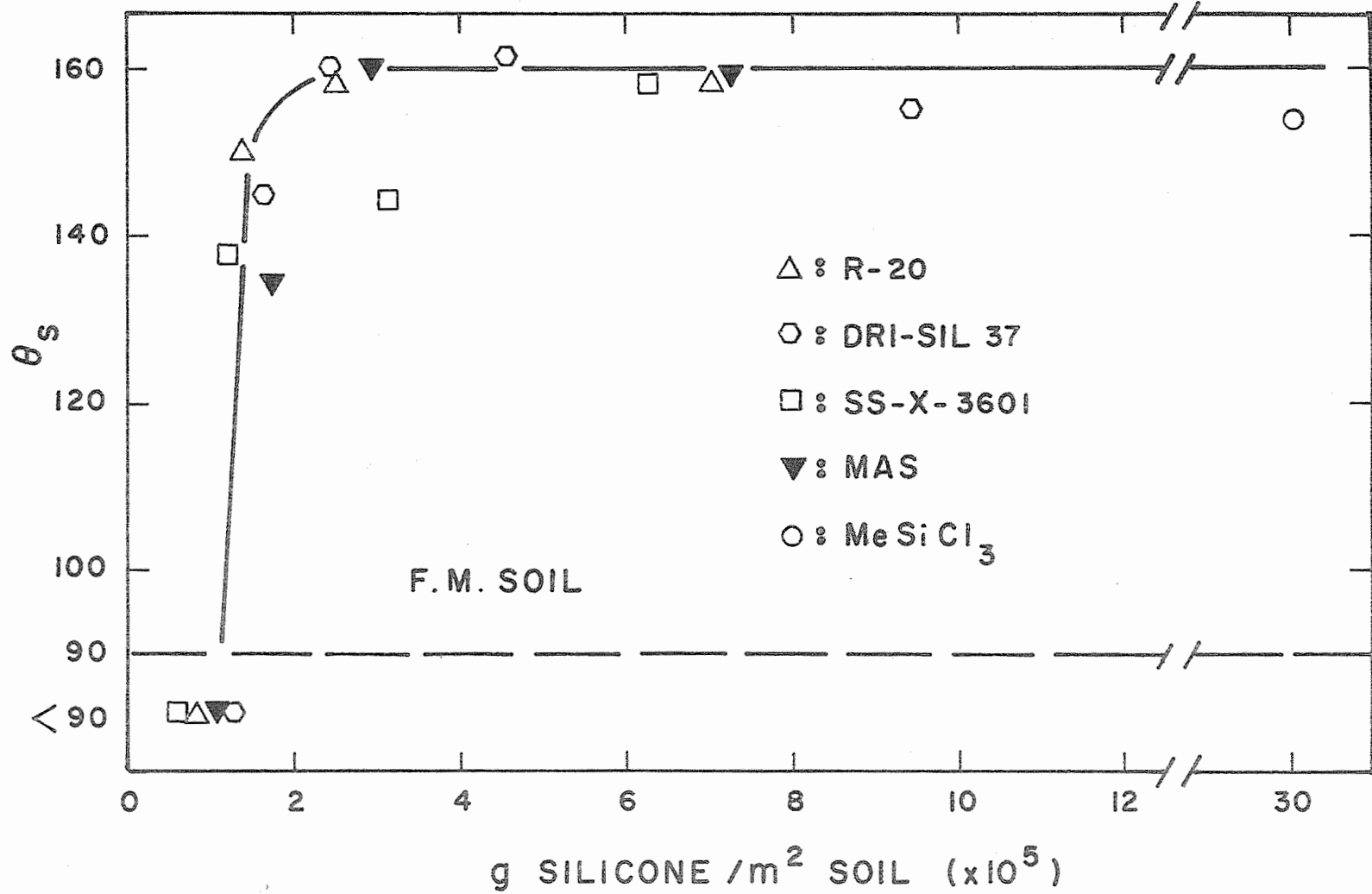


Figure 2. Contact angle of water on soil surfaces treated with silicones.

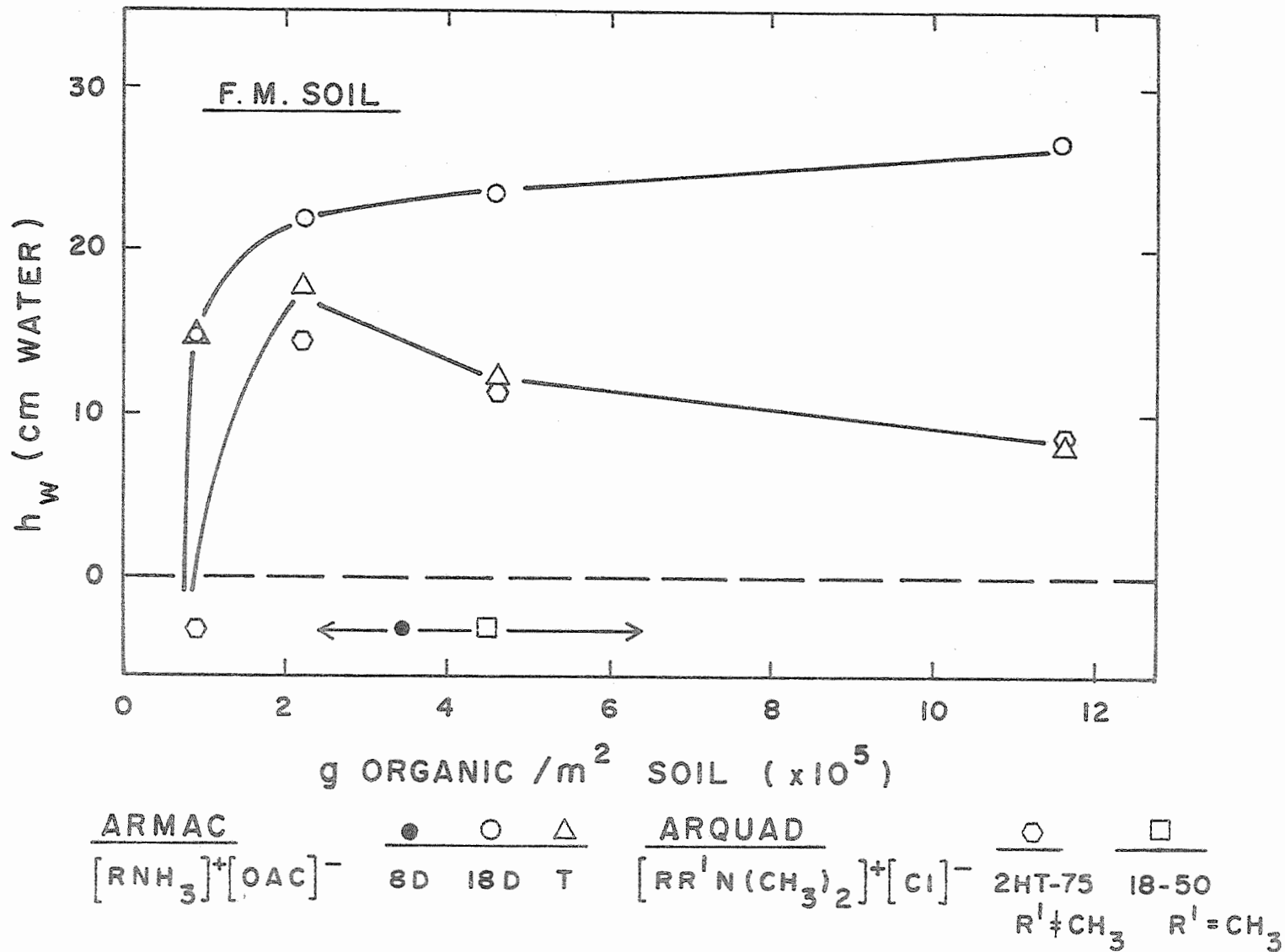


Figure 3. Breakthrough pressures for several primary amine and quaternary ammonium salts.

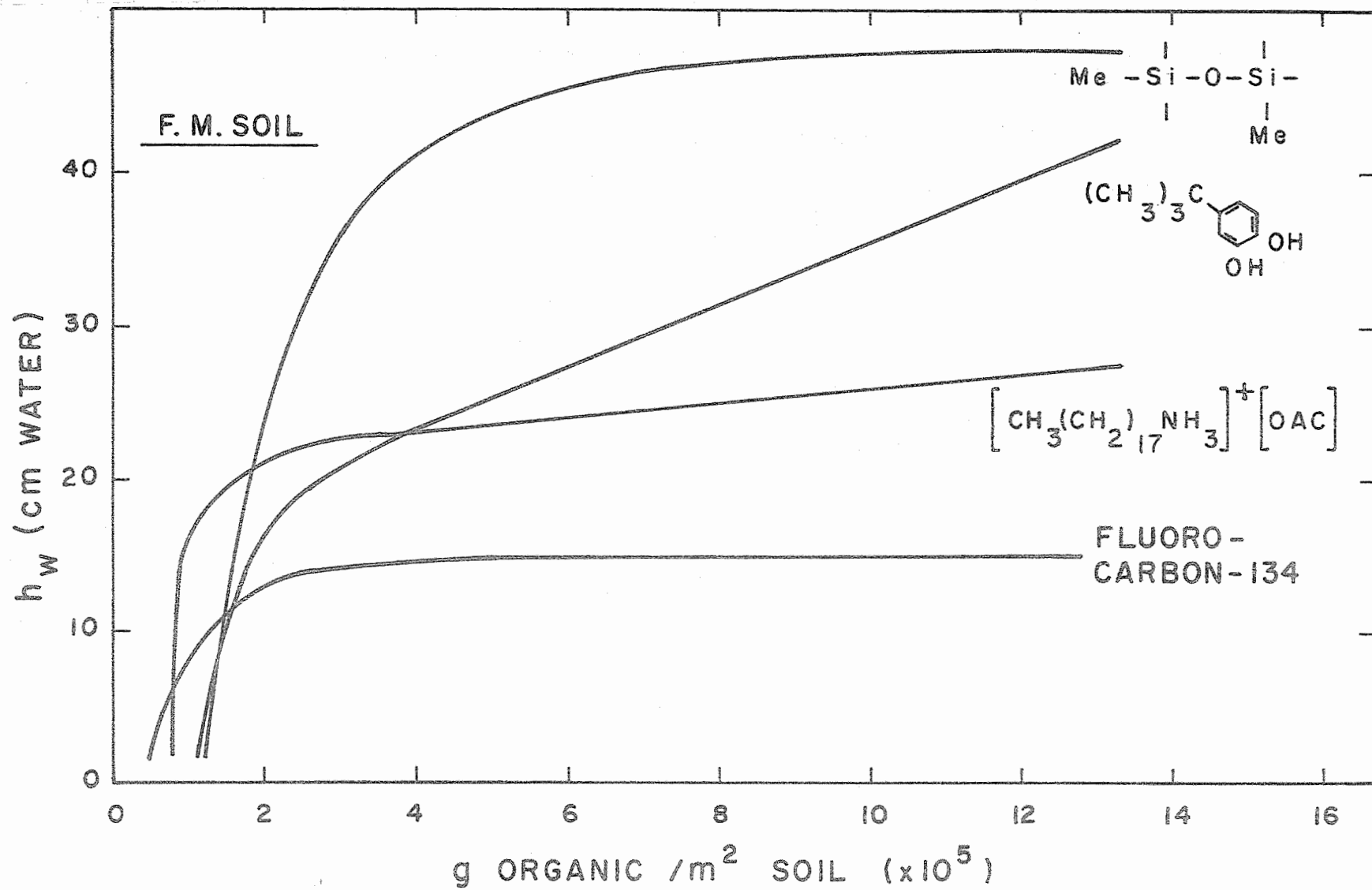


Figure 4. Breakthrough pressure curves for several types of organic coating materials.

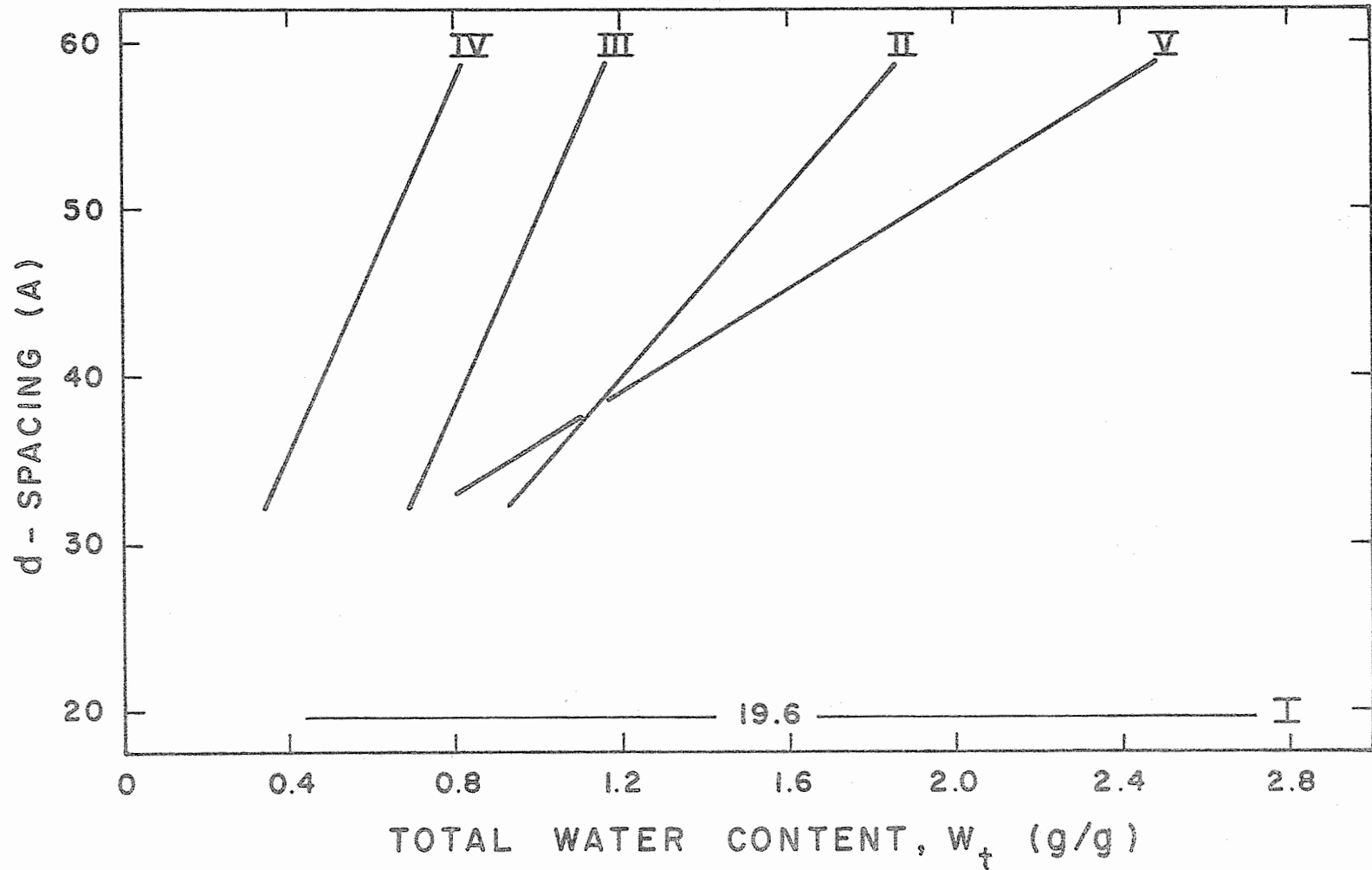


Figure 5. Actual and conjectured plots of swelling of mixed Na-, Ca-bentonite assuming either complete mixing or complete demixing of the ions.

TITLE: THE USE OF FLOATING SOLID AND GRANULAR MATERIALS  
TO REDUCE EVAPORATION FROM WATER SURFACES

CRIS WORK UNIT: SWC W7 gG-3 CODE NO.: Ariz.-WCL 67-3

INTRODUCTION:

The economics of using floating materials to reduce evaporation has been demonstrated (see 1965 Annual Report WCL-9). However, since no ideal material has been discovered, and due to an ever-increasing list of possible materials to use, continued research is necessary. Also, some materials may be economically feasible on small tanks, but are not practical on larger bodies of water.

Three lines of research, concerned with providing insight into the design of floating covers to reduce evaporation, are discussed in this report. The first consisted of testing materials on the 2.1 m diameter insulated evaporation tanks to determine their efficiency in reducing evaporation. The second was a field study of silicone treated perlite ore, on which data analysis is now complete. The third consisted of studying the complete heat budget of partially covered tanks, using a variety of sizes and shapes of covers.

PART I. EVAPORATION REDUCTION EFFICIENCY.

Procedure. Two new materials consisting of foamed wax chips and lily pads were tested on the tanks along with a new sample of foamed wax blocks (see 1967 Annual Report). The wax chips were made of a higher melting point wax than the foamed wax blocks. These chips were approximately 2 to 3 cm across and were irregular shaped; therefore, they covered more of the surface area than did the round foamed wax blocks.

Four lily pad plants were placed in wooden boxes filled with sand, and the boxes were lowered into an evaporation tank partially filled with water. After the plants were established, evaporation from all partially covered tanks was compared with evaporation from an open tank to determine the evaporation reduction efficiency of the various covers.

Results and Discussion. The efficiency of the materials tested in reducing evaporation is presented in Table 1. In all cases the efficiency decreased with time. For the wax materials this may be partially due to both increase in temperature and a discoloration from dust deposited on the wax. For the lily pads, as the heat increased the plants showed signs of stress, and the leaves turned to a darker green with yellow-brown portions. These changes would tend to decrease the reflected radiation and would therefore increase the energy available for evaporation, or decrease the evaporation reduction efficiency as the data indicate.

The efficiency of the lily pads decreased rapidly as the air temperature increased, and they were of little or no value at the end of the study period. This method of evaporation reduction may be economical in areas where conditions are conducive to the growth of lily pads, but was not under the conditions of this experiment. The effect of root growth on seepage would also need investigation.

The efficiency of the foamed wax blocks followed essentially the same pattern as the previous year, starting at 70% and decreasing to 60% as the top portion melted and changed color. The foamed wax chips did not melt on top, due to the use of higher melting point wax, but because of a different texture tended to draw the water up the sides and eventually over almost the entire surface, thus exposing more water area and reducing the efficiency.

#### PART II. FIELD STUDY OF PERLITE ORE:

Procedure. Silicone treated perlite ore was tested under field conditions on a 320 m<sup>2</sup> pond at Tucson, Arizona from 15 February to 30 November 1967. This study was conducted by the University of Arizona, Water Resources Research Center, under contract to the Laboratory. Evaporation on the treated, and a similar untreated control pond, were monitored to determine the efficiency of the perlite in reducing evaporation. The amount of perlite added, the

percentage of surface area covered, and wind speed and direction were also recorded. Two varieties of fish were placed in each pond to determine the effect of the perlite cover on their growth.

Results and Discussion. The results of the field study using silicone treated perlite ore to reduce evaporation are summarized by weekly periods in Table 2. This table shows that the perlite treatment reduced evaporation by 18.8% with a total of  $3.03 \text{ m}^3$  ( $107 \text{ ft}^3$ ) of perlite being lost from the surface, due to wind action or sinking. For an average surface area of  $320 \text{ m}^2$ , and a total savings of 28.22 cm (.926 ft) of water, this would amount to a savings of 89,000 liters (23,500 gallons). Relating the water saved to the perlite consumed, an average of 29,000 liters per cubic meter (220 gallons per cubic foot) is obtained. The cost of perlite during this study was \$10.60 per  $\text{m}^3$  (\$.30 per  $\text{ft}^3$ ), which when converted to cost of water saved, represents a cost of \$0.36 per 1,000 liters (\$1.36 per 1,000 gallons). This cost is considerably less than those reported for evaporation reduction on small ponds using monomolecular films, and silicone treated perlite would thus be economical for use on small ponds or stock tanks. This would be particularly true where water must be hauled if the supply is depleted.

As shown in Table 2, approximately two-thirds of the perlite either sank or blew away. Previous studies on evaporation tanks indicate that most of the loss is due to sinking. An improved silicone or other waterproofing treatment, both in respect to durability and coverage, would therefore be desirable. This could reduce the cost of water saved considerably, since less material (which is essentially the only cost because there is no dispensing equipment needed) would be required.

Measurements of the diurnal oxygen content of the two ponds indicated that, although variable from day to day, oxygen in the covered pond was lower over the study period than that in the control pond. This apparently had little effect, however, since

fish placed in each pond were weighed at the beginning and end of the period and no significant difference was noted in their growth rate. On the basis of this study, it appears that it will be possible to reduce evaporation using floating perlite ore without seriously disrupting fish growth.

### PART III. HEAT BUDGET STUDIES.

Procedure. The necessary meteorological, heat flow and evaporation data to determine a complete heat budget on each of the four insulated evaporation tanks was recorded. This data was monitored each 30 minutes by means of an automatic data acquisition system, and was recorded on paper tape for ease of processing. After measuring or calculating the energy components  $R_n$ ,  $G$  and  $LE$ , the energy or heat balance equation written as  $R_n + G + A + LE = 0$  was used to determine  $A$ . In this equation,  $R_n$  is the net radiation,  $G$  is the heat storage in the water,  $LE$  is the energy used in evaporation, and  $A$  is the sensible heat transfer to or from the air since the tanks were insulated.

Three different series of studies were conducted using two materials and several different shapes and sizes of covers. The materials used were 15 ml. butyl rubber painted white (see 1967 Annual Report), and white styrofoam of 5 cm thickness. All covers were round; however, during the last study a large section (94.6 cm diameter) was removed from the center of one cover, and twelve small sections (27.3 cm diameter) were removed from approximately equally spaced points on another cover. These two covers each covered 76 percent of the surface area. The percentage of surface area covered by other covers used varied from 87 to 26%.

The first study compared a white butyl cover (covering 86% of the surface area), and a white styrofoam cover (covering 80% of the surface area) with an open tank. The second study compared styrofoam covers of 87, 51, and 26 percent coverage, with an open tank. The last study was a comparison of a large styrofoam cover (covering 87%

of the surface area), and the two previously mentioned covers (which each covered 76% of the surface area and will be referred to as 1-hole and 12-hole covers), with an open tank.

Results and Discussion. Results of the heat budget studies are presented as daily summaries in Table 3, and the evaporation reduction data obtained during this series of studies is presented in Table 4. Analysis of the heat budget data indicates that the butyl cover is more efficient than the styrofoam covers, because it transfers energy to the atmosphere in the form of sensible heat, whereas the styrofoam covers obtain energy from the atmosphere, thus increasing the energy available to be used in the evaporation process. A look at Table 5, which presents the relationship between the reduction in net radiation and evaporation for the covered tanks as compared to the open tank, would again indicate that the butyl cover is more efficient. However, when Table 4 is considered, it appears that there is little difference in the efficiency of the two materials, as far as their ability to reduce evaporation is concerned. It should be noted that on 1 and 2 August, the net radiation over the butyl cover was considerably larger than that over the styrofoam cover, which actually covered a smaller percentage of the area. This may indicate that the albedo of the butyl was lower than that of the styrofoam, and if the two were equal, the butyl would then be significantly better. However, the temperature of the surface of the cover and the surface of the water not covered must also be considered, and data are not yet available to validate the above assumption.

The study with three different sized styrofoam covers produced savings of 84, 48, and 22% for areas covered of 87, 51 and 26%. This and previous studies indicate that the styrofoam covers will reduce evaporation within a few percent of the amount of surface area covered.

The study involving three styrofoam covers of different shape produced essentially the same results. It also pointed out that for

the same percentage of surface area covered, the cover with one large hole in the center was more efficient than the cover with 12 small holes. Since the net radiation was the same over both covers, the difference must either be due to a difference in roughness, or a difference in vapor gradient. In other words, even on this very small scale, the fetch may be important. Neither roughness nor vapor gradients were measured on the necessary scale to allow any more conclusive comments.

#### SUMMARY AND CONCLUSIONS:

Foamed wax has many of the properties desired in a floating material to reduce evaporation, such as white color, ease of transportation and application, and relatively high reduction efficiency. However, undesirable properties, such as low melting point or rough texture of the samples studied to date, make it necessary to develop new samples before field studies are conducted on this material.

The use of lily pads to reduce evaporation may be economical in areas where conditions for their growth are favorable. The effect, if any, of the root system on seepage from unlined ponds would have to be investigated to see if benefits from evaporation reduction were greater than loss from increased seepage.

Silicone treated perlite ore was used to reduce evaporation on a 320 m<sup>2</sup> pond, and proved to be both practical and economical. Fish placed in the pond experienced essentially the same growth rates as those in an untreated pond. A better silicone treatment would reduce the amount of perlite lost, and would probably decrease the cost of water saved, which was \$0.36 per 1,000 liters (\$1.36/1,000 gal.) in this study.

Heat budget studies indicate a thin cover, such as butyl rubber, may be more efficient than a thick cover such as 5 cm thick styrofoam. However, evaporation reduction measurements showed the two to be essentially the same. More research is therefore needed to determine

which would be best if both had the same albedo. Results using both types showed that the evaporation reduction was essentially the same as the percentage of area covered.

PERSONNEL: Keith R. Cooley

CURRENT TERMINATION DATE: December 1970.

Table 1. Evaporation reduction using floating materials.

Period	Open	Foamed Wax Blocks			Foamed Wax Chips			Lily Pads		
	Evap.	Evap.	Red.	Area	Evap.	Red.	Area	Evap.	Red.	Area
	(cm)	(cm)	(%)	Covered (%)	(cm)	(%)	Covered (%)	(cm)	(%)	Covered (%)
3 May - 17 May	10.00	3.03	70	Estimated 75-80	5.49	45	Estimated 85-90	8.73	13	Estimated 10-15
17 May - 3 Jun	13.08	4.66	64		9.47	28		12.62	4	
3 Jun - 19 Jun	12.50	5.04	60		9.12	27		12.20	2	
Totals	35.58	12.73	64	-	24.08	32	-	33.55	6	-

50-8

Table 2. Weekly evaporation data on test using perlite conducted on two 53 x 78 ft reservoirs located at Water Resources Research Center Field Laboratory, February 15, 1967 - November 30, 1967.

Period	Miles	Evaporation in Feet			Control P.:-Treated P.:	Percent Savings	Date and Amount of Treatment in Cu. Ft.
		Treated Pond	Control Pond	Control P.: Percent Savings			
<u>Calibration</u>							
Feb 15-22	397	0.071	0.069	-0.002			
" 22-Mar 1	535	.089	.089	-			
Mar 1-8	535	.096	.099	+ .003			
Totals		0.256	0.257	0.001			
<u>Measurement</u>							
Mar 8-15	355	.055	.073	.018	24.6	Mar 8 (42)	
" 15-22	478	.081	.111	.030	27.0	" 16 (6)	
" 22-29	479	.100	.126	.026	26.0	" 23 (3)	
" 29-Apr 5	505	.078	.103	.025	24.3		
Apr 5-12	544	.118	.143	.025	17.7		
" 12-19	442	.085	.101	.016	15.8	Apr 14 (3)	
" 19-26	476	.121	.142	.021	14.8	" 21 (3)	
" 26-May 3	486	.125	.155	.030	19.4		
May 3-10	463	.111	.145	.034	23.4	May 4 (3)	
" 10-17	517	.146	.180	.034	13.5		
" 17-24	373	.121	.155	.034	21.9	" 23 (3)	
" 24-June 1	- Drained and Filled Ponds						
Jun 1-7	546	.120	.147	.027	18.4	" 31 (9)	
" 7-14	632	.181	.218	.037	17.0		
" 14-21	464	.142	.180	.038	21.1	Jun 16 (6)	
" 21-28	451	.141	.177	.036	20.3		
" 28-Jul 5	475	.159	.213	.054	25.3	Jul 3 (6)	
Jul 5-12	474	.102	.127	.025	19.7	" 6 (6), Jul 7 (6)	
" 12-19	462	.122	.159	.037	23.3	" 18 (9)	
" 19-26	417	.138	.176	.038	21.6		
" 26-Aug 2	330	.106	.126	.020	15.9		
Aug 2-9	310	.120	.138	.018	13.0		
" 9-16	377	.106	.112	.006	5.9	Aug 11 (6)	
" 16-23	358	.135	.146	.011	7.5	" 16 (6)	
" 23-30	440	.150	.156	.006	3.8		
Aug 30-Sep 6	680	.118	.166	.048	28.9		
Sep 6-13	263	.104	.113	.009	8.0	Sep 12 (12)	
" 13-20	332	.121	.143	.022	15.4		
" 20-27	670	.124	.160	.036	22.5	" 25 (8)	
" 27-Oct 4	451	.102	.136	.034	25.0		
Oct 4-11	271	.093	.112	.019	17.0	Oct 4 (8)	
" 11-18	440	.099	.177	.018	16.2	" 16 (8)	
" 18-25	264	.079	.103	.024	23.3		
" 25-Nov 1	370	.080	.102	.022	21.6	Nov 1 (4)	
" 1-8	215	.051	.070	.019	27.2		
" 8-15	343	.066	.079	.013	16.5		
" 15-22	283	.054	.061	.007	11.5		
" 27-30	260	.042	.051	.009	17.6		
Totals		4.922	3.996	.926	18.8		157 cu ft

AUGUST 1968

Tank	Variable / Date	1	2	14	15	16	22	23	24
	Cover & % Area	White Butyl (86%)		Styrofoam (87%)			Styrofoam (87%)		
Tank #1	Rn	125	141	31	20	33	34	29	29
	G	-37	-29	32	41	26	23	19	9
	LE	-56	-55	-93	-71	-95	-79	-64	-52
	A	-32	-57	30	10	36	22	16	14
	Cover & % Area	Open		Open			Open		
Tank #2	Rn	459	480	412	402	435	414	416	422
	G	27	-8	78	-53	14	69	-116	-55
	LE	-462	-434	-517	-371	-519	-467	-352	-362
	A	-24	-38	27	22	70	-16	52	-5
	Cover & % Area	Styrofoam (80%)		Styrofoam (51%)			Styrofoam (76%-1 hole)		
Tank #3	Rn	85	77	184	173	197	81	81	84
	G	-18	-8	62	36	37	28	15	-11
	LE	-86	-112	-312	-204	-291	-132	-118	-76
	A	19	43	66	-5	57	23	22	3
	Cover & % Area			Styrofoam (26%)			Styrofoam (76%-12 hole)		
Tank #4	Rn			298	290	325	81	81	84
	G			67	9	18	30	10	-8
	LE			-448	-317	-423	-146	-132	-96
	A			83	18	80	35	41	20
	$\bar{U}_a$ (cm/sec)	108	124	111	97	148	115	75	88

50-10

Table 4. Evaporation reduction using floating materials.

Cover	Open	White Butyl			Styrofoam					
Period	Evap. (cm)	Evap. (cm)	Red. (%)	Area Covered (%)	Evap. (cm)	Red. (%)	Area Covered (%)	Evap. (cm)	Red. (%)	Area Covered (%)
22 Jul - 3 Aug*	4.98	.74	85	86	1.17	76	80	-	-	-
17 Sep - 1 Oct**	6.84	1.66	76	80	1.75	74	80	-	-	-
11 Oct - 18 Oct	2.69	.66	75	80	.56	79	80	-	-	-
	Open	Styrofoam			Styrofoam			Styrofoam		
10 Aug - 19 Aug	6.37	1.05	84	87	3.31	48	51	4.96	22	26
	Open	Styrofoam			Styrofoam 1-hole			Styrofoam 12-hole		
19 Aug - 29 Aug	5.58	.92	84	87	1.35	76	76	1.67	70	76
29 Aug - 10 Sep	6.97	1.16	84	86	1.87	73	76	2.12	70	76

\* Only 7 days of good data during this period due to rain and filling tanks.

\*\* Only 10 " " " " " " " " " " " " " " " "

50-11

Table 5. Reduction in net radiation compared to evaporation reduction.

	% Reduction in net radiation as compared to open tank	% Reduction in evaporation as compared to open tank	
		Measured	Calculated
Period 1 - 2 Aug 1968			
White Butyl (86% cover)	72	88	84
Styrofoam (80% cover)	83	78	81
Period 14 - 16 Aug 1968			
Styrofoam (87% cover)	93	82	83
" (51% cover)	56	43	42
" (26% cover)	27	16	17
Period 22 - 24 Aug 1968			
Styrofoam (87% cover)	93	83	85
" (76% - 1 hole)	80	72	72
" (76% - 12 hole)	80	68	71

50-12

TITLE: WASTE-WATER RENOVATION BY SPREADING TREATED SEWAGE  
FOR GROUND-WATER RECHARGE

CRIS WORK UNIT: SWC W4 gG1 CODE NO.: Ariz.-WCL 67-4  
PART A.

INTRODUCTION:

The year 1968 was the first year of full-scale operation of the project. In the spring, grass was seeded in four of the six basins, another basin was covered with a gravel layer, and the sixth basin was left in the original soil condition. All basins were subjected to the same inundation schedules which consisted of sequences of short inundation periods of about 2 days each and of long inundation periods of about 2 wks each. The laboratory for water quality analyses was fully staffed and equipped, and analytical procedures were established.

Additional observation wells were installed early in the year to permit sampling of renovated water from the grass basins and from the non-grassed basins. Also, wells were installed outside the basin area to sample renovated water at greater horizontal distances from the recharge basins, and to permit evaluation of ground-water table profiles.

The hydraulics of the recharge flow system beneath the water table was further analyzed with a resistance network analog and supplemented with field measurements. The analog was also used to develop guides for the design of a large-scale, multiple-basin recharge system capable of handling a significant part of the sewage effluent.

To facilitate orderly presentation of the results, the report is divided into five sections: I. Infiltration Studies, II. Water Quality Studies, III. Aquifer Studies, IV. Design of a Large-Scale Recharge System, and V. Symbols.

The excellent cooperation with the Salt River Project, which received a Demonstration Grant from the Federal Water Pollution Control Administration for partial support of the project, was continued in 1968.

## I. INFILTRATION STUDIES

### 1. Recharge basin management and infiltration rates

For the first 4 months of 1968, all six basins were operated with bare soil as bottom condition. The water depth was about 0.6 ft and the basins were operated in parallel. Infiltration rate was calculated from the difference between the inflow at the west end of each basin and the outflow at the east end of each basin. The layout of the recharge basins and the location of the observation wells within the basin area are shown in Figure 1.

The effluent from the 91st Avenue treatment plant, which started to deteriorate in quality and turn "black" in the fall of 1967, continued to be of poor quality in 1968 until about the middle of August when the effluent became clear again. Apparently, the quality degradation was mainly an increase in settleable solids content, since the COD and other chemical parameters were not much higher for the (filtered) black effluent than for the clear effluent.

Due to the high settleable solids content of the effluent in the last few months of 1967, the recharge basins entered the year 1968 with a substantial layer of black sludge. Upon drying, this sludge blanket shrank and formed curled-up flakes of about 1 x 1 inch to about 3 x 5 inch in size. Drying also caused horizontal shrinking and the dry flakes covered about 50 percent of the bottom area. As the flakes curled up, a layer of soil particles adhered to their bottom, thus yielding a clean and open soil surface.

The first recharge period in 1968 was from 15 to 19 January (Figure 2A). The initial infiltration rates were quite high (from 1.7 ft/day for basins 1, 2, and 6, to 2.5 ft/day for basin 5), probably because of the long preceding dryup period. Because of the high settleable solids content of the effluent and a tendency of the sludge flakes already present on the bottom to slake back to their original form, the infiltration rate underwent a rather rapid decrease (Figure 2A).

During the dryup period starting 20 January, the sludge layer in the recharge basins again dried as curled-up flakes. These flakes were removed by hand raking in all basins on 6 and 7 February. Also, a gravel dam was constructed across each recharge basin about 50 ft from the inlet end to create a presedimentation basin (Figure 1). The dams, which consisted of 3/8-inch gravel, were about 2 ft high and 10 ft wide. Initially, the effluent went through the dams and good filtration was obtained. Clogging occurred, however, and after a few weeks, most of the effluent went over the dams. The reduction in settleable solids was then essentially obtained by sedimentation. Because of this, water after an inundation period remained much longer in the presedimentation basins than in the recharge basins. Thus, a valved drainpipe was installed through each gravel dam to allow drying of the sedimentation basins and permit removal of the sludge deposits.

The next recharge period was from 7 to 10 February and the recharge rates were between 2 and 3 ft/day (Figure 2A). The ensuing dryup period was marked by shower activity from 10 to 13 February when 1.9 inches of rain was recorded. On 20 February, all basins were harrowed with a tooth harrow, after which three short recharge periods were held (29 February-2 March, 7-8 March, and 15-17 March). The intake rates for these periods ranged from 1.5 to 2 ft/day for most basins.

A sequence of four longer (5-day) inundation periods was started on 26 March to see if a decrease in the nitrate content of the renovated water from the 30-ft well in the center of the basin area (East Center Well or ECW, Figure 1) could be obtained. The infiltration rates again ranged from 1 to 2 ft/day. On 16 April, the water depth in all basins was raised from 0.6 ft to 1.1 ft by inserting a board in the outlet structures. As shown in Figure 2A, this increase in water depth almost doubled the infiltration rate. Thus, most of the head due to the water depth in the basins was dissipated over a relatively thin layer at or near the surface of the soil.

Because of a gradual accumulation of sludge, the basins were swept with a power lawn sweeper on 7 May, which was quite effective. All

basins were then harrowed and basins 3, 4, 5, and 6 were seeded with a mixture of Common and Giant Bermudagrass using a hand broadcaster. A heavy chain was dragged over the freshly harrowed soil to cover the seeds. In addition, a few 10-ft wide test strips of other grasses were planted to determine their suitability for growing under prolonged inundation by sewage effluent. These grasses were Tifway, Fescue, Sudangrass, Blue Panicum, and Giant Bermudagrass.

Following the seeding and planting of grass, basins 3, 4, 5, and 6 were irrigated with about 6 inches of effluent every 2 or 3 days. These irrigations, for which the infiltration rates were estimated as about 2 ft/day, are shown as dots in Figure 2B. During the period of irrigating the grass basins, basins 1 and 2 were left dry. On 23 May, basin 2 was covered with a 2-inch layer of concrete sand, followed by a 4-inch layer of 3/8-inch gravel. Basin 1 was left in the original soil condition. All basins received about 1 ft of water on 7 June and on 12 June a sequence of short, frequent inundations was started for all basins. The basins were again operated in parallel with a water depth of about 0.6 ft. The sequence ended on 17 August. The infiltration rates during this sequence generally ranged from 1.5 to 2 ft/day with little difference between the grass, gravel, and bare soil basins (Figure 2B).

At the end of August, the grass in basins 3, 4, 5, and 6 had reached a mature stand. The Giant Bermudagrass emerged as the dominant species where a mixture of Common and Giant Bermudagrass had been used. To evaluate the effect of the grass cover on the quality of the effluent flowing through the grass, series flow was started. For basins 4, 5, and 6, this was achieved by closing the outlet of basins 6 and 5 and opening the flume connecting basins 6 and 5 at the east end of the basin area, and the flume connecting basins 5 and 4 at the west end (Figure 1). The effluent was admitted into the west end of basin 6 from where it flowed in serpentine fashion through basins 6, 5, and 4

to be discharged by the outflow structure at the east end of basin 4. Deducting the 50-ft sedimentation basins from the total length of recharge basins, the effluent thus traveled a distance of 1950 ft through the grass. A similar series flow system was set up for basins 1, 2, and 3, where the effluent was admitted at the west end of basin 3 and discharged at the east end of basin 1. The series-flow arrangement and the locations where samples of the surface water were obtained are shown in Figure 3. The effect of overland flow on effluent quality is discussed in Section I.5.

The reason for also establishing series flow in basins 1, 2, and 3 was to evaluate the performance of the gravel and bare soil basins with effluent that was essentially free from settleable solids. Thus, basins 6 and 3 were mainly used to remove settleable solids and the effect of the grass, gravel, and bare soil condition on infiltration rates was studied for basins 5 and 4 (grass cover), basin 2 (gravel), and basin 1 (bare soil).

For the series flow system, the first basin receiving the sewage effluent must also carry the flow for the following two basins in the series. Therefore, the discharge and also the water depth in basins 6 and 3 was higher than when the basins were operated in parallel. To a lesser extent, this was also true for basins 4 and 2. The following water depths (measured in the center of each basin) prevailed during the period of series flow.

Basin	Water depth in ft
1	0.7
2	0.7
3	0.85
4	0.85
5	0.85
6	0.95

The water depth for the gravel basin refers to the original soil surface. Since the combined sand and gravel layer in basin 2 is 0.5

ft thick, the water depth above the gravel in basin 2 was 0.2 ft. For the last recharge period (2-17 Dec), the water depth in basin 5 was 1.15 ft. This was due to the heavy growth in the Tifway test strip at the west end of the basin.

Rather long inundation periods were selected for the series flow sequence because the effect of "grass filtration" on effluent quality and the effect of a grass or gravel cover on infiltration could become more pronounced with increasing time. Long inundation periods were also selected to see if the nitrate content in the renovated water, which had increased during the sequence of short inundation periods in the preceding months, could be brought down again.

For the period 15 August to 17 December, the effluent was relatively clear and after flowing through one grass basin, there were little or no settleable solids. Nevertheless, the grass basins (5 and 4) yielded much higher infiltration rates than the bare soil basin (1) and the gravel basin (2), as shown in Figure 2C. Accumulated infiltration depths for the six inundation periods in the period 20 August-17 December were as follows:

Basin 1 (bare soil)	72 ft
Basin 2 (gravel)	45 ft
Basin 4 (grass)	111 ft
Basin 5 (grass)	127 ft

Assuming that infiltration rate varies linearly with water depth in the basin, the accumulated infiltration in basins 4 and 5 would have been 91 ft and 105 ft, respectively, if the water depths in these basins had been the same as in basins 1 and 2 (0.7 ft). Thus, although a greater water depth may have been partly responsible for the higher intake rates in basins 4 and 5, most of the difference in infiltration must be attributed to the grass cover.

The low infiltration rates in basins 6 and 3, especially at the end of the long inundation period in October (Figure 2C), are probably caused by the settling of suspended material.

Since the influent for the grass basins 5 and 4 and the gravel and bare soil basins was essentially free from settleable solids, the higher intake rates for the basins 5 and 4 may be due to the fact that the grass prevented the growth of algae on the soil surface. In contrast to the grass basins, basins 1 and 2 exhibited a luxurious growth of algae at the soil and gravel surface, respectively. During the daylight hours, oxygen bubbles were formed and remained entrapped in the algae mat. For the bare soil basin, this caused the algae to break loose and float to the surface in flakes of about 3 x 4 inches. Usually, a layer of soil particles adhered to the bottom of the flakes. Thus, the soil surface in basin 1 was "rejuvenated" during inundation by the continuous process of algae flakes breaking loose and floating to the surface. This process did not occur in the gravel basin, probably because the gravel particles to which the algae mat was anchored were too heavy. The difference in algae behavior may be one reason why the gravel had a lower intake rate than the bare soil basin. Other reasons may be the smaller water depth above the gravel surface, the poor drying of the soil beneath the gravel layer during dryups, and dust settling in the gravel layer and at the interface between the gravel and the sand layer.

The Giant Bermudagrass appeared to be the most suitable grass. It dominated the Common Bermuda and developed a vigorous stand that was sufficiently dense for filtration and shading, yet sufficiently open for the effluent to flow "through" rather than "over" the grass. This made it possible to use inundation periods as long as a month without adverse effects on the condition of the grass. Excellent growth was also exhibited by Tifway. However, the sod was too dense to permit the effluent to flow through the grass. The resulting increase in water depth and complete inundation then caused the Tifway to die, particularly at the inflow end where solids settled on the grass. The Sudangrass also grew well, but the stand was not sufficiently dense to provide filtration and shading. Also, it died

after reaching maturity. The other grasses tested (Blue Panicum and Fescue) failed to survive. None of the grasses were mowed in 1968.

As regards the optimum schedule of inundations and dryups, it appears that dryup periods of 3 days or less are not effective in restoring infiltration rates. As a matter of fact, the infiltration rate after a short dryup period may be the same as if the inundation had continued (see for example, the dryup period of 17-19 September in Figure 2C). In contrast to this, a dryup of 1 to 2 weeks (depending on the season) is more effective in restoring infiltration rates (see the period 27 September-9 October, for example). Inundation periods much longer than 2 weeks do not seem desirable because of the reduction in infiltration rates toward the end of period. Also, mosquito emergence may become a problem. Thus, an optimum schedule of inundation (assuming that a low nitrate content in the renovated water is desired) appears to be 2 weeks wet-1 week dry in the summer, and 2 weeks wet-2 weeks dry in the winter. Using grass-covered basins and about 1 ft of water depth, it appears that a long-term infiltration rate (including the time occupied by dryup periods) of about 300 ft/yr should be attainable.

## 2. Effect of cover on wetting and drying of soil profile

To study the effect of the surface condition of the basins (bare soil, gravel, and grass) on the drying and wetting of the soil profile, measurements of the water content and soil water pressures (or tensions) were made at various depths. Access tubes for a water-content measuring neutron probe were installed about 75 ft from the east end of the basins. One (aluminum) tube in each basin reached to the fine sand-gravel interface, which generally occurred at a depth of about 3 ft (see Annual Report 1967). Another tube (galvanized steel) was installed in each basin with a rotary drill rig to extend below the fine sand-gravel interface. In addition to the tubes for water content measurements, tensiometers were installed around a neutron access tube in basins 1, 2, 5, and 6. The tensiometers were installed in 10-cm depth intervals, starting at 10 cm below the basin surface and down

to the fine sand-gravel interface.

Typical effects of the surface condition on the water content profiles are shown in Figure 4. The measurements were taken at 20 cm below soil surface, 20 cm above the fine sand-gravel interface, at the interface, and 10 cm below the interface. The point taken at the interface is indicated by a circle around the dot (Figure 4). On 16 September the basins had just started to drain. In fact, the water content profiles were identical to those taken on 13 September when the basins were inundated. The other profiles were measured on 19 September, 3 days after the basins had started to drain.

The profiles in Figure 4 show that basins 1 and 5 had a higher water content in the fine-sand layer (above the sand-gravel interface) on the 16th than did basin 2. The water content in basin 2 during inundation was lower than had been observed previously for that basin, before the gravel layer was placed. This indicates that the low infiltration rates observed in basin 2 were probably caused by a restriction at or near the bottom of the basin.

The water content change between the 16th and 19th was greatest in basins 1 and 5. Basin 1 seemed to drain the most, but this may be partly due to the fact that it had a deeper layer of fine sand in the vicinity of the neutron access tube than did basin 5, i. e., 129 cm compared to 94 cm for basin 5. Basin 2 has about the same depth of sand as basin 1. The reason for the slower drainage of the soil profile in basin 2 may be restricted entry of air at or near the bottom of the basin. Also, the gravel layer on the bottom acts as a mulch and reduces the drying of the upper soil layers by evaporation.

Figure 5 shows the pressure-head profiles for basins 2 and 5 on the same dates as previously discussed. The tensiometers in basin 1 were not installed until late November. Measurements were planned for a December drainage, but due to freezing weather, none of the tensiometers were operative. Figure 5 further supports the conclusion drawn from Figure 4, that during inundation the soil under basin 5 is

wetter (less negative pressures) than under basin 2 (particularly at greater depths) and that the soil profile of basin 2 does not drain as rapidly as that of basin 5. Thus, the grass-covered basins which gave the highest infiltration rates dried as fast as any other basin. The gravel-covered basin gave the lowest infiltration rate and drained slower than any other basin. The bare-soil basin was intermediate in infiltration but drained about as rapidly as the grass-covered basin over a 3-day period of drainage.

### 3. Calibration of neutron probes

Calibration of the neutron probe for soil moisture measurement was done for two new Troxler model 104 probes, Serial Nos. G23653E and G22096, and the model 600 scaler, Serial No. 119. The new equipment had not previously been calibrated. Galvanized steel pipe and aluminum access tubes were used in the calibration because both types of tubes are used in the recharge basins. A set of secondary standards was made from low-density polyethylene rods for recalibration of equipment following repair or substitution.

The calibration was performed in a 1 m x 1 m x 1 m steel bin filled with Flushing Meadows loamy sand at a uniform water content. An aluminum access tube was installed, and measurements were taken with the two probes at 10-cm intervals, starting at 20-cm below the surface. Four  $\frac{1}{2}$ -minute readings were taken at each depth. The high voltage was set at 1350 volts. Standard readings using a Troxler S-5 water bucket were taken before and after each probe was placed in the access tube. A 2-inch galvanized pipe was then placed in the sand, and four 1-minute readings were taken at each depth. Soil cores for gravimetric water content and bulk density were taken at 15-cm intervals, starting at 20-cm depth. Four samples were taken at each depth. This process was then repeated for water contents ranging from 3.6% to 36%.

The count rate in the soil,  $C$ , was referred to the count rate of the Troxler S-5 water bucket standard,  $C_S$ . The ratio,  $R = C/C_S$ , and

the water content data were fitted to a least-squares polynomial. A second order polynomial was required to get an index of determination above 0.99. A third order polynomial was required to get the percent error for every point below 10%. For the actual calibration curve, a fourth order polynomial was used which gave a percent error less than 7% at each point. The equations used are given in Table 1. A ratio was also developed between the Troxler standard and the Kaiser standard, so that the Kaiser standard could be used in the field. This ratio was 0.7737 and 0.7689 for probes No. G23653E and No. G22096, respectively.

A set of secondary standards was made from polyethylene rods. The rods were 3, 3½, 4, and 4½ inches in diameter and 18 inches long. A 14-inch deep hole with a diameter of 1.90 inches was drilled in the center of each rod to accommodate the probe. Ten ½-minute readings were taken in each standard with each probe. The Troxler S-5 water bucket was used as the reference standard. Average count rates and R-values for the four polyethylene rods are given in Table 2. The polyethylene standards can be used to periodically check out the moisture probes. This is simpler than going through the complete calibration process in a soil bin.

A comparison calibration was obtained with one of the new probes (Serial No. 22096) and an old Troxler probe (Serial No. 18138). This was done by taking alternate readings in an access tube with the two probes. The water content as measured with the old probe was used for the calibration. The access tubes were in Adelanto loam soil. The results (Figure 6) show that the comparison calibration is 2% higher at the 30% water content, and that the two calibrations agree at the 18% water content. The comparison calibration was not carried out below a water content of 18%. The variation of the two calibration curves can be explained in part by the fact that two different soils were used: Adelanto loam for the comparison calibration and loamy sand for the new calibration. Also, determination of the water

content in the new calibration at the high water-content values was somewhat difficult.

#### 4. Polysaccharides in bottom soil

To determine if the surface condition of the recharge basins had any effect on the polysaccharide formation in the soil during inundation, and on the breakdown of polysaccharides during dryup, soil samples were analyzed for polysaccharides by the anthrone method. Samples were taken from the top inch of soil at five different locations in each basin. These were mixed and subsamples were taken for analysis. A check sample was collected from the moist soil near the East Center Well outside the recharge basins. The samples were taken on 6 November immediately after a 30-day inundation period, and on 2 December after the subsequent 25-day dry period. The results are expressed below in mg of polysaccharide (glucose equivalent) per g of air dry soil.

Basin No.	1	2	3	4	5	6	Check
polysac. after inundation	1.5	1.4	1.4	1.3	1.2	1.1	1.2
polysac. after dry-up	2.2	1.3	1.7	1.4	1.6	1.3	1.3

Although the infiltration rates of basins 1 and 2 (bare soil and gravel covers) were considerably lower than those for the grass covered basins, there were essentially no differences in the polysaccharide concentrations. Also, the polysaccharide concentrations in the basin soils were little different from those in the check soil and they did not decrease during a dry period. These results indicate that the lower infiltration rates of basins 1 and 2 and the reductions in infiltration rates of all basins during long inundations were not caused by an accumulation of polysaccharides.

#### 5. Effect of grass filtration on quality of effluent

To evaluate the effect of flow through the grass on the quality of the effluent, henceforth referred to as influent, continuous samples were obtained at the pump (influent sample) and at the flumes between basins 5 and 6 (5-6), 5 and 4 (5-4), 3 and 2 (3-2), and 2 and 1 (2-1).

Continuous samples were also collected at the outflow flumes of basins 4 (4-out) and 1 (1-out). The location of the sampling points is indicated in Figure 3.

The samplers consisted principally of a plastic intake tube syphoning influent to an overflow reservoir (Figure 7). This constant-level reservoir was then connected by a long plastic tube of small diameter to a 2-gallon plastic bottle. The small-diameter tube enabled control of the flow to the bottle without danger of plugging, as may occur if the flow is controlled by clamps, valves, or other sudden restrictions. The elevation of the constant-level reservoir was adjusted so that the flow rate into the bottle was about 40 drops a minute which yielded a sample of about 1.5 gallons for a 24-hour period.

The samples, which were collected daily as much as possible, were analyzed for COD, nitrate, ammonium, and Kjeldahl N (see Section II.1. for analytical techniques). The results (Tables 3 and 4) show that, contrary to what might be expected, there was little effect of the flow through the grass on the influent quality, even when the flow distance was about 2000 ft, for which the travel time was 16 hrs. There seems to be a slight tendency for the COD to increase as the influent flows through the grass, and for the ammonium and nitrate concentrations to decrease. The flow through the non-vegetated basins (2 and 1) also seems to have little or no effect on the COD and ammonium content (Table 3).

Since the grass was not mowed, a dense mat of about 0.5 ft thick and consisting of fallen-over grass stems several ft in length formed in the basins. Most of the mass flow of the influent took place above this mat, through the green growth of the grass. However, what infiltrated into the soil had to move through the mat. To evaluate the effect of the flow through the mat on the influent quality, a perforated copper tube of about 3-ft length was placed in horizontal position on the soil surface below the mat. The location of this tube

was near the flume connecting basin 6 to basin 5 and the sample is referred to as "6-5 tube." Continuous samples were obtained using a device similar to that of Figure 7.

The results of the analyses (Table 4) showed that there was a tendency for the COD to increase as the influent moved through the grass mat, probably because of the decaying grass stems and leaves. Also, there seemed to be a reduction in the ammonium content, probably because of nitrogen fixation in the decaying portions of the mat. The nitrate content was not appreciably affected. The possible effect of the increase in COD on the degree of denitrification in the renovated water is discussed in the following section.

## II. WATER QUALITY STUDIES

### 1. Observation wells and analytical techniques

Five new observation wells were installed in April 1968. Each well is 20 ft deep and is equipped with nonperforated 6-inch steel casing to the bottom. The casing is covered at the top with a standard-pipe end cap. The wells are located on a line through the center of the basin area, normal to the direction of the basins. Well No. 1 is 200 ft north of the center, Well 1-2 is between basins 1 and 2 (Figure 1), Well 5-6 is between basins 5 and 6 (Figure 1), Well 7 is 200 ft south of the center, and Well 8 is 400 ft south of the center. A diagram of the well locations is presented in Figure 15. A hand-operated bailer was used to obtain water samples from these wells. Prior to obtaining the sample, the wells were bailed out several times to insure that "fresh" ground water was sampled.

The main source for obtaining renovated water was the East Center Well (ECW) which is 30 ft deep, and like the West Center Well (WCW), which is 100 ft deep, located in the center of the basin area (Figure 1) and equipped with a submersible pump. Samples from the East Center Well were obtained daily (except weekends and holidays) after pumping the well out a few times to remove the "stale" water. Other sources of renovated water were the 20-ft wells 1, 1-2, 5-6, and 7, which were sampled periodically. Well No. 8 and the 100-ft deep West Center Well were still yielding native ground water.

The water samples were routinely analyzed for COD, (dichromate technique), ammonium (initially by the Nessler method and later by the distillation technique), Kjeldahl nitrogen (micro technique), nitrate (brucine method), and coliforms (multiple-tube fermentation technique). Periodically, ground water and influent samples were analyzed for pH, electrical conductivity, phosphate (Murphy and Riley method), boron (curcumin method), and fluoride (SPADN method). Standard Methods was used as a guide in the analytical techniques.

## 2. Chemical Oxygen Demand

The COD of the influent as it is pumped from the channel and the COD of the renovated water from the East Center Well are shown in Figure 8. The COD of the influent was determined from the supernatant liquid in the sample bottle so that it would be characteristic of the influent as it would move into the soil, relatively free of suspended material. The influent COD was about 55 ppm until August when reductions in the influent COD were observed. The change to a lower COD was coincident with an improvement in the appearance of the sewage effluent from a dark to a clear liquid.

The COD of the renovated water from the East Center Well is much less than that of the influent and about the same as that of the native ground water (Table 5). The 91st Avenue well in this table is a Salt River Project irrigation well located about  $1\frac{1}{2}$  miles east of the recharge basins.

## 3. Biochemical oxygen demand

Through the courtesy of the laboratory of the 91st Avenue sewage treatment plant, 5-day BOD-values were determined periodically for the East Center Well water. The results showed a BOD range of 0 to 1.2 ppm with an average value of about 0.3 ppm. The influent BOD was about 20-30 ppm.

## 4. Nitrogen

The total influent nitrogen was about 25 ppm N (Table 5 and Figure 9), consisting of about 24 ppm ammonium N, 1 ppm organic N, and about 0.15 ppm nitrate N. For short inundation periods (3 days or less) with dryup periods of about the same length, the influent nitrogen was essentially all converted to nitrate in the renovated (ECW) water (Figure 9). However, for a sequence of long inundation periods (5 days or more per period), lower nitrate contents in the ECW water were observed. This is shown very clearly in Figure 9, where the sequence of long inundation periods starting 26 March 1968 was followed by a drop in nitrate content for the ECW water on about 8 April 1968. A

sequence of short inundation periods starting 10 May caused an increase in the nitrate content in the ECW water on 6 June. A change to long inundation periods on 2 September yielded a nitrate content reduction in the ECW water on 9 September. In the last four months of the year, nitrate-nitrogen concentrations of essentially zero were observed. With ammonium-nitrogen concentrations of 2 to 4 ppm, reductions in total nitrogen content of about 90% were thus realized.

The lower nitrate content in the renovated water during and after a sequence of long inundation periods is attributed to bionitrification. This conclusion is based on (1) the reproducibility in raising or lowering the nitrate-nitrogen content of the renovated water by the length of the inundation schedule, and (2) the fact that during a sequence of short inundation periods the nitrate-nitrogen content of the renovated water is about the same as the total nitrogen level of the influent. The latter rules out temporary hold-back of nitrogen in tissue of microorganisms.

Prior to planting grass, the nitrate-nitrogen content of the ECW water during and after a sequence of long inundation periods was about 9 ppm (see January, April, and May periods in Figure 9). After the grass had reached maturity, another sequence of long inundation periods yielded nitrate-nitrogen contents of less than 0.5 ppm in the ECW water (14-24 September, 24 October-5 December, and 16-31 December in Figure 9). A similar low nitrate-nitrogen content, i. e., about 0.1 ppm N, was observed in Well 5-6, which, like the East Center Well, is located between two grass basins. The nitrate content for Well 1-2, which is located between the gravel and bare soil basins, however, ranged from 4 to 7 ppm N for the same sequence of long inundation periods. Thus, the renovated water from the grass basins apparently has a lower nitrate content than that from the sand or gravel basins during sequences of long inundation periods. A possible explanation for this is that movement through the grass mat increased the COD of the influent (Table 4). This would represent an additional energy

source which could enable more complete bionitrification. Other factors may be an increase in COD due to decaying grass roots, oxygen uptake by the grass roots, and higher infiltration rates in the grass basins. As regards the possibility that the more complete removal of nitrogen below the grass basins is caused by direct uptake of nitrogen by the grass roots, this is ruled out because such uptake would be insignificant when compared to the large amount of nitrogen (about 100 lbs of N per acre per day) that is applied with the effluent during inundation.

The ammonium content of the renovated water was not appreciably affected by the length of the inundation period. For most of the year 1968, it was about 2 ppm N for the ECW, and about 1 ppm N for the other wells (Figure 9 and Table 5).

The delay in response of the nitrate content in ECW to a change in inundation period is due to the time required for the water to travel from the recharge basin to the bottom of the 30-ft well. In Section III. 4, the travel time to the East Center Well was calculated as 16 days for an infiltration rate of 1 ft/day in the basins. For the period starting 26 March, the average infiltration rate was 1.3 ft/day, which would give a travel time of  $16/1.3 = 12$  days. This is in agreement with the 13 days delay in the reduction of the nitrate content of ECW water. For the period starting 2 September, the calculated travel time is 10 days, whereas it took 7 days before the nitrate content in the East Center Well decreased.

Isolated peaks in the nitrate content of ECW water, such as observed on 14 October and 9 December (Figure 9), are probably caused by the arrival of water that remained as capillary water in the soil profile during dryups. Because of the aeration, this water can be expected to have a high nitrate content. When inundation is resumed, this water moves ahead of the newly infiltrated water and causes a nitrate peak in the water pumped from the ECW well. The peak on 9 December is particularly distinct. The average intake rate in

basins 3 and 4 for the week of 2-9 December was 1.2 ft/day, which would yield an arrival time of  $16/1.2 = 13$  days. This agrees well with the 11 days after the beginning of the inundation period that the nitrate content was on its way down after having reached a peak.

#### 5. Phosphates

Analysis of the influent for total phosphates yielded about the same value as analysis for orthophosphates. Hence, subsequent analyses were made for orthophosphates only. The phosphate content of the influent ranged from 15 to 36 ppm P with an average of about 20 ppm. For the renovated water of ECW, the phosphate concentration was 5 to 10 ppm P, yielding a phosphate removal of about two-thirds. The phosphate analysis on the "outlying" wells 1 and 7 (Table 5) showed that additional movement of the renovated water below the water table may further reduce the phosphate content. The low phosphate content of the 5-6 well may be due to the fact that this well extends into material with very low hydraulic conductivity (see III.6). Thus, this material contains more clay and other fine particles than the more permeable formations prevailing at the other wells (III.6).

#### 6. Fluorides

The fluoride content of 5.2 ppm of the influent (Table 5) is quite high. The fluoride content of the renovated water at ECW is about half of that of the influent (Table 5). Additional lateral movement below the water table apparently gives further reduction in the fluoride content, as indicated by the concentrations for wells 1 and 7. The fluoride content of Phoenix tap water is 0.5 ppm, and of the native ground water at Flushing Meadows 0.8 ppm.

#### 7. Boron

The boron content of the influent and the ECW water remained consistently at about 0.5 ppm. By comparison, the boron content of the native ground water is 0.63 ppm (Table 5). A boron content of 0.5 ppm in irrigation water is below the level whereby damage to even the more sensitive crops will occur.

## 8. Salts

The salt content was calculated by multiplying the electrical conductivity in millimhos by 640 to obtain ppm. Table 5 shows that the salt content of the renovated water is slightly higher than that for the influent. This is probably due to evaporation from the basins. Such evaporation does not only occur during inundation, but also during dryups (evaporation from soil, evapotranspiration from vegetated surface). Assuming a recharge rate of 300 ft/yr and an evaporation rate of 7 ft/yr, a salt content increase of about 2% can be expected.

The concentrations of the more important ions in the renovated water are listed in Table 6. The sodium adsorption ratio (SAR) of the renovated water is 4.6, which is below the range of 8-18 whereby damage to the structure of the soil can occur if the water is used for irrigation of soils containing clay. The SAR-value is calculated as  $Na^+ / \sqrt{(Ca^{++} + Mg^{++})/2}$ , where the concentrations are expressed in milliequivalents per liter.

## 9. pH

The pH of the effluent and the renovated water ranged (Table 5) from 7.1 to 8.4 with most values between 7.5 and 8, which is a desirable range for irrigation, recreation, and other uses of the water.

## 10. Coliforms

Test results for the presumptive, confirmed and fecal coliform counts are shown in Figure 11 as the most probable number (MPN) per 100 ml. There is some tendency for the coliform counts to be higher for a sequence of long inundation periods (April, October, and December). This tendency is particularly pronounced for the fecal coliforms, where the MPN was essentially 0 for sequences of short inundation periods. For longer inundation periods where denitrification is occurring, the MPN of fecal coliforms was generally about 10 per 100 ml. Some peaks in the presumptive MPN seem to occur in erratic fashion.

High values for the presumptive and fecal MPN were observed after the water from the inundation period in December had arrived. When the inundation was stopped and groundwater flow ceased, the MPN began to decrease and on 7 January 1969, the presumptive MPN was 3.5 per 100 ml (average of 2 and 5 yielded by duplicate tests). Thus, die-off of coliforms was essentially complete after 3 wks. This indicates that an additional underground detention time of about 3 wks is sufficient to remove the coliforms that have survived the percolation through the first 30 ft of riverbed material.

#### 11. Biostimulation

Four 55-gallon drums were filled with water from different sources at Flushing Meadows in August. The barrels were placed in the "back yard" of the U. S. Water Conservation Laboratory to study the behavior of the different waters when impounded and exposed to the atmosphere. One drum was filled with renovated water from the East Center Well with a high nitrate content as occurred after a sequence of short inundation periods. Another drum was filled with renovated water from the same source but with a low nitrate content as occurred after a sequence of long inundation periods. The third drum was filled with secondary sewage effluent from the channel and the fourth drum with native ground water from the West Center Well. The concentrations of nitrate-nitrogen and phosphorus and the COD of the water at the start and during the course of the test are presented in Table 7.

The growth of algae was studied by measuring the depth of visibility of the water in the drums with a Secchi disk (Figure 12). The high- $\text{NO}_3$  drum appeared to go through one brief algae cycle, after which it supported a considerable, steady algae growth. The low- $\text{NO}_3$  barrel exhibited almost no algae growth until the weather became cool and then only a slight algae growth appeared. In both cases, the algae were primarily of the one-celled variety and very little scum was present. The maximum disk reading obtainable was 80 cm, which was the water depth in the drums.

The depth of visibility in the sewage-effluent barrel after scum removal has been consistently greater than that of the high-NO<sub>3</sub> water. However, there was a considerable growth of multi-celled algae in the sewage effluent. The effluent was covered with a thick green scum until the advent of cool weather when the algae growth seemed to be converted to the one-celled variety. The depth of visibility of the native ground water has been maximum for the entire period and has shown almost no evidence of algae growth.

Measurements of the dissolved oxygen content of the water were made with a galvanic cell oxygen analyzer. The dissolved oxygen content was measured in the afternoon to obtain the maximum value. The barrels were then covered overnight and another measurement was taken early the following morning to obtain the minimum value of a 24-hr period. The following data are averages of three measurements made during September and October:

	East Center Well (high-NO <sub>3</sub> )	East Center Well (low-NO <sub>3</sub> )	Sewage effluent	West Center Well
Maximum DO ppm	17.6	11.6	11.1	7.5
Minimum DO ppm	11.9	9.2	4.9	7.2

The oxygen consumption during the night in the high-NO<sub>3</sub> water was considerable but the water still remained supersaturated. Dissolved oxygen saturation at 25 C is 8.4 ppm. The dissolved oxygen content of the low-NO<sub>3</sub> water did not fluctuate greatly and the water remained supersaturated. The minimum dissolved oxygen content of the sewage effluent would be marginal for the growth of some species of fish.

The following measurements were made on 15 January 1969:

	East Center Well (high-NO <sub>3</sub> )	East Center Well (low-NO <sub>3</sub> )	Sewage effluent	West Center Well
Maximum DO ppm	11.1	10.6	8.8	9.3
Minimum DO ppm	6.6	8.2	4.4	8.7

The minimum dissolved oxygen measurements made during the winter were below saturation but the sewage water concentration of 4.4 ppm was the only one below the 5.0-ppm level which is generally considered the minimum safe level for game fish. The low-NO<sub>3</sub> reclaimed water contained only slightly less dissolved oxygen than it did during the fall. The dissolved oxygen content of the West Center Well water did not fluctuate much during either season, indicating very little algae growth.

Two goldfish were placed in each drum on 30 September 1968 and all have survived except one in the West Center Well water. Goldfish, however, can tolerate lower levels of dissolved oxygen than many species of game fish.

The NO<sub>3</sub> content has declined to a low level in all four drums except the one with water from the West Center Well (Table 7). Much of the nitrate has probably been incorporated into algae cells. The algae growth probably caused the increase in COD also.

The NO<sub>3</sub>- and PO<sub>4</sub>-concentrations in the West Center Well water are several times more than the generally recognized maximum levels to avoid algae growth. However, the algae growth in this barrel of water as indicated by Secchi disk and dissolved oxygen measurements was very slight. The low-NO<sub>3</sub> water also contained a considerable amount of PO<sub>4</sub> but it did not support much algae growth. This might have been due to its low NO<sub>3</sub> content.

The data obtained so far indicate that the low-NO<sub>3</sub> reclaimed water at Flushing Meadows would probably not present an algae problem if placed in lakes.

### III. AQUIFER STUDIES

#### 1. Depth of impermeable layer

In previous analyses of the underground flow system, the depth of the impermeable layer was taken as 230 ft (see Annual Report 1967). This value was based on logs of irrigation wells in the vicinity of the project. To obtain a more accurate value of the depth of the clay deposit forming the lower boundary of the flow system, the 200-ft observation well east of the recharge basin area (East Well, Figure 1) was deepened. The material below 200 ft consisted mainly of fine sand to a depth of 247 ft where the clay layer started. Thus, the impermeable boundary of the flow system is 247 ft below field surface.

#### 2. Improved analysis of ground-water flow system

The flow system below the water table as presented in the 1967 Annual Report was based on the simplification that the upper boundary of the system was a horizontal water table. The water table beneath the recharge basins was then taken as a line-source equipotential. The rest of the water table was taken as a line-sink equipotential. This simplification neglected the flow above the original water table and caused all equipotentials to come together at the point separating the source and the sink. This situation of course does not occur in reality and the resulting system was only an approximation.

An improved flow system was obtained by including the ground-water mound in the representation of the flow medium by resistors on the resistance network analog. In the previous report, the height,  $h_c$ , of the center of the groundwater mound above the original water table was calculated as 3.8 ft. Using this value, the shape of the rest of the mound was estimated and represented on the analog. A uniform current input for the portion of the mound beneath the recharge basin area was then established and the potentials along the upper boundary of the flow system were evaluated. From these potentials, an improved estimate of the shape of the mound was obtained which was simulated on the analog, etc. This procedure was

repeated until the correct shape of the mound was obtained. The improved flow system with equipotentials and streamlines is shown in Figure 13. Since reversal of the boundaries for determining streamlines was not possible in this case, the streamlines were taken from the simplified flow system as shown in the previous report.

The equipotentials in the improved flow system yield a water level rise of 2.62 ft in the East Center Well and of 0.78 ft in the West Center Well. This agrees quite closely with the values observed in the field, i.e., 2.7 and 0.7 ft, respectively, so that the 16-fold ratio between horizontal and vertical hydraulic conductivity still holds. The values of the hydraulic conductivity in horizontal direction,  $K_h$ , and that in the vertical direction,  $K_v$ , yielded by the improved analysis were 282 ft/day and 17.6 ft/day, respectively. These values are somewhat lower than those yielded by the simplified analysis, probably because the additional resistors representing the groundwater mound changed the network configuration immediately below the recharge basins.

### 3. Effective transmissibility

The groundwater mound of the flow system in Figure 13 is shown in Figure 14 with the vertical scale exaggerated. Treating the flow system on the basis of the Dupuit-Forchheimer assumption, i. e., ignoring all vertical flow components, the flow beneath the groundwater mound can be described by the following equation:

$$\bar{I} x = - T \frac{dh}{dx} \quad (1)$$

where  $\bar{I}$  = intake rate for recharge basin area (ft/day)  
 $T$  = effective transmissibility of the aquifer (ft<sup>2</sup>/day)  
 $h$  = height of groundwater mound above original water table  
 $x$  = horizontal distance from symmetry line.

In contrast to  $I$ , which refers to the actual infiltration rate in a basin,  $\bar{I}$  represents the gross recharge rate for the total area in

which the basins are located. This area includes the area between recharge basins and that occupied by dry basins. Of course, the recharge basins should be sufficiently frequent to permit treatment of the area as one recharge unit.

Integrating equation (1) for the region beneath the percolation zone yields

$$h_c - h_e = \frac{\bar{I} W^2}{8T} \quad (2)$$

where  $h_c = h$  at center of mound

$h_e = h$  at edge of mound ( $x = W/2$ )

$W =$  width of recharge basin area

For the mound in Figure 14,  $h_c = 3.80$  ft,  $h_e = 2.35$  ft,  $\bar{I} = 1.91$  ft/day, and  $W = 220$  ft. Substituting these values in equation (2) yields a value of  $7,970$  ft<sup>2</sup>/day, or rather  $8000$  ft<sup>2</sup>/day, for the effective transmissibility of the aquifer as applying to a recharge area  $220$  ft wide. Since the hydraulic conductivity in horizontal direction is  $282$  ft/day, the effective height of the flow system is  $7,970/282$  or  $28$  ft. According to Figure 13, this depth corresponds approximately to the 60% streamline.

In applying the effective transmissibility to the design of a large-scale, multiple-basin recharge system, as discussed in Section IV, the question arises of whether the effective transmissibility value is constant or dependent on the width of the recharge basin area. If the high value of  $K_h$  is due to a single layer of very high hydraulic conductivity, the effective transmissibility will not depend on the width of the recharge basin area. If the aquifer is uniform or uniformly anisotropic, however, the effective transmissibility will vary in direct proportion with the width of the recharge basin area, until the effective height of the flow system is about equal to the height of the water table above the impermeable boundary. For the

Flushing Meadows area, this height is 237 ft.

The well logs at Flushing Meadows (see 1967 Annual Report) show a rather irregular succession of sand and gravel layers. Hence, the aquifer at that location should probably be considered as uniformly anisotropic and the effective transmissibility should be taken in proportion to the width of the recharge basin area. For the conditions at the Flushing Meadows site, the effective transmissibility can be calculated as:

$$T_w = \frac{W}{220} 8000 \quad (3)$$

where  $T_w$  is the effective transmissibility for a recharge basin, or area of recharge basins, of width  $W$ .

The analysis of the flow system in Figure 13 and the development of equation (2) are based on the assumption that the recharge basin area is of infinite length. Hence, flow components not perpendicular to the main direction of the recharge basin area are ignored. In practice, this assumption will be valid if the length of the recharge basin area is at least several times the width.

The hydraulic properties discussed in this section apply only to the Salt River bed at the Flushing Meadows location. Modification of the data may be desirable if the results are to be used for the design of a recharge system at different locations in the Salt River bed.

#### 4. Arrival times of renovated water

The time required for the renovated water to reach the bottom of the East Center Well and that of the West Center Well was calculated from the potentials on the symmetry line in Figure 13. The assumptions were made that (1) the aquifer is uniformly anisotropic (thus ignoring the effect of any distinct layers of low permeability that may have an overriding effect on the arrival time), (2) the difference in density between the reclaimed water and the more saline native ground water has no effect, and (3) dispersion effects can be ignored and the native ground water is displaced in piston-like manner.

Assuming an infiltration rate of 1 ft/day in the basins, the potentials in ft of water on the vertical symmetry line in the flow system of Figure 13 are presented in Table 8. In the third column, the vertical hydraulic gradients are shown. Assuming a porosity of 33% in the sand and gravels of the aquifer and taking the hydraulic conductivity in vertical direction at 17.6 ft/day, the macroscopic velocity is calculated in column 4. The sixth column shows the time required for the water to travel each depth increment, and the accumulated times are shown in the last column. Thus, for a sustained infiltration rate of 1 ft/day in the basins, it takes about 16 days for the water to reach the bottom of the 30-ft ECW well, and 315 days to reach the bottom of the 100-ft WCW well.

Usually, the infiltration rates vary between 1 and 2 ft/day during the first week of an inundation period. For an infiltration rate of 2 ft/day, the renovated water will reach the East Center Well in about 8 days. As discussed in Section II.4, calculated arrival times agree reasonably with arrival times evaluated from the nitrate behavior in ECW.

For the West Center Well, the arrival time of the water is much longer. At the time this report was prepared (December 1968), reclaimed water had still not arrived at the 100-ft West Center Well. The average long-term infiltration rate since the start of the Flushing Meadows Project in September 1967 is about 0.62 ft/day. At this rate, it will take  $315/0.62$  or 508 days before the native ground water at the bottom of the West Center Well will be replaced by reclaimed water. According to these data, therefore, a drop in the salt content from the present 3000 to 4000 ppm of the native ground water to the 1000 ppm of the reclaimed water can be expected for the 100-ft West Center Well in the second year of operation.

##### 5. Response of water table to ground-water recharge

In April 1968, additional observation wells were installed in a line through the center of the recharge basin area normal to the

direction of the basins. The location of these wells, each of which is about 20 ft deep and cased to the bottom with 6-inch nonperforated steel pipe, is shown in the upper part of Figure 15. The lower part of Figure 15 shows typical water level profiles yielded by these wells. The profile of 7 October was measured at the end of a 12-day dryup period. The profile of 14 October was measured after 1 wk of inundation, and the profile of 21 October was measured after 2 wks inundation. The water levels on 21 October are lower than on 14 October (except for well 7) because the infiltration rates decreased during the recharge period. The "irregularities" in the curves of Figure 15 reflect the nonuniformity of the underground formations. Since the East Center Well is 30 ft deep as compared to 20 ft for the newly installed wells, the water level in the East Center Well during recharge will be lower than in a comparable 20-ft well because of head loss due to the downward movement of the water. The water level in well 5-6 rises very slowly after the well has been pumped out. For this reason, well 5-6 is only used to obtain water samples for quality analysis and not for water level measurements.

As in 1967, the water level in the observation wells rose during the first few days of the recharge period to assume a pseudo-equilibrium level. After the recharge period, the water levels returned to essentially their original positions. The water table during recharge was about 9 ft below the bottom of the basins, and during dryup about 10 ft.

#### 6. Hydraulic conductivity of aquifer

As shown in the lower part of Figure 15, the water level in the East Center Well rose 1.0 ft during the first week of the recharge period which started 9 October. The average infiltration rate for all basins on 14 October was 1.4 ft/day. Because the height of the pseudo-equilibrium position of the water table above the original ground-water table is proportional to the infiltration rate, the water level rise per unit infiltration rate can be calculated as

1.0/1.4 = 0.71 days. A year ago (September 22-27, 1967), the pseudo-equilibrium position of the water level in the East Center Well was 2.7 ft above the original water table for an average infiltration rate of 3.5 ft/day in the basins (see Annual Report 1967). The water level rise per unit infiltration rate calculated for these data is 0.77 days, which is only slightly higher than the value of 0.71 calculated for October 1968. Thus, the hydraulic conductivity of the aquifer has not undergone a significant change during the first year of operation of the project.

On 25 November, the hydraulic conductivity, K, of the soil material below each observation well was determined with the tube method of Kirkham and Frevert. With this technique, the water level in the well is lowered a few feet below its equilibrium position, after which the rate of rise of the water level is measured for calculation of K. The following results were obtained:

<u>Well</u>	<u>K in ft/day</u>
1	2.5
1-2	173
ECW	34
WCW	270
5-6	0.1 (estimated)
7	775
8	620

The above values of K can be divided into two groups, one with relatively high values and one with relatively low values. This would be in agreement with the nature of the alluvial deposits, which is an irregular succession of gravelly materials with relatively high permeability and sandy and silty materials with relatively low permeability. The average of the values in the low group (0.1, 34, and 2.5) is 12.2 ft/day. The average of the values in the high group (173, 270, 775, and 620) is 458 ft/day. If aquifer material is considered to consist of alternate, equally thick layers of relatively

fine and relatively coarse material, the permeability in horizontal direction can be calculated as the arithmetic mean of the permeabilities of the layers, and that in vertical direction as the harmonic mean. Applying this approach to the group averages of 12.2 and 458 ft/day yields a horizontal permeability of 236 ft/day and a vertical permeability of 23.7 ft/day. This is in good agreement with the values of 282 ft/day and 17.6 ft/day obtained by electrical analog (Figure 13) from the recharge rate and the water level response in ECW and WCW.

#### IV. DESIGN OF A LARGE-SCALE RECHARGE SYSTEM

##### 1. Layout of system and principles of operation

As stated in Section I. 1, it is expected that an annual recharge rate of 300 ft/yr can be maintained. Thus, for every 1000 acre-ft of sewage effluent to be reclaimed annually, approximately 3 acres of recharge basin are required. For the projected flow of 300,000 acre-ft per year, 1000 acres of recharge basins would thus be necessary. A possible arrangement of recharge basins for such a large-scale system is shown in Figure 16. The basins are concentrated in two parallel "strips" on each side of the Salt River bed. Midway between the strips would be a series of wells to pump up the reclaimed water. As presented in Figure 16, the system consists of 50 acres of recharge basins which would be capable of handling 15 mgd of effluent. The reclaimed water could be pumped directly into the canals for indiscriminate irrigation, or part of the reclaimed water could be passed through a series of lakes. These lakes could be combined with park developments and they could be used for fishing, boating, picnicking, etc. The recharge strips could be expanded in westward direction to utilize water from the 91st Avenue treatment plant. The lakes and parks could be expanded eastward to include development at several parts in the Salt River bed between 23rd Avenue and Mesa. The presence of recreational lakes and parks in portions of the Salt River bed would undoubtedly enhance the value of the Salt River bed to the community.

A schematic plan and cross section of the system of recharge basins and wells presented in Figure 16 is shown in Figure 17. To minimize the spread of reclaimed water into the aquifer north and south of the Salt River bed and to minimize the inflow of native ground water into the recharge flow system, the system in Figure 17 should be operated so that the ground-water table below the outside edges of the recharge strips is kept as much as possible at its original position. In that case, all the water infiltrated through the recharge basins will flow to the wells with little or no movement to or from the aquifer outside the recharge flow system.

The highest position of the water table will occur beneath the outside edges of the recharge strip opposite the point midway between the wells (point C in Figure 17). The best way in practice to maintain the water table at point C, or the average position of the water table beneath the outside edges of the recharge strip, at its original "pre-recharge" position will be to install an observation well at point C, and operate the system of basins and wells so as to avoid a change in the water table elevation at that point. To obtain some idea of the water table elevations beneath the recharge basins and near the wells and how these elevations are affected by the geometry of recharge basins and wells, analyses were performed with an electrical resistance network analog.

## 2. Analog studies

The analyses were performed to determine the difference between the water table elevation at point C and that adjacent to the well in relation to system geometry, recharge rate, and aquifer transmissibility. The analyses were carried out for a plan model of the system. Thus, vertical flow components were ignored. A constant transmissibility was used, neglecting the effect of a change in water table position on the transmissibility of the aquifer. Use of a plan model with constant transmissibility is valid for a flow system of the type in Figure 17, provided that the transmissibility value used is the effective transmissibility for the "active" flow region, which is usually less than the transmissibility of the entire aquifer.

Assuming that all water entering the soil at the recharge basin will be pumped out by the wells and that there is no inflow of native ground water from outside the system, the spacing,  $S$ , of the wells can be calculated as

$$S = \frac{Q_w}{2 \bar{W}I} , \quad (4)$$

where  $Q_w$  is the discharge per well. A graph based on this equation showing  $\bar{W}I$  as a function of  $S$  for different well discharges expressed

in gpm is presented in Figure 18. Thus, if the well discharge is 4000 gpm,  $\bar{I} = 1$  ft/day and  $W = 800$  ft, the well spacing should be 480 ft.

The flow beneath the recharge strip was assumed to be in linear direction, parallel to BC (Figure 17). The water table drop between B and C,  $\Delta H_{B-C}$ , was calculated with equation (2) in Section III.3. Since there is no symmetry in the center of the recharge strip, the equation applying to the system of Figure 17 is

$$\Delta H_{B-C} = \frac{\bar{I} W^2}{2T} \quad (5)$$

Thus, the value of  $W$  for the system in Figure 17 is twice the value of  $W$  in equation (2). Because the flow beneath the recharge strip is assumed to be linear,  $\Delta H_{E-A}$  is equal to  $\Delta H_{B-C}$ . The water table at E and A will be lower than at C and B, however.

Because of the symmetries in the flow system, only one quadrant of the flow system around each well needed to be represented on the analog (Figure 19). The flow system from BA to the well was analyzed by resistance network analog. Because of the assumption of one-directional flow in section ECBA, the line BA in the analog model was a line source with uniform inflow distribution. The well was a point sink. The node arrangement in the analog for the case where AB is equal to the distance from A to the well ( $L = S/2$ ) is indicated in Figure 19. The difference between the water table elevation at A and that adjacent to the well is called  $\Delta H_A$ . Using different values for AB and the distance  $L$  between A and the well, the relationship between flow rate, transmissibility, and  $\Delta H_A$  was evaluated. A dimensionless plot of the results is presented in Figure 20. The ratio of the elevation difference,  $\Delta H_B$ , between the water table at B and that at the well, to  $\Delta H_A$ , is shown in Figure 21, again as a function of  $L/S$ . Figure 21 shows that as long as  $(L/S) > 0.5$ , the water table has about the same elevation at A as at B. This supports the validity of the assumption of one-

directional flow in the section ABCE.

To illustrate the use of Figures 20 and 21, the elevation difference between the water table at points, A, B, and C on the one hand, and the water table adjacent to the well on the other hand, will be computed for the following values:

$$\bar{I} = 1 \text{ ft/day}$$

$$W = 400 \text{ ft}$$

$$L = 500 \text{ ft}$$

$$Q_w = 4000 \text{ gpm}$$

$$T = 20,000 \text{ ft}^2/\text{day}.$$

The first step is to evaluate the value of  $S$  so that the well discharge equals the recharge volume. Figure 18 shows that for the above values of  $\bar{I}$ ,  $W$  and  $Q_w$ ,  $S = 950 \text{ ft}$ . Thus,  $L/S = 0.526$ , which according to Figure 20 yields a value of 1.43 for the ratio  $2WS\bar{I}/T \Delta H_A$ , from which  $\Delta H_A$  is calculated as 26.7 ft. Figure 21 shows that for  $L/S = 0.526$ ,  $\Delta H_B/\Delta H_A = 1.032$ , so that  $\Delta H_B = 27.5 \text{ ft}$ . The value of  $\Delta H_{B-C}$  is calculated with equation (5) as 4 ft so that the water table at point C will be 31.5 ft higher than at the well, or  $\Delta H_C = 31.5 \text{ ft}$ .

Using the above procedure, a graph was constructed showing the relationship between  $T\Delta H_C/\bar{I}$  and  $S$  for different well discharges and a constant  $L$ -value of 500 ft (Figure 22). Similar graphs can be developed for other values of  $L$ , thus enabling rapid evaluation of  $\Delta H_C$  for a number of situations.

The analysis so far applies to a constant value of  $T$ , which implies that the effective transmissibility for the recharge flow system beneath and adjacent to the recharge strips and the effective transmissibility for the subsequent lateral flow toward the well are the same. However, in reality, the transmissibility for the well flow system may exceed the effective transmissibility for the recharge flow system. This is because the well may penetrate the aquifer to greater depth than the effective depth of the recharge flow system. To account for this in the solution of the flow system,

the evaluation of  $\Delta H_A$  and  $\Delta H_B$  according to Figures 20 and 21 can be done for the appropriate value of T for the well flow system. The value of  $\Delta H_{B-C}$  can then be calculated with equation (5) using the effective transmissibility value for the recharge flow system. For example, if for the previous example the value of T for the well flow system were 40,000 ft<sup>2</sup>/day and for the recharge flow system 10,000 ft<sup>2</sup>/day, the following values would have been obtained:  $\Delta H_A = 13.4$  ft,  $\Delta H_B = 13.8$  ft,  $\Delta H_{B-C} = 8$  ft, and  $\Delta H_C = 21.8$  ft.

The value of L is governed by the distance and time of travel of the renovated water through the aquifer necessary to provide removal of bacteria, viruses, and odor. Quantitative information regarding desired values of L is scarce and the selection of the value for L depends on such factors as the intended use of the reclaimed water, the additional treatment provided, the soil materials of the aquifer, the possibility of short circuiting through cracks, fissures, or other large openings, etc. In view of experiences obtained elsewhere, L for the Salt River bed with its fine and coarse sands and gravel should not be much less than about 500 ft. In practice, L may also be affected by the availability of land and by the width and topography of the river bed. As regards the desired underground detention time to yield renovated water of a desirable quality, a time of about 3 weeks seems sufficient for complete removal of the coliform bacteria (see II. 10). Longer times may be required for the removal of virus, taste, and odor.

The analysis presented in this report applies to two parallel recharge basin strips with the wells located midway between the strips. Thus, all the recharge water that has infiltrated into the basins must travel to the wells midway between the recharge strips. In some cases, it may be desirable to install more than two parallel recharge basin strips. In such a multiple-strip system with wells midway between the strips (Figure 23), the center line of each strip becomes a symmetry line. Hence, to apply the analysis of the flow system as presented

in this section to the multiple-strip system, W should be taken as  $\frac{1}{2}$  the width of the recharge-basin strip.

## V. SYMBOLS

- $h$  = height of water-table mound above original water table
- $h_c$  = height of center of water-table mound above original water table
- $h_e$  = height of water-table mound at edge of percolation zone above original water table.
- $\Delta H_A$  = elevation difference between water table at point A and water table adjacent to well
- $\Delta H_B$  = as  $\Delta H_A$ , but for point B
- $\Delta H_C$  = as  $\Delta H_A$ , but for point C
- $\Delta H_{B-C}$  = elevation difference between water table at points B and C
- $I$  = infiltration rate in recharge basin (length/time)
- $\bar{I}$  = infiltration rate for gross area covered by recharge basins (length/time)
- $K$  = hydraulic conductivity of soil (length/time)
- $K_h$  =  $K$  in horizontal direction
- $K_v$  =  $K$  in vertical direction
- $L$  = distance between edge of recharge basin and well
- $P$  = soil-water pressure head (cm of water)
- $Q_w$  = discharge of well
- $S$  = distance between wells
- $T$  = transmissibility of aquifer (length<sup>2</sup>/time)
- $T_w$  =  $T$  for a recharge-basin area of width  $W$
- $W$  = width of area covered by recharge basins

## SUMMARY AND CONCLUSIONS:

The year 1968 was the first year of full-scale operation of the Flushing Meadows Project. In the beginning of the year, additional observation wells were installed to permit sampling of renovated water below the grassed and the non-grassed basins, and at greater horizontal distances from the recharge basins. Four basins were seeded to grass, one basin was covered with a 4-inch layer of fine gravel, and the sixth basin was left in the original condition. In each basin, gravel dams were installed about 50 ft from the inlet end to create sedimentation basins for removal of suspended solids in the effluent.

Of the various grass varieties planted, Giant Bermuda appeared the most suitable for sewage-effluent recharge basins, and it emerged as the dominant species where a mixture of Common and Giant Bermuda-grass had been used. The grass basins yielded the highest infiltration rates and the gravel basins the lowest. Accumulated infiltration amounts for the last 4 months in 1968 were 98 ft for the grass basins, 72 ft for the bare soil basin, and 45 ft for the gravel basin. Flow through the grass did not appreciably affect the chemical oxygen demand and the ammonium and nitrate contents of the effluent.

The effect of the surface condition of the basins on the wetting and drying of the soil profile during intermittent inundation was studied by determining soil water contents, soil water pressures, and polysaccharide concentrations. The grass basins, which gave the highest infiltration rate, also exhibited the fastest rate of drying when inundation was stopped. The gravel basin, which gave the lowest infiltration rate, also had the lowest rate of drying. The bare soil basin drained about as rapidly as the grass basin for the first 3 days of drying. Although the basins showed different infiltration rates, there was essentially no difference in the polysaccharide concentration of the surface soil. Also, the polysaccharide concentrations in the basin soils were little different from those in the soil outside the basins. No appreciable difference was found between the polysaccharide

content in the soil after an inundation period and after a dryup period.

The inundation schedules in 1968 were the same for all basins and consisted of sequences of short inundation periods of about 2 days each and sequences of long inundation periods of about 2 wks each. Dryup periods varied from about 2 days to about 2 wks. For the short inundation periods, almost all the nitrogen in the effluent was converted to nitrate as it percolated through the soil to the 30-ft deep well in the center of the recharge basin area. For the long inundation periods, 90% removal of the nitrogen in the effluent was achieved, probably because of biodenitrification in the soil. Denitrification was more complete below the grass basins than below the bare soil and gravel basins. Phosphates were reduced from 25 to 6 ppm P, fluorides from 5 to 2.5 ppm F, chemical oxygen demand from 45 to 12 ppm, and biochemical oxygen demand from 20 to 0.2 ppm. Boron, total salt, and pH of the reclaimed water were about the same as of the effluent, i. e., 0.5 ppm, 950 ppm, and 7.9, respectively. The number of coliform bacteria in the reclaimed water from the 30-ft well was higher during long inundation periods than during short periods, when the MPN of fecal coliforms was essentially zero. Optimum inundation schedules for maximizing the quantity of reclaimed water per unit basin area and minimizing the nitrate content of the reclaimed water appeared to be about 2 wks inundation and 1 wk dryup in the summer and 2 wks inundation and 2 wks dryup in the winter. With this schedule, recharge rates of about 300 ft/yr should be attainable. Thus, for every thousand acre-ft of sewage effluent to be reclaimed per yr, approximately 3 acres of recharge basins are required.

The biostimulative properties of the sewage effluent, the high-nitrate reclaimed water, the low-nitrate reclaimed water, and the native ground water were studied in 55-gallon drums with goldfish. Algae growth in the drums was evaluated by measuring the depth of

visibility with a Secchi disk. The high-nitrate reclaimed water supported a steady, heavy growth of algae of the one-cellular type. The low-nitrate reclaimed water exhibited much less algae growth and would probably be suitable for use in recreational lakes. Except for the sewage effluent drum, dissolved oxygen levels never dropped below a value where fish may be endangered. During the impoundment, nitrate and phosphate concentrations decreased and the COD increased. Fish survived in all drums, except in the native ground-water drum where one mortality was observed.

An improved analysis of the recharge flow system below the ground-water table was made with the resistance network analog. The values for the horizontal and vertical hydraulic conductivity yielded by this analysis were 282 and 17.6 ft/day, respectively. These values were in good agreement with the 236 and 23.7 ft/day, respectively, calculated from the results of permeability measurements with the tube method on the observation wells.

From the improved flow system analysis, the times of travel for the water to reach the 30-ft well and the 100-ft well in the center of the basin area were calculated. The travel time for the 30-ft well was about 10 days, which was in excellent agreement with the travel times deduced from the nitrate behavior in the water samples from the 30-ft well. For the 100-ft well, the travel time of the water was estimated as about 500 days. Native ground water at the 100-ft well had not yet been replaced with reclaimed water when this report was written, which is about 450 days after the start of the recharge operations.

The effective transmissibility of the aquifer at the Flushing Meadows Project was evaluated by applying the Dupuit-Forchheimer theory to the ground-water mound as evaluated by the analog analyses. The resulting value was  $8000 \text{ ft}^2/\text{day}$ . This value can be used in the analysis of a multiple-basin system by representing a horizontal plan of the system on the resistance network analog.

A plan for a large-scale multiple-basin recharge system capable of handling a significant volume of the effluent was developed. The system consists essentially of two "strips" of recharge basins, one strip along the north side of the river bed and one along the south side. The reclaimed water will be pumped up by a series of wells which is located midway between the recharge-basin strips. Analyses were performed with the resistance network analog to predict the water table positions in relation to the geometry of the recharge basins and of the wells pumping the reclaimed water, the recharge rates, and the effective transmissibility of the aquifer.

PERSONNEL: Herman Bouwer, J. C. Lance, R. C. Rice, F. D. Whisler, and E. D. Escarcega.

Salt River Project: Paul Kuechelmann and Geoffrey Ekechukwu.

CURRENT TERMINATION DATE: 1972.

Table 1. Moisture Probe Model 104-A Calibration Coefficients for Fourth Order Polynominal.

Tubing	Probe	Coefficient <sup>1/</sup>				
		A	B	C	D	E
2" Aluminum	G-22096	1.2398	-0.9988	0.1892	0.5388	-0.0269
	G-23653E	1.9137	-2.1879	0.8577	0.3856	-0.0174
2" Galvanized Pipe	G-22096	59.9687	-53.6572	16.8553	-1.3673	0.0541
	G-23653E	16.1071	-15.7617	5.5274	-0.0124	-0.0029

<sup>1/</sup> Coefficient for the equation  $\theta = AR^4 + BR^3 + CR^2 + DR + E$

Where  $R = \frac{\text{Count Rate in Soil}}{\text{Count Rate in Troxler Standard}}$

High voltage set at 1350 volts.

Table 2. Summary of Secondary Polyethylene Standards. Readings  
for Troxler Model 104A Moisture Probe.

Diameter of Poly. Standard	Probe No. G-23653E		Probe No. G-22096	
	C	R = C/C <sub>S</sub>	C	R
3	13,770 ± 147	0.170	11,860 ± 74	0.167
3.5	27,700 ± 176	0.441	23,950 ± 197	0.338
4	41,760 ± 177	0.515	35,980 ± 208	0.508
4.5	55,670 ± 364	0.686	48,420 ± 237	0.683

$$C_S = 81,140 \pm 568$$

$$C_S = 70,860 \pm 296$$

High voltage set at 1350 volts.

Table 3. Effect of flow through basins on COD, NH<sub>4</sub>, and NO<sub>3</sub> content of influent.

	COD, ppm O <sub>2</sub>				NH <sub>4</sub> , ppm N					NO <sub>3</sub> , ppm N	
	28-29 Aug	4-5 Sep	24-25 Sep	26-27 Sep	4-5 Sep	11-12 Sep	12-13 Sep	25-26 Sep	26-27 Sep*	28-29 Aug	12-13 Sep
Influent (pump)	50	48	28	47	26.5	24.3	27.5	26.2	27.1	0.11	0.14
6-5	46	49	47	56	24.9	26.5	26.7	26.3	27.6	0.06	0.02
5-4	50	53	40	43	26.1	26.6	27.8	27.2	28.7	0.05	0.02
4-out	57	58	39	43	26.0	26.0	24.7	25.5	?	0.08	0.05
3-2	46	49	?	?	26.8	26.2	24.8	?	?	0.05	0.07
2-1	46	56	42	43	25.5	26.8	24.9	25.9	26.1	0.07	0.02
1-out	?	55	40	42	24.9	22.3	26.3	25.0	25.9	?	0.02

\*Kjeldahl N

Table 4. Effect of flow through grass basins and grass mat on COD, NH<sub>4</sub>, and NO<sub>3</sub> of influent.

	14-15 Oct	15-16 Oct	22-23 Oct	29-31 Oct	3-4 Dec	4-5 Dec	5-6 Dec	6-9 Dec	10-11 Dec	11-12 Dec	12-13 Dec	13-16 Dec	16-17 Dec
<u>COD, ppm O<sub>2</sub></u>													
Influent (pump)	43	38	41	25	68	63	?	?	22	43	?	61	49
6-5 tube	55	40	45	46	63	58	49	62	32	?	50	?	48
5-4	43	33	33	25	?	?	47	49	20	40	56	?	?
4-out	44	33	39	29	82	63	59	58	47	52	51	54	53
<u>NH<sub>4</sub>, ppm N</u>													
Influent (pump)	21.4		21.0	23.5	27.0	28.1	?	?	24.4	24.9	31.7	31.2	27.7
6-5 tube	20.8		17.7	17.3	29.1	28.9	28.0	29.6	19.5	?	26.4	?	27.9
5-4	20.4		17.8	19.3	?	?	29.4	28.6	39.3	35.0	30.5	?	?
4-out	18.8		17.5	17.1	32.2	28.9	30.8	30.5	34.6	29.5	31.6	34.3	28.5
<u>Kjeldahl, ppm N</u>													
Influent (pump)			22.2	24.8	32.6	31.9	?	?					
6-5 tube			18.9	19.6	30.8	30.9	31.5	31.6					
5-4			19.2	21.0	?	?	32.4	31.8					
4-out			18.8	18.9	36.6	31.3	33.4	30.1					
<u>NO<sub>3</sub>, ppm N</u>													
Influent (pump)	?			0.33	0.0	0.2	?	?	0.2	0.00	0.02	0.05	0.02
6-5 tube	0.00			0.10	0.2	0.1	0.0	0.2	0.05	?	1.9	?	0.00
5-4	0.06			0.26	?	?	0.2	0.1	0.0	0.02	0.02	?	?
4-out	0.00			0.86	0.1	0.0	0.0	0.05	0.0	0.05	0.02	0.00	0.00

97-15

Table 5. Quality parameters of influent, renovated water in aquifer, and native ground water (continued on next page).

	Water	Salt conc. ppm	pH	COD ppm O <sub>2</sub>	Kjeldahl ppm N	NH <sub>4</sub> ppm N	NO <sub>3</sub> ppm N
Influent (pump)	treated sewage	800- 992	7.9-8.1	22-68 <sup>a</sup>	18.7-32.6 <sup>b</sup>	17.5-31.7	0 - 0.5
Well No. 1	renov.	1024-1182	7.9	10-12		0.8- 2.9	0.2-16 <sup>c</sup>
Well No. 1-2	renov.	909-1216	7.1	10-20		0.6- 2.0	4.2-50 <sup>d</sup>
East Center Well	renov.	832-1158	7.3-8.4	7-26 <sup>e</sup>	0.2-2.9	0.2- 3.8	0 -36.6 <sup>d</sup>
Well No. 5-6	renov.	1024-1088	7.7	11-21		0.1-3.8	0 - 3.6 <sup>d</sup>
Well No. 7	renov.	1024-1152	7.6	12-16		0.2-0.5	1.3-3.2 <sup>c</sup>
Well No. 8	native	2048-2176	7.9	10-12		0.1-0.5	0.2-4.2
West Center Well	native	2291-3712 <sup>f</sup>	7.4-8.3	11-23 <sup>g</sup>	0 -0.6	0 -0.6	0 -7.6 <sup>h</sup>
91st Ave Well	native			10-17	0 -0.6	0 -0.6	6.4-6.7

a most values between 40-60 (see Figure 8 for graphical presentation).

b see Figure 9 for graphical presentation.

c depending on length of inundations.

d depending on length of inundations (see Figure 10 for graphical presentation).

e most values between 10 and 16 (see Figure 8 for graphical presentation).

f increasing trend.

g most values between 14 and 18.

h most values between 1 and 4.

Table 5. (Continued)

	NO <sub>2</sub> ppm N	PO <sub>4</sub> ppm P	B ppm B	F ppm F
Influent (pump)	0 -0.4	15.3-35.9	0.43-0.50	5.0-5.5
Well No. 1		0.1-0.3		1.2-1.7
Well No. 1-2	0.06-0.23	10.5-14.2		2.1-2.8
East Center Well	0.02-0.58	4.8-10.1	0.43-0.56	2.1-2.5
Well No. 5-6		0.2-0.9		1.8-2.3
Well No. 7		1.1-1.6		1.8-1.9
Well No. 8		0 -0.2		0.8
West Center Well	0.2-0.6	0 -0.5	0.63	0.8
91st Ave. Well			0.64	

Table 6. Concentration of main ions in renovated water.

<u>ion</u>	<u>ppm</u>
HCO <sub>3</sub> <sup>-</sup>	381
Cl <sup>-</sup>	213
SO <sub>4</sub> <sup>--</sup>	107
CO <sub>3</sub> <sup>--</sup>	0
Na <sup>+</sup>	200
Ca <sup>++</sup>	82
Mg <sup>++</sup>	36
K <sup>+</sup>	<u>8</u>
Total	1027

Table 7. COD, nitrate, and phosphate concentrations of various waters in drums.

	East Center Well High-NO <sub>3</sub>			East Center Well Low-NO <sub>3</sub>			Sewage Effluent			West Center Well		
	NO <sub>3</sub> ppm N	PO <sub>4</sub> ppm P	COD ppm O <sub>2</sub>	NO <sub>3</sub> ppm N	PO <sub>4</sub> ppm P	COD ppm O <sub>2</sub>	NO <sub>3</sub> ppm N	PO <sub>4</sub> ppm P	COD ppm O <sub>2</sub>	NO <sub>3</sub> ppm N	PO <sub>4</sub> ppm P	COD ppm O <sub>2</sub>
Start	22.8	4.8	10.5	0.2	5.5	12.5	0.1	17.5	50.0	6.4	0.5	31.0
Sept 20	8.4	-	-	-	-	-	-	-	-	-	-	-
Oct 8	5.8	-	-	<0.1	-	-	0.1	-	-	6.3	-	-
Nov 7	0.6	0.5	81	<0.1	1.1	49	<0.1	1.1	91	5.4	0.4	59
Jan 6	0.2	-	-	0.2	-	-	0.2	-	-	5.0	-	-

51-50

Table 8. Calculation of arrival time for different depths below center of basin area.

Depth below field surface	Potential I = 1 ft/day	vertical hydraulic gradient	V <sub>macr</sub>	Δt	t
<u>feet</u>	<u>feet of water</u>		<u>ft/day</u>	<u>days</u>	<u>days</u>
10	1.09				0
		0.0325	1.72	2.3	
14	0.96				2.3
		0.0188	0.993	20.1	
34	0.583				22.4
		0.0096	0.507	39.4	
54	0.391				61.8
		0.0051	0.269	74.3	
74	0.289				136.1
		0.0031	0.164	121.9	
94	0.226				258.0
		0.0020	0.106	56.6*	
100					314.6
114	0.186				

\* for 6-ft distance to reach 100-ft well

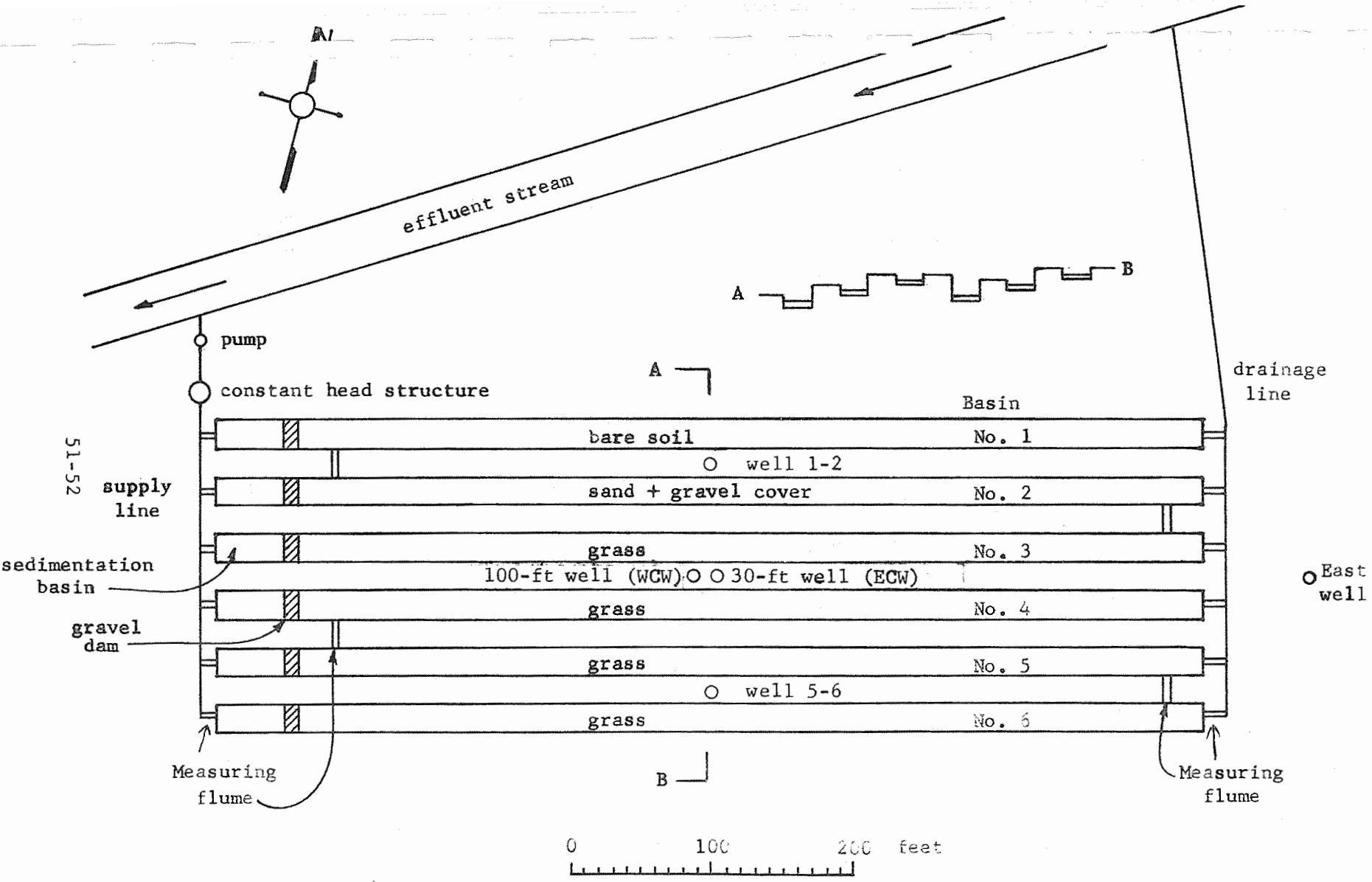


Figure 1. Schematic of Flushing Meadows project.

Sludge flakes removed by hand raking  
and gravel dams installed in all basins

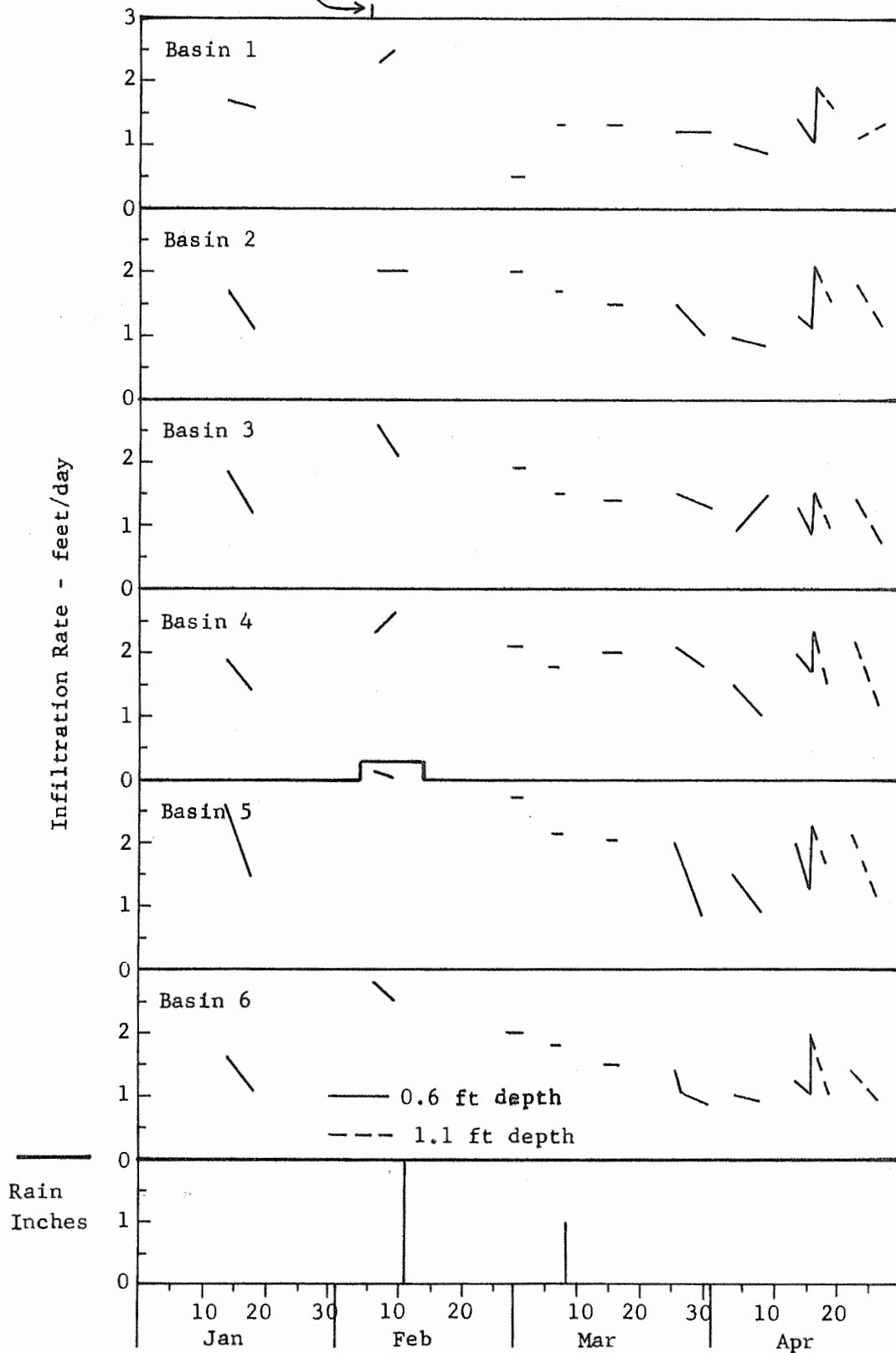


Figure 2A. Infiltration rates of recharge basins for January, February, March, and April 1968.

All basins swept and harrowed and basins 3, 4, 5, and 6 seeded with grass sand and gravel

installed in basin 2

dust storm

dust storm

end of parallel flow

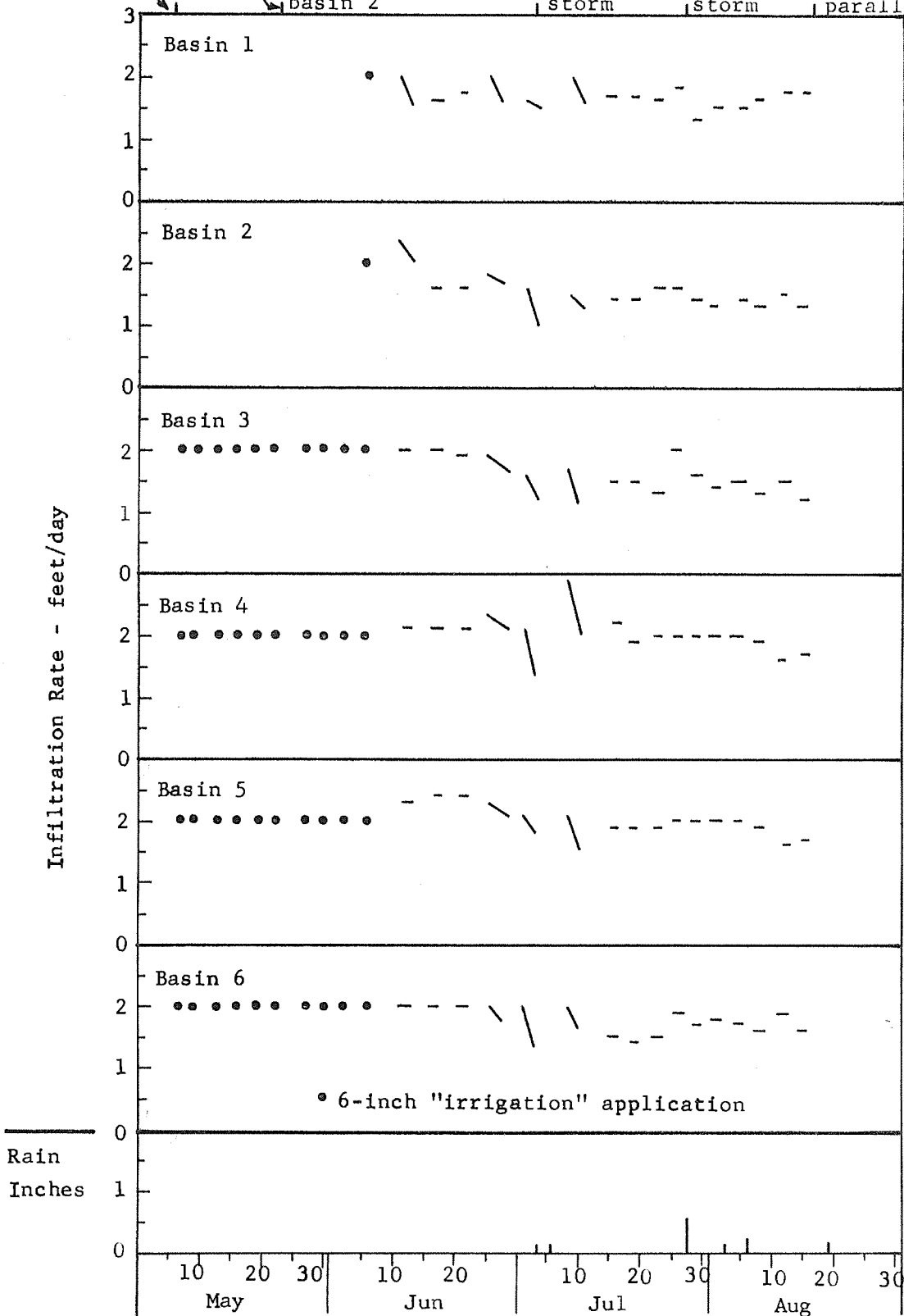


Figure 2B. As Figure 2A, but for May, June, July, and August 1968.

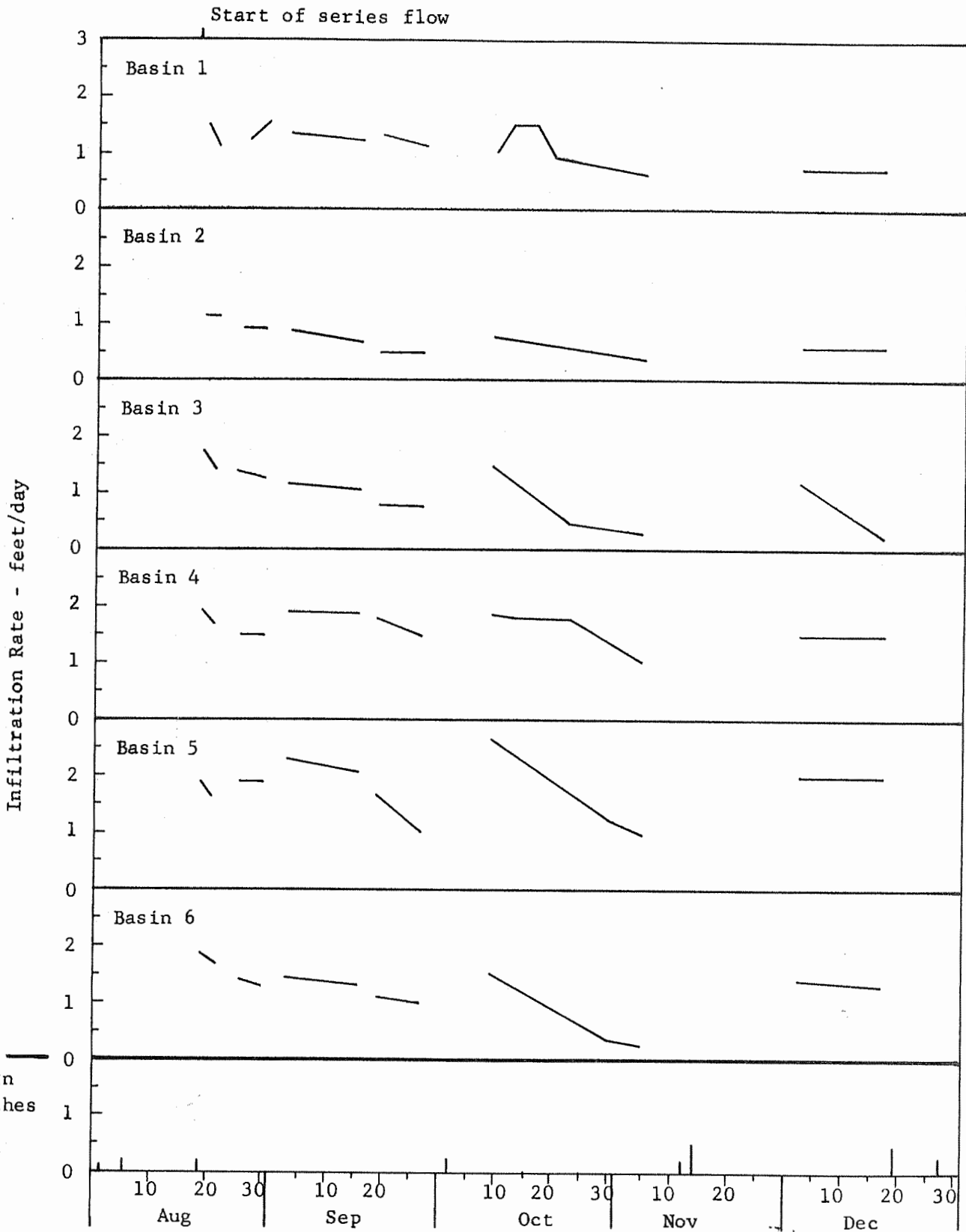


Figure 2C. As Figure 2A, but for August, September, October, November, and December 1968.

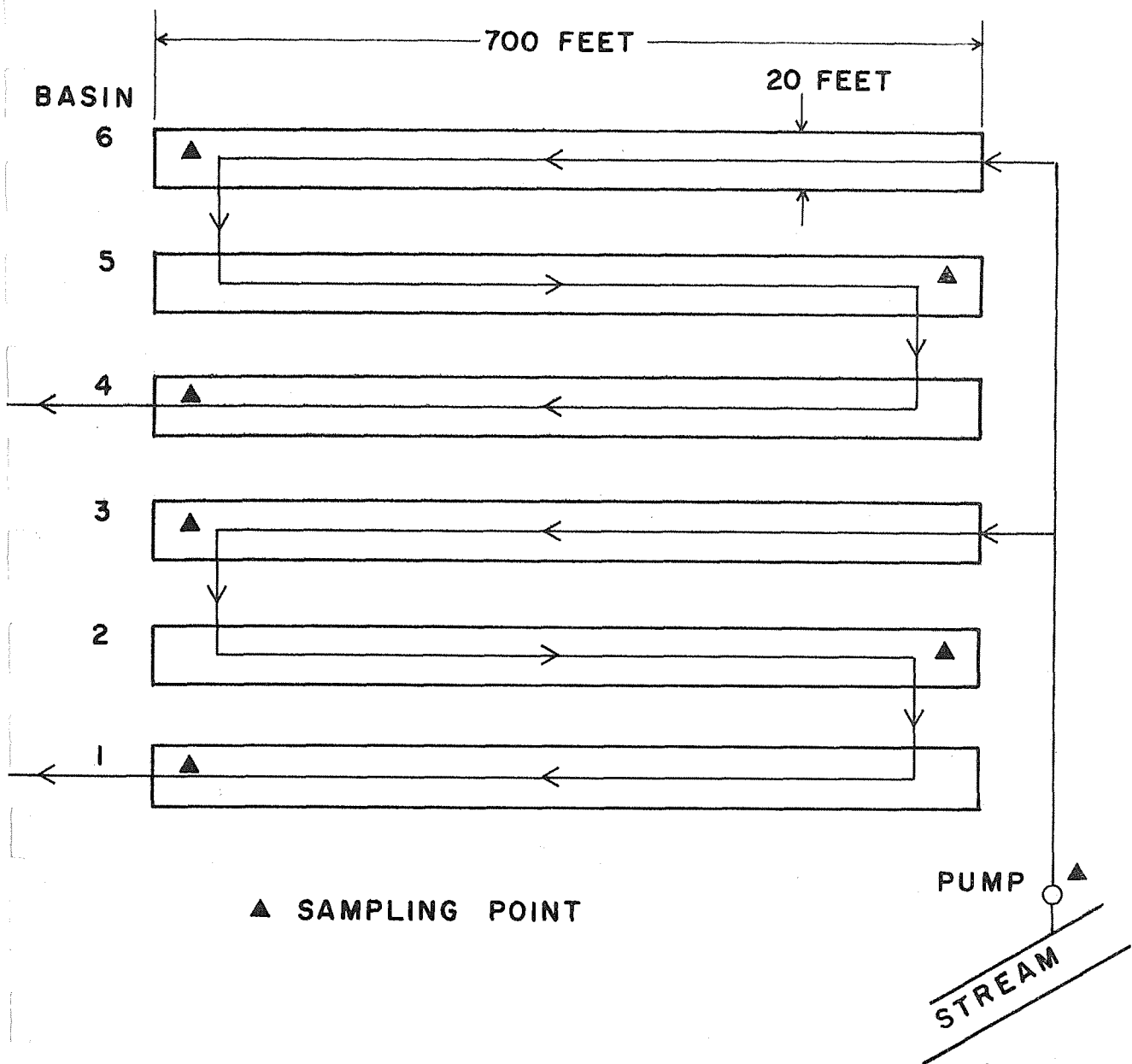


Figure 3. Schematic of series flow and points for sampling surface flow.

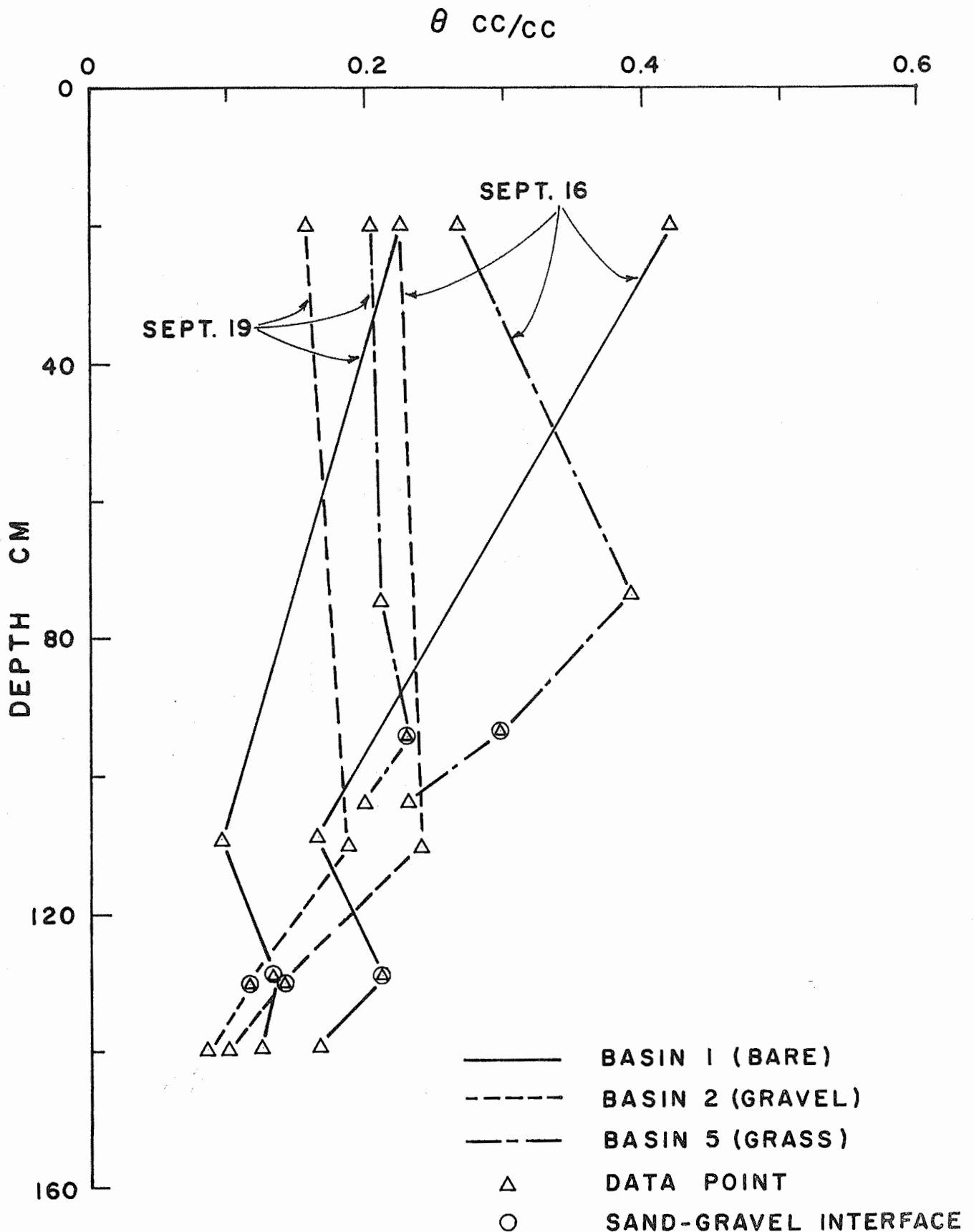


Figure 4. Soil water content as a function of depth during drying of basins 1, 2, and 5.

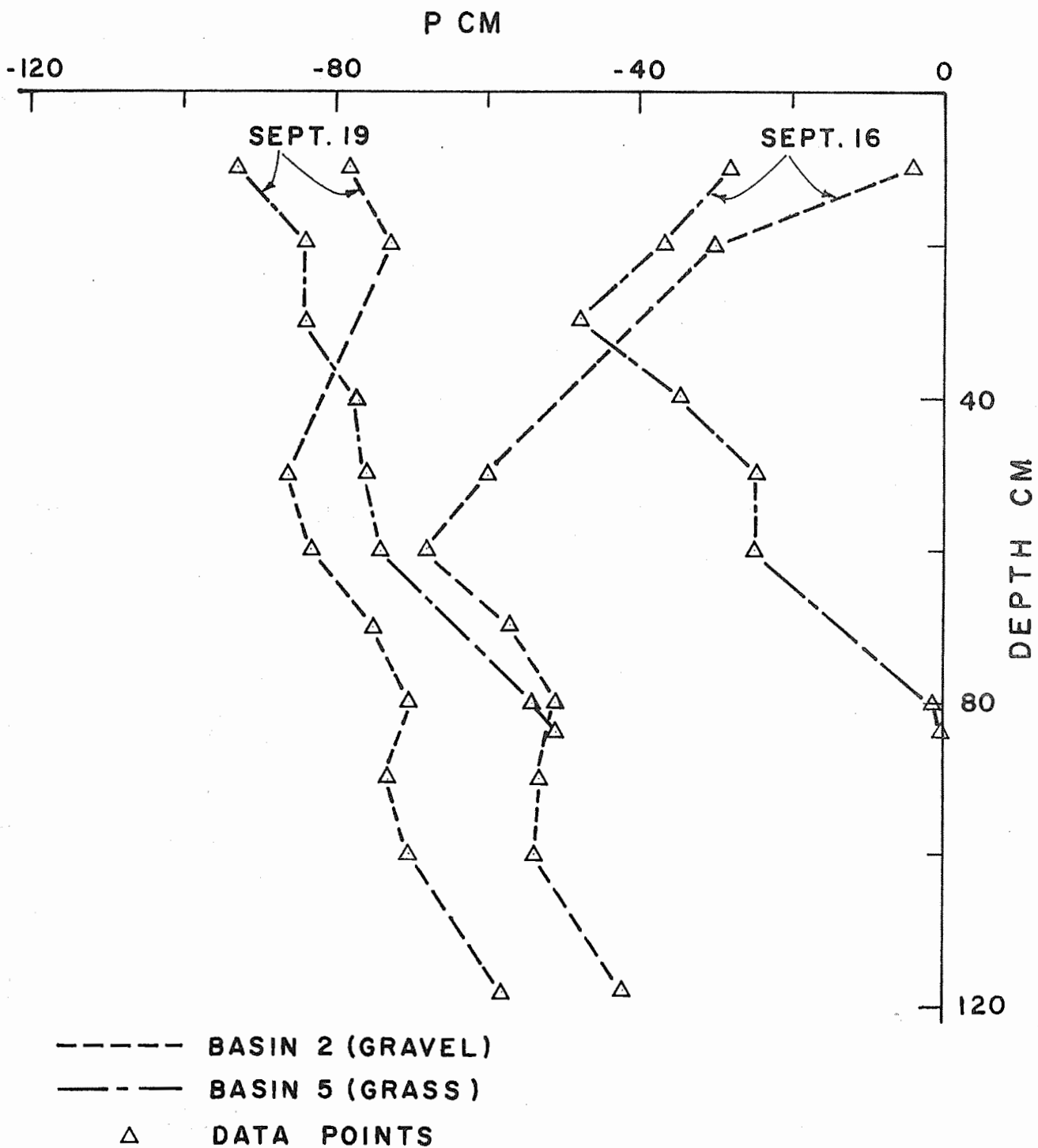


Figure 5. Soil water pressure as a function of depth during drying of basins 2 and 5.

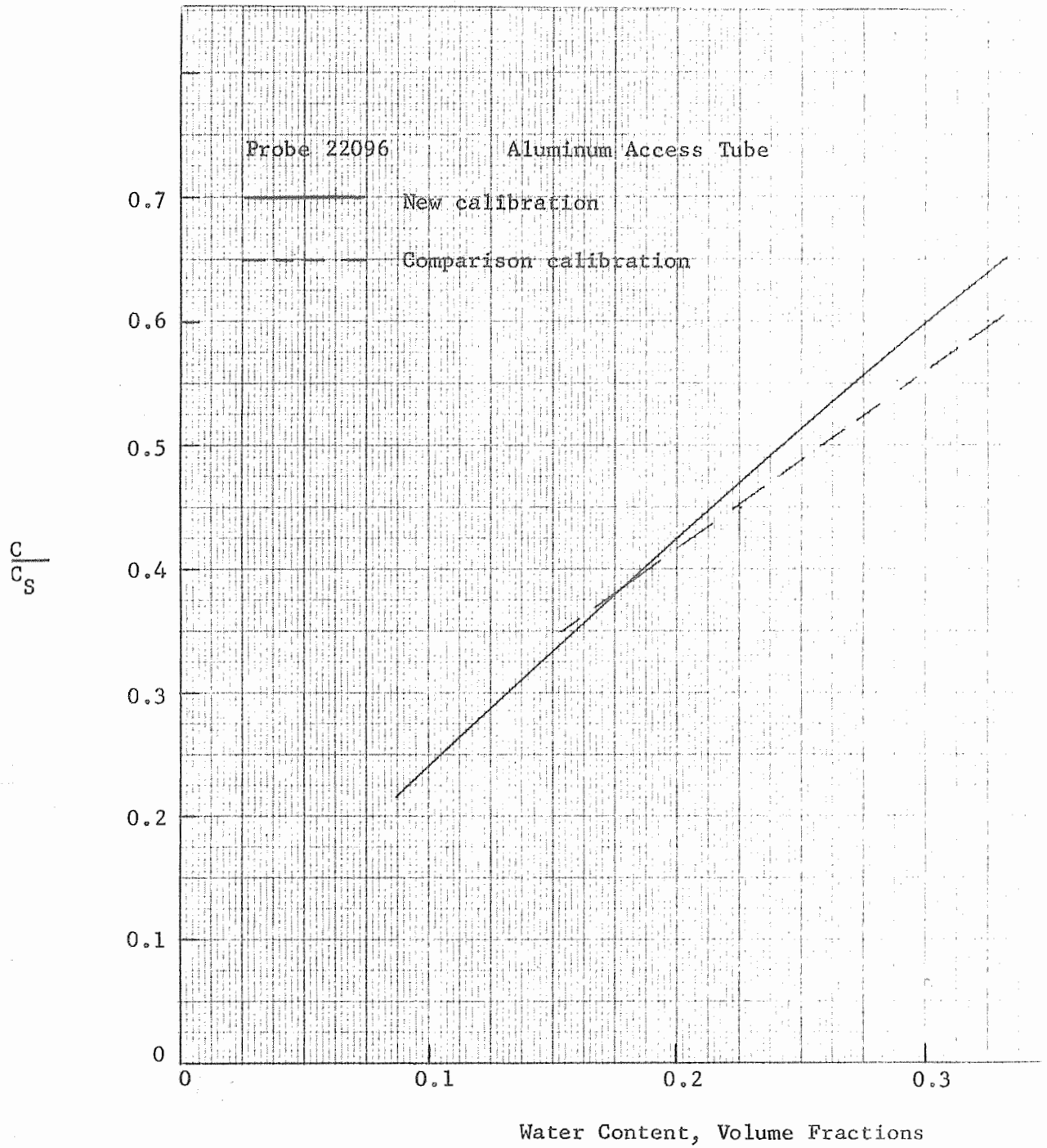
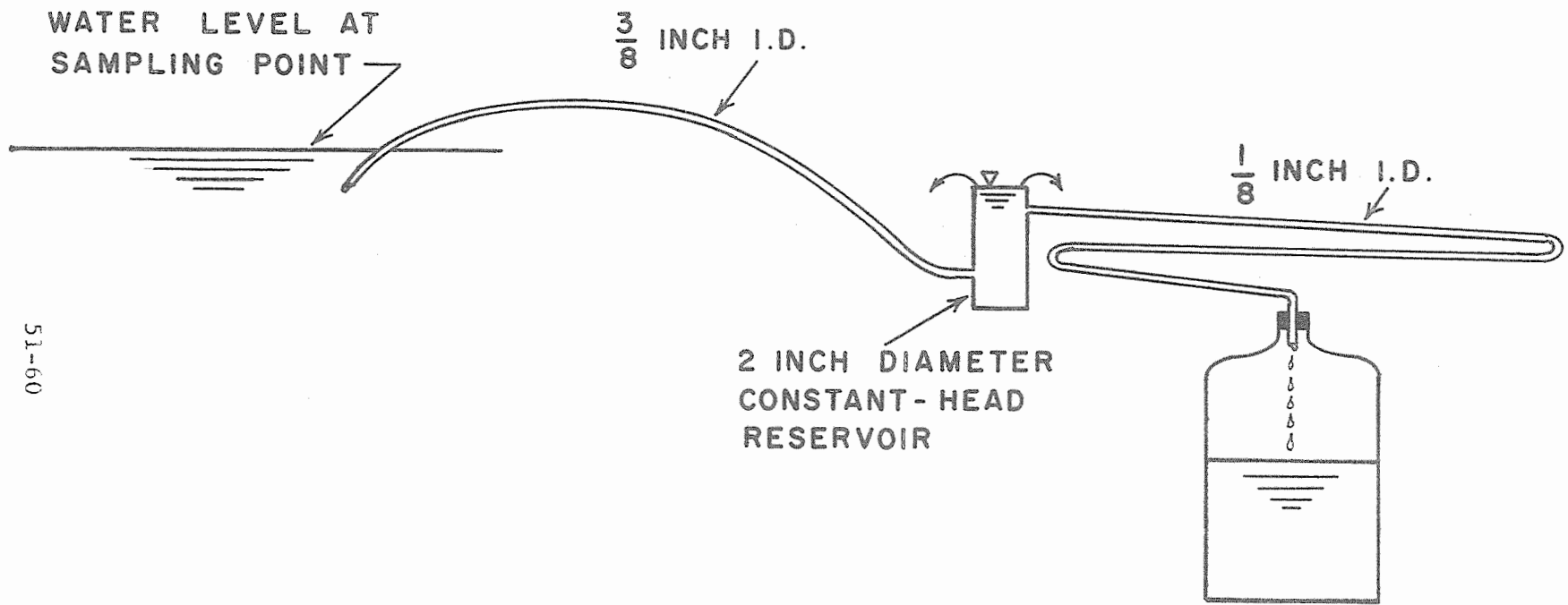


Figure 6. Calibration curves of new and comparison calibration methods for probe 22096.



51-60

Figure 7. Schematic of apparatus for collecting continuous samples of effluent in basins.

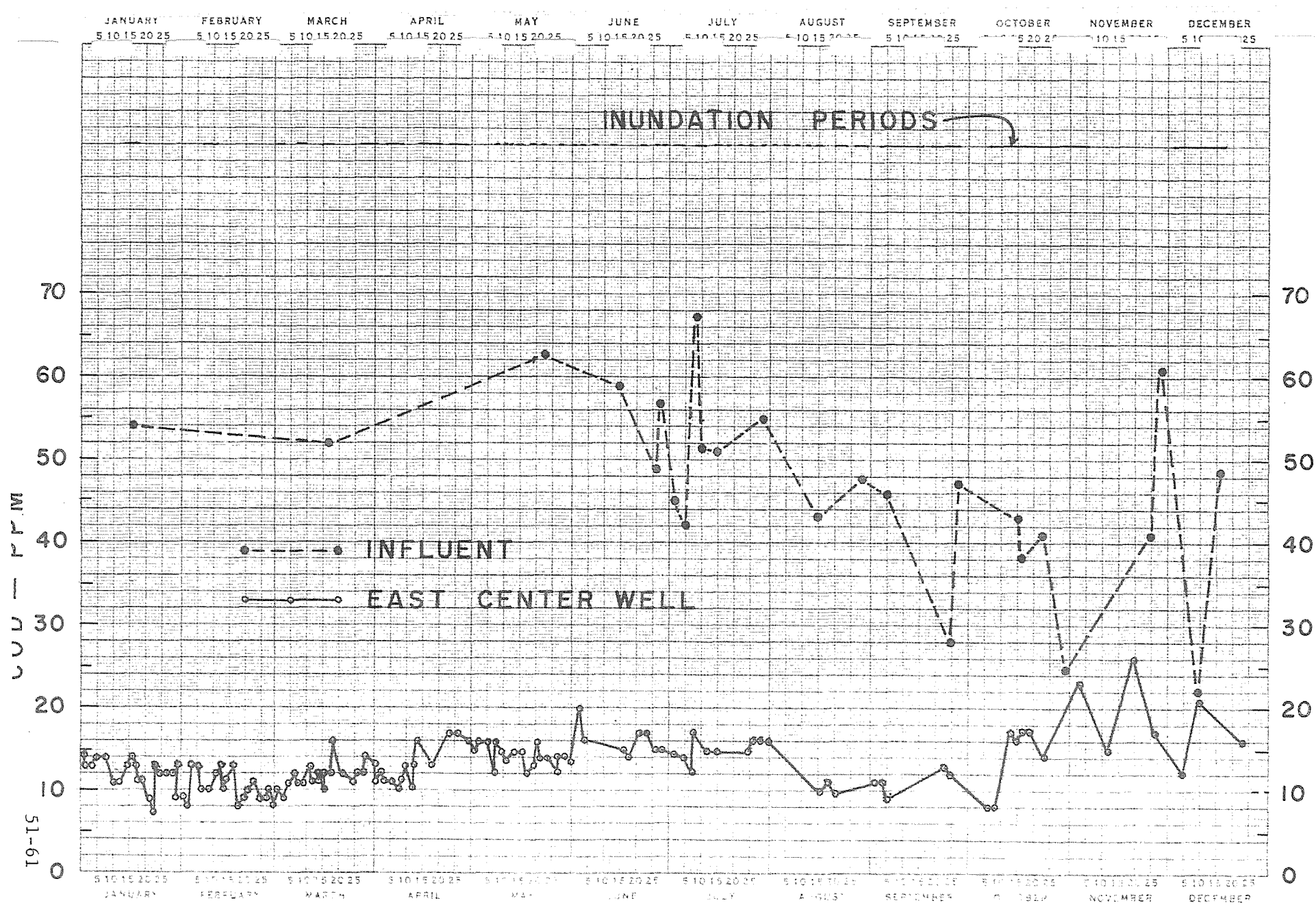


Figure 8. COD of influent and of renovated water from East Center Well.

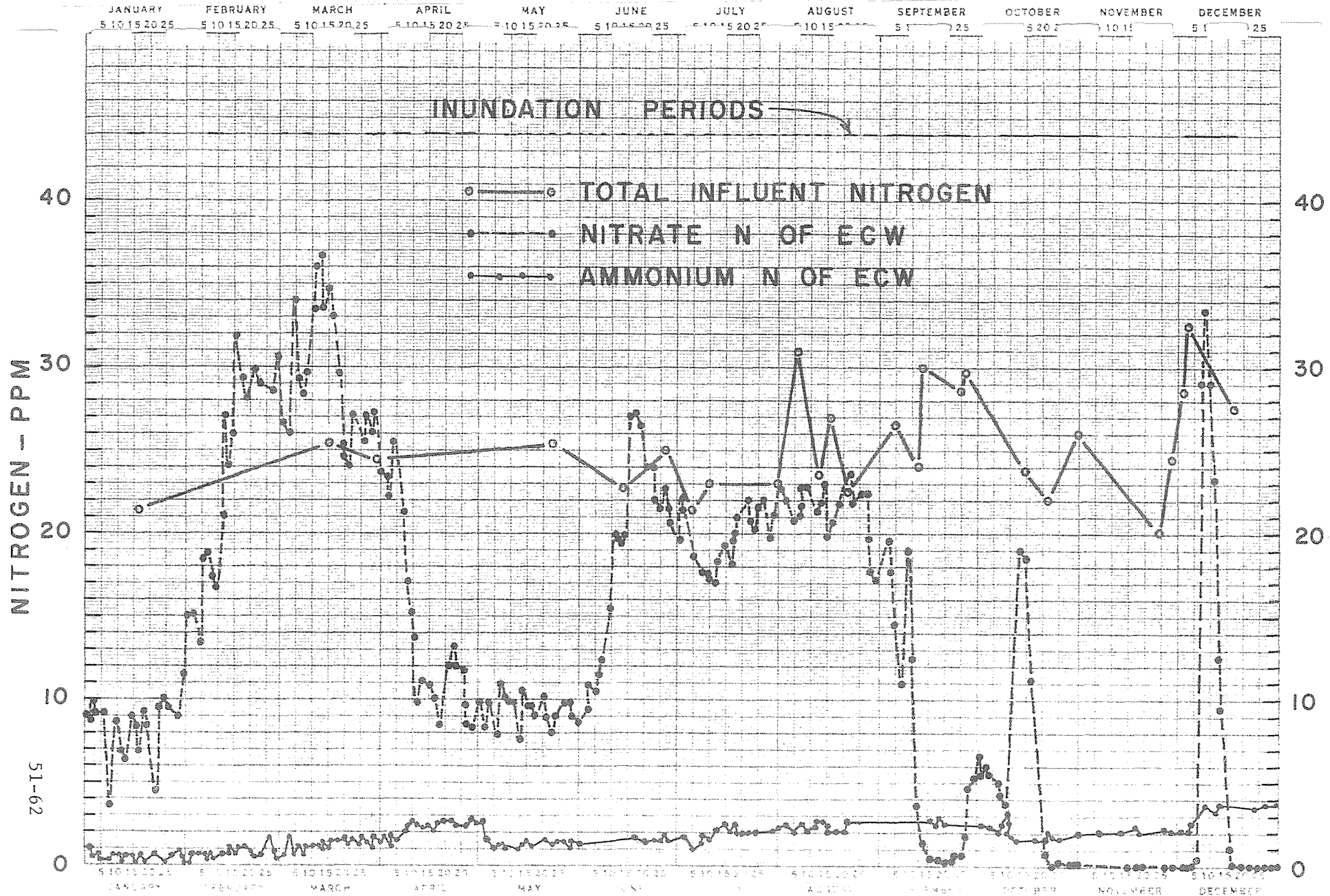


Figure 9. Total nitrogen in influent, and nitrate and ammonium nitrogen in renovated water from East Center Well.

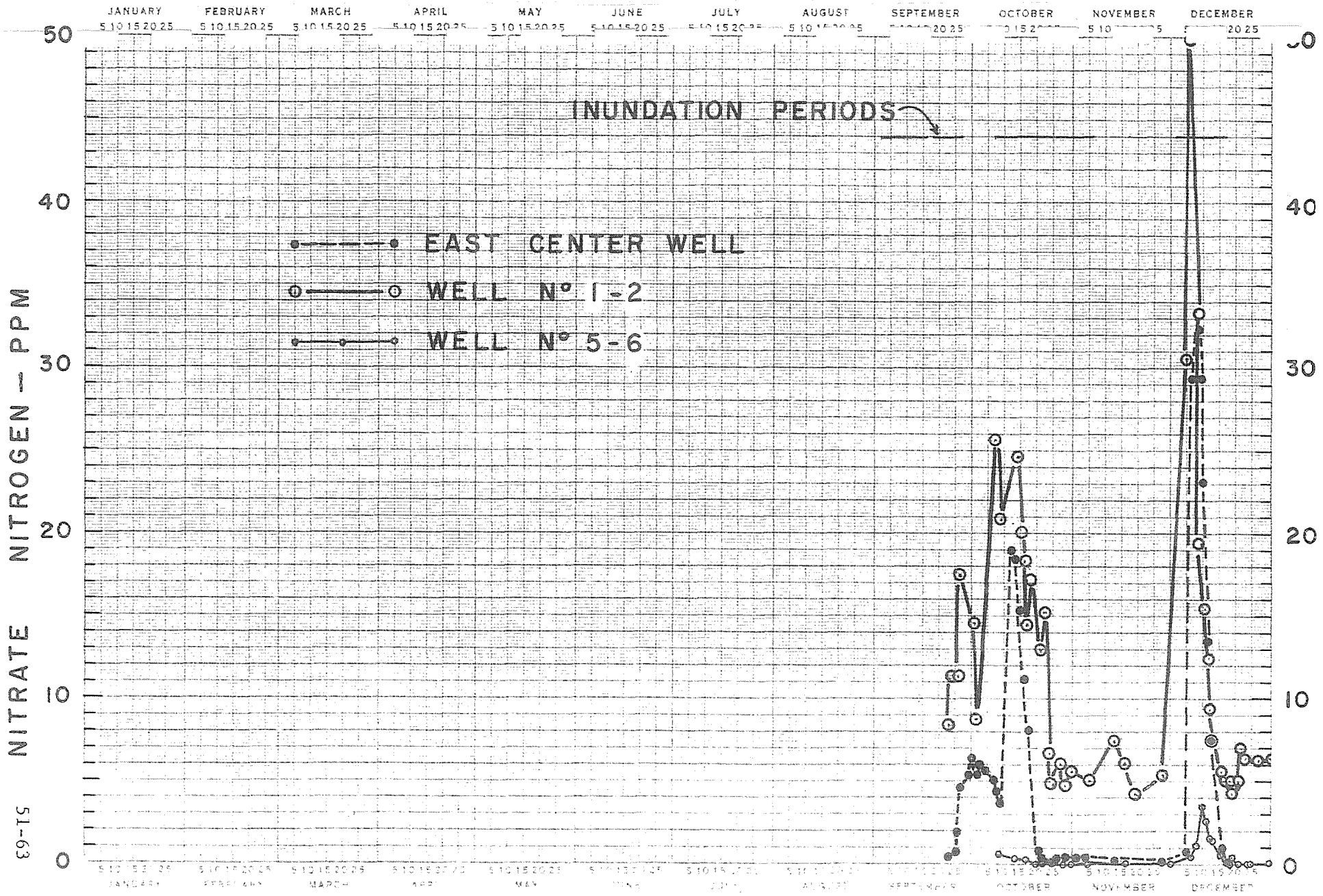


Figure 10. Nitrate nitrogen in renovated water from East Center Well, Well 1-2, and Well 5-6.

49-15

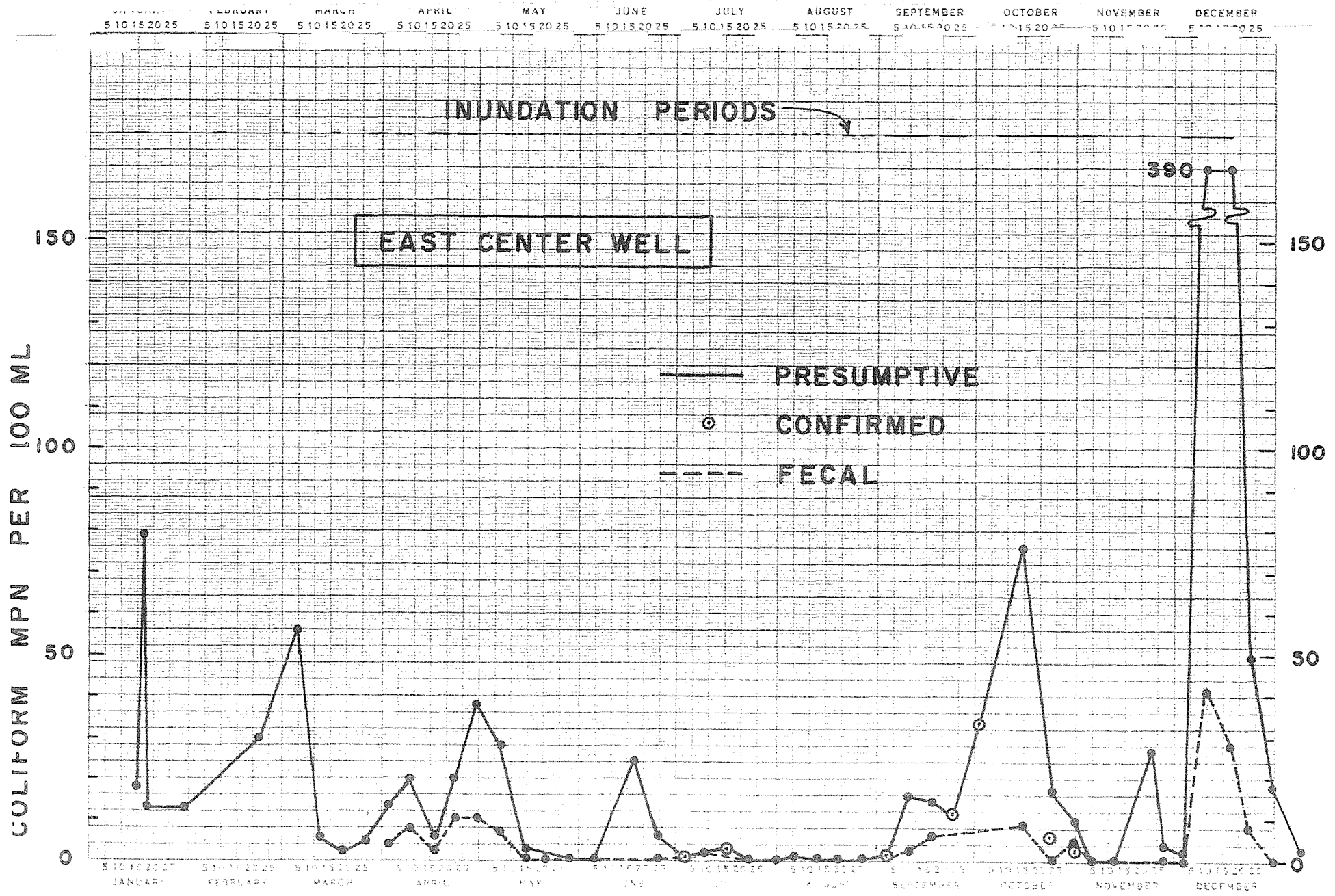


Figure 11. Presumptive and confirmed MPN of coliforms and MPN of fecal coliform bacteria in renovated water from East Center Well. Annual Report of the U.S. Water Conservation Laboratory

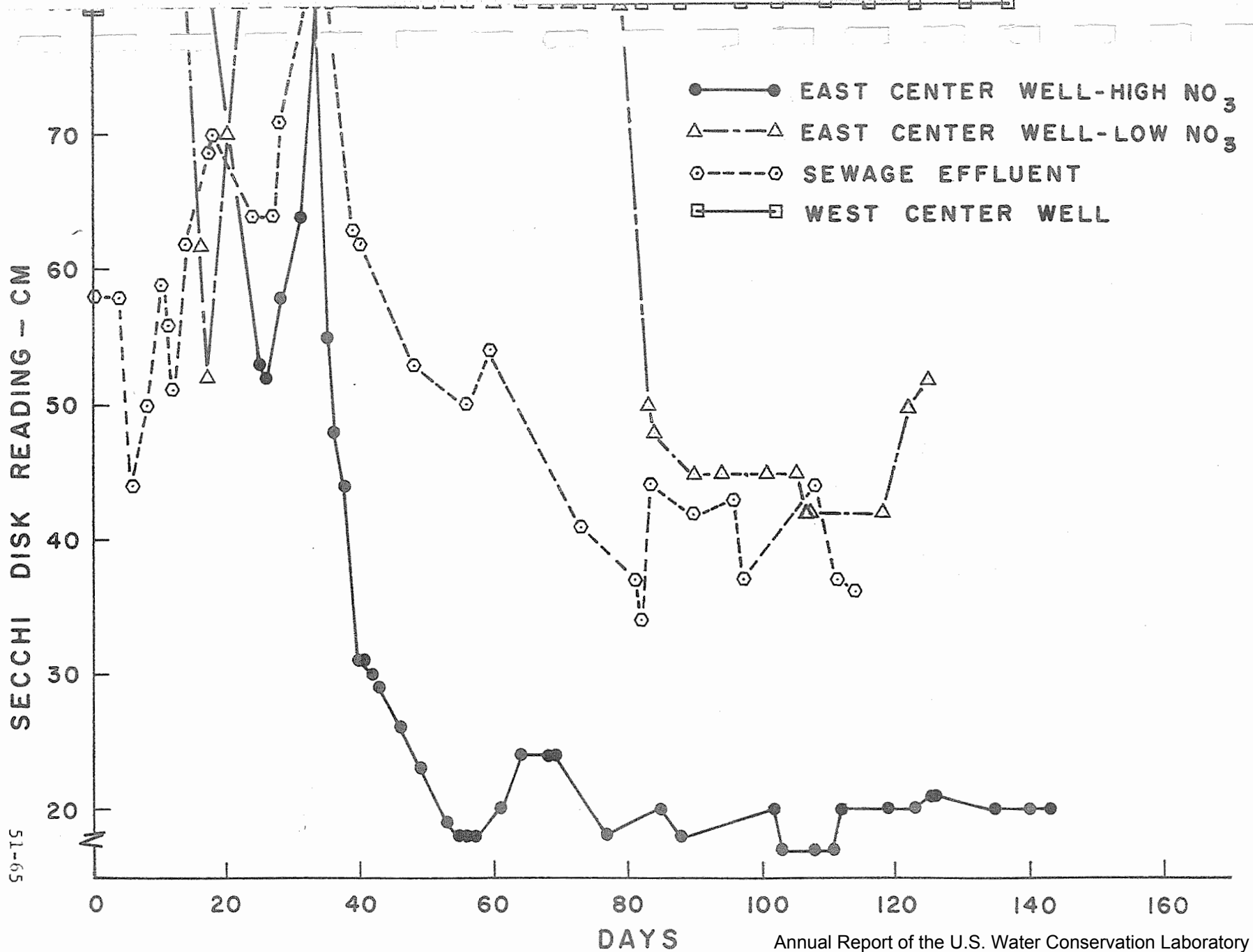


Figure 12. Secchi disk readings of various waters in drums.

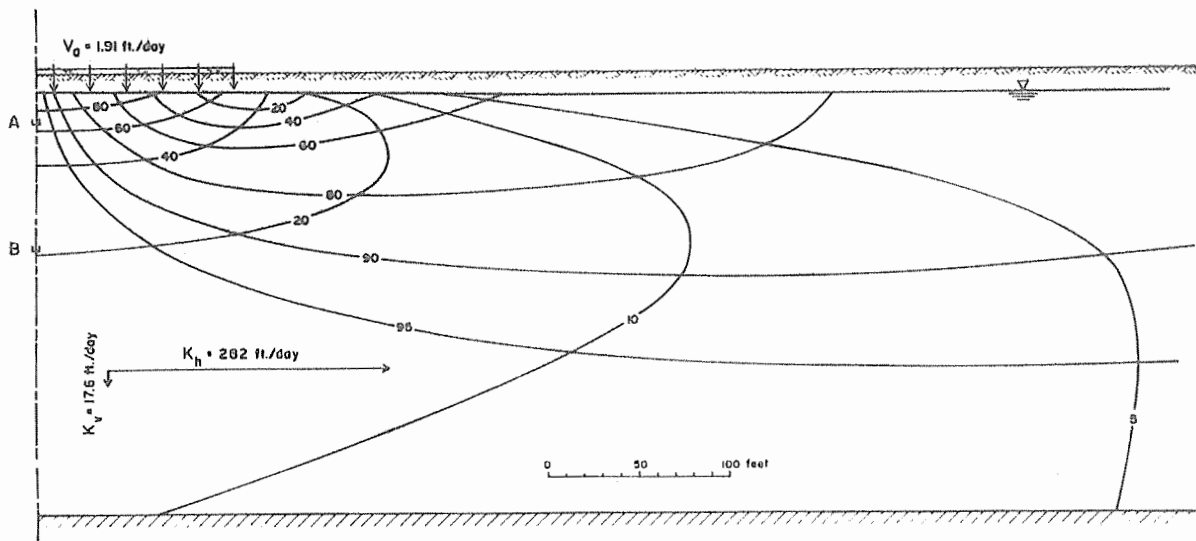
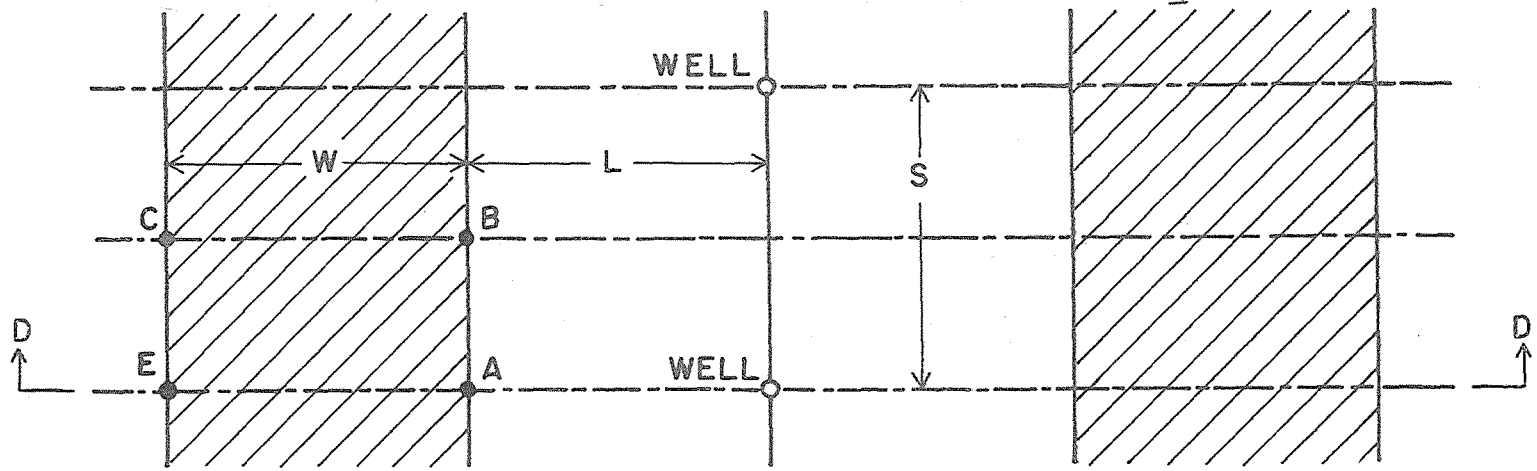
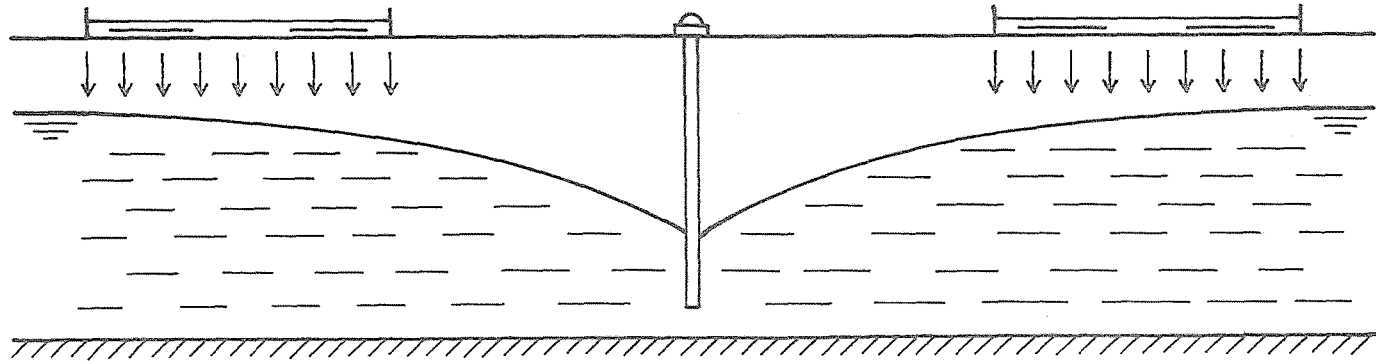


Figure 13. Streamlines and equipotentials for ground-water flow system during recharge.



PLAN



CROSS SECTION D-D

51-70

Figure 17. Schematic of recharge-basin strips and wells.

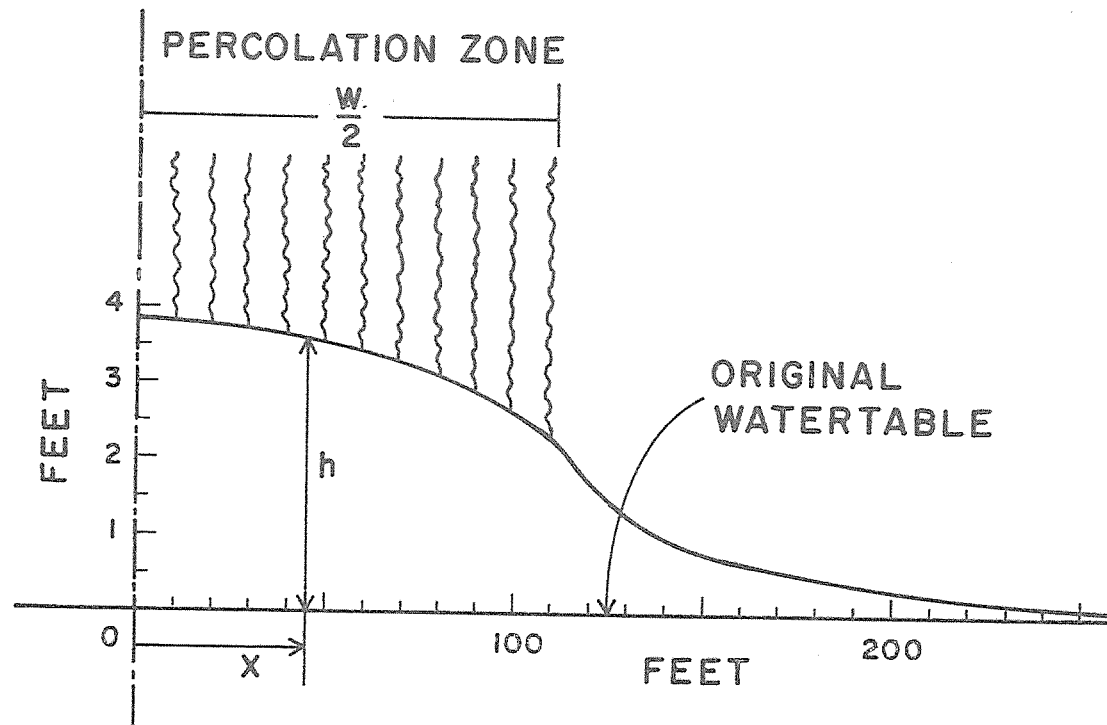
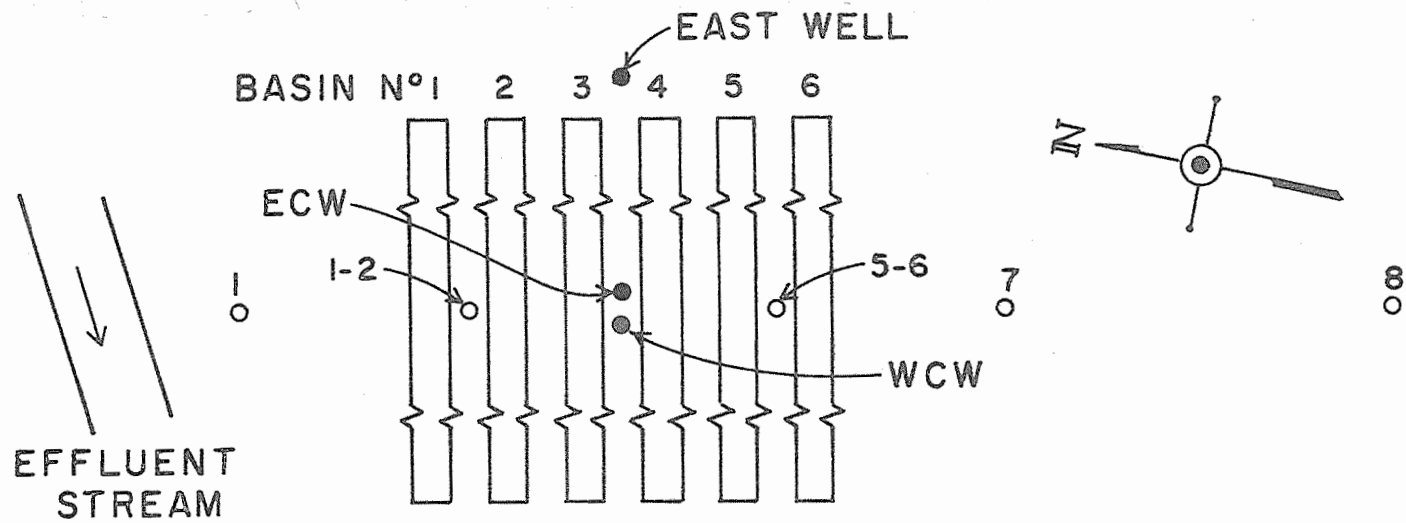
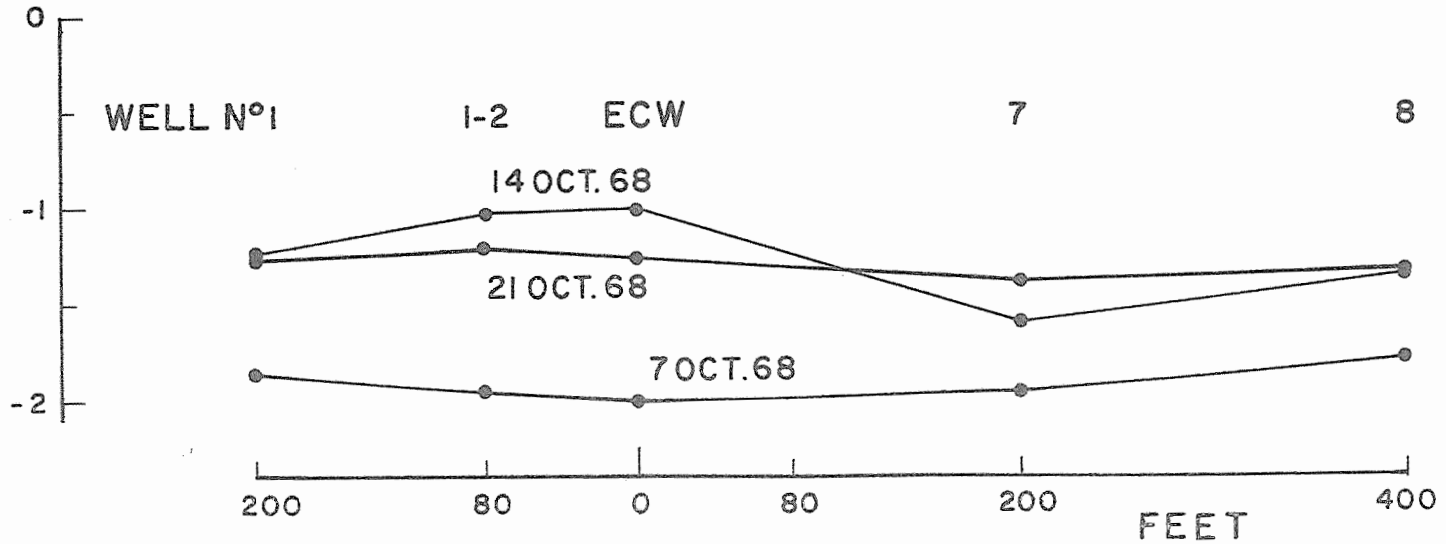


Figure 14. Water-table mound during recharge.



AVERAGE ELEVATION OF BASIN BOTTOMS: 7.85 FT.  
 ELEVATION OF WATER SURFACE IN STREAM: 1.0 FT.

ELEVATION IN FEET  
 LOCAL BM



51-68

Figure 15. Location of observation wells (top) and typical water-level profiles (bottom).  
 Annual Report of the U.S. Water Conservation Laboratory

EASTWARD EXTENSION TO MESA, ARIZ.

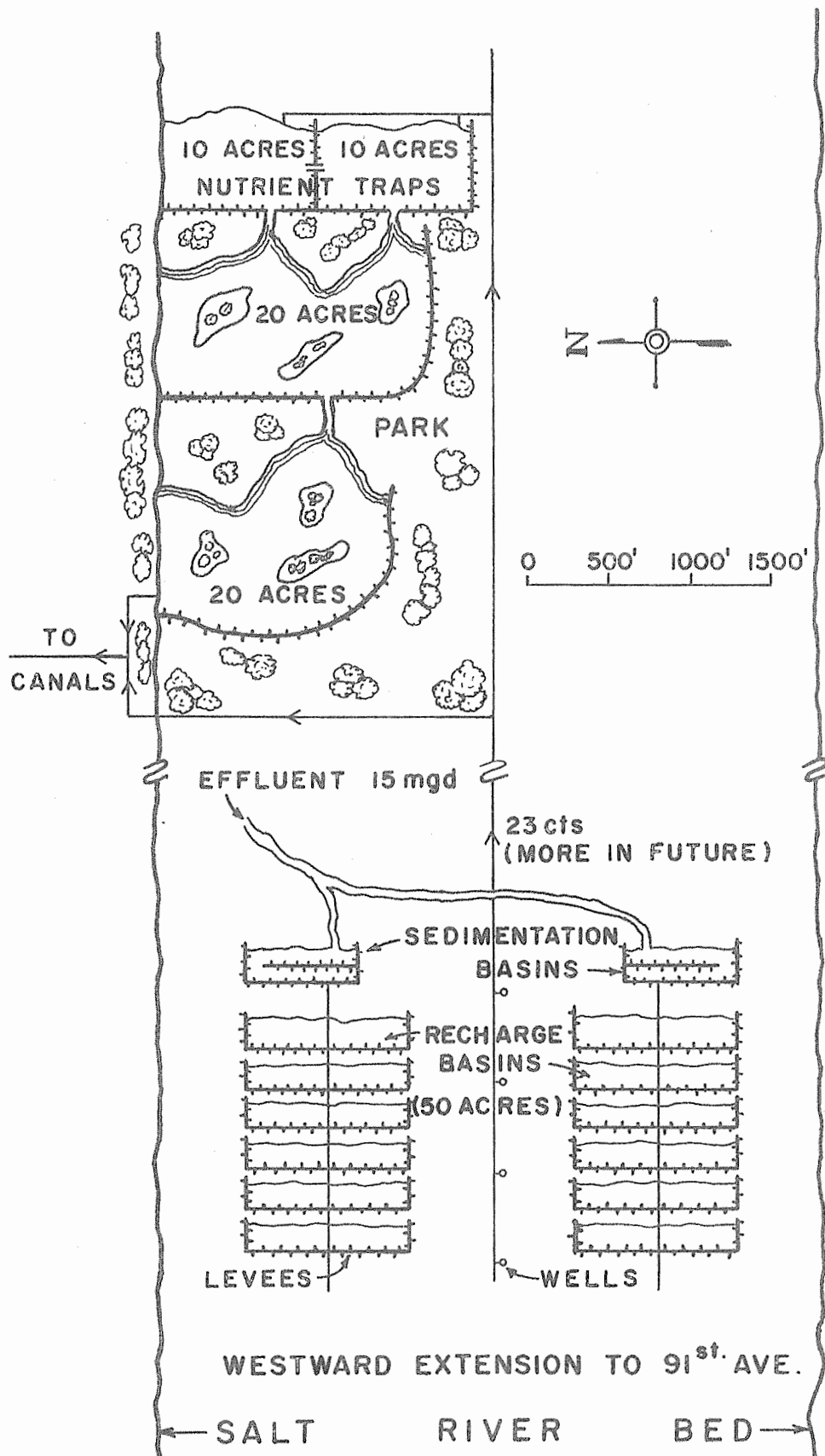


Figure 16. Layout of recharge basins, wells, and recreational lakes for larger-scale system. Annual Report of the U.S. Water Conservation Laboratory

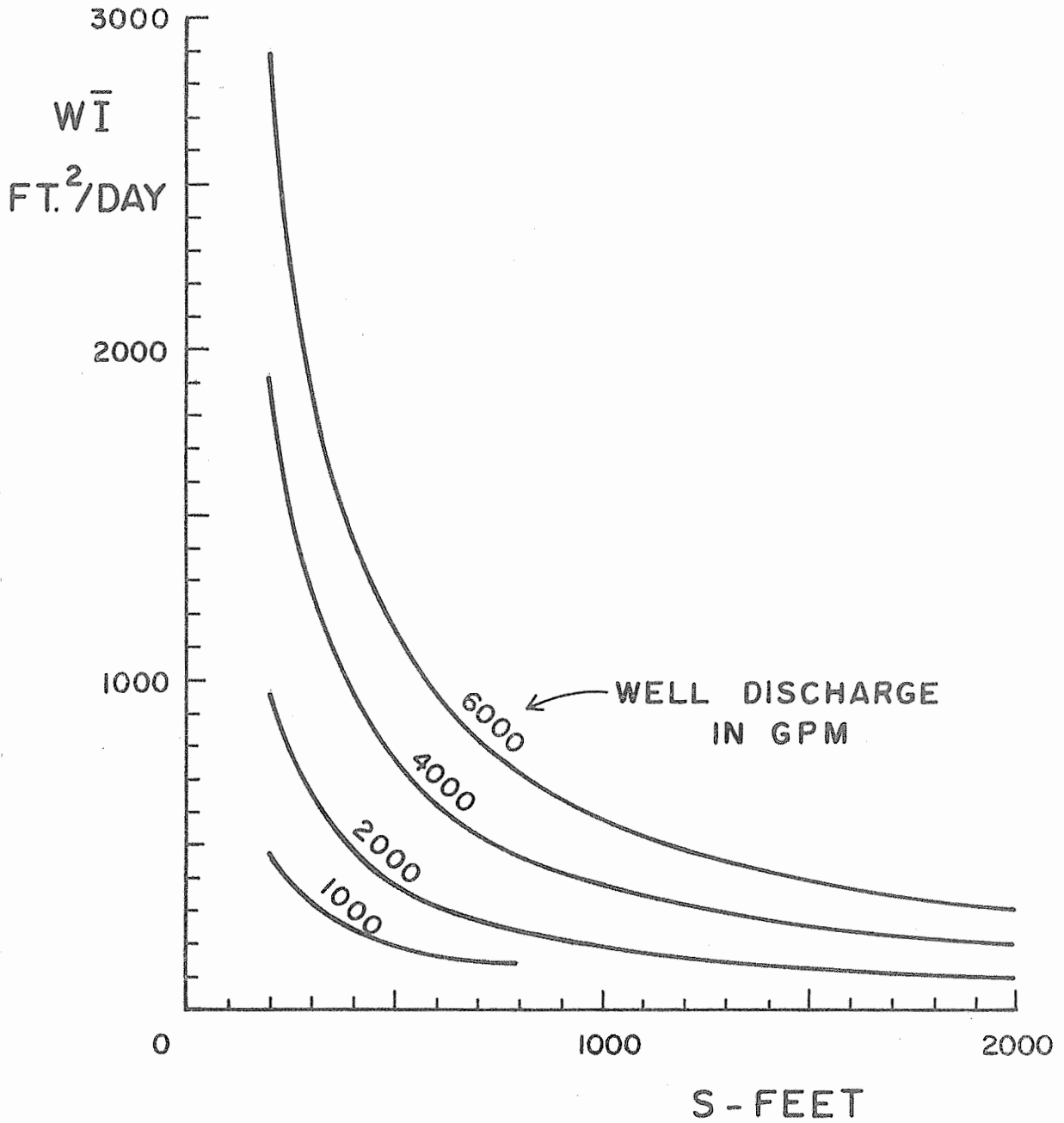


Figure 18. Graph of  $\bar{W}$  as a function of  $S$  for different values of the discharge per well.

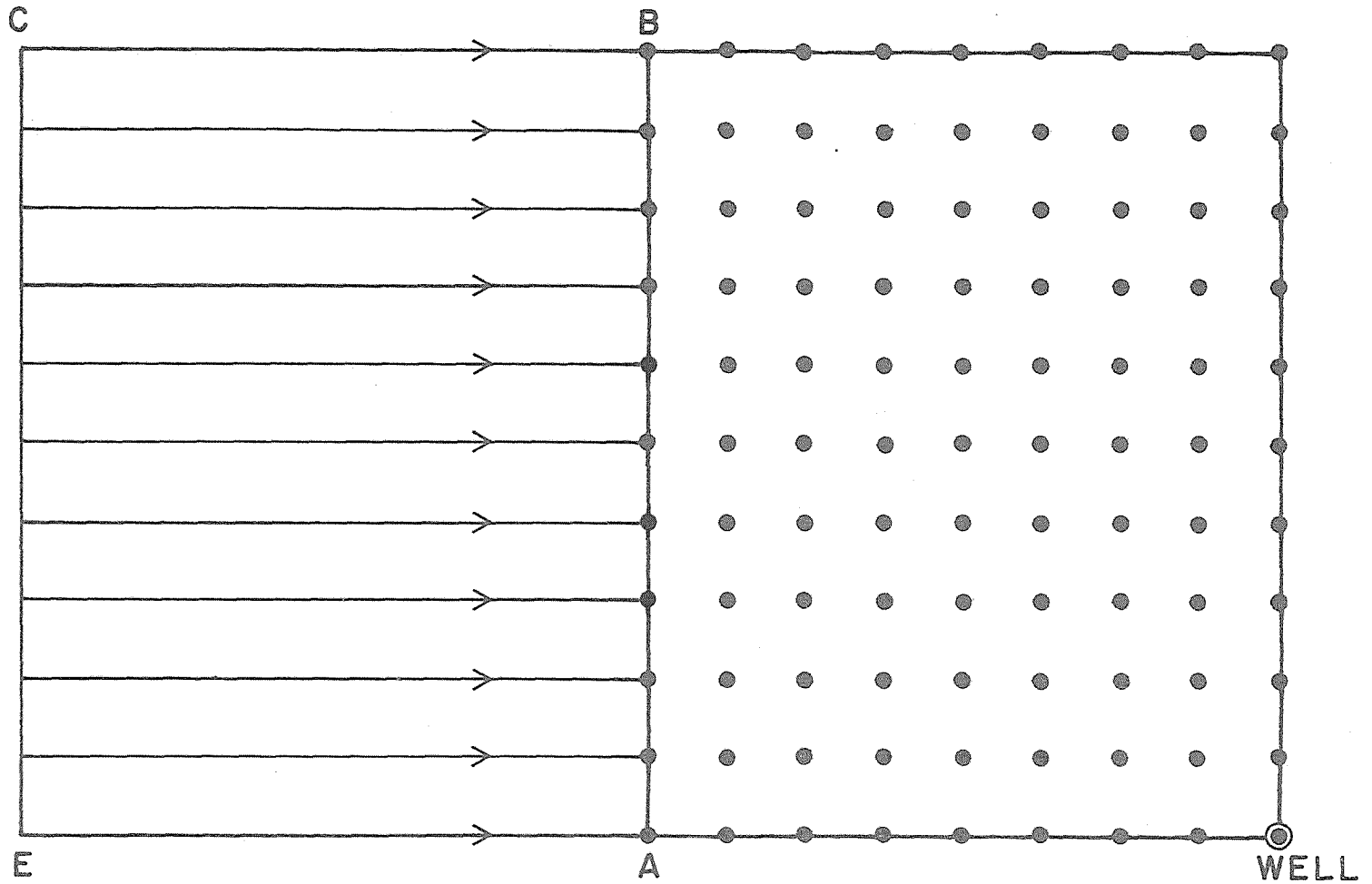


Figure 19. Node arrangement of flow system analyzed by electric analog.

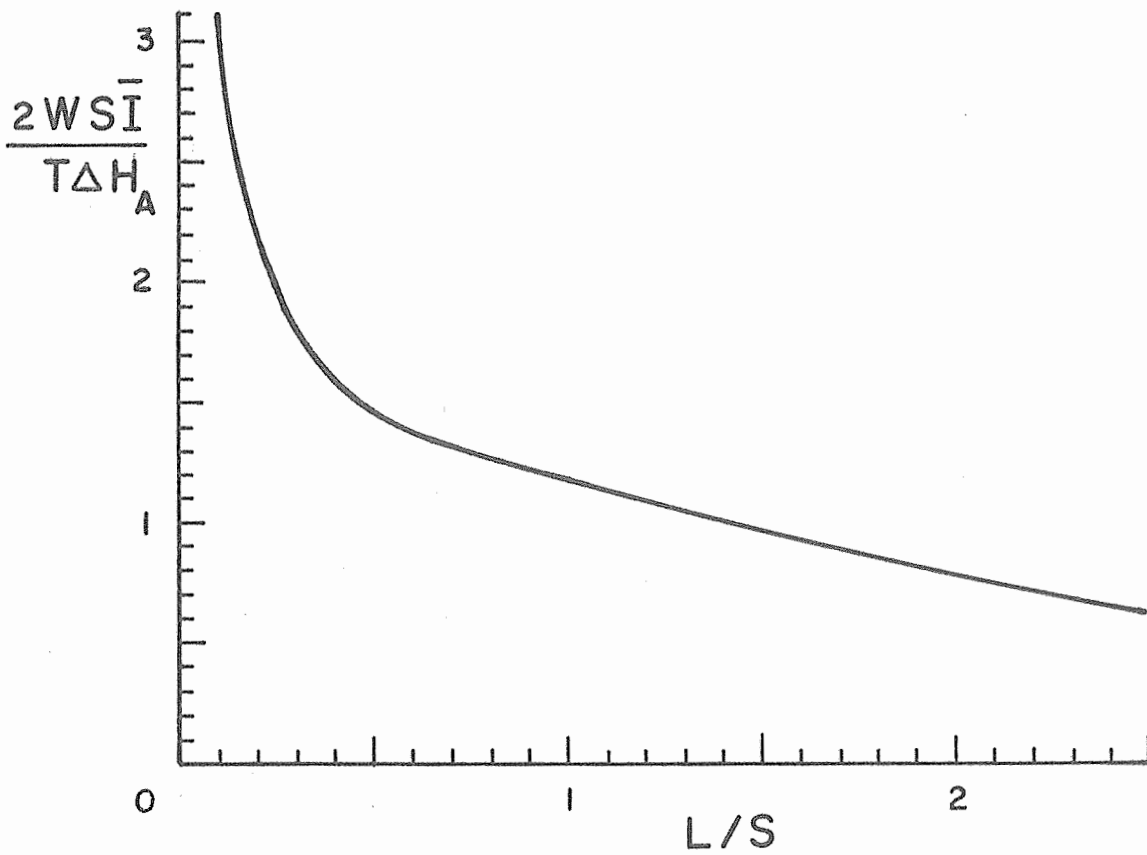


Figure 20. Dimensionless graph of  $2 \overline{WSI} / T\Delta H_A$  versus  $L/S$ .

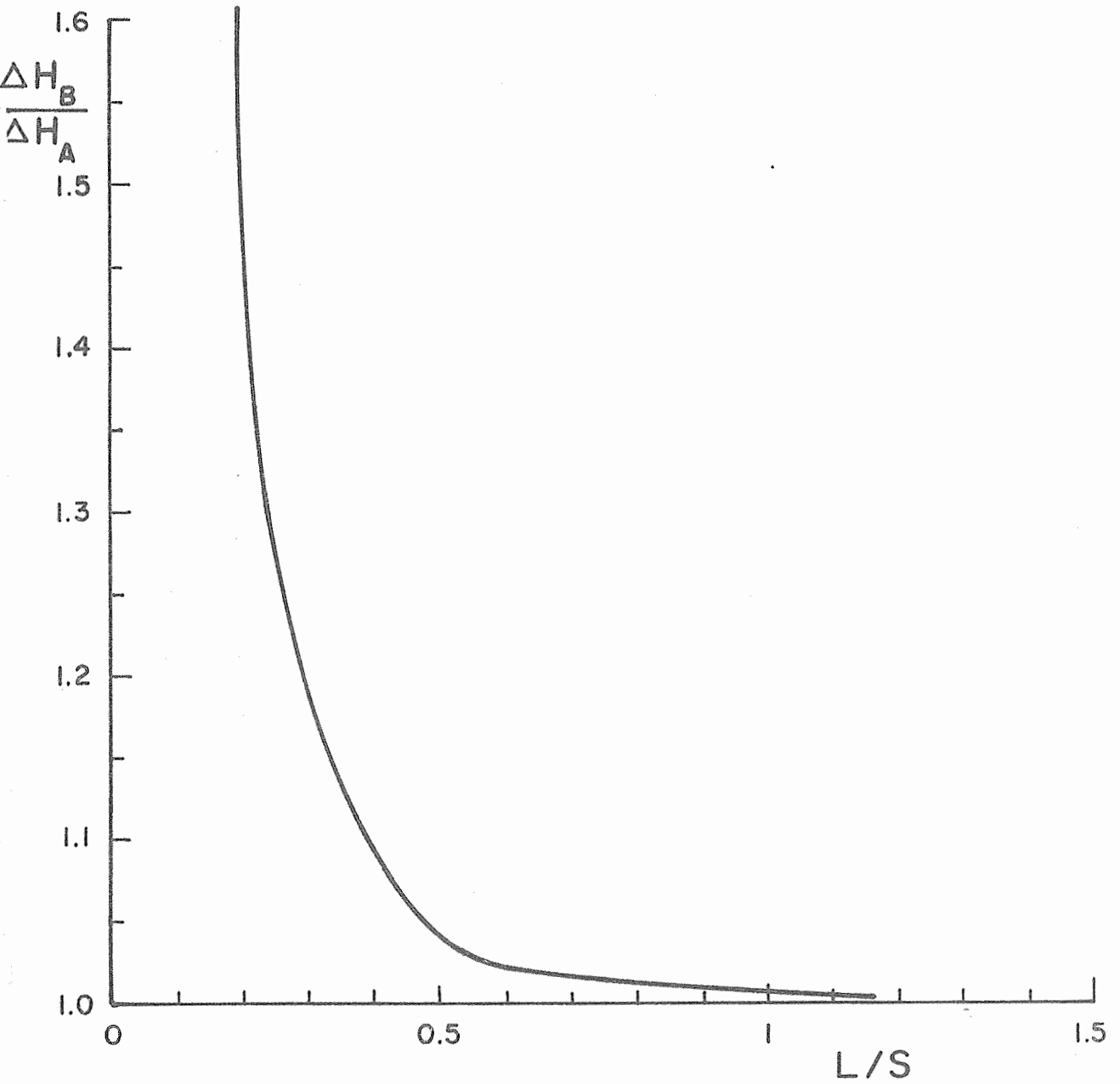


Figure 21. Dimensionless graph of  $\frac{\Delta H_B}{\Delta H_A}$  versus  $L/S$ .

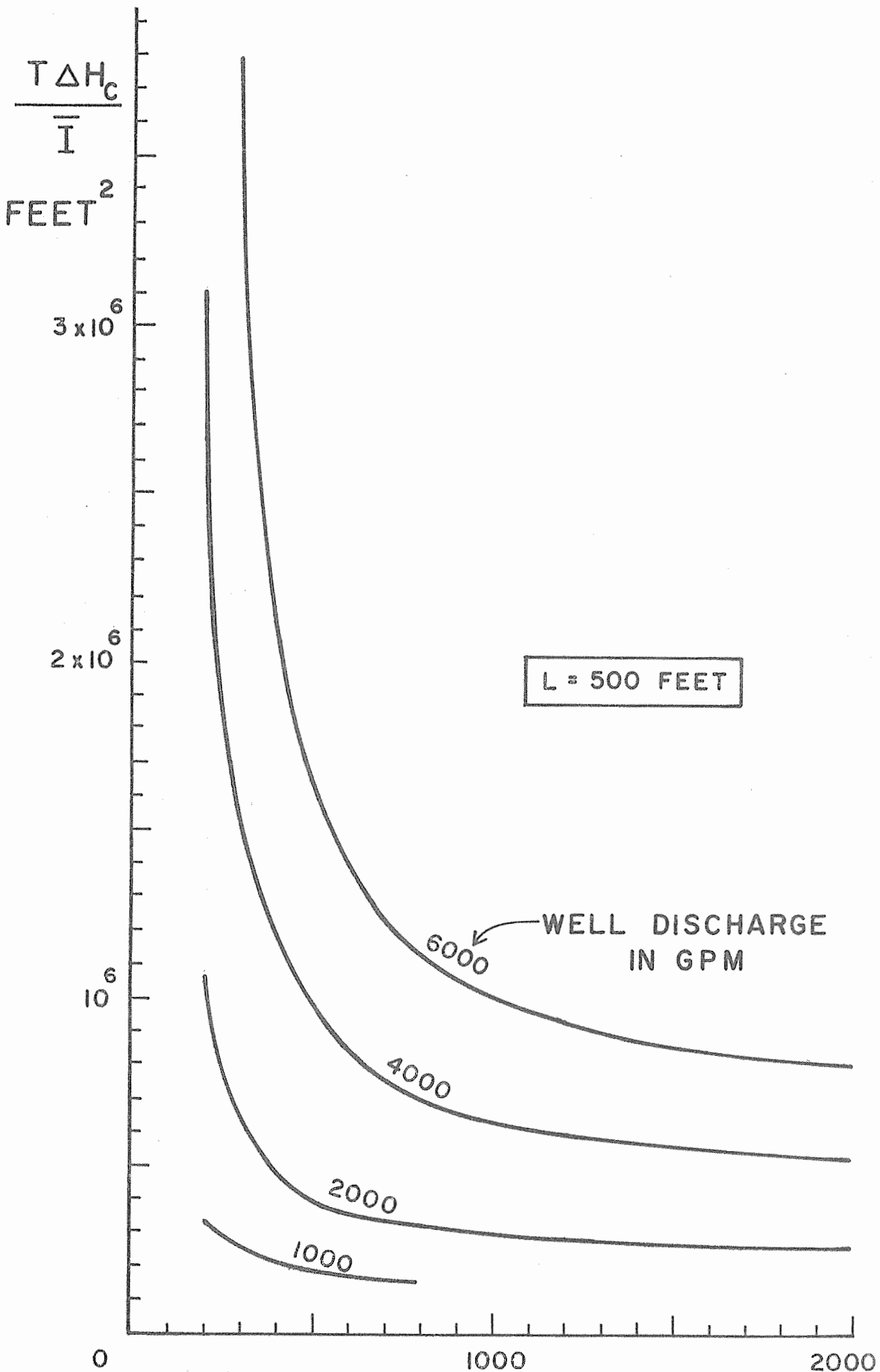


Figure 22. Graph of  $T\Delta H_c / \bar{I}$  as a function of  $S$  - FEET for different values of the discharge per well. Annual Report of the U.S. Water Conservation Laboratory 51-75

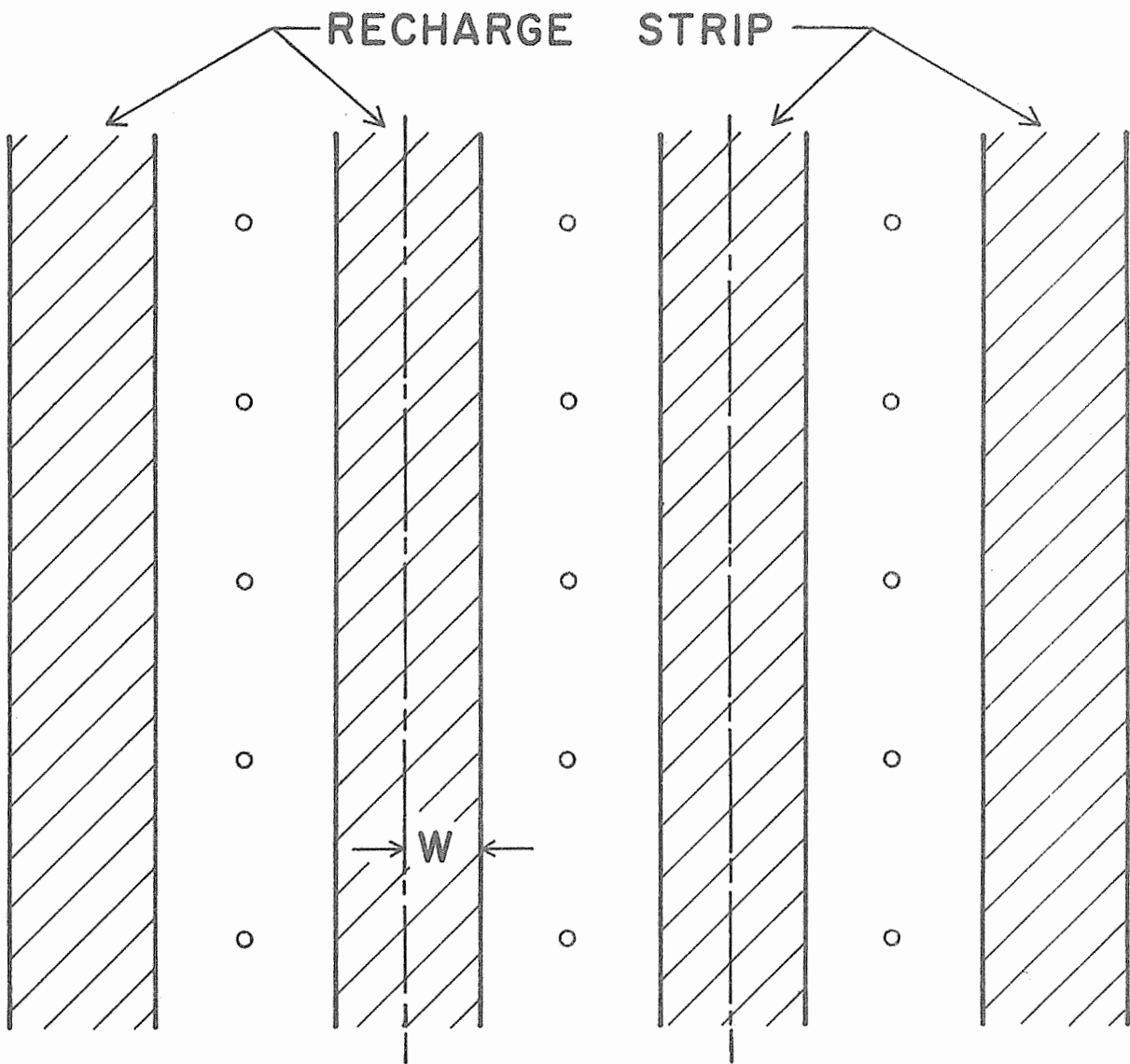


Figure 23. Schematic of multiple-strip recharge system and wells.

PART B. EVALUATING EVAPOTRANSPIRATION AND DRAINAGE  
USING A FAST-RESPONSE TENSIO-METER SYSTEM

INTRODUCTION:

Knowledge of the disposition of water after it has been applied to the root zone of a crop is important in irrigation efficiency and salt balance studies, so that the evapotranspiration rate and deep percolation to the ground water can be determined. Also, when crops are irrigated with liquid wastes for disposal or waste water reclamation and ground-water recharge, it is important to know how much water passed through the root zone to the ground water. The objective of the study in Part B of this report is to determine if evapotranspiration and drainage components of water applied to land can be evaluated in situ with the fast-response recording tensiometer system developed earlier at the Laboratory.

PROCEDURE:

Field system. Details of the tensiometer system are given in Annual Reports 1966 and 1967. New tensiometer cups were installed at 5, 10, 15, 20, 30, 40, 60, 80, 100, and 120 cm depths. The higher concentration of tensiometers in the top 30 cm was necessary to obtain a good measurement of the hydraulic gradient in the zone where it is likely to change the most.

Temperature effects on tensiometers. An increase in the pressure head was noticed in the late afternoon and evening at depths 5 to 60 cm. To determine whether this was a real pressure change in the soil, or whether there was a temperature effect on the tensiometer system, the plot was covered preventing evaporation, but allowing temperature changes in the soil and around the tubing. Next, the 20-cm tensiometer lead was kept at a constant temperature using a constant-temperature water coil placed along the side of the tubing and the cover was

removed to allow evaporation. Pressures were measured on the 20-cm tensiometer for a 24-hour period in each case.

Measurement of water uptake by roots. The evapotranspiration rate of a crop can be calculated from pressure-head data when the relationship between water content,  $\theta$ , hydraulic conductivity,  $K$ , and pressure head,  $P$ , is known. The  $\theta - K - P$  relationships were measured as outlined in Annual Report 1967, except that the  $P - \theta$  curve for the 5, 10, and 15 cm depths were obtained using the pressure-outflow method and core samples. After the  $\theta - K - P$  relationships were established, several wetting and drying cycles were conducted. The evapotranspiration was then calculated for three days during the year.

#### RESULTS AND DISCUSSION:

Temperature effects. The temperature experiments confirmed that the measured diurnal pressure fluctuations were real. When the plot was covered, the pressure of the 20-cm tensiometer decreased gradually (Figure 24a). The rate of pressure decrease changed very little with time of day. When evaporation was allowed with temperature control around the tensiometer lead, the diurnal pattern was present (Figure 24b). The pressure would decrease in the early morning, reach a minimum in the late afternoon, and then increase during the night. The magnitude of the pressure change decreased with depth.

The pattern of pressure change is characteristic of vapor flow and condensation. As the soil heats up in the morning, the increased evaporation and the transpiration by the plant causes the soil-water pressure to decrease. When the soil temperature decreases at night, condensation of water vapor occurs which increases the water content and soil-water pressure. Because temperature changes are greater at the shallower depths, the increase of soil-water pressure at

nights is also greater at these depths. The magnitude of the pressure decrease during the daylight hours is also greater at the shallower depths. This is illustrated in Figure 25 where the total head for the different depths is shown for a 24-hour period.

Measurement of water uptake by roots. The uptake of water by roots can be calculated using the following equation:

$$q_z = \frac{\partial v}{\partial z} - \frac{\partial \theta}{\partial t} \quad (1)$$

where

$q_z$  = rate of water removed or added at depth  $z$   
per unit volume of soil

$v$  = flux =  $K \frac{dh}{dz}$

$h$  = pressure head plus elevation head

$K$  = hydraulic conductivity

$\theta$  = water content

$t$  = time

The term  $q_z$  is the rate at which water is added to, or abstracted from, the soil at depth  $z$ . This may be water uptake by the roots or vaporization and condensation of water within the soil profile. As the temperature of the soil increases, both vaporization of water and root extraction occur, resulting in a negative value of  $q_z$ . When condensation occurs within the soil profile in excess of root extraction, a positive value of  $q_z$  is obtained. The condensation is heaviest at night when the soil cools below the dew point, while the root uptake during this period is usually small. The positive  $q_z$  values can also be referred to as the net return vapor flow, since this is the portion of the vapor that does not leave the soil

profile. Direct return of water to the soil by roots is unlikely.

Integrating  $q_z$  for a 24-hour period yields the soil-water removal rate,  $r_z$ , at depth  $z$ . Integrating  $r_z$  over the depth of the root zone then yields the total evapotranspiration for the day. Both the evaporation and the transpiration rate are obtained since the net vapor loss in the profile is accounted for.

The value of  $q_z$ , calculated from equation (1) and using the data in Figure 25, is shown in Figure 26 for different depths during the 24-hour period on 15 July. Depths 30, 100, and 120 cm were not operating during this period. The magnitude of  $q_z$  is greater at the shallower depths, indicating a higher rate of soil-water withdrawal at these depths. Also,  $q_z$  is negative at the 80-cm depth and only slightly positive at 60 cm. Assuming that the root zone extended to a depth of 90 cm, the estimated evapotranspiration for this day was 7 mm, and the return vapor flow was 1 mm. Evapotranspiration calculated in a similar manner for 15 August and 13 October was 6.2 mm and 2 mm, respectively. These three values agree favorably with evapotranspiration rates of 7.1 mm, 5.8 mm, and 2.3 mm measured by Van Bavel (Annual Report 1963) on bermuda-grass, using a weighing lysimeter.

The calculation of  $q_z$  does not take hysteresis into account. Thus, the actual return vapor flow may not be as large as calculated because the typical hysteresis-loop patterns usually indicate little change in water content for an increase in pressure head immediately after rewetting starts.

The amount of water lost to deep percolation can be calculated from the flux between two tensiometers located below the root zone. Because the 100 and 120 cm tensiometers

were inoperative, this calculation could not be made. However, because small amounts of water were added, the deep percolation losses were expected to be small. Assuming this to be true, the evapotranspiration should be equal to the soil-water depletion. The soil-water depletion for 15 July, 15 August, and 13 October is 7.01 mm, 6.0 mm, and 1.8 mm, respectively, which agrees with the calculated evapotranspiration rates on those days.

Future studies will include the measurement of evapotranspiration and drainage losses in a weighing lysimeter. Temperatures in the soil profile will also be measured for determination of vapor flow within the profile.

#### SUMMARY AND CONCLUSIONS:

Using a fast-response, recording tensiometer system, disposition of water in a bermudagrass root zone following an irrigation was evaluated. Soil-water pressures as measured by the tensiometer system decreased during the daylight hours, reached a minimum about 1800, and increased during the night. The magnitude of the pressure change decreased with depth. Investigations showed that these fluctuations were real and not caused by temperature effects on the tensiometer system. The decrease in pressure is the result of root extraction and evaporation within the soil profile, while the increase is caused by condensation of vapor at night when the temperature of the soil decreases below the dew point. The net amount of water extracted from the root zone can be considered the evapotranspiration rate when drainage losses are accounted for. The evapotranspiration calculated for three days during the year agreed favorably

with that measured on similar days in previous years using a lysimeter.

PERSONNEL: Herman Bouwer and R. C. Rice

CURRENT TERMINATION DATE: December 1972

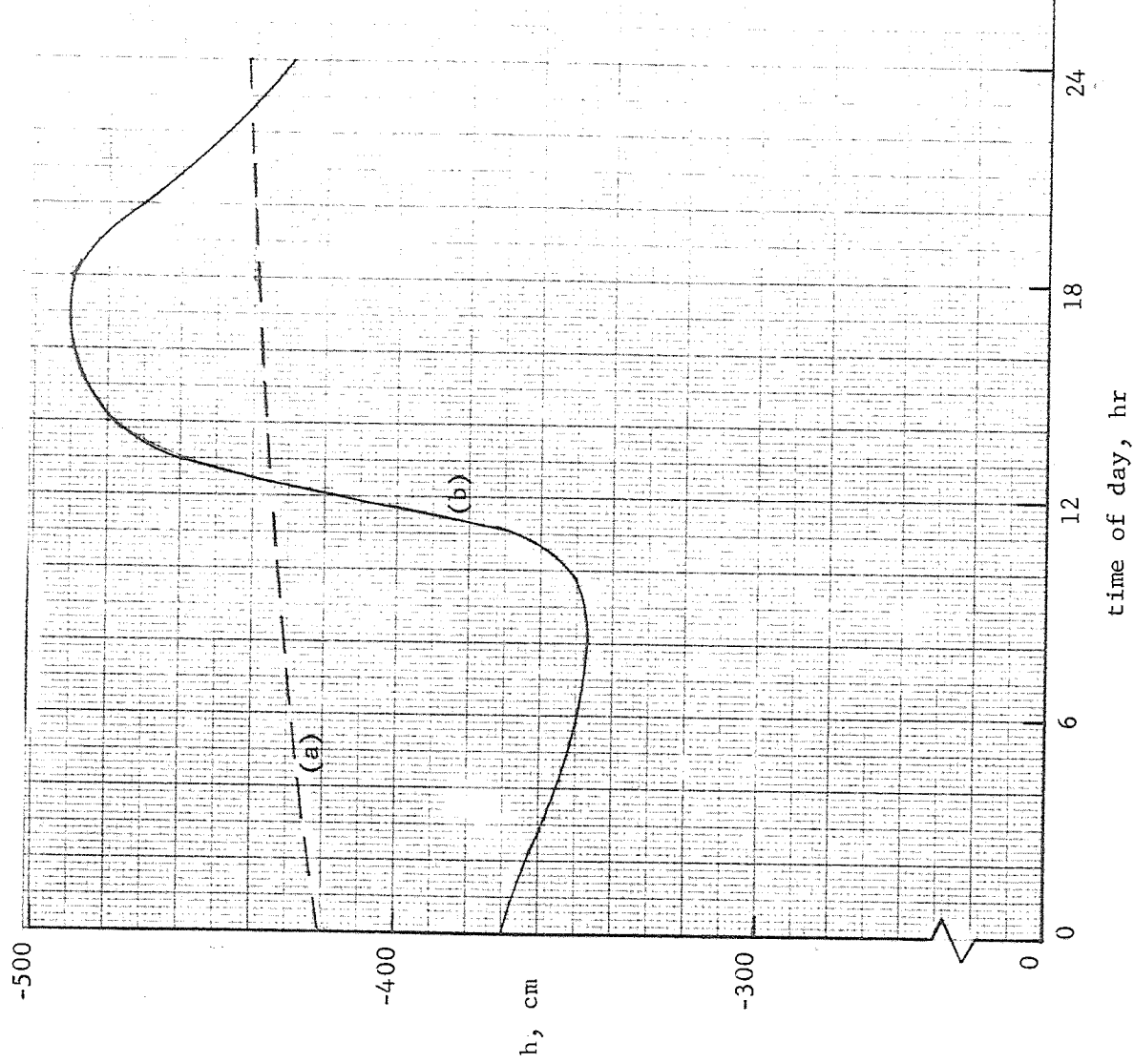


Figure 24. Diurnal total pressure trend at 20-cm depth for two conditions: (a) plot covered and (b) tensiometer tubing kept at constant temperature allowing evaporation.

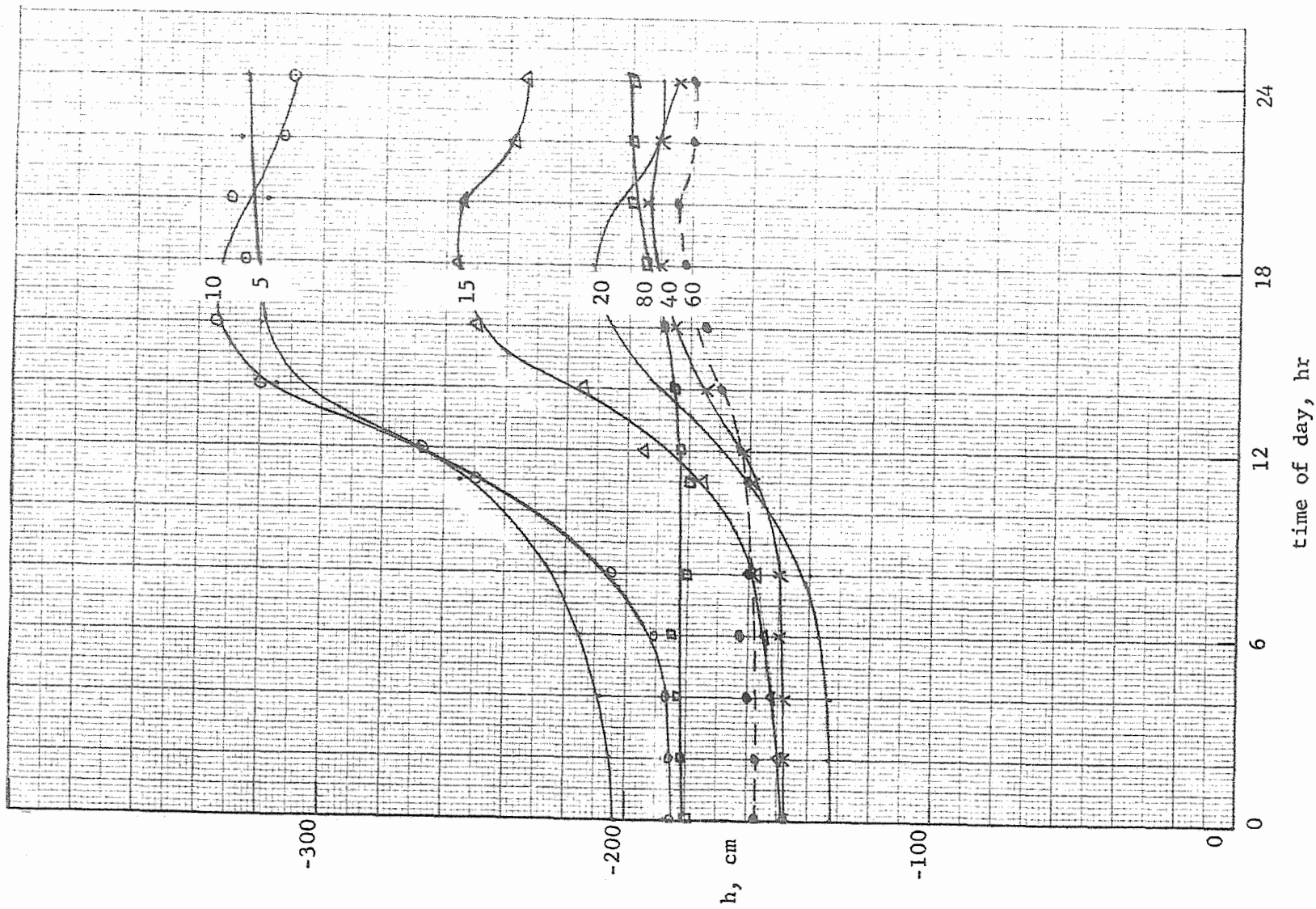


Figure 25. Total head,  $h$ , versus time of day for different depths in centimeters.

51-84

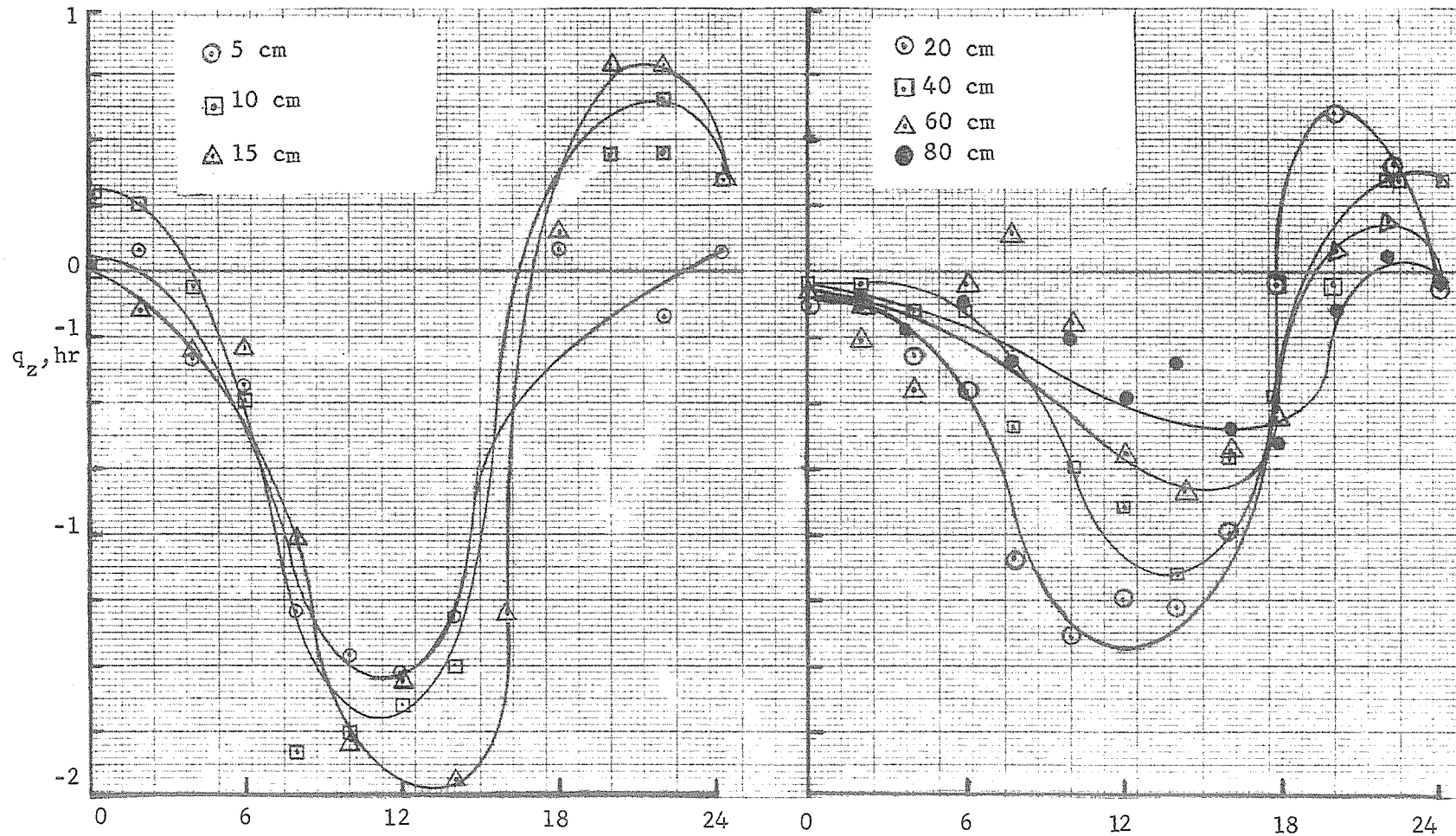


Figure 26.  $q_z'$  as a function of time of day for different depths.

TITLE: FABRICATED IN PLACE, REINFORCED RESERVOIR LININGS.  
CRIS WORK UNIT: SWC W7 gG-2 CODE NO.: Ariz.-WCL 68-2

INTRODUCTION:

Many water storage reservoirs are ineffective because of water loss by seepage. The use of water harvesting catchments has been restricted because of a lack of low-cost facilities to store the collected water between runoff events. At present, in many areas, construction site conditions often require the use of expensive materials such as steel tanks, butyl bags, or reinforced butyl linings for reservoirs. Materials for these structures are relatively bulky, increasing transportation costs to construction sites which can often be reached only in four-wheel drive vehicles. There is an urgent need for the development of materials and procedures which will permit construction of in-place, high-strength, low-cost storage structures for use with various types of water harvesting catchments.

Experimental linings of asphalt-fiberglass have been installed on two reservoirs in Arizona in cooperation with the Bureau of Indian Affairs (see 1962 and 1963 Annual Reports for WCL-7). These linings were constructed for a total cost of 75 cents per square yard, which was significantly lower than the cost of conventional reinforced materials. The linings have performed very well under severe conditions, including trampling by deer and cattle. To investigate the possibility of further lowering lining costs and improving performance, a series of laboratory studies were started to investigate various combinations of different asphalts and fiberglass mattings.

PROCEDURE:

A set of five pressure plates, 12 inches in diameter, were constructed to determine the head of water the linings would support over various subgrades. A disk of 18-mesh bronze screen is placed in the bottom section, which is then filled with the subgrade material. The lining material is laid over the subgrade material

and clamped into place between the two plates. The upper plate is connected to an air supply through a pressure regulator. The air pressure is initially set at 2 psi for 30 minutes, then increased by 2 psi every 2 hours. This is continued until the lining begins to leak air as indicated by air bubbling from a plastic tubing connected to the lower plate and immersed in a beaker of water.

The initial studies are with various types of fiberglass matings and asphalts. The fiberglass is cut into disks, 13 inches in diameter, and each disk weighed. Then asphalt is sprayed on the fiberglass disks at a rate which saturates the matting. The samples are allowed to cure for 2 weeks, then reweighed to determine the quantity of asphalt applied. The samples are then placed in the pressure plates for testing.

#### RESULTS AND DISCUSSION:

The studies were started in December 1968 and the results are not complete. In these first studies, two types of asphalts are being used. These are SS-2 anionic asphalt emulsion and MC-250 cut-back asphalt. The present indications are that the MC-250 is not satisfactory because the flow curing rate would make it impractical for field use.

#### SUMMARY AND CONCLUSIONS:

Asphalt fiberglass linings were installed in two 160,000 gallon reservoirs for a total cost of 75 cents per square yard. The linings are in excellent condition after six years of severe exposure, including trampling by deer and cattle. Laboratory investigations have been initiated to determine optimum combinations of various types of fiberglass, asphalt and application procedures. Preliminary results indicate that medium-cure cutback asphalts will not ordinarily be satisfactory because of their slow curing time.

PERSONNEL: G. W. Frasier and L. E. Myers

CURRENT TERMINATION DATE: December 1971.

TITLE: COLUMN STUDIES OF THE CHEMICAL, PHYSICAL, AND  
BIOLOGICAL PROCESSES OF WASTEWATER RENOVATION  
BY PERCOLATION THROUGH THE SOIL.

CRIS WORK UNIT: SWC W4 gG-1

CODE NO.: Ariz.-WCL 68-3

INTRODUCTION:

More information about the chemical, physical, and biological processes operating during groundwater recharge by sewage spreading is needed so that the efficiency of this water renovation can be improved. Most of the oxygen demand of wastewater must be satisfied if the water is to be adequately renovated. Therefore, the soil surface can only be flooded intermittently since the profile must be periodically recharged with oxygen. The oxygen use efficiency, then, must be known in order to calculate the maximum length of inundation period that can be used for a given dry period. One objective of this experiment is to prepare an oxygen balance sheet for soil columns during wastewater renovation which can be used in determining this oxygen use efficiency.

The reduction in the nitrate content of renovated water produced at Flushing Meadows during long inundation periods has been attributed to denitrification. Another objective of this experiment is to prepare a nitrogen balance sheet for soil columns during wastewater renovation and determine if nitrogen loss is indeed due to denitrification.

PROCEDURE:

Six soil columns of material from the basins at Flushing Meadows have been packed in the laboratory. Effluent collected at Flushing Meadows from the 91st Avenue sewage treatment plant in Phoenix is passed through the columns. Each column consists of a 2.75-meter length of 10-cm (I.D.) polyvinyl chloride pipe filled with 6 cm of pea gravel at the bottom and 250 cm of soil above that (Figure 1). The almost air-dry soil was packed to

an average bulk density of 1.6 g/cc. A constant head of 8 cm of water is maintained above the soil by means of a Mariotte siphon. The pipe is sealed 10 cm above the level of the constant head. This space is filled with water at the beginning of the inundation period, and air lost through the top of the soil column is collected by displacement of this water. The air volume is measured and sampled by withdrawing it through a serum cap with a syringe. A constant water level is maintained 5 cm above the lower end of the column, and air forced out the bottom is collected through a tube inserted into the gravel layer just above this water level. This air is collected by displacement of water from an inverted water bottle connected to a constant-head device. The air in the bottle is sampled through a serum cap and its volume is measured by weighing the water displaced through the constant-head device.

The flow rate and cumulative flow through the columns is measured by weighing the effluent at regular time intervals. The effluent and influent are analyzed periodically for coliform bacteria, organic N,  $\text{NH}_4^+$ , COD, and P. The air collected from the column is analyzed for  $\text{O}_2$  and  $\text{N}_2$  with a gas chromatograph equipped with a precision sampling valve and a molecular sieve column. Standard curves for  $\text{O}_2$  and  $\text{N}_2$  have been prepared using standard gases.

#### RESULTS AND DISCUSSION:

The columns were only recently put into operation and no data were available by the end of the year.

PERSONNEL: J. C. Lance, F. D. Whisler, Herman Bower, R. C. Rice

CURRENT TERMINATION DATE: October 1971

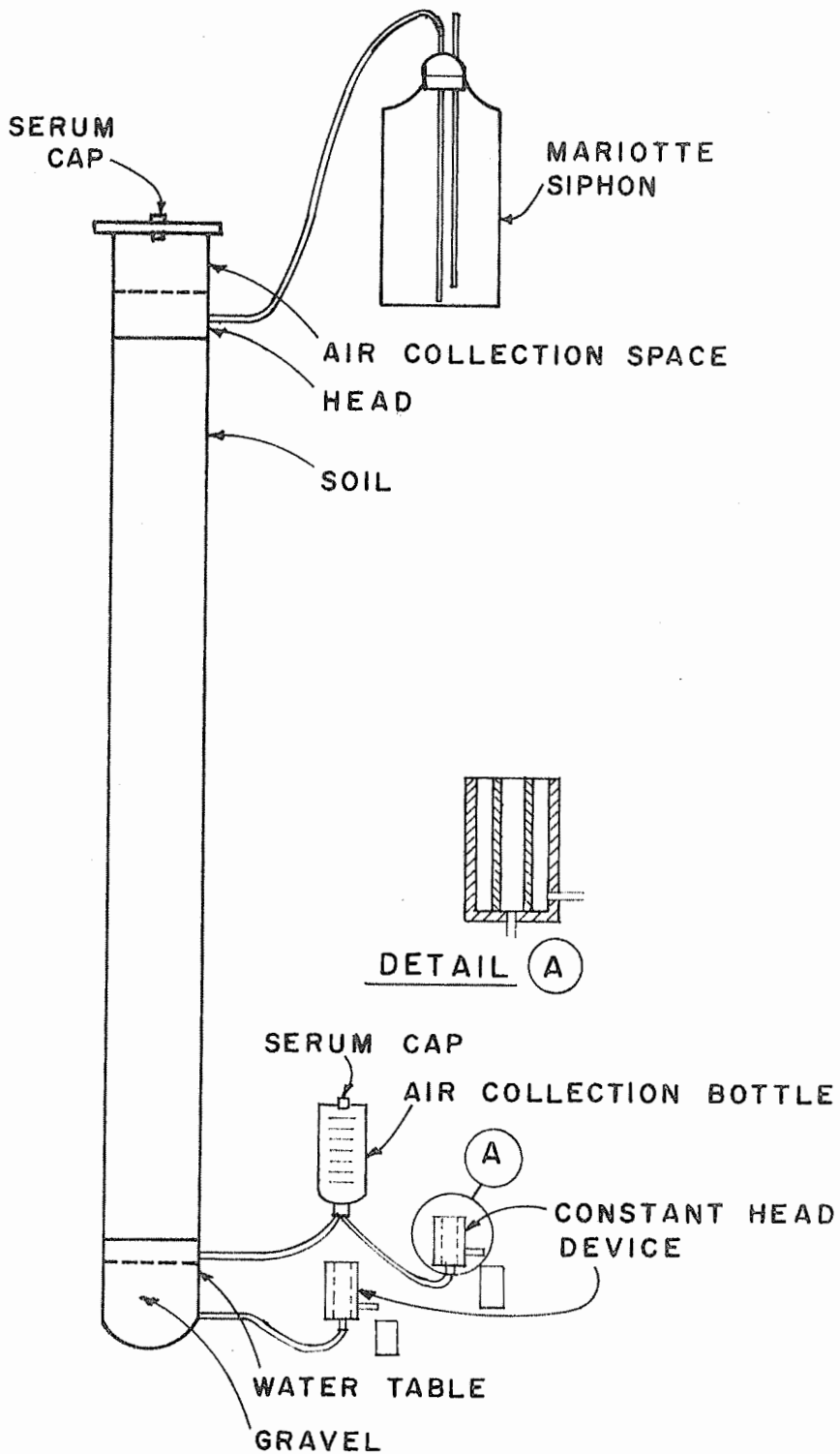


Figure 1. Soil column for wastewater renovation studies.

TITLE: WATER STRESSES IN PLANTS

CRIS WORK UNIT: SWC W9 gG6

CODE NO.: Ariz.-WCL 68-4

INTRODUCTION:

Prior to the commencement of work on this project outline, there existed no unified or general theory of the natures, causes, and effects of water stresses in plants. Thus, it was difficult to harmonize the many different aspects of water stress work. In particular, growth chamber and field work and work done in different climatic areas on the same or different plants did not always appear compatible in results. Indeed, much that seemed contradictory existed. Thus, the work herein described was begun in an attempt to develop a theory of water stresses in plants that could comfortably account for the variety of phenomena observed and currently appearing in the literature with respect to soil-plant-atmosphere water relations.

PROCEDURE:

The foundation of the theoretical framework which was constructed consisted of two basic hypotheses. These were: (1) that since transpiration is the physical movement of water from plant leaves to air, it is controlled essentially by the free energy gradient of water in the soil-plant-atmosphere continuum (SPAC), and (2) that whereas photosynthesis is the chemical reaction involving water in dry matter production, it is controlled chiefly by the actual free energy of water in the vicinity of the chloroplasts. From these two assumptions, the relative importances of atmospheric and soil water to the processes of transpiration and photosynthesis were derived. Certain apparent contradictory experiments were then harmonized by this analysis.

After thus establishing the general basis of the theory, some more refined postulations were advanced. These included second-order effects of transpiration rate and leaf temperature on photosynthesis rate. Their development evolved from considerations of

electric circuit analogy and irreversible thermodynamics. The results obtained were used to explain some "anomalous" fluctuations in CO<sub>2</sub> fixation observed by Troughton and Cowan (15).

#### RESULTS AND DISCUSSION:

It was demonstrated from principles implied in a discussion by Philip (13) dealing with the SPAC and from the two basic hypotheses defining the controlling mechanisms of photosynthesis and transpiration that whereas photosynthesis may come within 10% of being completely decoupled from the direct effects of atmospheric moisture content, transpiration may be independent of soil moisture to a similar degree. However, apparent effects of atmospheric and soil moisture may be greater than this. When compared with maximum potential rates under optimum conditions of each moisture source, however, this discrepancy is removed.

The predictions of the basic theory were found in harmony with the earlier theories of both Gardner (6) and Cowan (4), concerning water movement in soils and transpiration. Similarly, they harmonized with the experimental findings of Martin (12), Slatyer (14), Denmead and Shaw (5), Baker and Musgrave (1), and Van Bavel (16). On the other hand, they appeared to be completely contradictory of the results of Brix (3), who found both photosynthesis and transpiration to be similarly affected by soil moisture depletion. An analysis of all pertinent factors showed that his findings too, however, could still be explained by the theory.

All of this information is discussed in reference (7). In addition, an interesting exchange of ideas (conflicting) on the transpiration portion of the theory may be found in (10, 8, 11, and 17). The second and fourth, of course, are pro and the first and third are con.

As the theory was extended to include some second-order effects, electrical analogy (Figure 1) was used to determine the change in the free energy value at the site of the chloroplasts, or more

simply, the water chemical potential, with stomatal resistance as

$$\left( \frac{\partial E_c}{\partial R_{ST}} \right)_{E_A, E_{SS}, R_R, R_X, R_B} = (E_{SS} - E_A) \left( 1 + \frac{R_R + R_X}{R_{ST} + R_B} \right)^{-2} \frac{(R_R + R_X)}{(R_{ST} + R_B)^2} \quad (1)$$

where  $E_C$  = water chemical potential in vicinity of leaf chloroplasts

$E_A$  = water chemical potential of atmosphere moisture

$E_{SS}$  = water chemical potential of soil solution

$R_R$  = resistance to water flow of roots

$R_X$  = resistance to water flow of xylem vessels

$R_{ST}$  = resistance to water vapor transport of stomates

$R_B$  = resistance to water vapor transport of boundary-layer air.

As long as  $E_{SS} > E_A$  and water flows from the soil through the plant to the atmosphere, the expression in equation (1) will always be positive, implying that  $E_C$  and  $R_{ST}$  vary in phase with each other. This has recently been confirmed experimentally by Barrs and Klepper (2). Then, since  $R_{ST}$  and transpiration vary in an inverse manner, equation (1) and the postulate relating photosynthesis to water chemical potential predict the possibility of a photosynthetic depression when stomates are fully open and transpiration is at a maximum.

A similar but more detailed prediction of this phenomenon derives from considerations involving irreversible thermodynamics. It is specifically expressed by the equation

$$\mu_{WC} = \mu_{WSS} \left( \frac{T_C}{T_{SS}} \right) - K_W^{-1} J_W - \frac{K_U}{K_W} (T_C - T_{SS}) \quad (2)$$

where  $\mu_{WC}$  = water chemical potential in vicinity of chloroplasts  
 $\mu_{WSS}$  = water chemical potential of soil solution  
 $T_C$  = chloroplast or leaf temperature  
 $T_{SS}$  = temperature of soil solution  
 $J_W$  = transpiration rate  
 $K_W$  = conductance of plant system for water  
 $K_U$  = conductance of plant system for heat.

Again, it is evident from equation (2) that as transpiration rate increases,  $\mu_{WC}$  becomes more negative, implying a possible decrease in photosynthesis. Furthermore, since water chemical potential is always negative in sign, for any increase in  $T_C$ , this relationship will be enhanced. Experimentally, these predictions have been confirmed by the work of Troughton and Cowan (15) depicted in Figures 2 and 3. With all else constant, they observed photosynthesis to be depressed during the middle portions of the open parts of a rhythmic, plant controlled cycling of its stomatal apertures. The photosynthetic depressions were greater the higher the leaf temperature above the threshold for the effect of 37.5 C. A more detailed discussion of this phenomenon is included in reference (9).

#### SUMMARY AND CONCLUSIONS:

A new theory of water stresses in plants has been developed which concerns the two plant processes of photosynthesis and transpiration. The theory links photosynthesis most directly with soil moisture conditions and transpiration with atmospheric moisture conditions. It also predicts a second-order effect of transpiration rate on photosynthetic rate and describes the influence upon this latter effect of leaf temperature. The theory has received considerable substantiation from reports in the literature but cannot truly be said to be definitely established in its entirety. Pertinent experimental work will thus soon be initiated.

## REFERENCES:

1. Baker, D. N., and Musgrave, R. B. The effects of low level moisture stresses on the rate of apparent photosynthesis in corn. *Crop Sci.* 4:249-253. 1964.
2. Barrs, H. D., and Klepper, B. Cyclic variations in plant properties under constant environmental conditions. *Physiol. Plant.* 21:711-730. 1968.
3. Brix, H. The effect of water stress on the rates of photosynthesis and respiration in tomato plants and loblolly pine seedlings. *Physiol. Plant.* 15:10-20. 1962.
4. Cowan, I. R. Transport of water in the soil-plant-atmosphere system. *Jour. Appl. Ecol.* 2:221-239. 1965.
5. Denmead, O. T., and Shaw, R. H. Availability of soil water to plants as affected by soil moisture content and meteorological conditions. *Agron. Jour.* 54:385-390. 1962.
6. Gardner, W. R. Dynamic aspects of water availability to plants. *Soil Sci.* 89:63-73. 1960.
7. Idso, S. B. Atmospheric- and soil-induced water stresses in plants and their effects on transpiration and photosynthesis. *Jour. Theoretical Biol.* 21:1-12. 1968.
8. Idso, S. B. Comments on paper by Richard Lee, "The hydrologic importance of transpiration control by stomata." *Water Resources Res.* 4:665-666. 1968.
9. Idso, S. B. Water chemical potential and photosynthesis. *Jour. Theoretical Biol.* Submitted. 1969.
10. Lee, R. The hydrologic importance of transpiration control by stomata. *Water Resources Res.* 3:737-752. 1967.
11. Lee, R. Reply. *Water Resources Res.* 4:667-669. 1968.
12. Martin, E. V. Effect of soil moisture on growth and transpiration in Helianthus annuus. *Plant Physiol.* 15:449-466. 1940.
13. Philip, J. R. The physical principles of soil water movement during the irrigation cycle. In Third Congress on Irrigation and Drainage, Reports for Discussion 8, R7, 8:125-154. San Francisco. 1957.

14. Slatyer, R. O. The influence of progressive increases in total soil moisture stress on transpiration, growth, and internal water relations of plants. Austral. Jour. Biol. Sci. 10:320-336. 1957.
15. Troughton, J. H., and Cowan, I. R. Carbon dioxide exchange in cotton: some anomalous fluctuations. Science 161:281-283. 1968.
16. Van Bavel, C. H. M. Changes in canopy resistance to water loss from alfalfa induced by soil water depletion. Agr. Met. 4:165-176. 1967.
17. Van Bavel, C. H. M. Further to the hydrologic importance of transpiration control by stomata. Water Resources Res. Submitted. 1968.

PERSONNEL: Sherwood B. Idso

CURRENT TERMINATION DATE: October 1971

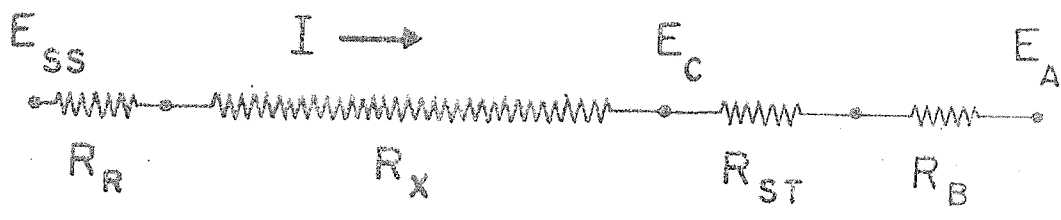


Figure 1. Electrical analogue for the transport of water in a plant.

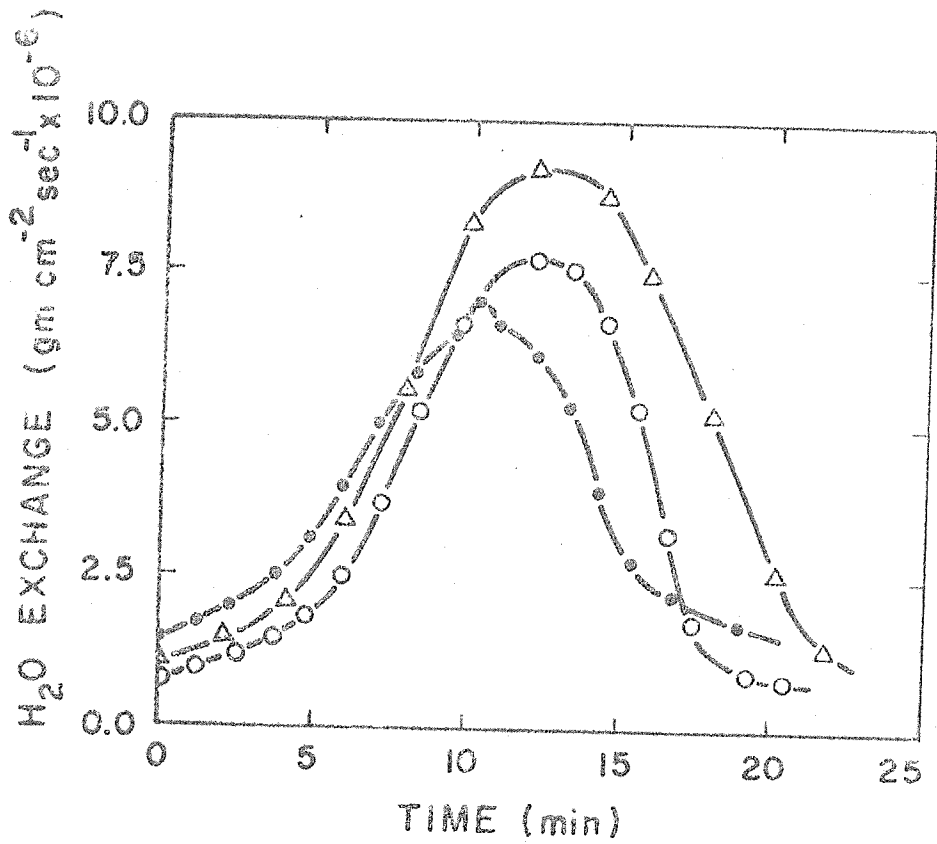


Figure 2. Transpiration during the opening and closing of cotton stomates as influenced by leaf temperature;  $\Delta = 37.5^{\circ} \text{C}$ ,  $\circ = 40.0^{\circ} \text{C}$ ,  $\bullet = 42.5^{\circ} \text{C}$ . After Troughton and Cowan (1968).

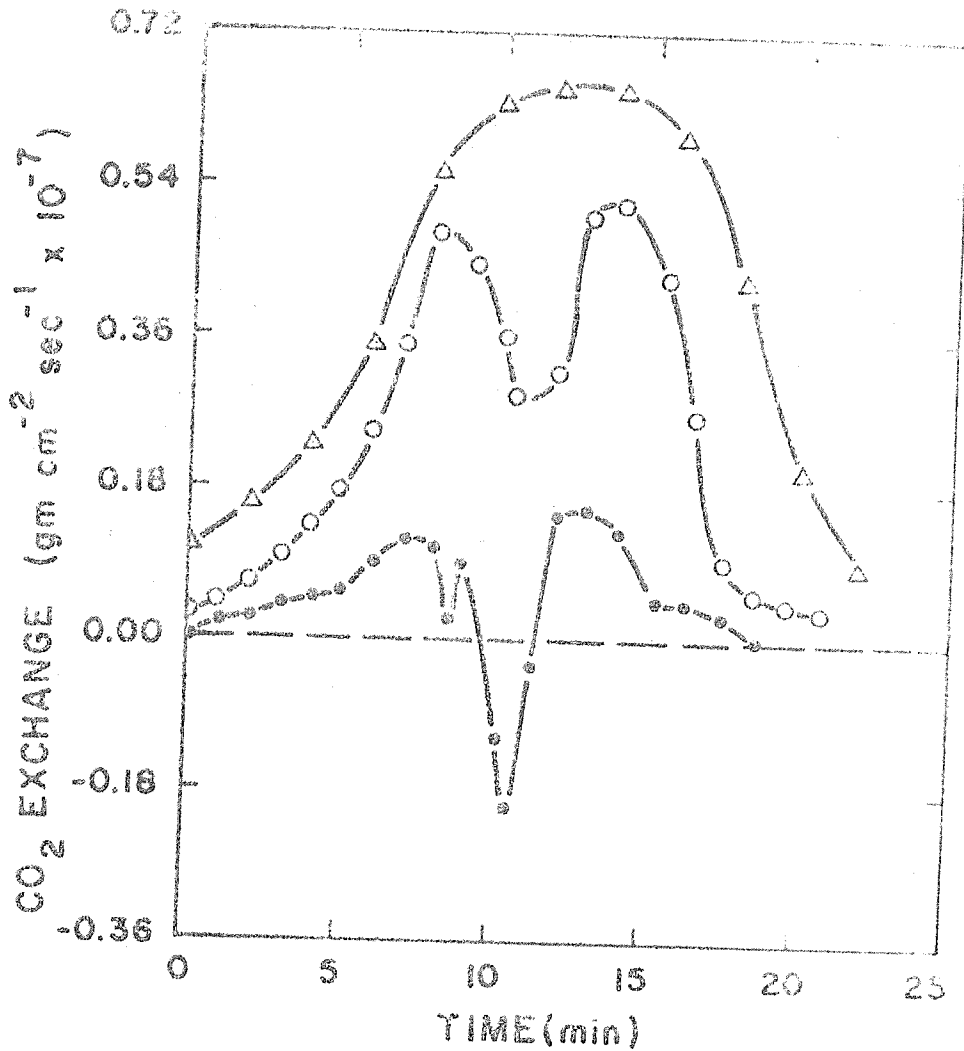


Figure 3. Net photosynthesis during the opening and closing of cotton stomates as influenced by leaf temperature;  $\Delta = 37.5^{\circ} \text{C}$ ,  $\circ = 40.0^{\circ} \text{C}$ ,  $\bullet = 42.5^{\circ} \text{C}$ . After Troughton and Cowan (1968).

TITLE: ASSESSING THE ENERGY ENVIRONMENT OF PLANTS

CRIS WORK UNIT: SWC W9 gG6

CODE NO.: Ariz.-WCL-68-5

INTRODUCTION:

That the naturally varying energy environment can have an enormous effect upon plant productivity was demonstrated by work reported on last year (8). As a result, this project outline was initiated to study various aspects of that environment and means of monitoring it. Within this framework a continuation was made of the infrared thermometry work reported in last year's annual report and subsequently published (9, 10). This included: 1) characterizing an additional source of error in infrared thermometry, 2) comparing two established procedures for determining the infrared emittances of bare soils, and 3) developing a new method for determining infrared emittance of both soils and leaves. In addition, a new theory of thermal radiation from clear skies was also produced.

PROCEDURE:

Infrared Thermometry Errors. The first set of experiments we conducted was designed to obtain a quantitative evaluation of the deterioration of the infrared thermometers' output signals at high ambient temperatures. In a controlled temperature room successively kept constant at four different ambient temperatures, Barnes IT-2 and IT-3 infrared thermometers simultaneously viewed a black plate, as their internal temperatures were raised from a point low in their suggested operating ranges to above their signal deterioration points. Plate temperature, internal instrument temperature, and instrument signals were all recorded.

The second phase of the experiment was conducted out-of-doors. A watertight chamber was constructed which contained two viewing ports, at the bases of which were two blackened cones. This chamber was immersed in a mixture of ethylene glycol, the temperature of which could be controlled between -30 and +50°C. The

infrared thermometers viewed the blackened cones continuously for several days at several different bath temperatures within this range. This allowed a calibration of the instruments' output signals as a function of blackbody radiation while the instruments were subjected to diurnal climatic variations; and it also established the relation between internal console temperature and ambient air temperature for the clear sky conditions which prevailed at that time.

Comparison of Emittance Measurement Methods. The two emittance measurement methods we compared were developed by Buettner and Kern (4) and Fuchs and Tanner (7). To accomplish the comparison, we acquired the apparatus essential to both methods and followed their outlined procedures to determine the infrared emittances of four bare soils. These procedures are described in detail in references (5, 7).

Development and Use of a New Emittance Measurement Method. From theory contained in reference (13), it is demonstrable that the energy sensed by an infrared thermometer perpendicularly viewing a horizontal surface outdoors may be expressed as

$$R_o = \epsilon f(T) \frac{\sigma T^4}{\pi} + (1-\epsilon) f(T_s) B_s \quad (1)$$

where  $\epsilon$  = average emittance of surface, weighted for the spectral sensitivity of the infrared thermometer employed

$\sigma$  = Stefan-Boltzmann constant

$T$  = surface temperature

$T_s$  = radiative temperature of surroundings

$B_s$  = total hemispherical radiation from surroundings divided by  $\pi$

and  $f(T)$  and  $f(T_s)$  are "lumped filter functions" defined as

$$f(T) = \frac{\int_0^{\infty} f(\lambda) E(\lambda, T) d\lambda}{\int_0^{\infty} E(\lambda, T) d\lambda} = \pi \frac{\int_0^{\infty} f(\lambda) E(\lambda, T) d\lambda}{\sigma T^4} \quad (2)$$

$$f(T_s) = \frac{\int_0^{\infty} f(\lambda) B(\lambda, T_s) d\lambda}{\int_0^{\infty} B(\lambda, T_s) d\lambda} = \frac{\int_0^{\infty} f(\lambda) B(\lambda, T_s) d\lambda}{B_s} \quad (3)$$

where  $f(\lambda)$  = spectral sensitivity of the infrared thermometer employed

$E(\lambda, T)$  = spectral distribution of normal blackbody radiation at temperature  $T$

$B(\lambda, T_s)$  = spectral distribution of hemispherical radiation from the surroundings of radiative temperature  $T_s$  divided by  $\pi$ .

The technique we developed used equation (1) in two different ways. First, a metal plate painted with a mixture of aluminum spray lacquer and flat black paint to yield an infrared emittance near 0.5 is placed in the center of an open expanse outdoors. By means of thermocouples imbedded just beneath its upper surface, its temperature is then monitored, along with  $R_o$  (obtained with an infrared thermometer), as it warms or cools to ambient temperature after having been previously cooled or heated. The data thus obtained are used to plot  $R_o$  as a function of  $f(T)\sigma T^4/\pi$ , whereby  $\epsilon$  is obtained as the slope of this regression line, and  $f(T_s)B_s$  is then calculated from the intercept. The average value of  $f(T_s)B_s$  obtained by this means for the clear sky conditions of a particular

location has been demonstrated by Idso and Jackson (9) to vary by not more than  $\pm 15\%$ . This variation has practically no effect on the calculations that follow.

The second usage of equation (1) yields either a soil or leaf emittance. In the case of a leaf, a 0.1-mm-diameter copper-constantan thermocouple is threaded diagonally into the leaf mid-rib just beneath the upper leaf surface. The temperature obtained from this thermocouple and the energy sensed by an infrared thermometer concurrently viewing the leaf then yield leaf emittance according to the relation

$$\epsilon = \frac{R_o - f(T_s)B_s}{\frac{1}{\pi} f(T)\sigma T^4 - f(T_s)B_s} \quad (4)$$

In the case of a soil, a thin layer of the soil is spread over the top of a piece of styrofoam, through which four thermocouples protrude to lie flat against the upper surface. Everything else remains the same.

Thermal Radiation From Clear Skies. A theoretical analysis of expressions proposed by Brunt (3), Angstrom (1, 2), and Swinbank (16) to describe thermal radiation from clear skies revealed that all lacked the generality to describe such radiation at all earth latitudes and temperatures. Thus, a new theoretical framework was developed to accomplish the objective of so describing this radiation. The details of the derivation are contained in reference (12). The new equation was tested with data obtained from Alaska, Arizona, Australia, and the Indian Ocean.

#### RESULTS AND DISCUSSION:

Infrared Thermometry Errors. For the IT-2 infrared thermometer, the internal temperature at which the output signal deteriorated was

about 48°C; and for the IT-3 it was about 58°C. The significance of these values is only appreciated, however, when the relations between internal temperatures and ambient air temperature are known. During the clear sky period when the instruments were operated outside, air temperature was generally around 9°C during the coolest part of the night and 25°C during the warmest part of the day. The corresponding internal console temperatures of both the IT-2 and IT-3 at these times were 23 and 50°C. Thus, on all of the days during which the instruments were in operation outdoors, the output signal of the IT-2 deteriorated during midday.

In the stability test of the instruments' calibration curves, no systematic effect could be discovered for the IT-2. The IT-3, however, was very definitely temperature dependent in this respect. The information in Table 1 indicates that the uncertainty introduced into a temperature measurement with the IT-3 by this effect may far exceed the accuracy of  $\pm 0.2^\circ\text{C}$  routinely claimed for this instrument (6, 7).

Comparison of Emittance Measurement Methods. The results of our comparison of the Buettner and Kern (BK) and Fuchs and Tanner (FT) emittance measurement methods are contained in Table 2. Based upon that evidence, we have concluded that both methods give essentially the same results, and that both are thus equally good (11).

Development and Use of a New Emittance Measurement Method. As a test of the accuracy of our method of emittance measurement, we compared it against the BK and FT methods applied to these soils. The results of this test are recorded in Table 3. The differences between our method and the other two were on the average less than 0.3%, or even better agreement than that between the BK and FT methods compared against each other. We thus concluded that our method (IJ) was equally as good as the other two.

Having established the method's validity, we then employed it to determine the infrared emittances of several plant leaves, an objective to which the BK and FT methods could not be applied, due to size limitations. The results of these measurements are tabulated in Table 4. Since there was no apparent correlation between the various plant species and their emittances, it was made evident that this parameter could not be merely estimated for very accurate work but instead required a measurement of the type we performed.

Thermal Radiation From Clear Skies. The equation we derived to describe thermal radiation from clear skies was

$$R = \sigma T^4 \left[ 1 - c \cdot e^{-d(273-T)^2} \right] \quad (5)$$

where c and d are constants and the remaining terms as previously defined. To this equation we fit experimental data from Alaska (15), Australia (16), Arizona (12), and the Indian Ocean (16), which covered a temperature range of from  $-45^{\circ}\text{C}$  to  $+45^{\circ}\text{C}$ . The coefficients c and d determined from these data were 0.261 and  $7.77 \times 10^{-4}$ , respectively. Plotted against the predictions of equation (5), these data analyzed by linear regression yielded a slope of 0.9993, an intercept of  $-0.2100 \text{ mw cm}^{-2}$ , and a correlation coefficient of 0.992.

#### SUMMARY AND CONCLUSIONS:

Two sources of error in infrared thermometry were documented and quantitatively assessed. Taking cognizance of them, two methods for determining the infrared emittances of bare soils were experimentally compared and were both found to be equally good. A new method of emittance measurement was then developed which in addition to being

used with soils could also be applied to plant leaves. It was found to be equally as good as the others. Thereupon it was used to determine the infrared emittances of many leaves. Finally, a general relation between clear sky atmospheric thermal radiation and screen-level air temperature was developed that appears to be valid at any latitude and for any air temperature obtainable on earth.

#### REFERENCES:

1. Angstrom, A. The study of radiation of the atmosphere. Smithsonian Inst., Misc. Coll. 65:1-159. 1918.
2. Angstrom, A. Effective radiation during the second international Polar Year. Medde. Stat. Met. Hydrogr. Anst., Stockholm, 6, No. 8. 1936.
3. Brunt, D. Notes on radiation in the atmosphere. Quart. J. Roy. Meteorol. Soc. 58:389-418. 1932.
4. Buettner, K. J. K., and Kern, C. D. The determination of infrared emissivities of terrestrial surfaces. J. Geophys. Res. 70:1329-1337. 1965.
5. Conaway, J., and Van Bavel, C. H. M. Remote measurement of surface temperature and its application to energy balance and evaporation studies of bare soil surfaces. Tech. Report ECOM 2-67P-1. 1966.
6. Conaway, J., and Van Bavel, C. H. M. Evaporation from a wet soil surface calculated from radiometrically determined surface temperatures. J. Appl. Meteorol. 6:650-655. 1967.
7. Fuchs, M., and Tanner, C. B. Infrared thermometry of vegetation. Agron. J. 58:597-601. 1966
8. Idso, S. B., and Baker, D. G. The naturally varying energy environment and its effects upon net photosynthesis. Ecology 49: 311-316. 1968.
9. Idso, S. B. and Jackson, R. D. The significance of fluctuations in sky radiant emittance for infrared thermometry. Agron. J. 60: 388-392. 1968.

10. Idso, S. B., and Jackson, R. D. A note on the role of sky radiance in infrared thermometry. J. Appl. Meteorol. 7: 521-522.
11. Idso, S. B., and Jackson, R. D. Comparison of two methods for determining infrared emittances of bare soils. J. Appl. Meteorol. 8: In press. 1969.
12. Idso, S. B., and Jackson, R. D. Thermal radiation from clear skies. J. Geophys. Res. Submitted. 1969.
13. Idso, S. B., Jackson, R. D., Ehrler, W. L., and Mitchell, S. T. Infrared emittance determinations of leaves. Ecology. Submitted. 1969.
14. Jackson, R. D., and Idso, S. B. Ambient temperature effects in infrared thermometry. Agron. J. 61: In press. 1969.
15. Lieske, B. J., and Stroschein, L. A. Radiative regime over Arctic tundra. Sci. Rept., Office of Naval Research, Contract 477(24)(NR 307-252), 23 pp. 1968.
16. Swinbank, W. C. Long-wave radiation from clear skies. Quart. J. Roy. Meteorol. Soc. 89:339-348. 1963.

PERSONNEL:

Sherwood B. Idso and Ray D. Jackson.

CURRENT TERMINATION DATE: October 1971

Table 1. The uncertainty in surface temperature of a blackbody created by the divergence of calibration curves for the IT-3 infrared thermometer obtained at internal temperatures of 25 and 50°C.

True surface temperature, °C	Uncertainty, °C
-30	8.0
-20	6.5
-10	4.8
0	3.6
10	2.7
20	1.9
30	1.0
40	0.4
50	0.0

Table 2. Emittances of four soils determined by the Buettner and Kern (BK) and Fuchs and Tanner (FT) methods with a Barnes IT-3 infrared thermometer. Each value is the average of 5 measurements.

	Silica sand $\epsilon \pm \text{std. dev.}$	Superstition sand $\epsilon \pm \text{std. dev.}$	Pine silty clay $\epsilon \pm \text{std. dev.}$	Adelanto loam $\epsilon \pm \text{std. dev.}$
BK	$0.893 \pm 0.005$	$0.945 \pm 0.003$	$0.968 \pm 0.006$	$0.964 \pm 0.007$
FT	$0.893 \pm 0.005$	$0.952 \pm 0.008$	$0.963 \pm 0.004$	$0.969 \pm 0.007$
BK-FT	$0.000 \pm 0.010$	$-0.007 \pm 0.011$	$+0.005 \pm 0.010$	$-0.005 \pm 0.014$

56-10

Table 3. Infrared emittances of three soils determined by the BK and FT methods and the IJ method. The BKFT values are the means of 5 BK and 5 FT measurements and IJ values are the means of 10 IJ measurements.

Method	Silica sand $\epsilon \pm \text{std. dev.}$	Superstition sand $\epsilon \pm \text{std. dev.}$	Adelanto loam $\epsilon \pm \text{std. dev.}$
BKFT	0.893 $\pm$ 0.005	0.949 $\pm$ 0.007	0.966 $\pm$ 0.007
IJ	0.894 $\pm$ 0.002	0.954 $\pm$ 0.005	0.967 $\pm$ 0.006

Table 4. Infrared emittances of plant leaves, determined as the means of approximately 12 measurements for each species by the IJ method.

Plant	$\epsilon \pm \text{std. dev.}$
<u>Phaseolus vulgaris</u> cv. Bountiful (center leaflet)	0.938 $\pm$ 0.008
<u>Zea mays</u> cv. Mexican June	0.944 $\pm$ 0.004
<u>Nymphaea odorata</u>	0.957 $\pm$ 0.006
<u>Opuntia ficus indica</u>	0.957 $\pm$ 0.002
<u>Opuntia engelmannii</u>	0.961 $\pm$ 0.004
<u>Ligustrum vulgare</u> cv. Japanese	0.964 $\pm$ 0.003
<u>Gossypium hirsutum</u> cv. Deltapine 16	0.964 $\pm$ 0.007
<u>Phaseolus vulgaris</u> cv. Bountiful (lateral leaflet)	0.964 $\pm$ 0.005
<u>Opuntia linguiformis</u>	0.965 $\pm$ 0.001
<u>Cordyline terminalis</u>	0.967 $\pm$ 0.003
<u>Gossypium hirsutum</u> cv. Hopicala	0.967 $\pm$ 0.011
<u>Aralia seboldi</u>	0.968 $\pm$ 0.006
<u>Hedera helix</u> var. Algerian	0.969 $\pm$ 0.005
<u>Opuntia santa rita</u>	0.969 $\pm$ 0.002
<u>Opuntia orbiculata</u>	0.971 $\pm$ 0.006
<u>Citrus aurantium</u>	0.972 $\pm$ 0.008
<u>Nicotiana tabacum</u>	0.972 $\pm$ 0.006
<u>Lophocereus schottii</u>	0.973 $\pm$ 0.004
<u>Cereus bridges</u> II	0.973 $\pm$ 0.001
<u>Cocculus laurifolius</u>	0.973 $\pm$ 0.003
<u>Citrus jambhiri</u>	0.975 $\pm$ 0.008
<u>Morus alba</u>	0.976 $\pm$ 0.008
<u>Opuntia rufida</u>	0.977 $\pm$ 0.002
<u>Populus Fremontii</u>	0.977 $\pm$ 0.004

Table 4. Infrared emittances of plant leaves, determined as the means of approximately 12 measurements for each species by the IJ method. (continued)

Plant	$\epsilon \pm \text{std. dev.}$
<u>Opuntia basilaris</u>	0.978 $\pm$ 0.002
<u>Persea drymifolia</u>	0.979 $\pm$ 0.009
<u>Gossypium barbadense</u> cv. Pima S-4	0.979 $\pm$ 0.008
<u>Capsicum frutescens</u> cv. Long Green	0.979 $\pm$ 0.005
<u>Lycopersicon esculentum</u> cv. Pearson Improved	0.982 $\pm$ 0.004
<u>Carica papaya</u>	0.988 $\pm$ 0.002
<u>Philodendron selloum</u>	0.990 $\pm$ 0.010
<u>Pelargonium domesticum</u> var. Martha Washington	0.992 $\pm$ 0.002
<u>Rosa</u>	0.993 $\pm$ 0.006
<u>Saccharum officinarum</u>	0.995 $\pm$ 0.004

TITLE: SIMULATION OF PLANT COMMUNITIES FOR DETERMINING  
WATER USE EFFICIENCY

CRIS WORK UNIT: SWC W9 gC6

CODE NO.: Ariz.-WCL 68-6

INTRODUCTION:

To understand fully the growth response of a crop and its concurrent efficiency in utilizing water, all aspects of the crop's environment must be considered; yet, in field experiments this is rarely feasible. It is also desirable to modify one or several environmental factors in a particular fashion under controlled conditions. Many of the combinations required, however, are not within the capacity to attain of even the most sophisticated controlled environmental chambers. Computer simulation stands as a ready solution to several of these problems. However, the results it yields are no better than the theoretical framework upon which its operations are based. The purpose of the research carried out under this project outline has been to improve the quality of this information and thus better the approximation of reality made by the computer.

The basic philosophy of this research was elucidated in last year's annual report and is also described in reference (11). The objective this year has been to improve upon various aspects of the general scheme there presented. Two particular phases have been dealt with: (1) describing the photosynthetic response of a crop to its environment, and (2) describing the light relations in plant canopies.

PROCEDURE:

Photosynthetic Response. In deriving an analytical expression for the carbon dioxide fixing response of a plant to its environment, models proposed by several other workers were investigated. These included photosynthesis models of Monteith (18), Duncan, et al. (7), de Wit (6), and Idso (11). Monteith's model considered only light

intensity as affecting photosynthesis, as did Duncan's. De Wit, in addition, considered CO<sub>2</sub> concentration of the ambient air; and Idso further included leaf temperature and water availability. It was decided that the latter scheme, being more inclusive of pertinent factors, must thus form the basis of any extended work. However, since it was not analytical but empirical, much needed to be done with it. By studying literature references, an analytical expression was finally constructed for CO<sub>2</sub> fixation in terms of five environmental variables and seven plant constants. Procedures were then outlined for measuring or calculating the five pertinent variables at the various leaves of a plant canopy.

Light Relations. The de Wit (6) - Idso (11) theory of light relations in a plant canopy was extended to provide useful information, not only for photosynthesis calculations, but also for remote sensing applications. A comparison of the predictions of the theory was then made with experiment. This was accomplished by applying the theory to a corn crop growing at Ithaca, New York, during the fall of 1961. Since this crop was thoroughly investigated and reported on in the literature (1, 2, 4, 22, 23, 24), it provided a good test of the new model.

#### RESULTS AND DISCUSSION:

Photosynthetic Response. The final equation constructed for the description of net CO<sub>2</sub> fixation in terms of environmental variables was

$$P_N = \left( \frac{M_L - M}{M_L - M_O} - \frac{100 - RH}{600} \right) \left( \frac{CDC}{300} \right) \left( \frac{P_{MAX} I}{I + I_2} - R \right) e^{-B(T_L - T_O)^2} \quad (1)$$

where  $P_N$  = net photosynthesis  
 $M$  = soil moisture tension of root zone  
 $RH$  = relative humidity of canopy air  
 $CDC$  = CO<sub>2</sub> concentration of canopy air

- I = intensity of solar radiation and skylight incident on leaf
- $T_L$  = leaf temperature
- $M_L$  = limiting soil moisture tension for net photosynthesis
- $M_O$  = optimum soil moisture tension for net photosynthesis
- $P_{MAX}$  = asymptotic rate of gross photosynthesis at very high light intensities
- $I_2$  = light intensity at  $P_{MAX}/2$
- R = rate of dark respiration
- B = constant.

The form of the first parenthetical term of equation (1) was determined chiefly from the theoretical water stress papers of Idso (10, 13). The second parenthetical term was deduced from Monteith's (18) evaluation of  $CO_2$  effects; and the third parenthetical term expresses de Wit's (6) analysis of light intensity effects. The exponential term involving leaf temperature was determined from data of several investigators (8, 16, 17, 20, 21). The complete derivation of equation (1) and the outline for obtaining values of the parameters necessary for its solution are found in reference (12).

Light Relations. The extended de Wit-Idso (D-I) theory was first used to calculate canopy profiles of reflection and transmission of solar radiation and skylight. These calculations were made for a solar altitude of  $65^\circ$ , which occurred one-half hour before and after solar noon. Figure 1 shows the results of the calculations along with measured values of these two parameters obtained over a similar, but slightly greater, interval of time. The degree of correspondence between the two representations is truly remarkable, especially considering that upper and lower limits of these two parameters were not set equal to measured fluxes as boundary conditions. Rather, they too were calculated from the

theory; and as may be seen from Figure 1, they agree to within better than 1% of the measured values.

Figure 2 shows the variation in the crop albedo during the day as calculated by the theory. Although no similar measurements for the crop investigated were available, these results are in harmony with those found by others for other crops (5, 9, 15, 19). This ability to account for variation in crop albedo with solar altitude is what gives D-I theory superiority over Kubelka-Munk, or K-M (3), theory as regards remote sensing.

Technical aspects of the theory and calculating procedures may be found in reference (14).

#### SUMMARY AND CONCLUSIONS:

A new analytical expression for net photosynthesis as a function of five microclimatic variables and seven plant constants has been developed, along with improved procedures for calculating values of the five pertinent variables at the plant leaves. Of the five variables, light intensity has received particular attention. An extension of de Wit-Idso theory of light relations in plant canopies has been made which predicts canopy reflectance and transmittance to within better than 1% of measured values. Variations with solar altitude are also predicted and are in harmony with experiment.

#### REFERENCES:

1. Allen, L. H., and Brown, K. W. Shortwave radiation in a corn crop. *Agron. Jour.* 57:575-580. 1965.
2. Allen, L. H., Yocum, C. S., and Lemon, E. R. Photosynthesis under field conditions. VII. Radiant energy exchanges within a corn crop canopy and implications in water use efficiency. *Agron. Jour.* 56:253-259. 1964.
3. Allen, W. A., and Richardson, A. J. Interaction of light with a plant canopy. *Jour. Optic. Soc. Amer.* 58:1023-1028. 1968.
4. Baker, D. N., and Musgrave, R. B. Photosynthesis under field conditions. V. Further plant chamber studies of the effects of light on corn. *Crop Sci.* 4:127-131. 1964.

5. Chia, L-S. Albedos of natural surfaces in Barbados. *Quart. Jour. Roy. Met. Soc.* 93:116-120. 1967.
6. de Wit, C. T. Photosynthesis of leaf canopies. *Agr. Res. Rpt.* 663. Centre for Agr. Pub. and Doc. Wageningen. 57 p. 1965.
7. Duncan, W. G., Loomis, R. A., Williams, W. A., and Hanau, R. A model for simulating photosynthesis in plant communities. *Hilgardia* 38:181-205. 1967.
8. El-Sharkawy, M. A., and Hesketh, J. D. Effects of temperature and water deficit on leaf photosynthetic rates of different species. *Crop. Sci.* 4:514-518. 1964.
9. Fritschen, L. J. Net and solar radiation relations over irrigated field crops. *Agr. Met.* 4:55-62. 1967.
10. Idso, S. B. Atmospheric- and soil-induced water stresses in plants and their effects upon transpiration and photosynthesis. *Jour. Theoretical Biol.* 21:1-12. 1968.
11. Idso, S. B. A holocoenotic analysis of environment-plant relationships, with special emphasis being given to the calculation of net photosynthesis, transpiration, and sensible heat exchange. *Minnesota Agr. Expt. Sta. Tech. Bul.* In Press. 1968.
12. Idso, S. B. A theoretical framework for the photosynthetic modeling of plant communities. *Adv. Frontiers of Plant Sci.* In Press. 1968.
13. Idso, S. B. Water chemical potential and photosynthesis. *Jour. Theoretical Biol.* Submitted. 1969.
14. Idso, S. B. Light relations in plant canopies. *Jour. Optic. Soc. Amer.* Submitted. 1969.
15. Idso, S. B., Baker, D. G., and Blad, B. L. Relations of radiation fluxes over natural surfaces. *Quart. Jour. Roy. Met. Soc.* In Press. 1969.
16. Lundegardh, H. *Environment and Plant Development.* Trans. and edited by E. Ashby. Edward Arnold and Co., London. 1931.
17. Milner, H. W., and Hiesey, W. M. Photosynthesis in climatic races of *Mimulus*. I. Effect of light intensity and temperature on rate. *Plant Physiol.* 39:208-213. 1964.

18. Monteith, J. L. Light distribution and photosynthesis in field crops. *Ann. Bot., N.S.* 29:17-37. 1965.
19. Monteith, J. L., and Szeicz, G. The radiation balance of bare soil and vegetation. *Quart. Jour. Roy. Met. Soc.* 87:159-170. 1961.
20. Scott, D., and Billings, W. D. Effects of environmental factors on standing crop and productivity of an alpine tundra. *Ecol. Monog.* 34:243-270. 1964.
21. Waggoner, P. E., Moss, R. A., and Hesketh, J. D. Radiation in the plant environment and photosynthesis. *Agron. Jour.* 55:36-39. 1963.
22. Wright, J. L., and Lemon, E. R. Photosynthesis under field conditions. VIII. Analysis of windspeed fluctuation data to evaluate turbulent exchange within a corn crop. *Agron. Jour.* 58:255-261. 1966.
23. Wright, J. L., and Lemon, E. R. Photosynthesis under field conditions. IX. Vertical distributions of photosynthesis within a corn crop computed from carbon dioxide profiles and turbulence data. *Agron. Jour.* 58:265-268. 1966.
24. Yocum, C. S., Allen, L. H., and Lemon, E. R. Photosynthesis under field conditions VI. Solar radiation balance and photosynthetic efficiency. *Agron. Jour.* 56:249-253. 1964.

PERSONNEL: Sherwood B. Idso

CURRENT TERMINATION DATE: October 1971

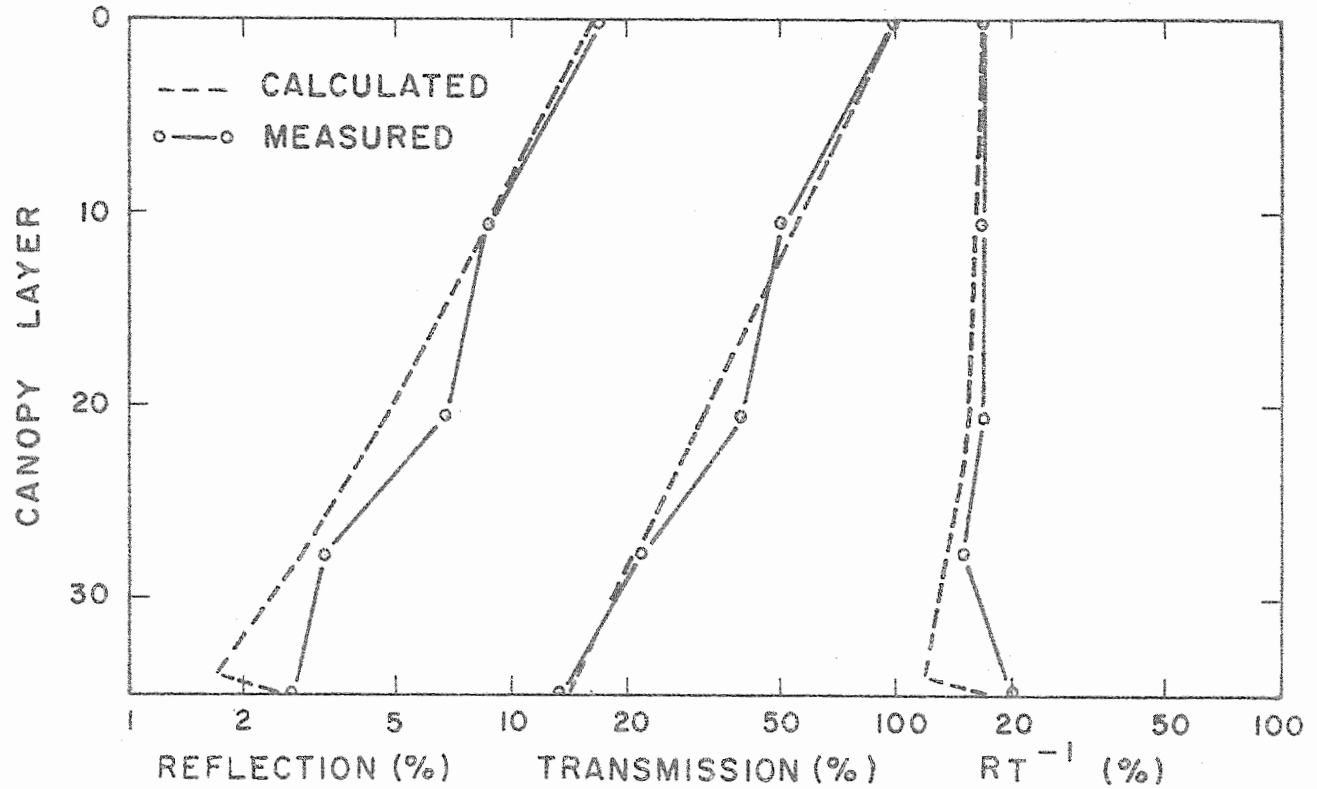


Figure 1. Calculated and measured profiles of reflection,  $R$ , and transmission,  $T$ , in a corn crop.  $R$  is computed as upward moving radiation divided by incident radiation and  $T$  as downward moving radiation divided by incident radiation.

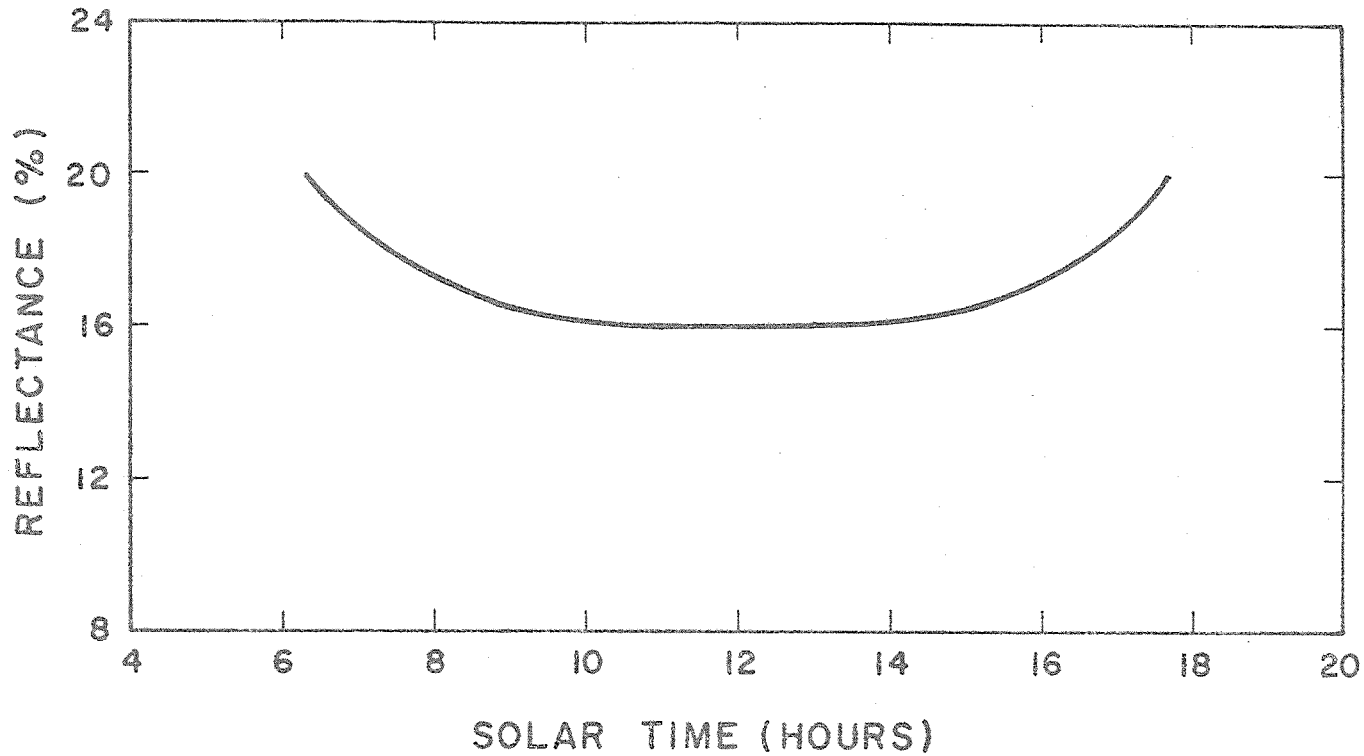


Figure 2. Calculated reflectance of a corn crop as a function of time for clear day conditions.

APPENDIX I

LIST OF PUBLICATIONS PREPARED OR PUBLISHED IN 1968

	<u>MS No.</u>
SWC W4-gG-1 Methods for water quality improvement and its storage underground.	
<u>Bouwer, Herman.</u> Salt balance, irrigation efficiency, and drainage design. (In press)	248
<u>Bouwer, Herman.</u> Water quality improvement by ground-water recharge. Second Seepage Symposium Proc., Phoenix, Ariz. 25-27 March 1968. (In press)	255
<u>Bouwer, Herman.</u> Returning waste to the land: A new role for agriculture? Jour. Soil and Water Conserv. 23(5):164-168. Sept-Oct 1968.	263
<u>Bouwer, Herman.</u> Putting waste water to beneficial use -- the Flushing Meadows Project. Ariz. Watershed Symposium Proc., Phoenix, Ariz. 18 Sept 1968. (Submitted for publication)	268
<u>Bouwer, Herman.</u> Infiltration of water into nonuniform soil. Jour. Irrig. & Drain. Div., Amer. Soc. Civil Engin. Proc. (Submitted for publication)	276
<u>Watson, Keith K.</u> The response behavior of a tensiometer-pressure transducer system under conditions of changing pore air pressure. Soil Sci. 104(6):439-443. 1967. (Issued in 1968)	192
<u>Watson, Keith K., and Whisler, F. D.</u> System dependence of the water content--pressure head relationship. Soil Sci. Soc. Amer. Proc. (Note) 32(1):121-123. Jan-Feb 1968.	202

- Whisler, F. D., and Watson, Keith K.  
One-dimensional gravity drainage of uniform columns of porous materials. Jour. Hydrol. 6(3):277-296. May-June 1968. 213
- SWC W7-gG-2 Theory and practice for conservation of massed water supplies for agricultural use.
- Bouwer, Herman, and Rice, R. C. A salt penetration technique for seepage measurement. Jour. Irrig. & Drain. Div., Amer. Soc. Civil Engin. Proc. 94(IR 4):481-492. Dec 1968. 205
- Bouwer, Herman, and Rice, R. C. Review of methods for measuring and predicting seepage. Second Seepage Symposium Proc., Phoenix, Ariz. 25-27 March 1968. (In press) 254
- Myers, Lloyd E., and Reginato, Robert J. Current seepage reduction research. Second Seepage Symposium Proc., Phoenix, Ariz. 25-27 March 1968. (In press) 251
- Myers, Lloyd E., Gen. Chairman & Editor Second Seepage Symposium Proc., Phoenix, Ariz., 25-27 March 1968. USDA-ARS 41-147. (In press) 264
- Nielsen, D. R., and Jackson, Ray D. Changes in water quality during seepage. Second Seepage Symposium Proc., Phoenix, Ariz. 25-27 March 1968. (In press) 252
- SWC W7-gG-3 Suppression of evaporation from water surfaces.
- Frasier, Gary W., and Myers, Lloyd E. Stable alkanol dispersion to reduce evaporation. Jour. Irrig. & Drain. Div., Amer. Soc. Civil Engin. Proc. 94(IR 1):79-89. March, 1968. 211

	<u>MS No.</u>
SWC W7-gG-4 Principles, facilities and systems for water harvest.	
<u>Frasier, Gary W., and Myers, Lloyd E.</u> Protective spray coatings for water harvesting catchments. Amer. Soc. Agric. Engin. Trans. (Submitted for publication)	274
<u>Myers, Lloyd E.</u> New-old water abracadabra reverses disappearing act. Chap. 59, "Science for Better Living" (1968 Yearbook of Agriculture) U. S. Dept. of Agriculture. Pp. 135-141.	229
<u>Myers, Lloyd E.</u> Saving water with asphalt. Amer. Chem. Soc., Symp. on New Uses for Asphalt Proc., Atlantic City, N.J. Sept. 1968.	258
SWC W7-gG-5 Soil water movement in relation to the conservation of water supplies.	
<u>Brust, K. J., Van Bavel, C. H. M., and Stirk, G. B.</u> Hydraulic properties of a clay loam soil and the field measurement of water uptake by roots: III. Field and laboratory measurement of conductivity and retention compared. Soil Sci. Soc. Amer. Proc. 32(3): 322-326. May-June 1968.	215
<u>Fink, Dwayne H., and Myers, Lloyd E.</u> Synthetic hydrophobic soils for harvesting precipitation. Symposium on Soil Wettability Proc., Riverside, Calif. 6-10 May 1968. (Submitted for publication)	261
<u>Fink, Dwayne H., Rich, C. I., and Thomas, G. W.</u> Determination of internal surface area, external water, and amount of montmorillonite in clay-water systems. Soil Sci. 105(2):71-77. Feb 1968.	193
<u>Nakayama, F. S.</u> Review of book, "Water in the Service of Man", by H. R. Vallentine. Quart. Rev. Biol. 43(1):116. March 1968.	218
<u>Nakayama, F. S.</u> Review of book, "Water: The Vital Essence", by Peter Briggs. Quart. Rev. Biol. 43(2):223. June 1968.	220

- Nakayama, F. S. Calcium activity, complex and ion-pair in saturated  $\text{CaCO}_3$  solutions. Soil Sci. 106(6):429-434. Dec 1968. 239
- Nakayama, F. S. Review of book, "The Problem of Water: A World Study," by Raymond Furon. Quart. Rev. Biol. 43(3):353. Sept 1968. 243
- Nakayama, F. S. Review of book, "Movement of Water in Plants," by G. E. Briggs. Soil Sci. Soc. Amer. Proc. 32(2):iv. Mar-Apr 1968. 245
- Nakayama, F. S. Magnesium complex and ion-pair in the  $\text{MgCO}_3\text{-CO}_2$  solution system. Jour. of Chem. & Engin. Data. (Submitted for publication) 262
- Nakayama, F. S. Hydrolysis of sodium carbonate. Jour. Chem. Ed. (Submitted for publication) 269
- Van Bavel, C. H. M., Brust, K. J., and Stirk, G. B. Hydraulic properties of a clay loam soil and the field measurement of water uptake by roots: I. Interpretation of water content and pressure profiles. Soil Sci. Soc. Amer. Proc. 32(3):310-317. May-June 1968. 208
- Van Bavel, C. H. M., Brust, K. J., and Stirk, G. B. Hydraulic properties of a clay loam soil and the field measurement of water uptake by roots: II. The water balance of the root zone. Soil Sci. Soc. Amer. Proc. 32(3):317-321. May-June 1968. 209
- Watson, Keith K., and Whisler, F. D. A semi-numerical approach for determining the hydraulic conductivity of unsaturated porous material. Trans., Inst. of Engineers, Australia. (Submitted for publication) 266

- Whisler, F. D. Analyzing steady-state flow in an inclined soil slab. Soil Sci. Soc. Amer. Proc. (Submitted for publication) 217
- Whisler, F. D., and Watson, Keith K. Analysis of infiltration into draining porous media. Jour. Irrig. & Drain. Div., Amer. Soc. Civil Engin. Proc. (Submitted for publication) 273
- SWC W9-gG-6 Factors governing evapotranspiration of water from cropped fields.
- Ehrler, W. L. Review of book, "Crop Responses to Water at Different Stages of Growth," by P. J. Salter and J. E. Goode. Soil Sci. (Submitted for publication) 272
- Ehrler, W. L., and Van Bavel, C. H. M. Leaf diffusion resistance, illuminance and transpiration. Plant Physiol. 43(2):208-214. Feb 1968. 212
- Erie, Leonard J. Management: A key to irrigation efficiency. Jour. Irrig. & Drain. Div., Amer. Soc. Civil Engin. Proc. 94(IR 3):285-293. Sept 1968. 222
- Erie, Leonard J., and French, Orrin F. Irrigate to satisfy cotton plant moisture needs. Univ. of Ariz. Agric. Ext. Serv. Bul. P-9, "COTTON", Pp. 20-21. Feb 1968. 238
- Erie, Leonard J., and French, Orrin F. Water management on fall-planted sugar beets in the Salt River Valley of Arizona. Amer. Soc. Agric. Engin. Trans. (Submitted for publication) 250
- Erie, Leonard J., French, Orrin F., and True, Lowell. Lawn watering need not be wasteful. Univ. of Ariz. Agric. Ext. Serv. Folder 143. 10 pp. Nov 1968. 267

- Hilgeman, R. H., Ehrler, W. L., Everling, C. E. and Sharp, H. O. Apparent transpiration and internal water stress in Valencia oranges as affected by soil water, season and climate. Internat'l. Citrus Symposium Proc., Riverside, Calif. March 1968. (In press) 259
- Idso, Sherwood B. An analysis of the heating coefficient concept. Jour. Appl. Met. 7(4): 716-717. (Note) Aug 1968. 224
- Idso, Sherwood B. Comments on "The Hydro-logic Importance of Transpiration Control by Stomata" by Richard Lee. Water Resources Res. 4(3):665-666. June 1968. 231
- Idso, Sherwood B. Atmospheric and soil induced water stresses in plants and their effects upon transpiration and photosynthesis. Jour. Theoret. Biol. 21:1-12. 1968. 233
- Idso, Sherwood B. A theoretical framework for the photosynthetic modeling of plant communities. In "Advancing Frontiers of Plant Sciences." (India) (In press) 270
- Idso, Sherwood B. Water chemical potential and photosynthesis. Jour. Theoret. Biol. (Submitted for publication) 271
- Idso, Sherwood B., and Baker, Donald G. The naturally varying energy environment and its effects upon net photosynthesis. Ecology 49(2):311-316. 1968. 242
- Idso, Sherwood B., and Jackson, Ray D. The significance of fluctuations in sky radiant emittance for infrared thermometry. Agron. Jour. 60(4):388-392. July-Aug 1968. 240
- Idso, Sherwood B., and Jackson, Ray D. A note on the role of sky radiance in infrared thermometry. Jour. Appl. Meteorol. 7(3):521-522. June 1968. 241

Idso, Sherwood B., and Jackson, Ray D.  
Comments on "Thermodynamic Aspects of Developmental Biology", by Zotin and Zotina.  
Jour. Theoret. Biol. 20:126-127. 1968.  
(Letter to Ed.) 247

Idso, Sherwood B., and Jackson, Ray D.  
Comparison of two methods for determining infrared emittance of bare soils.  
Jour. Appl. Meteorol. (Submitted for publication) 260

Idso, Sherwood B., and Jackson, Ray D.  
Thermal radiation from clear skies.  
Jour. Geophys. Res. (Submitted for publication) 275

Idso, Sherwood B., Jackson, Ray D., Ehrler, W. L., and Mitchell, S. T.  
Infrared emittance determinations of leaves.  
Ecology. (Submitted for publication) 265

Jackson, Ray D., and Idso, Sherwood B.  
Ambient temperature effects in infrared thermometry. Soil Sci. Soc. Amer. Proc. (Submitted for publication) 253

Longenecker, D. E., and Erie, Leonard J.  
Irrigation water management - Cotton.  
Chap. 11 in "Advances in Production and Utilization of Quality COTTON: Principles and Practices", pub. by Ortho Div., Chevron Chem. Co., at Iowa State Univ. (Pp. 321-345). Sept 1968. 201

Van Bavel, C. H. M., and Ehrler, W. L.  
Water loss from a sorghum field and stomatal control. Agron. Jour. 60(1):84-86. Jan-Feb 1968. 204

- Haise, Howard R., Kruse, Gordon E., and Erie, Leonard J. Hydraulically controlled butterfly gates in farm lateral turnouts for automation of surface irrigation systems. Amer. Soc. Agric. Engin. Trans. (Submitted for publication) 257
- Replogle, John A. Discussion of: "Rectangular cutthroat flow measuring flumes" by G. V. Skogerboe and M. Leon Hyatt. Jour. Irrig. & Drain. Div., Amer. Soc. Civil Engin. 94(IR 3):359-362. Sept 1968. 249
- Replogle, John A. Flow measurement with critical depth flumes. Internatl. Comm. on Irrig. & Drainage, 7th Cong. Proc. Mexico City (To be held in April, 1969). (Submitted for publication) 256
- Replogle, John A., Myers, Lloyd E., and Brust, Kenneth J. Digest: Flow measurements with fluorescent tracers." Amer. Soc. Civil Engin. Trans. 133:23-29. 1968. 225
- Replogle, John A., Myers, Lloyd E., and Brust, Kenneth J. Closure: Flow measurements with fluorescent tracers. Jour. Hydraul. Div., Amer. Soc. Civil Engin. Proc. 94(HY 2):552-555. March 1968. 228
- Replogle, John A., Myers, Lloyd E., and Brust, Kenneth J. Closure: Evaluation of pipe elbows as flow meters. Jour. Irrig. & Drain. Div., Amer. Soc. Civil Engin. Proc. 94(IR 3):335-339. Sept 1968. 244
- Replogle, John A., Myers, Lloyd E., and Brust, Kenneth J. Digest: Evaluation of pipe elbows as flow meters. Amer. Soc. Civil Engin. Trans. 133:373-374. 1968. 246

APPENDIX II  
SUMMATION OF IMPORTANT FINDINGS

SWC W4 gG-1 Methods for water quality improvement and its storage underground.

Studies near Phoenix, Arizona have shown that 90 percent of the total nitrogen in secondary sewage effluent can be removed by properly managed filtration through soil. Ponding water in groundwater recharge basins for short periods of time, 2 days wet and 3 days dry, yielded nitrate-nitrogen concentrations of 20-30 ppm in water that percolated down through the soil to a depth of 25 ft. Longer ponding periods, 2 wks wet and 1 wk dry, yielded nitrate-nitrogen concentrations of 0-1 ppm. These findings are of great importance in managing waste waters to minimize nitrate pollution of ground water. (WCL 67-4)

SWC W7 gG-2 Evaluation and control of seepage from water storage and conveyance structures.

Tough and durable asphalt-fiberglass linings installed in two 160,000 gallon reservoirs are in excellent condition after 6 years of severe northern Arizona exposure, including trampling by deer and cattle. The linings were fabricated in place by spraying fiberglass matting with asphalt emulsion at a total cost of 75 cents per square yard. Maintenance has required only 15 minutes spent pouring asphalt emulsion over small flaws in one lining. This lining, which requires little equipment or labor for installation, represents an important advance in the development of high performance, lower-cost reservoir linings. (WCL 68-2)

SWC W7 gG-3 Suppression of evaporation from water surfaces.

Silicone treated perlite ore, floated on the water surface to reduce evaporation from a 320 m<sup>2</sup> pond, proved to be both practical and economical. The cost of water saved was \$0.36 per 1000 liters (\$1.36 per 1000 gal.) for an 8-month period during which the perlite treatment reduced evaporation 18.8%. Fish placed in the treated pond experienced essentially the same growth rates as those in an untreated pond. (WCL 67-3)

SWC W7 gG-4 Principles, facilities, and systems for water harvest.

Runoff from a 180 m<sup>2</sup> bare soil catchment near Phoenix, Arizona, sprayed with a water repellent chemical in 1965, has averaged 75 percent of the 10-inch average annual rainfall. The treatment, which cost 5 cents per square yard, shows no sign of deterioration 3.5 years after application. Water collected to date has cost 31 cents per 1000 gallons. A similar catchment in a 20-inch rainfall zone would collect water for less than 20 cents per 1000 gallons.

(WCL 60-7)

SWC W7 gG-5 Soil water movement in relation to the conservation of water supplies.

Simple graphs have been developed for predicting the relative amounts of calcium ions, complexes, and ion-pairs in sulfate-carbonate solutions. These graphs resulted from theoretical investigations of solution equilibria of the sulfate, bicarbonate, and carbonate anions of calcium. The carbonate complexes and ion-pairs decrease the net available calcium ions as much as 50 percent in solutions where sulfates are added to alkaline carbonates. This information explains why some gypsum treatments have not been successful in reclaiming alkali soils. (WCL 64-6)

SWC W9 gG-6 Factors governing evapotranspiration of water from cropped fields.

Although a soil water deficit depressed the early growth of three varieties of field-grown cotton near Phoenix, Arizona, compensatory growth after a drought-breaking irrigation resulted in final values of dry weight and height not significantly different from those of the frequently irrigated controls. These data suggest the persistence of net photosynthesis in spite of plant water stress.  
(WCL 62-10)

A new, simple, and accurate method of measuring infrared emittances from plant leaves, as well as from soils and other surfaces has been developed. Emittances of leaves from 34 different plant species were measured and reported. Previous methods for measuring emittance were difficult or impossible to use on plant leaves because of the size of required equipment. This new method will be of great value in measuring the energy balance of plants in studies of photosynthesis and the utilization of water by plants.  
(WCL 68-5)

SWC W10 gG-7 Irrigation systems for efficient water use.

A procedure has been developed for using pipe elbow rate meters as recording flow meters by connecting turbine-type household meters to the pressure taps on the elbow meters. The relationship between main line flow and flow through the turbine meter is sufficiently linear to provide an indication of total flow through the main line with only  $\pm 4$  percent error. This system provides a low-cost totalizing meter with accuracy sufficient for many irrigation applications. (WCL 60-2)